Investigating the role of the exocyst complex in infection-related development of the rice blast fungus *Magnaporthe oryzae*

Submitted by Yogesh Kumar Gupta

to the University of Exeter as a thesis for the degree of Doctor of Philosophy, in Biological Sciences

September 2014

I certify that all material in this thesis which is not my own work has been identified and that no material has been previously submitted and approved for the award of a degree by this or any other University.

Yogesh Kumar Gupta

Abstract

Host colonization is mediated through the secretion of effector proteins in order to neutralize host immune responses. However, the mechanism of the effector delivery during biotrophic invasion is not well defined in *M. oryzae*. In this thesis, I define the role of the exocyst complex, an evolutionarily conserved octameric protein complex involved in vesicle docking to the plasma membrane (composed of Sec3, Sec5, Sec6, Sec8, Sec10, Sec15, Exo70 and Exo84), during infection-related development in *M. oryzae*. Like other filamentous fungi, *M. oryzae,* exocyst components localize to the vegetative hyphal tip distinct from the Spitzenkörper. However, at the initial stage of infection-related development all the exocyst components localise as a ring at the cortex of the appressorium and re-assembles around the appressorium pore in an actin-dependent manner in mature appressoria. I report that the septin network is required for the transition of exocyst ring from periphery to the appressorium pore. Deletion of Exo70 and Sec5 showed significant reduction in protein secretion and plant infection. I show that Sec6 is required for the exocyst assembly around the appressorium pore and effector secretion from the appressorium. I report that, during biotrophic invasion, effectors are secreted through a distinct pathway. Apoplastic effectors, Bas4 and Slp1 are secreted via a Golgi-dependent pathway while secretion of cytoplasmic effectors, Pwl2 and Bas1 meditates through a Golgi-independent pathway in which exocyst components Exo70 and Sec5 are involved.

Table of contents

Giraldo, M.C., Dagdas, Y.F., Gupta, Y.K., Mentlak, T.A., Yi, M., Martinez-Rocha, A.L., Saitoh, H., Terauchi, R., Talbot, N.J. and Valent, B. (2013) Two distinct secretion systems facilitate tissue invasion by the rice blast fungus *Magnaporthe oryzae*. *Nature Communication* **4**: 1996. doi: 10.1038/ncomms2996.

List of Figures

List of Tables

Acknowledgements

I would like to thank Les and Claire Halpin of their support and funding which gives me opportunity to join Nick Talbot's group and I really feel honoured to be a Halpin scholar. I would like to express my eternal gratitude to my supervisor Nick Talbot for his guidance, keen interest, encouragement and full support during whole course. He is truly a great and inspirational scientist who always motivates me.

I would like to thank Yasin Dagdas and Muhammad Islam for their support during my study. I spent a lot of time with them even outside of the lab.

Special thanks to George Littlejohn for his help in thesis writing and providing support on confocal microscopy and Marian Littlejohn who construct model diagram of the exocyst paper.

I am grateful to Barbara Valent, Martha Giraldo, Ryohei Terauchi, and Hiromasa Saitoh to work with me in collaboration on effector secretion project.

I thank Michael Kershaw and Tina Penn for their support in lab.

I appreciate the technical staff of School of Biological Sciences for providing technical support throughout my study.

A big thanks to all the current and past lab members of the Halpin laboratory including Nick Tongue, Lauren Ryder, Miriam Oses-Ruiz, Magdelana Martin Urdiroz, Magdalena Basciewicz, Termizi Yosouf, Muhammad Badaruddin, Darren Soanes, Ana-Lilia Martinez Rocha, Min He, Xia Yan, Wasin Sakulkoo, David Mwongera, Richard Lindsay, Vincent Were, Kenichi Ikeda, Kanako Inoue-Ikeda, Kae Yoshino and Barbara Saddler.

Many thanks to Yogesh and Neha Chaudhari for their support in curicial time of thesis writing. We spent wonderful time together.

I would not be able to achevie this without blessings and support of my parents and my lovely sisters, Jyoti and Monika. I would like to thank my parents-in-law, Shilpa and Shikhar for their well wishes. Last but not the least, very special thank to my wife, Shikha for being with me all the time to share joy and sorrows. It's immense pleasure for me to have your support all the way through in my life. Words cannot express to thank my son, Medhansh, who bring so much happiness to our life.

Dedicated to my parents,

For their endless love, blessings, support and encouragement.

Abbreviations

°C	degrees celcius
BFA	brefeldin A
BIC	biotrophic interfacial complex
bp	base pair
cAMP	cyclic 3', 5' adenosine monophosphate
cDNA	complementary dna
CM	complete medium
DMSO	dimethyl sulphoxide
DNA	deoxyribonucleic acid
EDTA	ethylenediaminetetracetic acid
EIHM	extra-invasive hyphal membrane
g	Grams
GFP	green fluorescent protein
kb	Kilobase
L	Litre
Lat A	latrunculin A
M	Molar
MAPK	mitogen-activated protein kinase
mg	Milligram
mL	Millilitre
mm	Millimetre
mM	Millimolar
MM	minimal media
mRNA	messenger RNA
NADPH	nicotinamide adenine dinucleotide phosphate
ng	Nanogram
ORF	open reading frame
PCR	polymerase chain reaction
RFP	red fluorescent protein
RNA	ribonucleic acid
RNase	ribonuclease

ROS	reactive oxygen species
rpm	revolutions per minute
sec	Second
SPK	spitzenkörper
TS	temperature sensitive
wt	wild type
X-gal	5-bromo-4-chloro-3-indolyl-β-d-galactosidase
µg	Microgram
µL	Microliter
µm	Micrometre

Chapter 1. Introduction

1.1 Global significance of plant pathogens

Due to increasing population pressure, global agricultural production needs to increase more than three-fold over the next fifty years to satisfy increasing food demand (Godfray et al, 2010). Emerging threats to global food production are posed by crop pests and diseases (Fisher et al, 2012; Pennisi, 2010) and it has been suggested that more than 10% of global food production is lost annually due to plant parasites (Strange & Scott, 2005). Serious threats to global food production include wheat stem rust (*Puccinia graminis* Ug99), potato blight (*Phytophthora infestans*), rice blast (*Magnaporthe oryzae*), black sigatoka of banana (*Mycospharella fijiensis*), Asian soybean rust (*Phakospora pachyrhizi*) and cassava brown streak virus (Pennisi, 2010). A recent outbreak of panama disease on banana production caused by *Fusarium oxysporum* f. sp. *cubense* race TR4, for example posed a serious threat to a crop which is a staple food for approximately 400 million people worldwide (Butler, 2013).

Fungal diseases of trees such as Dutch elm disease caused by the fungus *Ophiostoma ulmi*, resulted in the loss of over 100 million elm trees in the UK and US (Giraud et al, 2010; Loo, 2009). Recently, ash dieback caused by *Chalara fraxinea*, has emerged as a serious threat to ash trees throughout Europe, it also poses a danger to several lichen species living specifically on ash trees (Ellis et al, 2012). Infections of trees also cause serious environmental issues and economic problems such as loss of habitat for animal species, loss of economically important trees, changes in the landscape and carbon release.

Recently, it has been suggested that diseases caused by fungi and fungus-like organisms may cause extinctions of several animal and plant species (Fisher et al, 2012). It is,

therefore, necessary to overcome these problems by sustainable and integrated disease control solutions which include climate forecasting and population genomics to understand molecular evolution and epidemiology (Fisher et al, 2012).

1.2 Rice and rice blast disease

Rice is a staple food for more than half of the world's population and it is estimated that, by 2020, global rice consumption will surge by an additional 90 million tons (Mohanty, 2009). Asian countries consume the most rice, and it was estimated that greater than 100 kg rice *per capita* is consumed annually, which provides more than 50% of the total calorific supply (Dawe, 2002). Rice production can be severely hampered by plant pathogens and one of the most important pathogens is *Magnaporthe oryzae* Couch (formerly *M. grisea* Cav.), which causes rice blast disease (Couch & Kohn, 2002). It is estimated that every year up to 30% of global rice production is lost due to rice blast disease (Skamnioti & Gurr, 2009; Wilson & Talbot, 2009). It was reported that in 1995, Bhutan lost over 1000 tonnes of their rice harvest covering over 700 hectares area due to *M. oryzae* (Talbot, 2003; Thinlay et al, 2000).

Recently, *M. oryzae* was voted one of the most destructive and important fungal pathogens of plants (Dean et al, 2012). *M. oryzae* is a heterothallic, filamentous ascomycete fungus which can infect over 50 different grass species, including agronomically important crops such as barley, wheat, oat, rye and finger millet (Skamnioti & Gurr, 2009; Talbot, 2003). More recently, *M. oryzae* has emerged as a serious threat to wheat producing areas in South America where significant yield loss has occurred due to wheat blast disease. It was first observed in 1985 in the state of Paraná, Brazil and now poses a serious threat to wheat production as there is a lack of understanding of the mode of infection and suitable fungicides (Cruz et al, 2012; Urashima et al, 2004).

Control measures, including use of resistance cultivars, are generally thwarted because *M. oryzae* is highly variable in field conditions and breaks resistance in only a few generations (Huang et al, 2014). It is, therefore, important to learn about infection-related biology in order to prevent rice blast disease and potentially other diseases too, which uses analogous mechanism of infection. The availability of genome sequences of both rice and *M. oryzae*, is highly advantageous to genome-wide association studies and expression profiling (Dean et al, 2005; International Rice Genome Project, 2005). The rice blast fungus can grow outside its host plant *in vitro*, can efficiently be transformed via protoplast or *Agrobacterium*-based methodologies, and possesses a tractable sexual cycle, which is helpful for molecular genetic studies. All these advantages make *M. oryzae* an attractive model organism to study host-pathogen interactions (Ebbole, 2007; Talbot, 2003). The ease with which fluorescent markers and targeted gene deletion mutation can be achieved through homologous recombination facilitates functional studies in *M. oryzae*. Molecular cell biology can be easily performed as *M. oryzae* spores germinate on glass coverslips, which potentially mimic the rice leaf surface and are therefore highly useful in studying pre-penetration events.

1.3 The life cycle of *Magnaporthe oryzae*

M. oryzae reproduces both sexually and asexually. The sexual cycle is difficult to detect as it is cryptic or facultative and has only been seen in restricted areas of south-east Asia (Saleh et al, 2012; Zeigler, 1998). The sexual cycle requires two opposite mating type strains (*MAT1*/-*MAT2*), in which at least one should be female fertile i.e. competent to produce perithecia (Zeigler, 1998). *M. oryzae* produce microconidia and macroconidia in their asexual cycle (Chuma et al, 2009; Kato et al, 1994; Zhang et al, 2014a). However all infection studies reported in *M. oryzae* use macroconidia. Recently, Zhang et al, (2014a) has reported that *M. oryzae* produce single celled microconidia which

only infects through wounded leaves of rice and barley (Zhang et al, 2014a). *M. oryzae* produces a three-celled macroconidium, which is responsible for rice blast infection and is commonly referred to as the conidium.

The infection cycle starts when the three-celled conidium lands on the hydrophobic leaf surface by aerosol or wind dispersal (Talbot, 1995; Wilson & Talbot, 2009). In the presence of water, the cell wall of the conidium is hydrated and spore tip mucilage is secreted from the apex of the spore and acts as a glue to allow the conidium to adhere to the hydrophobic leaf surface (Hamer et al, 1988). The apical cell of the conidium forms a polarised germ tube which starts swelling at the tip, 2-3 h after germ tube initiation starts and subsequently flattens against the leaf surface in a process called hooking (Bourett & Howard, 1990). The swollen tube then forms a dome-shaped, melanised infection structure called an appressorium which generates huge turgor pressure up to 8 MPa which is sufficient to rupture the plant cuticle (de Jong et al, 1997; Wilson & Talbot, 2009). The melanin layer is formed between the fungal cell wall and plasma membrane and allows accumulation of glycerol inside the appressorium which acts as an osmoticum, thereby allowing development of huge turgor in the appressorium (Chumley & Valent, 1990; de Jong et al, 1997; Howard et al, 1991). A penetration hypha emerges from the base of the mature appressorium, where the cell wall and melanin layer have been shown to be initially absent (Howard & Valent, 1996). After gaining entry to the host tissue, *M. oryzae* suppresses host immune responses and grows inside the host rice cells biotrophically (Kankanala et al, 2007; Khang et al, 2010). In the later stages of infection, *M. oryzae* secretes toxins to induce cell death and thereby causes necrotrophic lesions. Enormous amounts of inoculum are produced by these lesions, which carry on the infection cycle (Kankanala et al, 2007; Talbot, 1995; Talbot, 2003; Wilson & Talbot, 2009).

Recently, *M. oryzae* infection was observed in wheat growing regions in South America but still there is no direct evidence about which crop or grass species is responsible for the host jump to wheat. Interestingly, the infection of wheat blast was only observed on flowering heads and no symptoms were detected on leaves in field conditions (Cruz et al, 2012; Tufan et al, 2009). The infection cycle of the wheat blast pathogen is still unknown, and this is a challenge for effective control of wheat blast disease.

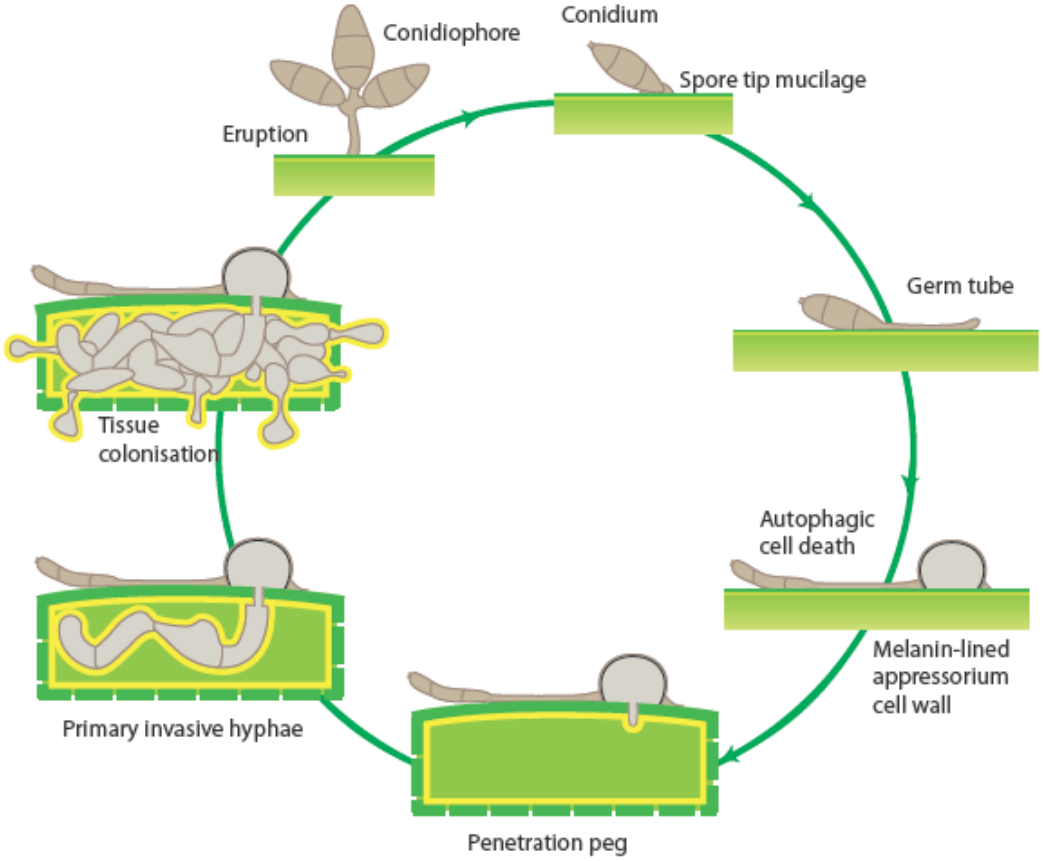

Figure 1.1 Disease cycle of the rice blast fungus, *M. oryzae* (Modified by Marian Littlejohn from Wilson & Talbot, *Nature Review Microbiology* 2009, 7:185-185).

The infection cycle of *M. oryzae* starts when a three cell conidium lands on the hydrophobic leaf surface and secretes spore tip mucilage to adhere to the surface. The conidium germinates from the apex and forms a polarised germ tube, which differentiates into a melanised dome-shaped infection structure called an appressorium. Mature appressoria generates huge turgor pressures to breach the leaf cuticle by means of mechanical force. A narrow penetration peg develops from the base of the appressorium, differentiates into primary invasive hyphae which then colonise host tissue. Necrotrophic lesions appear after 96 h and these lesions produce millions of spores which build an enormous amount of inoculum to carry on the infection cycle.

1.4 Appressorium mediated tissue invasion in *M. oryzae*

Fungal plant pathogens use diverse mechanisms to gain entry to host tissue. Some species form infection structures outside the host tissue, such as *M. oryzae, Ustilago maydis, Fusarium spp., Colletotrichum spp.* while some gain entry from the natural openings including *Cladosporium fulvum* and *Zymoseptoria tritici*. Physiological and biochemical cues from the plant surface are sensed by pathogens and are required for successful invasion (Gilbert et al, 1996; Howard & Valent, 1996; Tucker & Talbot, 2001). *M. oryzae* recognises an inductive plant surface which provides the signal for natural appressorium formation, but on non-inductive surfaces produces only extended growth of germ tubes, with no differentiation of appressoria (Tucker & Talbot, 2001; Wilson & Talbot, 2009). Formation of functional appressoria depends on surface recognition and downstream signalling pathways mediated through cyclic AMP and MAPK cascades (Li et al, 2012; Xu, 2000). Differentiation of the appressorium from the germ tube is tightly linked with cell cycle and autophagic cell death in the conidium (Kershaw & Talbot, 2009; Saunders et al, 2010a; Veneault-Fourrey et al, 2006; Wilson & Talbot, 2009).

1.4.1 Cyclic AMP signalling

The infection cycle of *M. oryzae* starts when a conidium lands on the leaf surface and senses inductive biochemical (cutin monomers, primary alcohols and leaf waxes) and physiological properties such as surface hardness and hydrophobicity (Gilbert et al, 1996), which result in induction of appressorium formation. In the early stages of infection-related development the cyclic AMP (cAMP) plays an important role in surface recognition and appressorium formation (Lee & Dean, 1993; Mitchell & Dean, 1995). The cAMP pathway is activated by the gene encoding adenylate cyclase, *MAC1*,

and targeted gene deletion mutant of *MAC1* results in spores unable to produce appressoria and consequently unable to infect rice plants (Choi & Dean, 1997). Interestingly, addition of exogenous cAMP to Δ*mac1* mutants restores the ability to form functional appressoria and remediates pathogenicity defects (Adachi & Hamer, 1998; Choi & Dean, 1997). cAMP generated *MAC1* can interact with the regulatory subunit of the cAMP-dependent protein kinase (Sum1), causing release of the catalytic subunit, CpkA (**Figure 1.2**) (Adachi & Hamer, 1998). Mutation in the regulatory subunit-encoding gene Sum1, causes detachment and constitutive activation of CpkA, which restores the wild type appressorium phenotype of Δ*mac1* as a consequence of over-riding the requirement of cAMP signalling (Adachi & Hamer, 1998). The catalytic subunit of cAMP-dependent protein kinase, CpkA, is required for normal appressorium formation and pathogenicity (Mitchell & Dean, 1995). However, Xu et al, (1997) showed that prolonged incubation on plants of Δ*cpkA* mutants can produce some appressoria but they are defective in penetration (Xu et al, 1997).

Heteromeric GTP-binding proteins (G-proteins) and their regulators are also involved in surface recognition. *M. oryzae* has three Gα subunits, MagA, MagB and MagC. Targeted deletion of the *MAGB* gene shows significant reduction in conidiation, appressorium formation and pathogenicity, while disruption of *MAGA* and *MAGC* has no significant effect on pathogenicity (Liu & Dean, 1997). Addition of exogenous cAMP in Δ*magB* mutants restores appressorium formation and a dominant active allele of *MAGB* can form appressoria on non-inductive hard surfaces. This suggests that MagB might have a first role in sensing surface cues and then in stimulating cAMP synthesis (Liu & Dean, 1997; Wilson & Talbot, 2009). The regulator of G-protein signalling, Rgs1, binds Gα subunits and negatively regulates appressorium development, as Δ*rgs1* mutants form normal apprresorium on both hydrophobic and

non-inductive, hydrophilic surfaces (Liu et al, 2007a). Furthermore, characterisation of seven additional regulators of G-proteins suggested their role in the control of intracellular cAMP levels and also implicated them in appressorium development and pathogenicity (Zhang et al, 2011). Another upstream component of cAMP signalling, MoRic8 (a regulator of GTP-binding proteins) has been shown to interact with MagB in a yeast two-hybrid assay. Targeted gene deletion mutants of *MoRic8* are impaired in appressorium development and plant infection (Li et al, 2010). Recently, Zhou and colleagues identified a Mac1-interacting protein, Cap1 (cyclase–associated protein 1), by co-immunoprecipitation and further confirmed this interaction by yeast two-hybrid assay (Zhou et al, 2012). Interestingly, Cap1:GFP localised with actin patches in vegetative hyphae and in appressorium development and deletion of *CAP1* abolished the effect of a dominant RAS2 allele (Ras GTPase) which can form appressoria on hydrophilic surfaces. Further characterisation suggests that *CAP1* is required for appressorium development and full virulence (Zhou et al, 2012). Downstream components of CpkA were identified in a screen for non-pathogenicity mutants in a T-DNA insertional library. MoSom1 has been shown to directly interact with CpkA by yeast two-hybrid analysis. In addition, two other transcription factors, MoStu1 and MoCdtf1 have been shown to interact with MoSom1 (**Figure 1.2**) (Yan et al, 2011). Functional characterisation of all three transcription factors shows them to be involved in appressorium morphogenesis and plant infection (Yan et al, 2011).

Three additional proteins in *M. oryzae* have been shown to be involved in surface recognition, including a class1 hydrophobin, Mpg1, which is highly expressed during germ tube extension (Kershaw et al, 1998; Talbot et al, 1993). Deletion of *MPG1* resulted in a non-pathogenic phenotype, which could be recovered by the addition of exogenous cAMP, which restores its ability to infect rice plants, suggesting that *MPG1*

might regulate the attachment of the germ tube and activate a signalling cascade required for appressorium development (Talbot et al, 1993). A G-protein coupled receptor (GPCR) protein, Pth11, deletion mutants of which cannot form appressorium, has been shown to be localised to the plasma membrane and is thought to be involved in sensing surface hardness and hydrophobicity. Pth11 contains seven trans-membrane domains and an extracellular cystenin-rich EGF like domain which suggests a mechanism whereby environmental cues maybe transmitted to secondary messengers to regulate appressorium development (DeZwaan et al, 1999). In addition, a novel chitin-binding protein, *CBP1*, was identified by screening a cDNA subtractive differential library and deletion mutants of *CBP1* were shown to be unable to generate appressoria on artificial surfaces. However, they can form functional appressoria on plant leaf surfaces, which suggests that *CBP1* may recognize physical or chemical properties of plant surfaces (Kamakura et al, 2002).

1.4.2 Mitogen-activated protein Kinase (MAPK) pathways

M. oryzae surface recognition is governed by a cAMP signalling pathway but there are three Mitogen-activated protein Kinase (MAPK) pathways, signalling via Pmk1, Mps1 and Osm1, which regulate appressorium development and tissue invasion (Li et al, 2012). In *M. oryzae*, Pmk1 encodes a MAPK orthologous to yeast Fus3/Kss1 and a null mutant of *PMK1* is not competent to form appressoria (Xu & Hamer, 1996). The Pmk1 pathway is regulated through the surface receptor Msb2 and other upstream components, including MAPKK Mst11, MAPK Mst7 and an adaptor protein, Mst50 (Park et al, 2006; Wilson & Talbot, 2009; Zhao et al, 2005). Mst50 is known to interact with Mst11 and Mst7 and act as a linker/adaptor for the Pmk1 pathway (Park et al, 2006; Zhao & Xu, 2007). A small GTPase, Cdc42, and Ras GTPase, Ras2, directly interact with the Mst50 adaptor protein and regulate the Mst11-Mst7-Pmk1 pathway

(**Figure 1.2**) (Park et al, 2006). A dominant active allele of *RAS2* can form appressoria on hydrophilic surfaces, suggesting that it might act upstream of the Pmk1 pathway. Direct interaction of Mst50 and Cdc42 (regulator of polarised secretion pathway) suggest that it may also have a role in cellular polarity establishment (Park et al, 2006). Mst12 is a transcription factor that acts as a downstream component of the Pmk1 pathway and null mutants of *MST12* produce normal, melanised appressorium which are unable to form penetration hyphae (Park et al, 2002). Further evidence that Mst12 acts specifically in penetration is provided by mutant study of the Mst12-interacting protein, MoMcm1, identified by affinity purification. Targeted gene deletion mutants of *MCM1* exhibit a defect in appressorium penetration and only a few appressorium can form narrow invasive hyphae but are restricted to first invaded rice cell (Zhou et al, 2011).

The second MAPK-encoding gene, *MPS1* is invovled in surface recognition and a functional homologue of the yeast *SLT2* which regulates the cell integrity pathway in *M. oryzae* (Xu et al, 1998). *M. oryzae MPS1* is regulated by the MAPKK *MCK1* which shows functional homology to *BCK1* from *S. cerevisiae* (Jeon et al, 2008). Targeted deletion mutants of Δ*mps1* and Δ*mck1* show severe reduction in conidiogenesis, hypersensitivity to cell wall degrading enzymes and produce non-functional appressoria, which are unable to penetrate the host cell (Jeon et al, 2008; Xu et al, 1998). *MPS1* regulates accumulation of cell-wall synthesizing enzymes, such as alpha-1, 3-glucan, which may protect from cell wall degrading enzymes during infection (Fujikawa et al, 2009). Mig1, a downstream target of Mps1 encodes a MADS-box transcription factor. Null mutants of *MIG1* show no sign of cell wall defects. However Δ*mig1* mutants lose their ability to carry out plant infection (Mehrabi et al, 2008). Interestingly, Δ*mig1* mutants can form functional appressoria, which can infect host

cells and develop primary invasive hyphae, but do not differeniate into secondary invasive hyphae (Mehrabi et al, 2008). It has been suggested that *MIG1* may regulate expression of genes which supress host immune responses (Mehrabi et al, 2008). Another transcription factor, MoSwi6, encodes the yeast homologue Swi6, a downstream target of Slt1 (Qi et al, 2012). MoSwi6 directly interacts with *MPS1* and is required for maintaining cell wall integrity, activity of extra-cellular enzymes and complete virulence on rice plants (**Figure 1.1**) (Qi et al, 2012).

The third MAPK-encoding gene in *M. oryzae*, *OSM1* (Osmoregulatory MAP kinase), is a functional homologue of S. cerevisiae *HOG1* and regulates the cellular response to hyperosmotic stress (**Figure 1.2**). Although *OSM1* is dispensable for glycerol accumulation and plant infection, Dixon et al, (1999) suggest that there might be an independent signalling pathway which regulates turgor generation (Dixon et al, 1999).

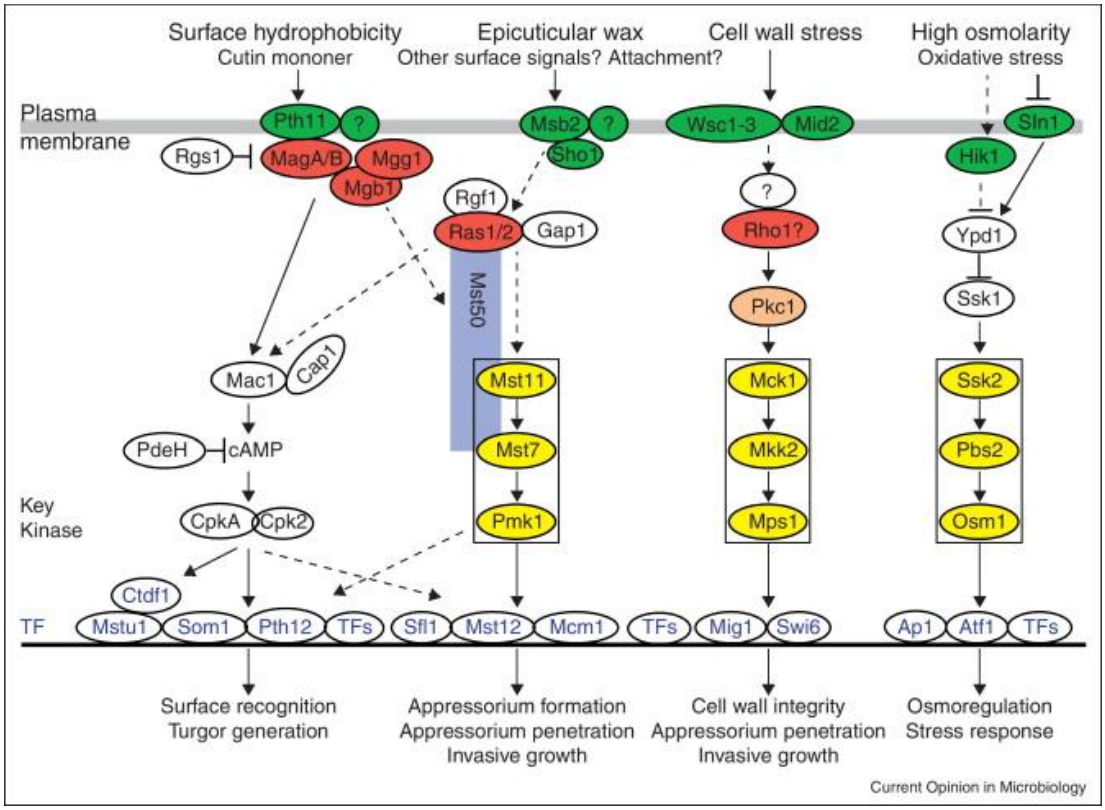

Figure 1.2 *M. oryzae* signalling pathways responsible for infection-related development (Taken from Li et al, *Current Opinion in Microbiology* 2012, 15:678-684).

A surface receptor (green box) senses the environmental cues and passes the signal to downstream components through small GTPases (red box), which activate MAPK cascades (yellow box). These MAPK genes act on the transcription factors and regulate morphogentic changes during infection-related development. The cAMP pathway is important for surface regnition and upstream components of this pathway may interact with the PMK1 MAPK pathway, which regulates appressorium devlopment and penetration peg emergence. The upstream components of the MPS1 pathway are not well studied and it controls cell wall integrity, penetration formation and invasive growth. The OSM1 pathway is not essential for plant infection but may be required for stress responses.

1.4.3 Control of cell-cycle and autophagic machinery in *M. oryzae*

M. oryzae forms an appressorium after the three cell conidium lands on an inductive surface. The conidium germinates and grows in a polarised fashion, before the tip of the germ tube grows isotropically, signalling initiation of appressorium development. During the maturation process, a melanin layer is deposited under the cell wall, ultimately providing a diffusion barrier, which allows the appressorium to generate huge turgor to gain entry to the host cell. This whole process is tightly linked with cell cycle progression and autophagic cell death in *M. oryzae* (Veneault-Fourrey et al, 2006). Saunders and colleagues used Histone-GFP as a marker to observe cell cycle progression during appressorium development. The nucleus of the apical cell of the conidium migrates into the germ tube at the beginning of appressorium development and undergoes mitotic cell division to generate two daughter nuclei after 3-4 h germination of conidia (Saunders et al, 2010a). After nuclear division, one of the daughter nuclei migrates into the emerging appressorium while the other nucleus returns back to the conidium for degradation (Saunders et al, 2010a). Initiation of appressorium development is regulated by the S-phase check point, which is demonstrable as addition of DNA replication inhibitor, hydroxyurea (HU), at 0-2 h post inoculation (hpi) shows no tip swelling and appressorium formation. However, if HU was applied after 6-8 hpi, no defect was observed in appressorium morphogenesis (Saunders et al, 2010a). Genetic evidence was provided by using a temperature sensitive allele of NimA (never in mitosis) ($nimA^{E37G}$), a serine/threonine kinase regulates entry into mitosis, which arrested in G_2 phase of cell cycle at the restrictive temperature (Veneault-Fourrey et al, 2006). Appressorium development and nuclear division was inhibited when $nimA^{E37G}$ was shifted to the restrictive temperature at 0-3 hpi, however no significant defects were observed when shifted after 6 hpi (Veneault-Fourrey et al, 2006). It was further demonstrated that mitotic exit is required for successful plant infection as conditional

inactivation of *bim* ^{F1763*} (blocked in mitosis) prevented mitotic exit, suggesting that repolarisation of the cytoskeleton and development of penetration peg requires the complete mitotic event (Saunders et al, 2010a). Overall, it was suggested that appressorium development and plant infection is regulated by three main checkpoints (G_1-S-G_2-M) of the cell cycle.

After successful completion of mitosis, cytokinesis is required for septum formation at the neck of the appressorium and this was observed by actomysosin ring formation (Saunders et al, 2010b). Septation is regulated by the Mitotic Exit Network and a temperature-sensitive mutation in Sep1^{G849R} (a serine/threonine kinase, which regulates septum formation) causes complete loss of virulence on susceptible rice plants (Saunders et al, 2010b).

After successful plant infection, the remaining three nuclei in the conidium are degraded through a process which involves autophagic cell death (Veneault-Fourrey et al, 2006). Systematic targeted deletion of autophagy-related genes (ATG) suggests that non-selective macroautophagy is required for successful plant infection (Kershaw & Talbot, 2009b). Autophagic cell death is coupled with mitotic entry and blocking mitotic entry prevents conidium death which suggests that recycling of the contents from the conidium to the appressorium is required for successful plant infection (Kershaw & Talbot, 2009; Veneault-Fourrey et al, 2006).

1.4.4 Turgor generation, melanin biosynthesis and cytosketelon remodelling

The appressorium melanin layer deposited inside the cell wall provides structural support to strengthen the appressorium and prevent leakage of osmolytes by forming an impermeable barrier, which is necessary for the generation of turgor pressure which may be as great as 8 MPa (Howard et al, 1991). Biosynthesis of melanin is critical for plant infection and melanin-deficient mutants (Δ*alb1*, Δ*buf1* and Δ*rsy1*) are unable to

cross the plant cuticle (Chumley & Valent, 1990). In the absence of a melanin layer, osmolytes responsible for turgor generation leak out and the appressorium is unable to generate sufficient turgor to breach the plant surface (Howard et al, 1991). It has been shown that glycerol is the most abundant solute present in the appressorium, which may be as high as 3.2 M during turgor generation. Melanin-deficient mutants accumulate significantly less glycerol compared to the wild type and are unable to produce turgor sufficient to invade host plants (de Jong et al, 1997).

Emergence of the penetration peg from the base of the appressorium is dependent on repolarisation of the cytoskeleton, which is regulated by septin GTPase. Septins are small GTPases, highly conserved from yeast to humans and are able to form hetero-oligomeric structures which regulate various morphogenetic processes including cytokinesis, septum formation, polarized growth and secretion (Caudron & Barral, 2009; Longtine & Bi, 2003). *M. oryzae* encodes septins, Sep3, Sep4, Sep5 and Sep6 which shows close homology to the core *S. cerevisae* septins, Cdc3, Cdc10, Cd11, and Cdc12, respectively (Dagdas et al, 2012). Dagdas and colleagues observed that all the septins form a ring-like structure at the base of the appressorium, which co-localises with the F-actin network. Targeted gene deletion of any one of the four septins, causes the subcellular localisation of the other septins and F-actin network to be completely disrupted. It suggests that all four septins act together to organise the F-actin network at the appressorium pore (illustrated in **Figure 1.3**). Distribution of septins and the F-actin network around the appressorium pore causes impairment of the infection process, because appressoria of these mutants are unable to concentrate the enormous turgor pressure at the point of infection. The septin and actin network around the appressorium pore is regulated by Cdc42, Chm1, Mst12 and Mps1 (Dagdas et al, 2012). It was observed that *M. oryzae* septins form a diffusion barrier around the appressorium pore,

which maintains the organisations of Bin-Amphiphysin-Rvs (BAR)-domain protein, such as Rvs-167 and the N-WASP protein, Las17, which play roles in membrane curvature and protrusion of the penetration peg (**Figure 1.3**) (Dagdas et al, 2012).

The generation of reactive oxygen species (ROS) is also involved in cell wall differentiation in the appressorium and it has been shown that disruption in generation of superoxide prevents appressorium formation (Egan et al, 2007). *M. oryzae* encodes two superoxide-generating NADPH oxidases, Nox1 and Nox2 and targeted deletion of these genes prevent plant infection (Egan et al, 2007). Recently, it was reported that Nox2 and NoxR (p67phox-like regulator) regulate the septin mediated assembly of F-actin network around the appressorium pore (Ryder et al, 2013). Nox1, however, is expected to regulate F-actin polymerisation required for development of penetration peg as Δ*nox1* mutants fail to elaborate a penetration peg into invasive hyphae. Furthermore, it has been shown that the actin binding protein gelsolin also forms a ring at the appressorium pore, the assembly of which is regulated by the Nox2-NoxR complex. Gelsolin localisation is sensitive to the ROS scavenger, ascorbic acid and the Nox inhibitor, diphenylene iodonium, suggesting that ROS production and initiation and maintenance of polarised growth are regulated by NADPH oxidases in *M. oryzae* (Ryder et al, 2013).

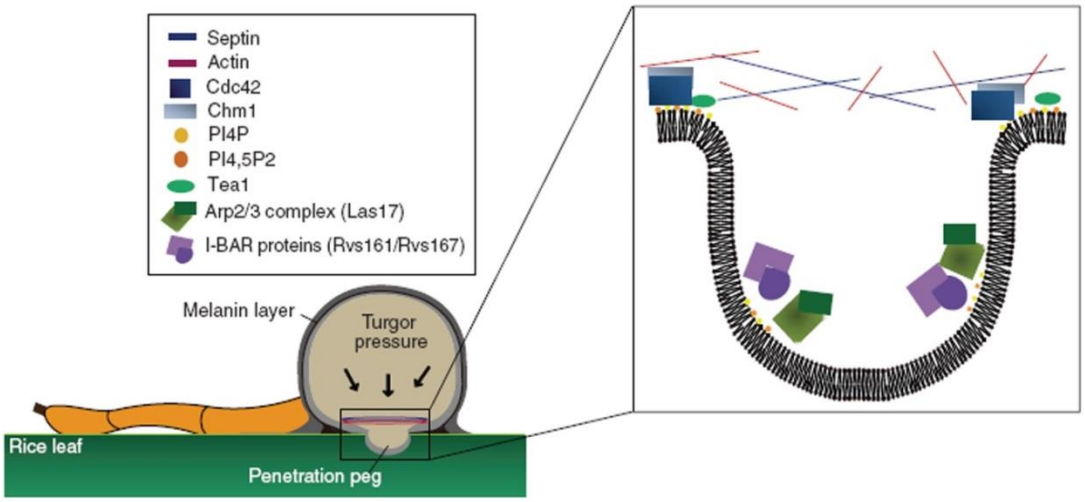

Figure 1.3 Septin mediated plant infection by *M. oryzae* (Taken from Dagdas et al, *Science* 2012, 336: 1590-1595).

Septins regulate formation of a toridal F-actin network and positioning of the ERM protein, Tea1, around the appressorium pore. This organisation is thought to provide the structural basis by which turgor pressure may be applied at the point of penetration. Septins form a diffusion barrier around the appressorium pore which holds protein that induce membrane curvature such as the N-WASP protein, Las17 and the Bin-Amphiphysin-Rvs (BAR) domain protein, Rvs-167. Organisation of septins is regulated by the small GTPase, Cdc42 and p-21 activated kinase, Chm1.

1.5 Polarised growth in fungi

In filamentous fungi, establishment of polarised growth requires continuous synthesis and targeting of materials required for cell wall biogenesis to specific domains in the plasma membrane of the hyphal tip (Riquelme, 2013). Once established, polarised growth is maintained by continued localisation of the secretory machinery to the growing hyphal tip. Establishment and maintenance of cell polarity during bud emergence is well defined in *S. cerevisae* and provides a powerful paradigm to understand hyphal tip growth in filamentous fungi. In filamentous fungi, three key components for vesicle trafficking were identified, The Spitzenkörper, the polarisome and the exocyst complex.

1.5.1 Role of the Spitzenkörper in polarised growth

During polarised growth secretory vesicles are delivered to the apex of the growing hyphal tip and accumulate at the Spitzenkörper (SPK), a sub-apical membrane rich region, prior to fusing with the plasma membrane (Read, 2011; Riquelme, 2013; Steinberg, 2007; Sudbery, 2011). The SPK acts as a vesicle supply centre and is only present in filamentous fungi, such as *Aspergillus nidulans*, *Neurospora crassa* and *M. oryzae*, and no such structure has been described in yeasts, such as *S. cerevisiae* and *S. pombe*. It suggests that filamentous hyphae require continuous rapid delivery of vesicles in order to extend the hyphal tip (Steinberg, 2007). In contrast, yeast or yeast like cells do not form true hyphae. The SPK is required for polarised growth where different cellular components such as ribosomes, microfilaments, granules and microtubules accumulate (Riquelme & Sanchez-Leon, 2014). The biochemical nature of the SPK is still not known, but using fluorescence microscopy it has revealed that in *N. crassa*, chitin synthases (CHS) carrying micro-vesicles called chitosomes form the core of the

SPK while glucan synthase (GS) related protein, GS-1, and a Rho1 specific guanine-nucleotide exchange factor (GEF), RGF1, were found in macro-vesicles which surrounds the core of CHS (Richthammer et al, 2012; Riquelme & Sanchez-Leon, 2014; Verdín et al, 2009). This suggests that the SPK is occupied by vesicles carrying enzymes for cell wall synthesis. However, more studies are required to establish the exact composition of the SPK. The SPK is a highly dynamic structure and is only found actively growing in highly polarised hyphae indicative of its involvement in polarised growth. The shape, size and position of the SPK varies among the fungal taxa and in *M. oryzae* the SPK was observed in growing vegetative hyphae (Giraldo et al, 2013) although it is still not known whether the SPK is present in infection hyphae or not. Very little is known about the role and regulation of the SPK in infection-related development, but it is crucial to determine its function in relation to effector secretion during invasive growth in *M. oryzae*, in order to fully understand the mechanism of *M. oryzae* infection of rice.

1.5.2 The role of the exocyst and polarisome complex in polarised secretion

The exocyst and the polarisome complex, together with the SPK, are essential for polarised growth. The exocyst complex is an evolutionarily conserved octameric complex, which consists of Sec3, Sec5, Sec6, Sec8, Sec10, Sec15, Exo70 and Exo84, and plays a crucial role in vesicle docking to the plasma membrane (Hsu et al, 1996; TerBush et al, 1996). Most fungi have a single homologue of each of the exocyst encoding genes. Studies in yeast have suggested a mechanism explaining how vesicles are delivered to the plasma membrane (He & Guo, 2009; Heider & Munson, 2012). Secretory vesicles are delivered to the site of secretion via actin cables. The exocyst components, Sec3 and a fraction of Exo70, are localised at the bud tip in an actin-independent manner (Boyd et al, 2004; Finger et al, 1998). The remaining exocyst

components are, however, delivered via secretory vesicles in an actin-dependent process (Zajac et al, 2005). This suggests Sec3 and Exo70 closely associate with the plasma membrane and target the vesicle after interacting with other exocyst components. In the filamentous fungus, *N. crassa*, Exo70 and Exo84 are closely associated with the outer layer of the SPK, while the remaining exocyst components localised with the plasma membrane of the hyphal tip, suggesting some cell specific function of the exocyst complex (Riquelme et al, 2014). The role and regulation of the exocyst complex is extensively discussed in detail in **Chapter 3**.

In *S. cerevisiae*, the polarisome complex, which consists of Pea2, Spa2, Aip3/Bud6 and the formin Bni1, is involved in nucleation of actin microfilaments at the growing hyphal tip (Evangelista et al, 2003; Sagot et al, 2002; Sheu et al, 1998). Spa2 plays a critical role in polarisome scaffolding through physical interaction with other components. MAPK proteins, Mkk1 and Mpk1 of the cell wall integrity pathway, interact with Spa2 and localise to sites of polarised growth in a Spa2-dependent manner which suggests that Spa2 scaffolds the cell wall integrity pathway, thereby regulating polarised growth (Sheu et al, 1998; van Drogen & Peter, 2002). Aip3/Bud6 is an actin and formin (Bni1)-interacting protein. Together, they are involved in actin cable assembly and organisation (Moseley et al, 2004). The filamentous fungus *N. crassa* encodes Spa2, Bud6 and Bni1 components of the polarisome complex. Spa2 co-localises with the SPK, while Bud6 and Bin1 show partial co-localisation (Lichius et al, 2012). SepA, a homologue of the formin Bni1 in *Aspergillus nidulans*, exhibits sub-apical localisation and co-localises with the SPK (Sharpless & Harris, 2002). However, *SPA2* in *Ustilago maydis*, *A. nidulans* and *M. oryzae*, partially overlaps with the SPK (Carbo & Perez-Martin, 2008; Li et al, 2014; Virag & Harris, 2006). Null mutants of *SPA2* in *M. oryzae* and *U. maydis* showed defects in hyphal growth but not in pathogenicity (Carbo & Perez-Martin, 2008;

Li et al, 2014). This suggests that Spa2 is involved in polarity establishment and has no role in infection-related development. Further characterisation of polarisome components is required to understand, how the polarisome regulates vesicle fusion with the plasma membrane and maintains polarity in filamentous fungi.

1.5.3 Polarity determinants in *M. oryzae*

Small GTPases play a crucial role in the establishment and maintenance of cell polarity (Wu et al, 2008). The Rho family of small GTPases directly interact with exocyst components and regulate polarised secretion. It has been shown in *S. cerevisae* that Rho1 and Cdc42 directly interact with Sec3 in a GTP-dependent manner and are required for Sec3 localisation at the bud tip (Guo et al, 2001; Zhang et al, 2001). The exocyst component, Exo70, interacts with Rho3 and Cdc42, suggesting that vesicle trafficking is controlled by Rho GTPases (Robinson et al, 1999; Wu & Brennwald, 2010). In *M. oryzae*, targeted gene deletion of *RHO3* is dispensable for hyphal growth but shows severe defects in conidiogenesis, appressorium development and plant infection (Zheng et al, 2007). Another Rho GTPase, MoCdc42, is required for plant infection and null mutants of *MoCdc42* can still form appressoria but are unable to generate enough turgor pressure to breach the leaf cuticle (Zheng et al, 2009). Recently, it has been suggested that MoCdc42 is required for septin-mediated repolarisation of F-actin network in appressorium (Dagdas et al, 2012). In addition a novel Rho GTPase, Rac1, is not present in *S. cerevisae* and *S. pombe*, but is found in higher eukaryotes, and plays a crucial role in polarity establishment (Nobes & Hall, 1995). In *M. oryzae*, Rac1 directly interacts with Chm1, PAK kinase, and NADPH oxidases (Nox), Nox1 and Nox2, which suggests that Rac1 may play an important role in Nox-mediated polarity establishment (Chen et al, 2008). Null mutants of *RAC1* are not competent to form appressoria and remain non-pathogenic (Chen et al, 2008). Although it is known that

polarity establishment and repolarisation are required for plant infection, the precise mechanism describing the regulation of polarised growth during infection-related development is yet to be elucidated.

During biotrophic invasion, *M. oryzae* forms bulbous invasive hyphae (IH) analogous to pseudo-hyphal cells of *C. albicans* (Khang et al, 2010). Kang et al, (2010) have shown that cytoplasmic effectors are accumulated at a sub-apical region of the bulbous IH (Khang et al, 2010). As the IH are characteristic of invasive growth, it is therefore, critical to understand polarised growth of bulbous IH and how polarised secretion of effectors occurs during host invasion.

1.6 Post-penetration events and host cell colonisation by *M. oryzae*

1.6.1 Cuticle rupture and entry to the host cell

M. oryzae breaches the plant cuticle as a narrow penetration hyphae emerging from the base of the appressorium where it is the focus of physical pressure at the point of infection (Dagdas et al, 2012; Howard & Valent, 1996; Talbot, 2003). After gaining entry to the host cell, penetration hyphae extend to form primary IH which further differentiate in bulbous secondary IH (Kankanala et al, 2007), that exhibit pseudohyphal-like growth. Prior to invasion of neighbouring plant cells, IH switch to filamentous growth. These IH, then swell from the tip, sensing the plasma membrane to establish a crossing point and upon passing through pit fields show severe constriction as they pass from rice cell-to-rice cell (Kankanala et al, 2007).

During biotrophic invasion, *M. oryzae* IH are enveloped by invaginated plant plasma membrane (PM), which is known as the Extra Invasive Hyphal Membrane (EIHM) (Kankanala et al, 2007). It has been shown that the lipophilic steryl dye FM4-64 cannot

be endocytosed by fungal IH when applied apoplastically but does stain the plant PM (Kankanala et al, 2007) consistent with the fungus being surrounded by plant membrane. Further to this, plant plasma membrane was visualised using rice transgenic lines expressing LTi6B:GFP, suggest that rice PM tightly covers the IH (Giraldo et al, 2013). Plant infection by oomycete phytopathogens, such as *Phytophthora infestans* and *Hyaloperonospora arabidopsidis* are also characterised by the presence of an Extra-Haustorial Membrane (EHM) which surrounds infection structures, or haustoria (O'Connell & Panstruga, 2006). This apparent similarity suggests that biotrophic pathogens may be surrounded by host membranes via similar mechanisms but more detailed study is required to understand the nature of the EIHM, such as the use of electron microscopy and high resolution imaging of infection hyphae.

1.6.2 Localisation of effector proteins during host invasion in *M. oryzae*

During host invasion, pathogens secrete virulence proteins, known as effectors, to suppress and bypass host immune responses, and which may also change host physiology and metabolism. Mosquera et al (2009) identified several putative biotrophic-associated secreted (BAS) proteins that showed distinct patterns of secretion in susceptible and resistant interactions (Mosquera et al, 2009). Some of these effectors, BAS1-4, were expressed more than 50-fold during biotrophic growth as compared to *in vitro* growth (Mosquera et al, 2009). Based on their localisation pattern, *M. oryzae* effector proteins can be broadly categorized in two groups; cytoplasmic effectors which are host-translocated and apoplastic effectors, which remain bound by the EIHM (Giraldo & Valent, 2013; Khang et al, 2010; Mosquera et al, 2009). Live cell imaging of effectors tagged with fluorescence proteins is very helpful in understanding host-pathogen interactions. It has been shown that cytoplasmic effectors, such as AvrPita, Pwl2, AvrPia, AvrPizt, accumulate at a host-derived membranous structure known as

the biotrophic interfacial complex (BIC) (Khang et al, 2010; Mosquera et al, 2009; Park et al, 2012; Yoshida et al, 2009). On the other hand apoplastic effectors such as Bas4, Slp1 and Bas113, remain inside the sealed compartment between the EIHM and fungal PM (Giraldo et al, 2013; Khang et al, 2010; Mentlak et al, 2012; Mosquera et al, 2009).

M. oryzae encodes a large number of secreted proteins which contain an N-terminal signal peptide (1,546), which is predicted to represent 20% of the total number of proteins (12,841) in the *M. oryzae* genome (Dean et al, 2005; Soanes et al, 2008). One of the earliest studied *M. oryzae* effectors, Avr-Pita, shows a virulence activity and induces a hypersensitive response on the resistant rice cultivar carrying the corresponding resistance (R) gene, Pita. Avr-Pita directly interacts with a Leucine Rich Domain (LRD) in Pita and induces a Pita-dependent resistance response (Jia et al, 2000). Avr-Pita was predicted to encode a putative metalloprotease and a single amino acid change in the LRD region of Pita or in the Avr-Pita encoding protein, results in disruption of physical interactions between both proteins (Jia et al, 2000). It has been shown that Avr-Pita is secreted via the BIC, but the precise molecular function has yet to be identified (Khang et al, 2010; Mosquera et al, 2009). Using association genetic mapping Yoshida et al (2009) identified Avr-Pia, Avr-Pii and Avr-Pik/Km/Kp avirulence proteins, which have been shown to be recognised by rice plants carrying cognate resistance genes (Yoshida et al, 2009). A novel avirulence gene, AvrPiz-t was first identified by map-based cloning and shown to be secreted from the BIC (Li et al, 2009; Park et al, 2012). AvrPiz-t has been shown to suppress flg11- and chitin-induced hypersensitive response, which suggests it has a possible role in suppression of pathogen-associated molecular pattern (PAMP)-triggered immunity in rice (Park et al, 2012). Further to this, AvrPiz-t interacts with a host RING finger ubiquitin E3 ligase, known as APIP6 (AvrPiz-t-interacting protein 6), which suppresses E3 ligase activity of

host. However, APIP6 also ubiquitinates AvrPiz-t and promotes its degradation (Park et al, 2012). More recently, Mentlak et al, (2012) characterised the chitin binding protein Slp1, secreted LysM protein 1, which is secreted into the apoplast between the fungal cell wall and EIHM (Mentlak et al, 2012). Slp1 binds with chitin oligosaccharides, and prevents chitin recognition by the chitin elicitor binding protein (CEBiP), thereby supressing chitin-induced plant defence responses. Targeted deletion of *SLP1* shows reduced virulence on a susceptible rice cultivar. However, no pathogenicity defect is observed on *CEBiP*-silenced rice lines (Mentlak et al, 2012). This evidence suggests that Slp1 acts as an apoplastic effector and prevents a PAMP-triggered defence response of rice.

Many *M. oryzae* effectors have been identified and shown to be secreted during biotrophic invasion, including Bas1, Bas2 and Pwl2 which accumulates at the BIC, Bas3 which localised at cell-wall crossing points, and Bas4 that accumulates between EIHM and the fungal cell wall. The localisation data is intriguing, because it provides information regarding the stage of infection at which each of these effectors is deployed but still their precise functions have yet to be described (Mosquera et al, 2009).

1.6.3 Translocation of effector proteins during host colonisation

M. oryzae enter into the host cell by extending penetration hyphae and, in response to fungal infection, the host plant cell develops a membranous structure, BIC, at the point of infection. The BIC closely associates with the growing IH and effectors are secreted from the tip of growing primary IH (Khang et al, 2010). This suggests that components involved in polarised secretion are involved in the early infection. As primary IH differentiate into bulbous secondary IH, the BIC remains attached to the sub-apical region and effectors accumulate at the BIC (Khang et al, 2010). Fluorescence Recovery

After Photobleaching (FRAP) experiments suggest that effectors actively accumulate at the BIC (Khang et al, 2010). Translational fusion of cytoplasmic effectors with fluorescent proteins has been extensively used to understand *M. oryzae* infection biology (Giraldo et al, 2013; Kankanala et al, 2007; Khang et al, 2010; Mosquera et al, 2009). One such translational fusion, Pwl2:mRFP, was shown to actively accumulate at the BIC (Khang et al, 2010; Mosquera et al, 2009). Host translocation of Pwl2 was confirmed by adding a nuclear-localisation signal (NLS) to the C-terminus of Pwl2:mRFP and observing the accumulation of mRFP signal in the host nucleus. Interestingly, Pwl2:mRFP was also detected in neighbouring non-invaded host cells (Khang et al, 2010), suggesting that effectors can move from cell-to-cell, prior to hyphal invasion. The symplastic nature of plant tissues makes it likely that effectors use plasmodesmata for translocation. However, it is still too early to know how many *M. oryzae* effectors pass through the fungal cell wall and across the host membrane to enter the host cytoplasm and how many remain inside the EIHM.

Research in oomycete pathogens has elucidated the importance of host-targeting domains which contain conserved motifs, such as the RXLR, LFLAK and CHXC amino acid sequences (Jiang et al, 2008). These motifs can be used to define the effector repertoire in different species and have been shown to be required for effector translocation into host cells (Birch et al, 2009; Whisson et al, 2007; Win et al, 2007). Kale and colleagues suggested that RXLR motifs of the effector proteins bind to extra-cellular phosphatidylinositol-3-phosphate (PI3P) and mediate effector entry to host cells (Kale et al, 2010). Mutation in an RXLR motif of the *P. sojae* effector Avr1b for example abolished entry to the host cell (Dou et al, 2008). However, more recent studies have challenged this hypothesis of RLXR-PI3P interaction-mediated host entry (Yaeno et al, 2011; Yaeno & Shirasu, 2013). Yaeno and colleagues have suggested that the

Phytophthora capsici effector AVR3a4, a close homologue of *P. infestans* AVR3a, contains positively charged amino acids in the conserved region, and not an RXLR motif, and that these positively charge residues are required for binding with PIPs (Yaeno et al, 2011). A criticism of many of these studies, however, is that the experiments were conducted using a strategy which is independent of the pathogen and the assays used in these studies are therefore under debate. Recently, Wawra and colleagues have observed that fluorescence proteins (FP) alone can be taken up by plant cells at a similar rate to that seen with effector-fluorescent protein fusion (Wawra et al, 2013). Further to this, Tyler and colleagues (2013) have proposed that a quantitative difference was observed when the same assay was used for single FPs versus effector-FP translational fusion and clarify that host cell uptake is more efficient for effector-FP than FPs alone (Tyler et al, 2013). Some other conflicting reports suggest that the RXLR domain of the *P. infestans* effector Nuk10 binds with PI3P inside the pathogen (Bhattacharjee et al, 2012). No conserved motif such as RXLR has been identified in the secreted proteome of *M. oryzae* (Soanes et al, 2008). In summary, more research and robust assays are required to understand how fungal and oomycete effector enter the host cells.

Very little is known regarding how *M. oryzae* effectors are secreted during host colonisation. It has been suggested that protein modification is required prior to secretion and targeted gene deletion of the ER chaperon *LHS1* exhibits a defect in the secretion of extracellular enzymes, including cytoplasmic effector proteins (Yi et al, 2009). Interestingly, null mutants of *LHS1* in a strain which carries AvrPita, failed to induce HR response on a rice cultivar carrying the resistance gene, Pita (Yi et al, 2009). Another gene encoding a ER localised protein, *ALG3*, encodes a α-1, 3-mannosyltransferase, and is required for N-glycosylation of apoplastic effectors such as

Slp1 and Bas4 (Chen et al, 2014). Null mutants of *AGL3* are not able to form secondary bulbous IH and show significant reduction in plant infection. It has been shown that Slp1 is glycosylated at three different sites in an Agl3-dependent manner (Chen et al, 2014), showing that post-transcriptional modification can also required for effector functions, particularly in the case of extracellular apoplastic effectors.

M. oryzae, encodes a type IV aminophospholipid translocase, *MgAPT2*, which is required for aminophosholipid distribution in cellular membranes (Gilbert et al, 2006). Targeted gene deletion mutants of *MgAPT2* showed defect in secretion of extracellular enzymes and have lost the ability to cause infection. Interestingly, *APT2* is required for the induction of the hypersensitive response during incompatible interactions. Indeed, Δ*apt2* mutants fail to induce AvrPita/Pita interactions in the rice cultivar IR-68, carrying the *Pita* resistance gene (Gilbert et al, 2006). This suggests that Apt2 might play an essential role in effector secretion during host infection.

In conclusion, we do not know the basic mechanism of effector secretion during host colonisation and the mechanism by which these effectors translocate to the host cell has also yet to be determined. Why only a few effectors enter the host plasma membrane and others do not, suggests that there might be more than one distinct mechanisms for effector secretion and this study set out to investigate this question.

1.7 Introduction to the current study

In the current study, I set out to understand the mechanism of polarised secretion of effector proteins during rice blast infections. I have characterised the role of the exocyst complex in appressorium-mediated infection and started to define its role in effector secretion. Furthermore, I have defined the regulatory mechanism by which the exocyst complex is recruited to the appressorium pore.

In **Chapter3**, genes encoding secretory components are identified in the *M. oryzae* genome and each of the components expressed as translational fusions with fluorescent proteins, which are then used to determine subcellular location using fluorescence microscopy to define their role in polarised growth. I show that the exocyst and other polarity determinants are localised to the growing tips of vegetative hyphae. The exocyst components are localised as a crescent structure, distinct from the SPK. I also show that exocyst components physically interact during vesicle trafficking using co-immunoprecipitation. During appressorium formation, exocyst components localise as a ring to the periphery of early stage appressoria which later contracts to locate specifically around the appressorium pore. This transition of the exocyst ring is an actin-dependent process.

In **Chapter4**, I report functional characterisation of the exocyst components. Targeted gene deletion mutants for *SEC5* and *EXO70* are reported and I show that exocyst components are required for successful plant infection. I demonstrate that secretory mutants exhibit protein secretion defects and are not able to secrete spore tip mucilage efficiently. A temperature sensitive mutation in SEC6 encoding region is also generated and this suggests that *SEC6* is critical for exocyst assembly at the appressorium pore. I show that the transition of the exocyst ring to the appressorium pore is a septin-dependent process.

In **Chapter 5**, I investigate infection-related development and conduct a series of experiments to understand effector secretion during host colonisation. This work was accomplished in collaboration with Prof. Barbara Valent and Prof. Ryohei Terauchi and part of this study has already been published in Giraldo et al, (2013) (**Appendix 1**). We showed that some polarity components (Mlc1, Snc1 and Sso1) that localised to hyphal tip are also observed in BIC-associated cells during invasive growth. We provide

evidence that fungal effectors are secreted via two distinct pathways, apoplastic effectors are secreted via an ER-Golgi pathway which is BrefeldinA-sensitive. Cytoplasmic effectors are secreted in a Golgi-independent pathway which involves the exocyst components, Sec5 and Exo70, and the SNARE protein, Sso1. My contribution to this study was to generate targeted gene deletion mutants for exocyst components and to generate the translational GFP fusions. Furthermore, the results I have shown in this chapter also suggest that effectors might be secreted from the appressorium pore in an exocyst-dependent manner. I show the localisation of the exocyst and other polarity determinants at the invasive hyphal tip which confirms the expectation that these proteins are involved in tip secretion.

When considered together, this study provides new insight into the mechanism of polarised secretion which is crucial to the infection strategy of *M. oryzae,* one of the main fungal pathogens threatening global food security.

Chapter 2. Materials and Methods

2.1 Growth and maintenance of fungal stocks

All isolates of *Magnaporthe oryzae* used in this study are stored in the laboratory of N. J. Talbot (University of Exeter). For long-term storage, *M. oryzae* was grown through filter paper discs (3 mm, Whatman International), which were desiccated for at least 48 h and stored at -20°C. The fungus was routinely incubated in a controlled temperature room at 24°C with a 12-hour light and dark cycle. *M. oryzae* was routinely cultured in complete medium (CM) (Talbot et al, 1993) consisting of 10 g L^{-1} glucose, 2 g L^{-1} peptone, 1 g L^{-1} yeast extract (BD Biosciences), 1 g L^{-1} casamino acids, 0.1% (v/v) trace elements (zinc sulphate heptahydrate 22 mg L^{-1}, boric acid 11 mg L^{-1}, manganese(II) chloride tetrahydrate 5 mg L^{-1}, iron sulphate heptahydrate 5 mg L^{-1}, cobalt chloride hexahydrate 1.7 mg L^{-1}, copper sulphate pentahydrate 1.6 mg L^{-1}, sodium molybdate dehydrate 1.5 mg L^{-1}, ethylenediaminetetraacetic acid 50 mg L^{-1}), 0.1% (v/v) vitamin supplement (0.1 g L^{-1} biotin, 0.1 g L^{-1} pyridoxine, 0.1 g L^{-1} thiamine, 0.1 g L^{-1} riboflavin, 0.1 g L^{-1} *p*-aminobenzoic acid, 0.1 g L^{-1} nicotinic acid), nitrate salts (sodium nitrate 6 g L^{-1}, potassium chloride 0.5 g L^{-1}, magnesium sulfate heptahydrate 0.5 g L^{-1}, potassium dihydrogen phosphate 1.5 g L^{-1}), pH adjusted to 6.5. For solid medium, 15 g L^{-1} agar was added to the medium.

20 X nitrate salts, 1000 X trace elements and vitamin solutions were prepared and stored at 4°C. Vitamin solution was kept in a dark bottle. Chemicals for 1000 X trace elements were mixed, boiled and cooled to 60°C before pH to 6.5 with 10 M NaOH. All chemicals were obtained from Sigma (Poole, Dorset), unless otherwise stated.

2.2 Nucleic Acid Analysis

2.2.1 Fungal genomic DNA extraction

Genomic DNA was extracted using a modified CTAB method. CTAB buffer contains 33 mM CTAB (Hexadecyltrimethylammonium bromide), 0.1 M Tris (Tris (hydroxymethyl) aminomethane), 7.8 mM EDTA and 0.7 M NaCl. Fungal strains were first grown on CM plates overlaid with a cellophane disc (Lakeland) and incubated for 10-12 days at 24°C until a mat of fungal mycelium had grown over the surface of the cellophane disc. The cellophane disc was then removed and placed into a mortar and ground to a fine powder with a pestle using liquid nitrogen. The powder was then transferred to sterile 1.5 mL microcentrifuge tubes. A 600 µL aliquot of preheated CTAB extraction buffer was added to microcentrifuge tubes and mixed by vortexing. Tubes were then incubated at 65°C for 30 min with occasionally shaking. An equal volume of chloroform:iso-amyl alcohol (CIA) (24:1) was added and the tubes shaken vigorously for 30 min at room temperature. Following centrifugation of the samples at 13,000 x *g* for 10 min using a microfuge (Beckman J2-MC), the supernatant was transferred to a fresh sterile 1.5 mL microcentrifuge tube and the CIA extraction step was repeated. The upper aqueous phase was transferred to a fresh microcentrifuge tube to which 1 mL of iso-propanol was added to facilitate nucleic acid precipitation and samples were incubated at -20°C for 20 min, followed by centrifugation at 13,000 x *g* for 10 min. The supernatant was discarded and pellet containing nucleic acid was re-suspended in 500 µL sterile deionized water and precipitated by adding 0.1 volumes of 3 M sodium acetate (pH 5.2) and 2 volumes of ice cold 100% ethanol and incubated at -20°C for 30 min. Overnight precipitation gave a higher yield. Purified nucleic acids were recovered by centrifugation at 13,000 x *g* for 20 min at 4°C and then washed with 70% ice cold ethanol. The supernatant was discarded and the nucleic acid pellet dried using a centrifugal evaporator

(Eppendorf) for 20-30 min. The pellet was then re-suspended in 50 to 100 μL of TE with 4 μL of DNase-free pancreatic RNase A (20 μg/mL; Promega). Genomic DNA samples were routinely stored at -20°C.

2.2.2 Digestion of genomic or plasmid DNA with restriction enzymes

Restriction endonucleases were routinely obtained from Promega UK Ltd. (Southampton, UK) or New England Biolabs (Hitchin, UK). DNA digestion was carried out using buffer solutions provided by the manufacturer in a total volume of 40 μL with 2-5 μg DNA and 5-10 units of enzyme. Southern blot analysis, 15-20 μg genomic DNA was used to digest with 50 units of enzyme in a total volume of 50 μL and incubated overnight at the optimum temperature for the restriction endonuclease used.

2.2.3 DNA gel electrophoresis

Normally, 0.8-1.4% (w/v) agarose gels were used for gel electrophoresis using a 1 x Tris-borate EDTA buffer (TE) (0.09 M Tris-borate, 0.002 M EDTA). For genomic DNA digestion, 0.8% (w/v) agarose gel was used. Visualisation of DNA was made possible by addition of ethidium bromide (final concentration 0.5 μg mL^{-1}). In order to determine the size of digested DNA products or PCR products, a one kb plus (Invitrogen) DNA size marker were used during gel electrophoresis. DNA was visualised using a gel documentation system (Image Master® VDS with a Fujifilm Thermal Imaging system FTI-500, Phamacia Biotech).

2.2.4 The polymerase chain reaction (PCR)

DNA fragments were amplified by Polymerase Chain Reaction (PCR) which was carried out using an Applied Biosystems GeneAmp® PCR System 2400 cycler using

either GoTaq® Flexi DNA Polymerase (Promega), GoTaq® Green Master Mix (Promega), Phusion® high fidelity DNA Polymerase (New England Biolabs, Thermo Scientific®) or Herculase® enhanced DNA Polymerase (Stratagene) according to manufacturer's instructions. For routine PCR, the GoTaq® Flexi Polymerase reaction, 50-100 ng of template DNA was used for amplification, along with the GoTaq Flexi DNA Polymerase buffer (5 x), 10 nM $MgCl_2$, 100 nM each dNTP, 0.25 pM of each primer, 2 units of GoTaq® Flexi DNA Polymerase, made up to a final volume of 50 µL using sterile water (Sigma).

The PCR was routinely carried out according to the following conditions: as initial denaturation step at 94°C for 5 min followed by 35 cycles of PCR cycling parameters of: denaturation at 94°C for 30 sec, annealing at 56-64°C for 30 sec and extension 72°C for 1 min/kb target length, followed by a final extension at 72°C for 10 min and hold at 4°C.

Phusion® high fidelity DNA Polymerase (New England Biolabs, Thermo Scientific®) was used for gene cloning experiments. In 50 µL reaction final reaction, 10 µL 5 x Phusion HF buffer, 200 µM dNTPs, 0.5 µM of each primer, 100-200 ng template DNA and 1 units of Phusion DNA polymerase was added in a microcentrifuge tube. PCR condition for Phusion® high fidelity DNA Polymerase (New England Biolabs, Thermo Scientific®) was: initial denaturation step at 98°C for 30 sec followed by 35 cycles of PCR cycling parameters of: denaturation at 98°C for 10 sec, annealing 58°C for 30 sec and extension 72°C for 30 sec/kb target length, followed by a final extension at 72°C for 10 min and hold at 4°C.

2.2.5 Gel purification of PCR Amplified DNA fragments

PCR amplified products were separated by size using gel electrophoresis and purified from agarose gels using a commercial kit according to manufacturer instructions (Wizard® SV Gel and PCR Clean-Up System, Cat. # A9282 Promega). Fragments were excised from the gel using a razor blade and placed in a pre-weighed microfuge tube. The mass of agarose removed from the gel was determined and Membrane Binding Solution (4.5 M guanidine isothiocyanate and 0.5 M potassium acetate, pH 5.0) added to the gel slice in a microfuge tube, at a ratio of 10 µL per 10 mg of agarose gel slice. Samples were incubated at 65°C and mixed by vortexing every 2-3 min until the gel slice had dissolved. A 750 µL of aliquot dissolved gel mixture was transferred to a Wizard® SV Minicolumn placed in 2 mL collection tube and incubated at room temperature for 1 minute. After centrifugation for 1 minute in an IEC, Micromax (16,000 x *g*) the DNA is bound to the Wizard® SV Minicolumn. The flow-through was discarded and the column placed in the collection tube. To wash the column, 0.70 mL of Membrane Wash Solution (10 mM potassium acetate (pH 5.0), 80% ethanol, and 16.7 µM (pH 8.0) ethylenediaminetetraacetic acid) was added and centrifugation carried out for 1 minute (16,000 x *g*). The flow-through was discarded and the column processed by centrifugation for 5 minutes (16,000 x *g*) with a further wash of 0.50 mL Membrane Wash Solution. The flow-through was discarded and the column placed in centrifuge for another minute and centrifugation repeated for 1 min. The Wizard® SV Minicolumn was placed in a clean microfuge tube, 30 µl of Nuclease-Free Water added, and after 2 minute incubation at room temperature, there was a further centrifugation step for 1 minute, at 16,000 x *g*. The DNA solution stored at -20°C.

2.3 DNA cloning

2.3.1 DNA ligation

PCR amplified products were routinely cloned using the StrataClone™ PCR Cloning Kit (Agilent Technologies) for blunt end cloning or pGEM®-T Easy Vector System (Promega) which allows T:A cloning. Standard ligation reactions for pGEM®-T Easy Vector System were carried out in total volume of 10 µL using 10 x reaction buffer (300 mM Tris-HCl (pH 7.8 at 25°C), 100 mM magnesium chloride, 100 mM dithiothreitol, and 10 mM adenosine triphosphate), 3 units of T_4 DNA ligase and vector and insert DNA in a 1:3 molar ratio. Ligation reactions were incubated for 3 h at room temperature or overnight at 4°C.

Ligation reactions for StrataClone™ PCR Cloning Kit (Agilent Technologies) were carried out by adding 3 µL StrataClone cloning buffer, PCR product (20–50 ng, typically a 1:10 dilution of a PCR reaction) and 1 µL StrataClone vector mix and incubating at room temperature for 5 min, then placing the reaction on ice.

2.3.2 Bacterial transformation

Bacterial transformations were carried out using *Escherichia coli* strain XL1 Blue (Stratagene). XL1 – Blue has genotype *sup*E44 *hsd*R17 *rec*A1 *end*A1 *gyr*A46 *thi rel*A1 *lac*$^-$ [F′ *pro* AB$^+$ *lac*I^q *lac*ZΔM15 *Tn*10 (*tet*^{r})] and competent *E. coli* JM109 cells (Promega, *rec*A1 *sup*E44 *end*A1 *hsd*R17 (r_k^- m_k^+) *gyr*A96 *rel*A1 *thi* Δ(*lac-pro*AB) [F′ *tra*D36 *pro*AB$^+$ *lac*I^q *lac*ZΔM15]). JM109 is a recombination-deficient strain that will support growth of vectors carrying amber mutations and will modify but not restrict transfected DNA. A 100 µL aliquot of competent cells was transferred to pre-chilled 15 mL tubes (Falcon 2059, BD Biosciences). The tubes were then incubated on ice for 10 min to thaw the competent cells completely. After incubation, 5 µL of ligation reaction was added and the mixture incubated on ice for a further 30 min. The tubes were then placed for heat-shock at 42°C for 45 sec and subsequently transferred to ice for 2 min.

A 800 µl aliquot of SOC (tryptone 20 g L^{-1}, yeast extract 5 g L^{-1}, sodium chloride 0.5 g L^{-1}, glucose 20 mM, magnesium sulfate 10 mM and magnesium chloride 10 mM) was added to each tube and the recovering cells incubated at 37°C for 1 hour with gentle shaking at 200 x *g*. Aliquots were plated on LB agar (10 g L^{-1} tryptone, 5 g L^{-1} yeast extract, 10 g L^{-1} NaCl and 15 g L^{-1} agar [pH to 7.5]) with the appropriate antibiotic. Where α-complementation selection was available (Sambrook *et al.,* 2000), the agar contained isopropyl-thiogalactoside (IPTG, 0.8 mg/mL per plate) (Calbiochem (VWR International Ltd.)) and 5-bromo-4-chloro-3-indolyl-β-D-galactopyranoside (X-gal, 0.8 mg/mL per plate) (Calbiochem (VWR International Ltd.)) which allowed blue/white selection. Plates were inverted and incubated at 37^{o}C overnight.

Bacterial transformation of StrataClone™ ligation reactions was carried out in StrataClone SoloPack competent cells (Tetr Δ(mcrA)183 Δ(mcrCB-hsdSMR-mrr)173 endA1 supE44 thi-1 recA1 gyrA96 relA1 lac Hte [F′ proAB lacIqZΔM15 Tn10(Tetr) Amy Camr]). The competent cells were thawed on ice and 2 µL of ligation reaction added to competent cells and incubated on ice for 20 min. After incubation cells were heat-shocked at 42°C for 45 sec and incubated on for 2 min. 250 µL pre-warmed SOC (tryptone 20 g L^{-1}, yeast extract 5 g L^{-1}, sodium chloride 0.5 g L^{-1}, glucose 20 mM, magnesium sulfate 10 mM and magnesium chloride 10 mM) was added to the transformation mixture and competent cells were allowed to recover for 1 hour at 37°C with gentle shaking at 200 x *g*. Transformation mixtures were spread on LB-ampicillin contained 5-bromo-4-chloro-3-indolyl-β-D-galactopyranoside (X-gal, 0.8 mg/mL per plate). Plates were incubated at 37°C overnight.

2.3.3 Bacterial plasmid DNA preparations

2.3.3.1 Bacterial DNA mini preparations (Alkaline lysis preparations)

Single colonies were picked and used to inoculate 5 mL LB broth (10 g L^{-1} tryptone, 5 g L^{-1} yeast extract, 10 g L^{-1} NaCl, [pH to 7.5]) containing the appropriate antibiotic in a universal bottle. Bacterial cultures were grown overnight at 37°C, with vigorous shaking (200 x *g*) in an Innova 4000 rotary incubator (New Brunswick Scientific). For the small-scale bacterial plasmid DNA preparations, modified method was used from Sambrook *et al.* (2000). For long-term storage of bacterial cells, a glycerol stock was prepared by adding 800 µL aliquot of bacterial solution in 1.5 mL microfuge tubes containing 200 µL sterile 100% glycerol. The suspension was vortexed rapidly (Whirlimixer, Fisher Scientific), snap frozen in liquid nitrogen, and stored at -80°C. The remainder of the culture was transferred to fresh 1.5 mL microfuge tubes and pelleted by centrifugation at 13,000 x *g* (Sigma) for 2 min. The supernatant was removed and the bacterial pellet re-suspended in 200 µL of ice-cold cell re-suspension solution (Solution I) (50 mM glucose, 25 mM Tris-HCl [pH 8.0], 10 mM EDTA [pH 8.0]) by vigorous vortexing using a Whirlimixer (Fisher Scientific). A 400 µL aliquot of freshly prepared lysis solution (Solution II) (0.2 M NaOH (freshly diluted from a 10 M stock), 1% SDS) was added to the cell suspension. The contents of the tube were mixed by inversion, ensuring that the entire surface of the tube came in to contact with the solution. The tubes were incubated on ice and then 300 µL of ice-cold neutralisation solution (Solution III) (3 M potassium acetate, 11.5% (v/v) glacial acetic acid) was added. The contents were mixed gently by vortexing in an inverted position for 10 sec to thoroughly mix solution III with the viscous bacterial lysate. The tube was stored on ice for 3-5 min, and then centrifuged at 12,000 x *g* for 5 min in a microfuge. The supernatant was transferred to a fresh tube and precipitated using an equal volume of isopropanol at room temperature. Centrifugation at 12,000 x *g* for 15 min was performed in a microfuge and the resulting supernatant, removed and discarded. The

pellet containing nucleic acids was washed with 500 µL of 70% (v/v) ethanol and centrifugation carried out at 12,000 x *g* for 5 min in a microfuge. The supernatant was discarded and the pellet dried for 5 min in a vacuum rotary desiccator (microfuge rotary concentrator 5301, Eppendrof). The pellet was re-suspended in 50 µL of TE (10 mM Tris-HCl [pH 7.5], 1 mM EDTA [pH 8.0]) containing DNase-free pancreatic RNase (20 µg/mL), vortexed briefly and incubated at 37°C for 20 min. The preparations were stored at -20°C.

2.3.3.2 High quality plasmid DNA preparations

To obtain high quality plasmid DNA for sequencing and cloning, a commercially available kit (Promega PureYield™ Plasmid Midiprep System) (Cat. #A2492) was used as per the manufacturer's instructions. Bacterial cultures of 50-100 mL were grown overnight in LB with appropriate selection and bacterial cells harvested by centrifugation for 10 min at 4,000 x *g*. The resulting pellet was re-suspended in 3 mL of cell re-suspension solution (50 mM Tris [pH 7.5], 10 mM EDTA, 100 µg/mL RNase A) by vortexing. 3 mL of cell lysis solution (0.2 M sodium hydroxide, 1% sodium dodecyl sulfate) was then added to the mixture, which was then mixed by inverting 5 times and incubated at room temperature for 3 min. After this, 5 mL of neutralization solution (4.09 M guanidine hydrochloride, 0.759 M potassium acetate, 2.12 M glacial acetic acid, [final pH 4.2]) was added. The cell lysate was mixed well by inverting 10 times and centrifuged for 15 min at 10,000 x *g* at room temperature. A column stack was then assembled by placing a PureYield™ Clearing Column on top of a PureYield™ Binding Column. The column stack was placed onto a vacuum manifold and the bacterial lysate poured into the column. A vacuum was applied to the column stack until the liquid had passed through both the clearing and binding columns. The vacuum was released slowly and clearing column was discarded. A 5

mL aliquot of endotoxin removal wash solution was added to the binding column and a vacuum applied, to draw the solution through the column. Then, 20 mL of column wash solution was added to the binding column, and the solution drawn through the column by applying a vacuum. A 30-60 sec burst of vacuum was applied to remove excess ethanol from the DNA binding membrane. The binding column was removed from the vacuum manifold and transferred to a 50 mL falcon ensure there was no ethanol on the wall of column. A total of 600 μL of nuclease-free water was then added to the binding column and left for 2 min at room temperature to re-suspend DNA. The centrifugation was then carried out for 5 min at 4,000 x *g*. The DNA solution was transferred to a microcentrifuge tube and stored at -20°C for further analysis.

2.4 Extraction of fungal RNA and cDNA synthesis

2.4.1 Preparation for RNA extraction

All RNA extraction equipment was routinely autoclaved at 121°C for 15 min. To prevent RNA degradation due to contaminating RNase enzymes, solutions was made with double-distilled water treated with diethyl pyrocarbonate (DEPC, Sigma) prior to use. DEPC-treated water was prepared by adding 0.1% (v/v) DEPC to double distilled water and incubating overnight at 37°C. Residual DEPC was removed by autoclaving the solution prior to use because autoclaving DEPC solution causes DEPC to be broken down by hydrolysis to give ethanol and carbon dioxide.

2.4.2 Extraction of total RNA from *M. oryzae*

Fungal strains were grown on CM agar plates for 10-12 days. A 2 cm^2 plug of mycelium was excised and blended with 150 mL of liquid CM and incubated for 48 hour with 150 rpm aeration at 24°C in an orbital shaking incubator. The mycelium was

harvested by filtering through sterile Miracloth, washed with sterile distilled water, and blotted dry with paper towels to prepare for RNA extraction using the lithium chloride method. Mycelium was ground in a chilled mortar to a fine powder in liquid nitrogen and transferred to a sterile microcentrifuge tube containing 400 µL of extraction buffer (0.1 M LiCl, 0.1 M Tris [pH 8.0], 10 mM EDTA, 1% SDS) and 400 µL phenol. The tube was inverted for 1 min before 0.5 volumes (400 µL) of chloroform was added. The sample was then mixed by inverting the tube for 30 sec, before being centrifuged at 13,000 × *g* for 30 min at 4°C. The aqueous phase was transferred into a fresh microcentrifuge tube and an equal volume of 4 M LiCl was added before incubating the sample at 4°C overnight. After that, the sample was centrifuged at 13,000 × *g* for 20 min at 4°C to yield a pellet containing RNA which was washed with 70% (v/v) ethanol (made with DEPC treated water) before being resuspended in 500 µL of DEPC treated water. An equal volume of phenol:CIA was added to the tube and the sample inverted for 30 sec before centrifugation at 13,000 × *g* for 10 min at 4°C. The aqueous phase was transferred to a fresh microcentrifuge tube and RNA precipitated by adding 0.1 volumes of 3 M sodium acetate (pH 5.2) and 2 volumes of ethanol and then incubated at -20°C overnight. The RNA was recovered by centrifugation at 13,000 × *g* for 20 min at 4°C. The pellet was washed with 70% (v/v) ethanol, air dried, resuspended in 50 µL DEPC water and stored at -80°C.

2.4.3 cDNA synthesis by reverse-transcriptase PCR

To generate double stranded cDNA from RNA, the AffinityScript Q-PCR cDNA Synthesis Kit (Agilent technologies) was used. First-strand cDNA synthesis reaction was performed in a microcentrifuge tube in a final volume of 20 µL in RNase-free water containing 10 µL of first strand master mix (2 X), 3.0 µL of oligo (dT) primer (0.1 µg/µL), 1.0 µL of AffinityScript RT/ RNase Block enzyme mixture and RNA (1–3 µg

total RNA). The reaction mixture was incubated at 25°C for 5 min to allow primer annealing and subsequently incubated at 42°C for 15 min in order to synthesis cDNA. Finally, the reaction was incubated at 95ºC for 5 min to terminate the cDNA synthesis reaction. The cDNA was stored at -20ºC for long term storage and used as template to amplify cDNA for any gene.

2.5 Protoplast-mediated transformation of *M. oryzae*

M. oryzae strains were grown on CM agar plates and after 8-12 days of growth, a 2.5 cm^2 section of mycelium was excised from the growing edge and blended in 150 mL complete medium with the appropriate antibiotic and incubated at 24°C with shaking at 125 rpm in an orbital incubator for 48 hours. The mycelium was harvested through sterile Miracloth (Calbiochem) by filtration and subsequently washed in sterile distilled water. The mycelium was blotted dry with a paper towel and transferred to a 50 mL centrifuge tube (Becton Dickinson) with 40 mL OM buffer (1.2 M magnesium sulfate, 10 mM (pH 5.8) sodium phosphate, Glucanex 5% (Novo Industries, Copenhagen) final pH 5.4). Centrifuge tubes were shaken gently at 75 rpm for 3 hours at 30°C in an orbital shaking incubator. The digested mycelium was then transferred to a sterile polycarbonate Oakridge tubes (Nalgene) and overlaid with an equal volume of ice cold ST buffer (0.6M sucrose, 0.1M Tris-HCl pH 7). Protoplasts were recovered at the interface by centrifugation at 5,000 x *g* and 4°C in a swinging bucket rotor (Beckman JS-13.1) in a Beckman J2.MC centrifuge. The protoplasts were recovered at the OM/ST interface and transferred to a sterile Oakridge tube with disposable pasteur pipette (Liquipette^{CTM}, Elkay). Cold STC buffer (1.2 M sucrose, 10 mM Tris-HCl pH7.5, 10 mM calcium chloride) was filled in to the Okaridge. Protoplasts were pelleted at 3,000 x *g* for 10 min at 4°C, (Beckman JS-13.1 rotor), washed twice more with 30 mL STC,

with complete re-suspension each time. Finally, protoplasts were re-suspended in 1 mL of STC and the concentration of protoplasts was determined by counting using a haemocytometer. Purified protoplasts (1×10^7 mL^{-1}) were added to 1.5 mL microfuge tubes with DNA (4-6 μg) in a total volume of 150 μL. The mixture was incubated at room temperature for 30 min and subsequently 1 mL of PTC (60% PEG 400, 10 mM Tris-HCl pH 7.5, 10 mM calcium chloride) was gently added (in 2-3 aliquots with gentle mixing after each addition of PTC). The mixture was incubated at room temperature for 15-20 min. The mixture was then added to 150 mL molten (45°C) 1.5% agar/OCM (osmotically stabilised CM with 0.8M sucrose) without antibiotic selection to allow protoplasts to recover cell walls, mixed gently and poured into 5 sterile Petri dishes (30 mL/plate). For selection of transformants on Hygromycin B (Calbiochem), plate cultures were incubated in the dark for at least 16 hours at 24°C and then overlaid with approximately 15 mL CM/1% agar containing 200 μg/mL hygromycin B freshly added to the medium from a stock solution of 50 mg/mL.

2.6 Southern blot analysis

Blot of agarose DNA gels was performed according to an adaptation of the method from Southern (1975). Genomic DNA was digested with appropriate restriction enzymes and fractionated through 0.8% agarose gel contains ethidium bromide (0.5 μg mL^{-1}). Digestions were confirmed by visualizing agarose gel on a UV transilluminator. Each gel was submerged in 0.25 M HCl for 15-20 min to de-purinate fractionated DNA and then denatured by immersing in gel blotting solution (0.4 sodium hydroxide, 0.6 M sodium chloride) for 30 min. The gel was transferred to neutralisation buffer (1.5 M sodium chloride, 0.5 M Tris-HCl, [pH 7.5]) for 30 min before capillary blotting onto Hybond-N (GE healthcare). Gel blots were performed

by placing the inverted gel onto a wet filter paper wick, which was supported on a perspex sheet with each end of the wick submerged in 20 X SSPE solution (3.6 M sodium chloride, 200 mM monosodium phosphate, 22 mM ethylenediaminetetraacetic acid). Hybond-N membrane was then placed on top of the gel and overlaid with five layers of wet Whatman 3 mm paper and five layers of dry Whatman 3 mm paper onto which a 10 cm high pile of paper towels was placed (Kimberley Clark Corporation) another perspex sheet put on top of the towels. Finally, a 500 g weight was placed on the stack and the blot left to stand at room temperature overnight (16 h). The blot was then dismantled and the Hybond-N membrane dried. The transferred DNA was cross-linked to the membrane using a BLX crosslinker (Bio-link®) and either probed immediately or wrapped in Saran wrap for storage.

2.6.1 Generation of radio-labelled DNA probes

DNA hybridisation probes were labelled by the random primer method (Feinberg and Vogelstein, 1983) using a Primer-It RmT random primer labelling Kit (Agilent technologies) according to the manufacturer's instructions. Single-use reaction tubes (which contained a dehydrated mixture of random primers, dNTPs, buffer and cofactors for use with [α-^{32}P]dCTP) were used for each probe. A 50 ng aliquot of DNA was made to a final volume of 46 µl in water and transferred to the reaction tube. The sample was then boiled for 5 min to denature the DNA and then chilled on ice for 2 min. The tube was briefly subjected to centrifugation and 3 µL of magenta DNA polymerase (4 U/µL) added. The reaction components were mixed thoroughly and 1 µL of [α-^{32}P]dCTP (3,000 Ci/mmol) added. The labelling reaction was then incubated at 37°C for 10 min before being stopped by addition of 100 µl of labelling stop dye (0.1% SDS, 0.06 M EDTA, 0.5% bromophenol blue, 1.5% blue dextran).

Un-incorporated isotope was removed by passing the labelling reaction through a Biogel P60 (Bio-Rad) column, and collecting the dextran blue-labelled fraction. The probe was denatured by heating at 100°C for 5 min and quenched on ice for 2 min, before adding to the hybridisation mixture.

2.6.2 DNA gel bot hybridisation

Standard procedures were followed from Sambrook et al, (2000) for DNA gel blot hybridisations. DNA blots were incubated in hybridisation bottles (Hybaid Ltd.) in a hybridisation oven (Hybaid) for at least 4 hours at 65°C in 30 mL of pre-hybridisation solution, (6 x SSPE (diluted from a 20 x stock prepared by dissolving 175.3 g of NaCl, 27.6 g of NaH_2PO_4 and 7.4 g of EDTA in 800 mL of ddH_2O, adjusting the pH to 7.4 with NaOH and making up to 1 litre with ddH_2O), 5 x Denhardt's solution (diluted from a 50 x stock prepared with 5 g Ficoll (type 400, Pharmacia), 5 g polyvinylpyrrolidone in 500 mL ddH_20), 0.5 % SDS), with 100 μL denatured herring sperm DNA (1% [w/v] in 0.1 M NaCl) (Sigma) added. A heat denatured radio-labelled probe was then added and the mixture incubated overnight at 65°C.

After hybridisation, the blot was washed at high stringency. The pre-hybridisation solution was discarded along with any unbound probe and 30 mL of 2 x SSPE wash (0.1% SDS, 0.1% Sodium pyrophosphate [PPi], 2 x SSPE (diluted from the 20 x SSPE stock) [pH 7.4]) added. The blot was then incubated in 2 x SSPE solution for 30 min at 65°C. The wash solution was removed and replaced with 30 mL of 0.2 x SSPE wash (0.1% SDS, 0.1% Sodium pyrophosphate [PPi], 0.2 x SSPE, [pH 7.4]) followed by another 30 min incubation at 65°C. The 0.2X SSPE wash was repeated and the membrane dried for 30 min on paper towels. The membrane was wrapped in cellophane and placed in a cassette with an intensifying screen (Amersham) with X-

ray film (Fuji medical X-ray film, Fuji Photo Film (U.K.) Ltd.) at -80°C. After 24-48 hours X-ray films were developed using Fuji chemicals (Devalex 153 x-ray developer (OptiMax X-ray processer) and Fixaplus 354 Fixer provide by Champion Imaging Ltd).

2.7 Assay of pathogenicity and infection-related development by *M. oryzae*

2.7.1 *M. oryzae* pathogenicity assay

Infection assays were carried out on dwarf Indica rice (*Oryza sativa*) cultivar, CO-39, which is susceptible to rice blast (Valent et al, 1991). *M. oryzae* strains were grown on CM agar for 9-12 days before harvesting the conidia. The spore suspension was filtered through sterile Miracloth (Calbiochem) and subjected to centrifugation (Sigma) at 7,000 x *g* for 5 min. The pellet of conidia was recovered and diluted to 5 x 10^4 conidia mL^{-1} for plant infections. Spray inoculation was performed by using an artist's airbrush (Badger Airbrush, Franklin Park, Illinois, USA). Rice plants were grown in pots (8-10 plants per pot) and inoculated at 15-18 days old (2-3 leaf stage). Following spray-inoculation, plants were wrapped in polythene bags and incubated in controlled environment chamber (REFTECH, Holland) at 24°C with a 12 hours light-12 hours dark photo-phase and 90% relative humidity according to (Valent et al, 1991). After 48 hours, polythene bags were removed and the plants further incubated for another 2-3 days. Lesion formation was monitored 3 days post-inoculation and lesion density was recorded 4-5 days after inoculation.

2.7.2 Assays for measuring germination and appressorium formation rates

Conidial germination and appressorium formation were monitored over time using a method adapted from Hamer et al, (1988). Conidia were harvested and a conidial

suspension of 5 x 10^4 conidia mL^{-1} generated in double-distilled water. Conidia were then inoculated onto the surface of borosilicate glass coverslips (Fisher Scientific UK Ltd.) before being incubated in a humidity chamber (humidity was maintained in to the closed chamber by adding water soaked paper towels to the base of the chamber) at 24°C. The percentage of conidia undergoing germination and appressorium formation was monitored over a period of 24 h and examined by microscopy.

2.7.3 Assays for examining intracellular infection-related development on rice leaves

The intracellular growth of *M. oryzae* was observed in rice leaf sheath tissue, based on a method adapted from Kankanala et al, (2007). 3-4 week old (3-4 leaf stage) rice plants were used and leaf sheath removed from the plants. A conidial suspension at a concentration of 1 x 10^5 conidia mL^{-1} was prepared in 0.2% gelatine (BDH) and inoculated into the leaf vein using a syringe and incubated in a humid chamber at 24°C. After a period of at least 26 h, an outer epidermal layer of leaf tissue was dissected using a blade before being mounted onto a slide for microscopic analysis.

2.8 Microscopy and live cell imaging

2.8.1 Microscopy analysis using the epifluorescence microscope

To visualize GFP and RFP expressing strains, epifluorescence microscope was routinely used an IX81 motorized inverted microscope (Olympus) equipped with a UPlanSApo 100X/1.40 Oil objective (Olympus). Excitation of fluorescently-labeled proteins was carried out using a VS-LMS4 Laser-Merge-System with solid state lasers (488 nm/70 mW and 561 nm/70 mW). The laser intensity was controlled by a VS-AOTF100 System and coupled into the light path using a VS-20 Laser-Lens-System (Visitron System).

Images were captured using a Charged-Coupled Device camera (Photometric CoolSNAP HQ2, Roper Scientific). All parts of the system were under the control of the software package MetaMorph (Molecular Devices).

2.8.2 Confocal microscopy

Zeiss LSM510 Meta and Leica SP8 confocal laser scanning microscope systems were used to generate 3-D construction and movies of GFP and RFP expressing strains. Argon (488 nm laser line) and helium-neon (543nm laser line) lasers were used to excite GFP and RFP fluorochromes, respectively, and images recorded under x63 (Zeiss) or x40 (Leica) oil objective lenses. All microscopic images were analyzed using MetaMorph (Molecular Devices), LSM Image browser (Zeiss) or LAS AF (Leica) software. FRAP experiments were carried out on a Leica SP8 confocal microscope, using an Argon (488 nm laser line) to excite GFP for imaging and a 405 nm diode laser to perform bleaching. Five pre-bleach scans and 100 post-bleach were captured at 1 sec intervals.

Chapter 3. Identification and localization of secretory components in rice blast fungus

3.1 Introduction

3.1.1 Polarised secretion in fungi

Polarised exocytosis is an essential biological process required for a wide range of cellular activities, such as cell expansion, migration and morphogenesis (He & Guo, 2009). Polarised expansion of fungal cells requires the fusion of secretory vesicles with the plasmamembrane to secrete enzymes and raw materials required for synthesis of new cell wall material (Riquelme, 2013). In filamentous fungi, during polarised frowth secretory cargos are transported along cytoskeletal elements to the hyphal tip (Read, 2011; Riquelme, 2013; Steinberg, 2007; Sudbery, 2011). Vesicles accumulate at the sub- apical region called 'the Spitzenkörper', which acts as a vesicle supply centre and directs secretory cargo to the hyphal tip (Riquelme et al, 2007; Verdin et al, 2009). The Spitzenkörper, together with the polarisome and the exocyst complex, plays a crucial role in hyphal tip growth (Sudbery, 2011; Taheri-Talesh et al, 2008). Secretory cargo is delivered to the site of polarised growth along actin cables (Pruyne et al, 1998) and the nucleation of F-actin is mediated through the polarisome complex, which consists of Pea2, Spa2, Bud6 and the formin Bni1 in *Saccharomyces cerevisiae* (Evangelista et al, 2003; Sagot et al, 2002; Sheu et al, 1998). The motive force for the cargo delivery is provided through Myo2, a class V myosin, which forms a complex with its regulatory light chain, Mlc1 (Schott et al, 1999). Post-Golgi secretory cargos are delivered to the site of polarised growth in a process requiring the Rab GTPase Sec4, which is activated through its guanine nucleotide exchange factor (GEF), Sec2 (Novick et al, 2006; Stalder et al, 2013). The active GTP-bound form of Sec4 binds to the exocyst complex through

Sec15 (Salminen & Novick, 1989) (**Figure 3.1**). The exocyst complex is an evolutionarily conserved octameric protein complex, comprising Sec3p, Sec5p, Sec6p, Sec8p, Sec10p, Sec15p, Exo70p and Exo84p and is required for vesicle docking to the plasma-membrane (Guo et al, 1999a; He & Guo, 2009; TerBush et al, 1996) (**Figure 3.1**). Vesicle fusion to the plasma-membrane also requires soluble N-ethylmaleimide-sensitive factor attachment protein receptors (SNAREs), with v-SNAREs present on vesicles and t-SNAREs located at the plasma membrane (Novick et al, 2006).

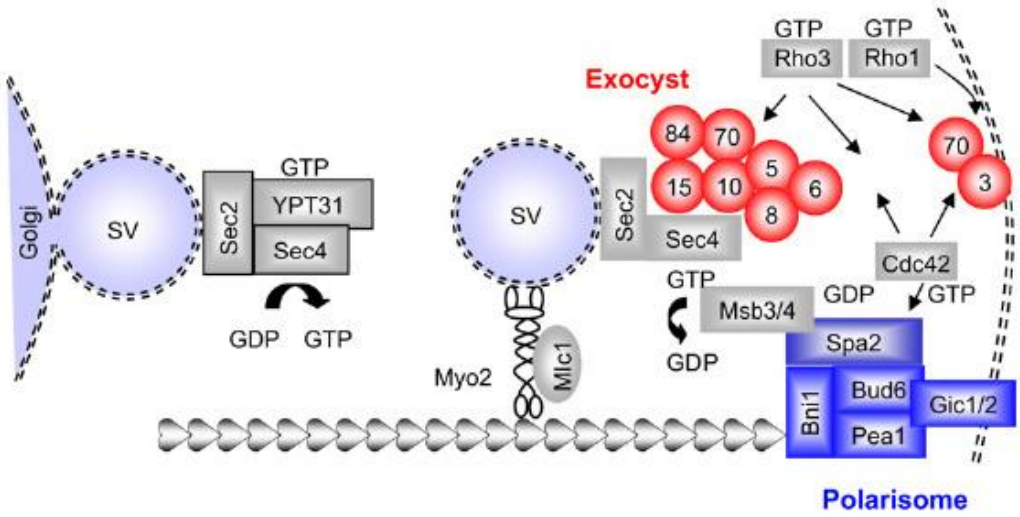

Figure 3.1 Schematic representation of polarised secretion via post-Golgi secretion pathway based on the information available in *S. cerevisiae*. (Taken from Sudbery, *Fungal Biology Reviews* 2008, 22:44-55).

3.1.2 Importance of the exocyst complex

The exocyst complex interacts, directly or indirectly, with membrane proteins, components of the cytoskeleton, small GTPases (of the Rab, Ral, and Rho subfamilies) and many other proteins directed to the growing point of the cell (Wu et al, 2008). Exocyst subunits are required for the formation of invadopodia, lamellipodia, and neural dendrites in animal cells, budding in yeasts, and cytokinesis in fission yeast, while in plants, the exocyst is essential for growth of root hairs, pollen tubes, cell elongation in hypocotyl, cytokinesis, seed coat formation and also formation of papillae during pathogen attack (Cole et al, 2005; Heider & Munson, 2012; Kulich et al, 2010; Pečenková et al, 2011; Synek et al, 2006; Synek et al, 2014; Vaskovicova et al, 2013).

3.1.3 Recruitment of the exocyst subunits with the plasma membrane

In budding yeast, it has been shown that secretory vesicles are transported to the bud tip along F-actin cables whereas, in contrast, localisation of Sec3 and a proportion of Exo70 is actin independent. The remaining exocyst subunits are dependent on actin cables for their localisation to the bud tip (Boyd et al, 2004). These results suggest that Sec3 and a pool of Exo70 proteins associate with the plasma membrane and interact with exocyst subunits when they arrive at the bud tip. Sec3 and Exo70 binds with phosphatidylinositol 4,5-bisphosphate (PIP_2) at the plasma membrane. It was reported that the C-terminal domain D of yeast Exo70 directly interacts with PIP_2 (He et al, 2007). Disrupting the interaction with PIP_2 causes severe growth and secretion defects (He et al, 2007; Liu et al, 2007b; Zhang et al, 2008) (**Figure 3.2**).

In yeast, Sec3 is a downstream target of both Cdc42 and Rho1. The N-terminus of Sec3 interacts with GTP-bound Rho1 and/or Cdc42 which suggests that Rho1 and Cdc42 control Sec3 localisation during different stages of cell growth (Guo et al, 2001; Zhang

et al, 2001) (**Figure 3.2**). Deletion of the N-terminus Sec3 showed growth defects like other exocyst mutants (Roumanie et al, 2005; Zhang et al, 2008). Similarly, it has been revealed that Exo70 interacts with the GTP-bound form of Rho3 which is a small GTPase (**Figure 3.2**). However, there was no effect on exocyst localisation when the interaction of Exo70 and GTP-bound Rho3 was blocked (Adamo et al, 1999; Hutagalung et al, 2009; Robinson et al, 1999).

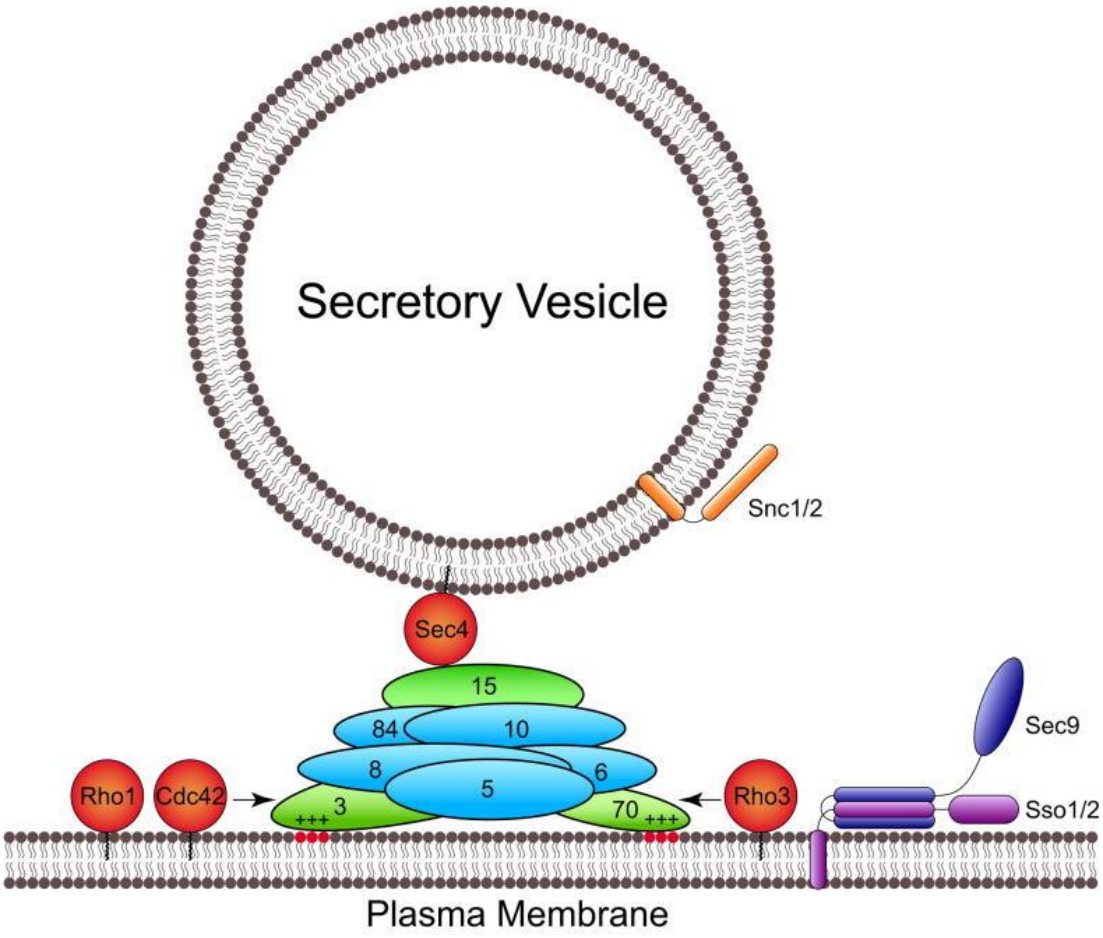

Figure 3.2 Schematic representation to show tethering of secretory vesicles to the plasma membrane in budding yeast. (Taken from He & Guo, *Current Opinion in Cell Biology* 2009, 21: 537-542).

3.1.4 Polarised secretion in *M. oryzae*

Rho-GTPases play an important role in infection related-development in *M. oryzae*. Deletion of *M. oryzae* Rho3, which interacts with Exo70, caused a severe defect in conidiation, appressorium development and virulence (Zheng et al, 2007). Similarly, the *M. oryzae* homolog of Cdc42 (small Rho-like GTPase) is required for full virulence of the fungus, null mutants of *M. oryzae* Cdc42 formed abnormally-shaped conidia and non-functional appressoria (Zheng et al, 2009). Another Rho-GTPase, Rac1, is only found in higher eukaryotes and is not present in yeasts such as *Saccharomyces cerevisiae* and *Schizosaccharomyces pombe*, and is a key regulator of actin cytoskeleton organization and cellular morphogenesis (Nobes & Hall, 1995). The *M. oryzae* homologue of Rac1 is required for conidiation and appressorium formation and null mutants of Rac1 showed severe defects in pathogenicity (Chen et al, 2008). It has been shown through yeast two hybrid analysis that *M. oryzae* Rac1 directly interacts with its downstream effector, the PAK kinase Chm1, and catalytic sub-units of the NADPH oxidase Nox1 and Nox2 (Chen et al, 2008). It was suggested that the Rac1-Chm1 interaction is required for conidiogenesis and the interaction with the NOX pathway is involved in appressorium development and pathogenicity (Chen et al, 2008). The *M. oryzae* Chm1, a PAK kinase and Cla4 homologue from yeast, is involved in appressorium-mediated plant infection (Li et al, 2004) and also required for septin and F-actin polymerisation at the appressorium pore (Dagdas et al, 2012).

More recently, Ye and coworkers (2014) characterised Rho GTPase-activating proteins (Rho GAPs) in *M. oryzae.* The RhoGAPs, Lrg1 is required for conidiation and appressorium formation, while Rga1 plays a role as a stage-specific regulator of conidial differentiation. Both Lrg1 and Rga1 directly interact with Cdc42 and Rac1 suggesting direct involvement in the regulation of Rho-GTPases (Ye et al, 2014).

In *M. oryzae*, no direct evidence has been reported regarding the mechanism of polarised secretion during appressorium-mediated plant infection. For this reason we decided to characterise the secretion pathway(s) in *M. oryzae*. In this chapter, the role of the polarised secretion pathway during appressorium-mediated plant infection by the rice blast fungus *M. oryzae* is described. Fluorescent markers fusion proteins involved in secretory pathway were analysed by live cell imaging and their expression investigated during appressoirum development. Polarity components including exocyst subunits, polarisome component, SNAREs, Rab-GTPase, and Rho-GTPase were all localised. All of the targeted proteins preferentially localised to the tips of growing hyphae and octameric exocyst complex was found at the hyphal tip, distal from the Spitzenkörper. In *M. oryzae* exocyst exists as a octameric complex and all the sub-units are physically interacts when SEC6:GFP and EXO84:GFP were co-immunoprecipitates with GFP-trap and followed by liquid chromatography–tandem mass spectrometry (LC-MS/MS). During initial stages of infection-related development, the exocyst is localised to the tip of the germ tube, but then adopts a cortical pattern of localisation in the developing appressorium, before specifically localising to the appressorium pore where it co-localises with F-actin network. The appressorium pore is a site for emergence of the penetration peg and localisation of the exocyst subunits around the appressorium pore suggests that the pore is an active site of secretion during plant infection. In the mature appressorium, the v-SNARE Snc1, the actin binding protein Fimbrin and Rho-GTPase showed punctate distribution within the appressorium pore. Furthermore, the requirement of an intact F-actin network for exocyst localisation at the appressorium pore is reported.

3.2 Materials and methods

3.2.1 Construction of GFP-tagged strains for localisation of polarity components

N- or C- terminal translational fusions for secretory compoenents were generated based on published reports in other fungi like *C. albicans* or *N. crassa* (Court & Sudbery, 2007; Jones & Sudbery, 2010; Riquelme et al 2014; Sudbery, 2011). N-terminal translational fusions were generated through cloning of GFP fragments between the native gene promoter and coding region of each native gene. A 1 kb fragment downstream of the stop codon was used as a terminator of each gene. To generate C-terminal translational fusions, primers were designed to amplify the gene of interest including 2 kb of sequence upstream of the start codon, and then fused to GFP and the TrpC terminator, *Aspergillus nidulans* (Sweigard et al, 1997). All primers used in this study are shown in **Table 3.1**. All plasmids for expressing GFP-translational fusion were generated by the GAP repair cloning method, which relies on homologous recombination in *S. cerevisiae* (Kevin et al, 1997). The pNEB-Nat-Yeast cloning vector which carries the *URA3* gene, was used to synthesise uracil and thereby complement *ura3* strain of *S. cerevisiae*. The Yeast cloning vector was linearized with *Hind*III and *Sac*I before the PCR products were transformed directly into a yeast uracil auxotrophic ura3 (-) strain. Primers for C- and N- terminal translational fusions carried overhangs corresponding to adjacent fragments. In each case, primers contained a 30 bp 5' overhang with adjoining fragments to allow assembly of fragments by homologous recombination. The PCR fragments and linearized vector were mixed together (600 ng of each) and used to transform DS94 a *ura3* strain of *S. cerevisiae* (*MAT*α, *ura3-52*, *trp1-1*, *leu2-3*, *his3-111*, and *lys2-801*) (Tang et al, 1996). The PCR fragments and linearised vector were assembled in the correct orientation through homologous recombination to generate a viable plasmid. In order to identify positive clones, yeast

colony PCR was performed and grown on minimal media to extract plasmids. The yeast plasmid was then used to transform *E. coli* XL10-Gold Ultracompetent cells (Agilent Technologies) to produce the plasmid in bulk.

Table 3.1 List of oligonucleotide primers used in this study.

Primer Name	DNA Sequence (5`-3`)
Sec6.SUR_F	GATTATTGCACGGGAATTGCATGCTCTCACCCGTCTTTTTGTTGTCGTCTCT
Sec6.GFP_R	GGTGAACAGCTCCTCGCCCTTGCTCACCATCTTGACTCTACTCATAATAG
Sur_vec.F	AACTGTTGGGAAGGGCGATCGGTGCGGGCCGTCGACGTGCCAACGCCACAGT GC
SurR	GTCGACGTGAGAGCATGCAATTCC
Cdc42.Pro_SUR	GATTATTGCACGGGAATTGCATGCTCTCACTCGTCATACTGGCTGCTTCC
Cdc42.Pro_GFP	GGTGAACAGCTCCTCGCCCTTGCTCACCATTGTTTAGAGCTGAGCGGGAG
Cdc42.Orf-GFP	ATCACTCACGGCATGGACGAGCTGTACAAGATGGTGGTTGCAACGATTAA
Cdc42.Ter-R	TTCACACAGGAAACAGCTATGACCATGATTCATCCAAACTTTACCTGCCC
GFP-F	ATGGTGAGCAAGGGCGAGGA
GFP-R	CTTGTACAGCTCGTCCATGC
Exo70.Sur_F	GATTATTGCACGGGAATTGCATGCTCTCACTTCTTCTCCACACCTCCCAGCA
EXO70.GFP_R	GGTGAACAGCTCCTCGCCCTTGCTCACCATGTAAAGGCTGGCGAAAACGGCA
SEC5-SUR-F	GATTATTGCACGGGAATTGCATGCTCTCACAGGAGTGGCCCAGTTAGAATGA
Sec5.GFP_R	GGTGAACAGCTCCTCGCCCTTGCTCACCATTACGGAATCCTTGCGCTCCGTT
EXO84.SUR_F	GATTATTGCACGGGAATTGCATGCTCTCACAGAGGGTGGATAGAAAAGGA
EXO84.GFP_R	GGTGAACAGCTCCTCGCCCTTGCTCACCATAGAGAGGCCGAGGCCAAGCG
Sec3.SUR_F	GATTATTGCACGGGAATTGCATGCTCTCACAATACAGGACTGGGAAACGC
Sec3.GFP_R	GGTGAACAGCTCCTCGCCCTTGCTCACCATCCCTCTCCCAAGGTTCGAAA
Sec4.Pro-Sur.F	GATTATTGCACGGGAATTGCATGCTCTCACTTTGGGTTCGTCGGGCTT
Sec 4.Pro-FP.R	GGTGAACAGCTCCTCGCCCTTGCTCACCATGGTGCTGCGTTTGGAGCA
Sec4.Orf-GFP.F	ATCACTCACGGCATGGACGAGCTGTACAAGATGGCCAACAGGAATTACGATG
Sec4.Ter.R	TTCACACAGGAAACAGCTATGACCATGATTAACGGACAACGACGCACTCTAT
Sec9.Sur-F	GATTATTGCACGGGAATTGCATGCTCTCACAATGATGCGGTGTCTTGAGT
Sec9.GFP-R	GGTGAACAGCTCCTCGCCCTTGCTCACCATACCCTTCTTGTAGATGCGGT
Sec15.SUR_F	GATTATTGCACGGGAATTGCATGCTCTCACGGCATCCATAAAGCGAAACT
Sec15.GFP_R	GGTGAACAGCTCCTCGCCCTTGCTCACCATGCTGAAACCAAAACGAGATG
SEC8-SUR-F	GATTATTGCACGGGAATTGCATGCTCTCACCCAGAGGGCATTACACAAAA
SEC8-GFP-R	GGTGAACAGCTCCTCGCCCTTGCTCACCATAACCGTCCCCAAACCTTCAG
SEC10.SUR_F	GATTATTGCACGGGAATTGCATGCTCTCACATCCGACGCTGTTGTTATCT
SEC10.GFP_R	GGTGAACAGCTCCTCGCCCTTGCTCACCATCAGTCCAGCGAGAACGCTCT
RAC1.Pro.SUR-F	GATTATTGCACGGGAATTGCATGCTCTCATCGCAGTAGTCACAACGGGC
RAC1.Pro.GFP-R	GGTGAACAGCTCCTCGCCCTTGCTCACCATGGTTCAGCGTGGTCTGGAAA
RAC1.ORF.GFP-F	ATCACTCACGGCATGGACGAGCTGTACAAGATGGCCGCCCCTGGGGTTCA
RAC1.TER.VEC-R	TTCACACAGGAAACAGCTATGACCATGATTGCACCTGGGGCAAAAGCGTCAA

3.2.2 Yeast transformation

For yeast transformations, single *S. cerevisiae* colonies of DS94 (Tang et al, 1996) were picked and used to inoculate 10 mL of YPD medium (10 g L^{-1} yeast extract, 20 g L^{-1} peptone and 20 g L^{-1} glucose) and incubated overnight at 30°C with continuous shaking at 200 x *g*. In order to obtain fresh yeast cells for transformation, a 2 mL aliquot from the overnight culture was inoculated into 50 mL YPD in a 250 mL sterile flask and incubated at 30°C for 5 h, with continuous shaking at 200 rpm. After 5 h, yeast cells were pelleted, by centrifugation at 2,200 × *g* for 5 min. The supernatant was discarded and the pellet of yeast cells re-suspended in 10 mL distilled water before centrifugation at 2,200 × *g* for 5 min. The supernatant was again discarded and the pellet re-suspended in 300 μL sterile distilled water. For transformation, linearized vector and PCR products (600 ng each) were combined in a fresh microcentrifuge tube with a 50 μL aliquot of yeast cells and 50 μL of 2 μg/μL salmon sperm DNA (denatured at 95°C for 5 min and cooled on ice for 2 min), 32 μL of 1 M lithium acetate and 240 μL of 50% PEG 4000 were added to the tube which was incubated at 30°C for 30 min. The tube was centrifuged at 2,000 × *g* for 2 min after heat shock at 45°C for 15 min. The supernatant was removed and the pellet re-suspended in 200 μL distilled water. A 10 x dilution of the 200 μL suspension was made and plated on yeast synthetic drop out agar (1.7 g L^{-1} yeast nitrogen base (without amino acids) (Fluka), 5 g L^{-1} ammonium sulfate, 5 g L^{-1} casein hydrolysate (Fluka), 0.02 g L^{-1} adenine (Sigma), 0.02 g L^{-1} tryptophan (Fluka), 20 g L^{-1} glucose and agar 10%) and incubated at 30°C. Transformants usually appeared after 2-3 days of incubation.

3.2.3 Selection for products of GAP repair cloning

Routinely, 16 colonies were picked from transformation plates and sub-cultured on yeast synthetic drop out plates. The colony PCR was performed using 2 x Thermo-start PCR master mix (Thermo Scientific) and a 1 kb gene fragment was used to amplify from yeast colonies in order to select positive clones. Each reaction contained 12.5 µL 2 x Thermo-start PCR master mix, 0.5 µM of each primer, a single yeast colony and the final volume was made up to 25 µL with sterile water.

The PCR conditions used for 2 x Thermo-start PCR master mix (Thermo Scientific) were as follows: an initial denaturation step at 95°C for 15 min, followed by 35 cycles of PCR: Denaturation at 95°C for 20 sec, annealing at 58°C for 30 sec and extension at 72°C for 1 min, followed by a final extension at 72°C for 5 min and a hold at 4°C, prior to evaluation of amplicons by gel electrophoresis.

3.2.4 Yeast plasmid extraction

Positive yeast clones were sub-cultured in 50 mL yeast synthetic drop out media and grown overnight at 30°C with continuous shaking at 200 rpm. The cells were recovered by centrifugation for 5 min at 3,000 × *g* and the pellet re-suspended in 0.5 mL sterile distilled water and transferred to a sterile microcentrifuge tube. The cells were centrifuged again for 5 sec at 13,000 × *g*, the supernatant discarded and the pellet vortexed and re-suspended in the water. After resuspension, 200 µL of yeast lysis buffer (2% (v/v) triton X-100 (Sigma), 1% SDS, 0.1 M sodium chloride, 1 mM ethylenediaminetetraacetic acid, 10 mM Tris), 200 µL phenol:chloroform: isoamylalcohol (25:24:1) and 0.3 g of acid washed glass beads (425-600 µm) were added to the tube. A 200 µL aliquot of TE (10 mM Tris and 1 mM EDTA, pH 8.0) was added to the tube after vortexed for 30 min. The tube was centrifuged for 10 min at

13,000 × *g* before the aqueous phase was transferred to a fresh microcentrifuge tube. A 0.1 volume of 3 M sodium acetate (pH 5.5) and 2 volumes of 96% ethanol were then added to the tube which was incubated at -20°C for 15 min. Subsequently the tube was centrifuged at 13,000 × *g* for 20 min to recover the pellet of plasmid DNA. The plasmid DNA pellet was then re-suspended in 400 µL of TE treated with 4 µL of RNase A (10 mg/mL) and incubated at 37°C until the pellet dissolved. A 10 µL aliqout of 4 M ammonium acetate and 1 mL of 96% (v/v) ethanol was added to the tube which was centrifuged at 13,000 × *g* for 20 min. The supernatant was discarded and the pellet washed with 500 µL of 70% ethanol before being air-dried and re-suspended in 50 µL of distilled water. In order to obtain increased amounts of plasmid DNA the plasmid was transformed into *E. coli*.

3.2.5 Bacterial transformation of yeast plasmid

Bacterial transformation was carried out using XL10-Gold Ultracompetent cells (Agilent Technologies). The genotype of XL-10 gold ultracompetent cells is Tet^rΔ(*mcrA*)*183* Δ(*mcrCB-hsdSMR-mrr*)*173 endA1 supE44 thi-1 recA1 gyrA96 relA1 lac* Hte [F´ *proAB* $lacI^q$ZΔ*M15* Tn*10*(Tet^r) Amy Cam^r]. Competent cells were thawed on ice and a 100 µl aliquot of transferred into pre-chilled 15 mL Falcon tubes and 4 µl of β-mercaptoethanol added. The tubes were incubated on ice for 10 min and tubes gently agitated every 2 min. A 10 µl aliquot of plasmid DNA was added to the competent cells and the mixture incubated on ice for a further 30 min. Tubes were placed heat-shocked at 42°C for 30 sec and subsequently transferred to ice for 2 min. A 900 µl aliquot of preheated NZY^+ broth (casein hydrolysate 10 g L^{-1}, yeast extract 5 g L^{-1} and sodium chloride 0.5 g L^{-1}, glucose 20%, magnesium sulfate 10 mM and magnesium chloride 10 mM) was then added and incubated at 37°C for 1 hour with

shaking at 200 rpm. A 10 x dilution of the transformation reaction was then made and plated onto LB agar (10 g L^{-1} tryptone, 5 g L^{-1} yeast extract, 10 g L^{-1} NaCl and 15 g L^{-1} agar [pH to 7.5]) with the appropriate antibiotic and incubated overnight at 37°C. Colony PCR was performed to identify positive clones which were cultured and plasmid DNA purified using the Promega PureYield™ Plasmid Midiprep System see section 2.3.3.2.

3.2.6 *FM4–64* staining and treatment with chemical inhibitors

Strains expressing GFP-tagged exocyst components were stained with the lipophilic dye FM4-64 at 4 μg mL^{-1} in water, as described previously (Bolte et al, 2004). A plug of mycelium was inoculated on a water agar slide. After 24h, a 10μL aqueous solution of FM4-64 was used to stain vegetative hyphae and incubated for 5 min before viewing by epifluorescence microscopy.

Chemical inhibitors were used to observe the effect on exocyst localization in mature appressoria. The microtubule disrupting agent methyl 1-(butylcarbamoyl)-2-benzimidazolecarbamate (benomyl; Fluka) was used at 30 μM (stock: 10 mM in DMSO) and the actin inhibitor latrunculin A (Enzo Life Sciences) was used at 10 μM (stock: 20 mM in DMSO). Inhibitors were added after 16 h of appressorium development and observations made after 24 h. A solution of 0.1% DMSO was used in the control experiment.

3.2.7 Co-immunoprecipitation (Co-IP) experiment and LC-MS/MS analysis

3.2.7.1 Protein extraction from fungal mycelium

Total protein was extracted from the modified protocol reported by Liu and coworkers (Liu et al, 2011). *M. oryzae* Guy11 strain expressing exocyst sub-units, Sec6:GFP and

Exo84:GFP were grown on CM plates for 10 days and afterwards a 2.5 cm^2 section of mycelium was excised from the growing edge and blended in 150 mL CM and incubated at 24°C with shaking at 125 rpm in an orbital incubator for 48 hours. The mycelium was harvested through sterile Miracloth (Calbiochem) by filtration and subsequently washed in sterile distilled water. The mycelium was blotted with paper towel, snap frozen in liquid nitrogen and freeze-dried in freeze dryer (Heto* PowerDry LL3000 Freeze Dryer, Thermo Scientific) before protein extraction. A 250 mg freeze dried mycelium from each strain was ground into fine powder in liquid nitrogen using mortar and pestle. Fine powdered mycelium was homogenised in 2 mL of freshly prepared and ice-chilled protein extraction buffer (GTEN (10% glycerol, 25 mM Tris-HCl (pH 7.5), 1 mM EDTA, 150 mM sodium chloride autoclaved and stored at 4°C), 2% w/v polyvinylpolypyrrolidone, 1X protease inhibitor cocktail (Sigma), 0.1% tween 20 (Sigma)). Samples were vigorously vortexed for 20 sec so that all the powder mixed properly in the extraction buffer. The lysate was centrifuged at 14,000 x *g* for 20 min at 4°C and the supernatant was transferred to a new sterile microcentrifuge tube which contains soluble proteins. The supernatant was stored in -80°C and used for the immunoprecipitation experiment.

3.2.7.2 Co-immunoprecipitation using GFP-Trap method

Total protein was extracted from mycelium of *M. oryzae* strains expressing Sec6:GFP, Exo84:GFP and ToxA:GFP (expressed in cytoplasm and used as a control) and used for immunoprecipitation using GFP-Trap protocol (ChromoTek) according to the manufacturers' protocol. A 25 µL GFP-Trap_A slurry beads was re-suspended in 500 µL ice cold dilution buffer and centrifuged at 2,500 x *g* for 2 min at 4°C. Supernatant was discarded and beads were washed twice with 500 µL ice cold dilution buffer. A 50

µL of protein extract was added to GFP-Trap_A beads and incubated with constant shaking for one hour at 4°C. Supernatant was discarded after centrifugation at 2,500 x *g* for 2 min at 4°C and beads were wash three times with 500 µL ice cold wash buffer. Beads were re-suspended in 100 µL 2 X SDS-Sample buffer and boiled for 10 min at 95°C to dissociate immunocomplexes from the beads. Supernatant was collected after centrifugation at 2,500 x *g* for 2 min at 4°C and SDS-PAGE was performed with the supernatant.

3.2.7.3 Mass spectrometery

Proteins were separated with sodium dodecyl sulphate/polyacrylamide gel electrophoresis (SDS/PAGE) and gels were cut into slices (∼5 Å~ 10 mm). Proteins contained in gel slices were prepared for liquid chromatography–tandem mass spectrometry (LC-MS/MS), as described previously (Ntoukakis et al, 2009). LC-MS/MS analysis was performed with a LTQ Orbitrap mass spectrometer (Thermo Scientific) and a nanoflow-HPLC system (nanoACQUITY; Waters Corp.), as described previously (Oh et al, 2009) with the following differences: MS/MS peak lists were exported in mascot generic fileformat by using Discoverer v2.2 (Thermo Scientific). The database was searched with Mascot v2.3 (Matrix Science) with the following differences: (**i**) The database searched with Mascot v2.3 (Matrix Science) was against *M. oryzae* protein database with the inclusion of sequences of common contaminants such as keratins and trypsin. (**ii**) Carbamidomethylation of cysteine residues was specified as a fixed modification, and oxidized methionine was allowed as a variable modification. Other Mascot parameters used were as follows: (**i**) Mass values were monoisotopic, and the protein mass was unrestricted. (**ii**) The peptide mass tolerance was 5 ppm, and the fragment mass tolerance was ± 0.6 Da. (**iii**) Two missed cleavages

were allowed with trypsin. All Mascot searches were collated and verified with Scaffold (Proteome Software), and the subset database was searched with X Tandem (The Global Proteome Machine Organization Proteomics Database and Open Source Software; www.thegpm.org). Accepted proteins passed the following threshold in Scaffold: 95% confidence for protein match and minimum of two unique peptide matches with 95% confidence.

3.3 Results

3.3.1 Identification of genes required for polarised growth in *M. oryzae*

Genes expected to be involved in polarized growth were identified by homology to genes of known function using the BLASTX programme provided by the Magnaporthe genome database (http://www.broadinstitute.org/). A list of the genes targeted in the current study is shown in **Table 3.2**. In the current study, the polarisome component Spa2 (MGG_03703), myosin light chain protein Mlc1 (MGG_09470), actin-binding protein fimbrin, Fim1 (MGG_04478), v-SNARE Snc1 (MGG_12614), t-SNARE Sec9 (MGG_00522), Rho-GTPase Cdc42 (MGG_00466), Rab-GTPase Sec4 (MGG_06135), Sec2 (MGG_02923) the guanine nucleotide exchange factor for Sec4 and all eight predicted subunits exocyst complex; Sec3 (MGG_03323), Sec5 (MGG_07150), Sec6 (MGG_03235), Sec8 (MGG_03985), Sec15 (MGG_00471), Exo70 (MGG_01760) and Exo84 (MGG_06098) were targeted for study.

Table 3.2 List of the genes used in this study

Name	*S. cerevisiae* Protein	*M. oryzae* protein	Size (aa)	Function	Blastp e-value
Spa2	YLL021W	MGG_03703	951	Polarisome component	1.9e-23
Mlc1	YGL106W	MGG_09470	147	Myosin light chain regulator	1.3e-23
Fim1	YDR129C	MGG_04478	651	actin-bundling protein, maintenance of the actin cytoskeleton and involved in endocytosis	1.3e-222
Sec2	YNL272C	MGG_02923	670	Guanyl-nucleotide exchange factor Rab-GTPase Sec4p	6.9e-23
Sec4	YFL005W	MGG_06135	206	Rab-GTPase involved in exocytosis and autophagy	2.2e-60
Sec3	YER008C	MGG_03323	1434	Exocyst subunit	4.9e-29
Sec5	YDR166C	MGG_07150	1055	Exocyst subunit	1e-22
Sec6	YIL068C	MGG_03235	755	Exocyst subunit	9.2e-37
Sec8	YPR055W	MGG_03985	1101	Exocyst subunit	1.3e-41
Sec15	YGL233W	MGG_00471	775	Exocyst subunit	1.3e-43
Exo84	YBR102C	MGG_06098	681	Exocyst subunit	5.4e-30
Exo70	YJL085W	MGG_01760	633	Exocyst subunit	5.4e-30
Sec9	YGR009C	MGG_00522	465	t-SNARE required for secretory vesicle-plasma-membrane fusion	4.2e-09
Snc1	YAL030W	MGG_12614	126	v-SNARE involved in exocytosis and endocytosis	2.3e-24
Cdc42	YLR229C	MGG_00466	194	Rho-like GTPase important for establishment and maintenance of cell polarity	1e-85
Rac1	-	MGG_02731	199	small GTPase involved in actin cytoskeleton organization and polarized cell growth	

3.3.2 Multiple alignment of amino acid sequence of putative homologues

To investigate the similarity *M. oryzae* exocyst proteins, the predicated amino acid sequences of each gene aligned with secretory proteins from related fungi using ClustalW (Chenna et al, 2003; Thompson et al, 1994). Amino acid sequences for proteins in *M. oryzae* were retrieved from the *M. oryzae* genome database (http://www.broadinstitute.org/annotation/genome/magnaporthecomparative/MultiHome. Html). A BLASTP search (Altschul et al, 1990) was performed with *M. oryzae* amino acid sequences. The putative homologous amino acid sequences were downloaded and aligned with *S. cerevisiae, C. albicans, A. nidulans, N. crassa* and *M. oryzae*, respectively (**Figure 3.3**).

A. Exo70 protein sequence alignment

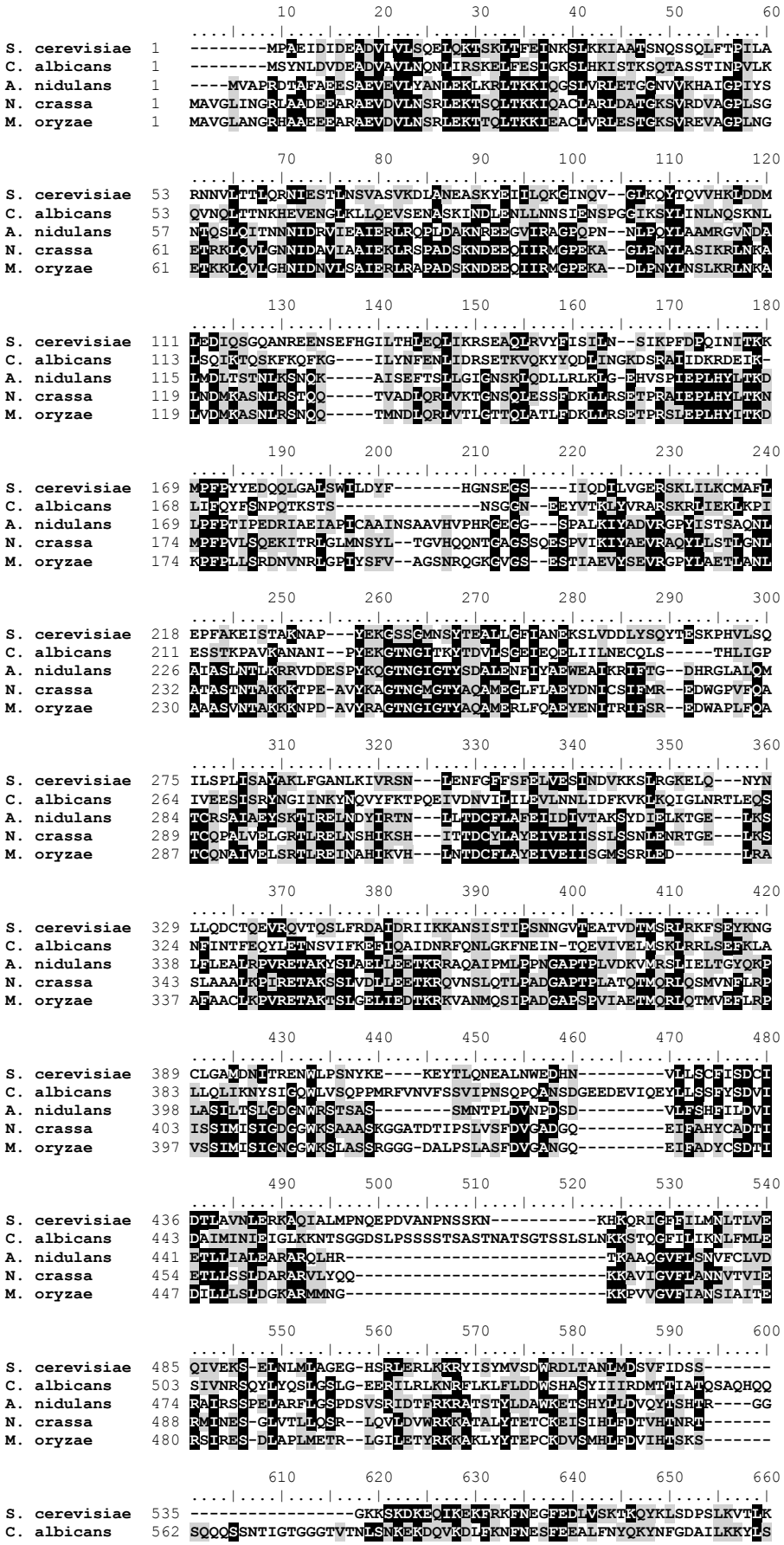

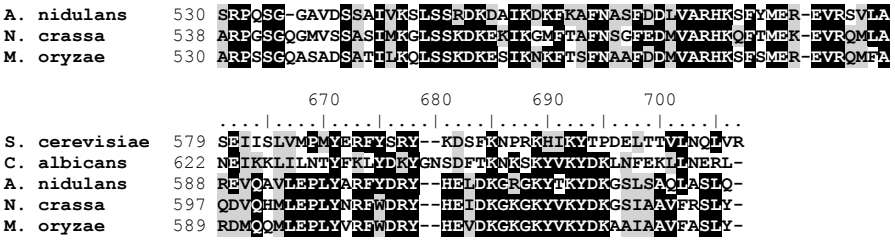

B. Sec15 protein sequence alignment

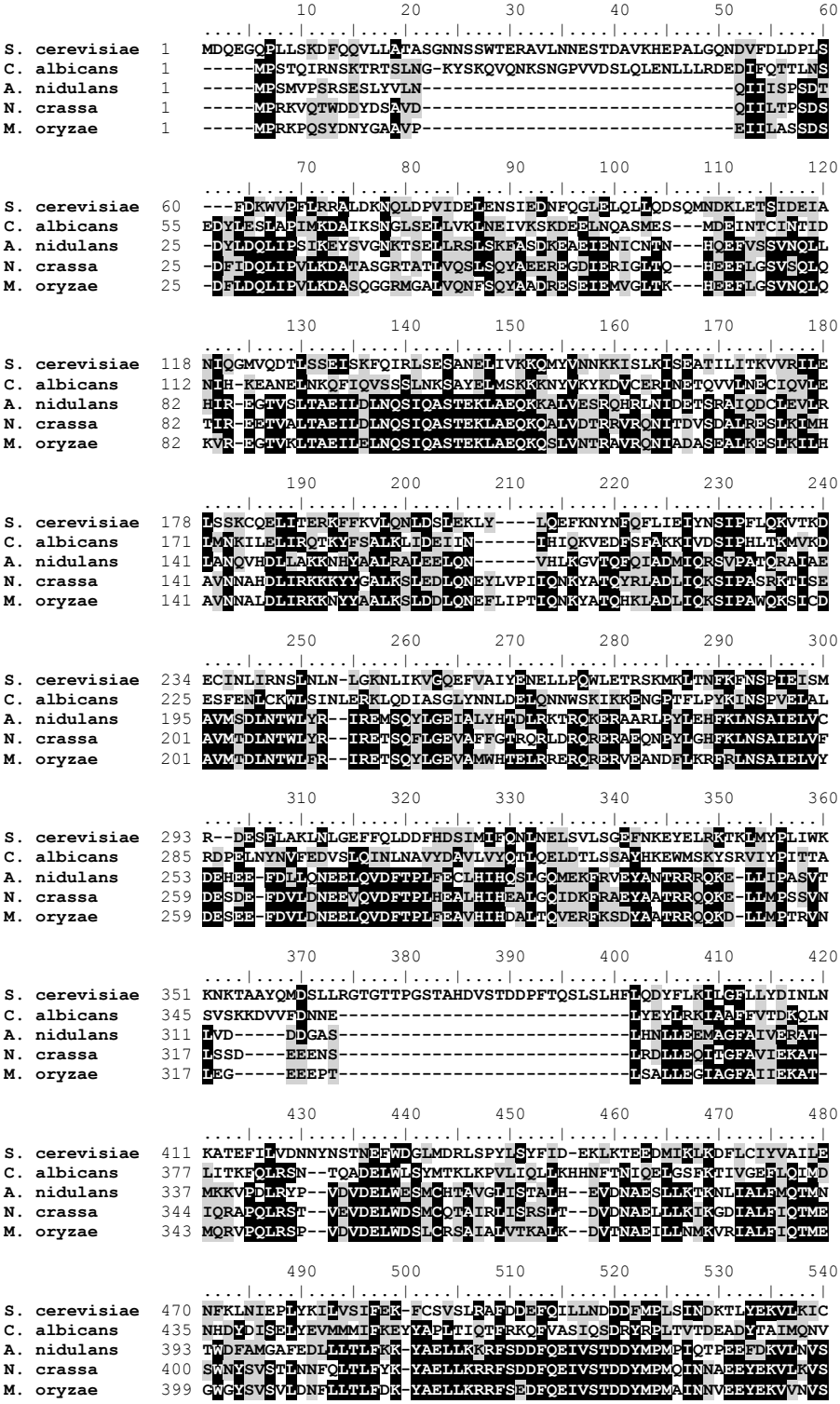

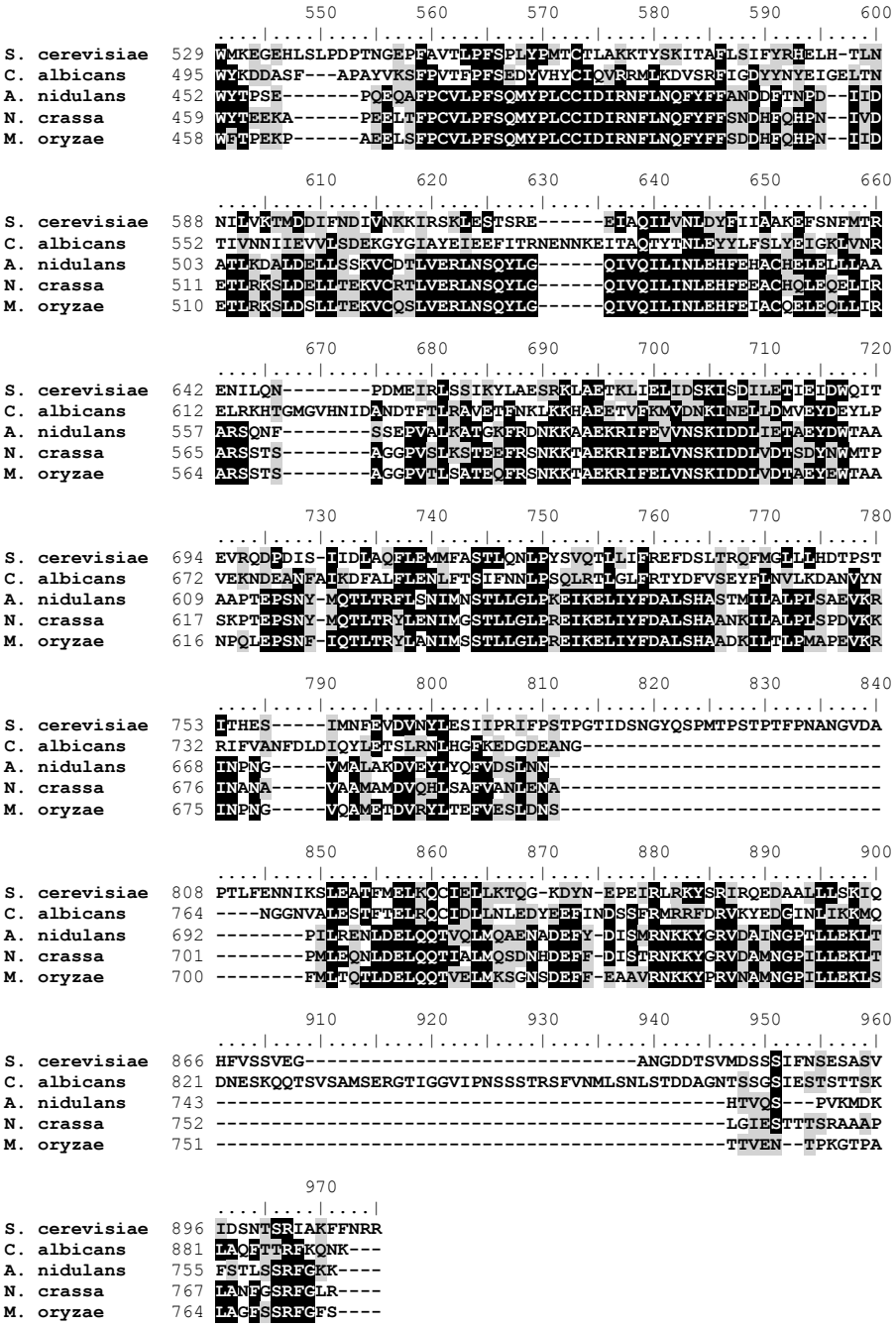

C. Sec8 protein sequence alignment

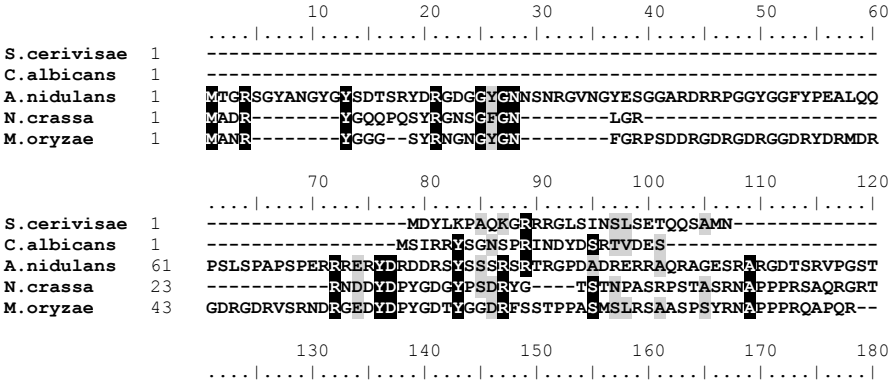

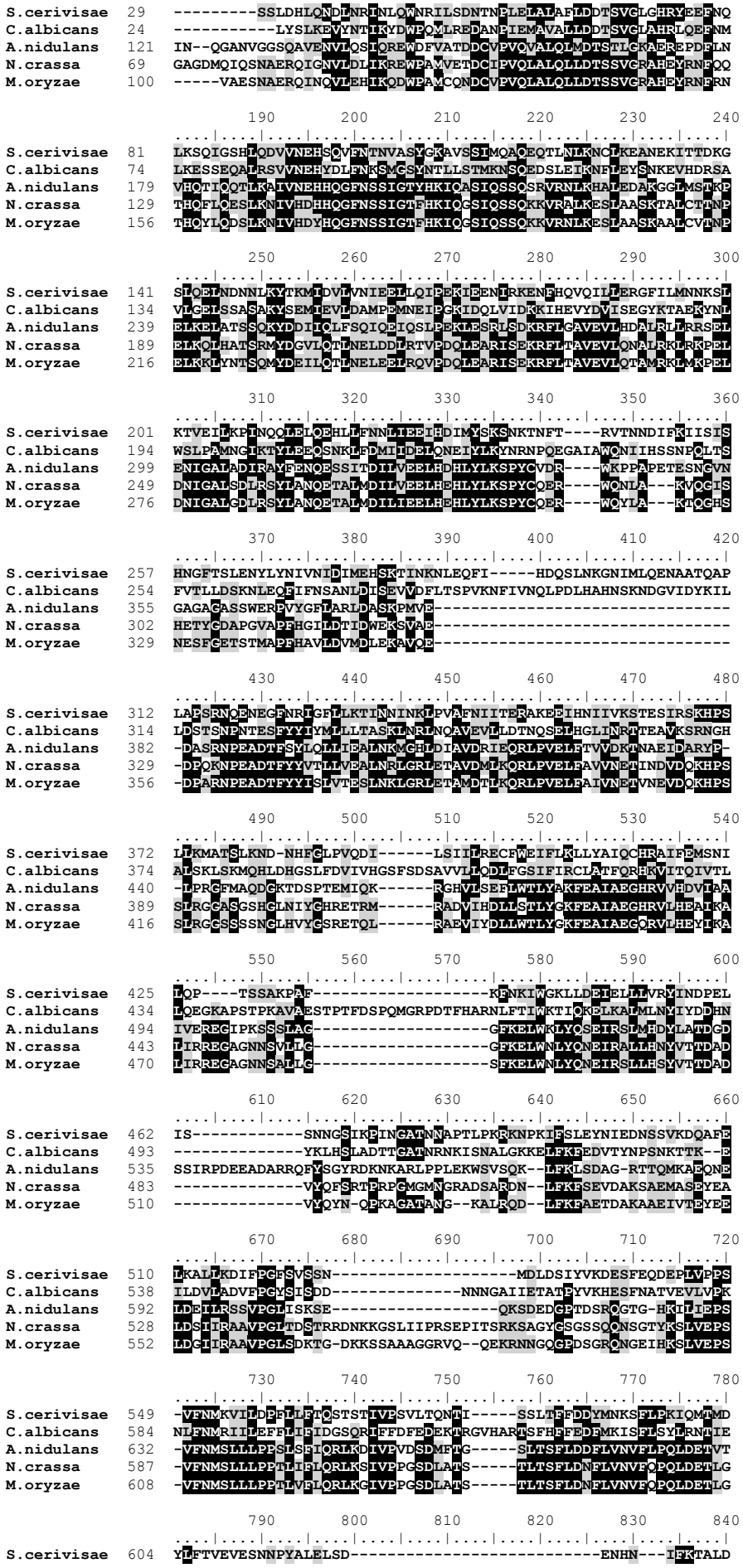
S.cerivisae 29 ---------SSLDHLQNDLNRINLQWNRILSDNTNPLELALAFLDDTSVGLGHRYEESNQ
C.albicans 24 ----------LYSLKEVYNTIKYDWPQMLREDANPIEMAVALLDDTSVGLAHRLQEPNM
A.nidulans 121 IN--QGANVGGSQAVENVLQSIQREWDFVATDDCVPVQVALQLMDTSILGKAERFPDELN
N.crassa 69 GAGDMQIQSNAERQIGNVLDLIKREWPAMVETDCIPVQLALQLLDTSSVGRAHEYRNFQQ
M.oryzae 100 -----VAESNAERQINQVLEHIKQDWPAMCQNDCVPVQLALQLLDTSSVGRAHEYRNFRN
190 200 210 220 230 240
S.cerivisae 81 LKSQIGSHLQDVVNEHSQVFNTNVASYGKAVSSIMQACEQTLNLKNCLKEANEKITTDKG
C.albicans 74 LKESSEQALRSVVNEHYDLFNKSMGSYNTLLSTMKNSQEDSLEIKNFLEYSNKEVHDRSA
A.nidulans 179 VHQTIQQTLKAIVNEHHQGFNSSIGTYHKIQASIQSSQSRVRNLKHALEDAKGGLMSTKP
N.crassa 129 THQFLQESLKNIVHDHHQGFNSSIGTFHKIQGSIQSSQKKVRALKESLAASKTALCTTNP
M.oryzae 156 THQYLQDSLKNIVHDYHQGFNSSIGTFHKIQGSIQSSQKKVRNLKESLAASKAALCVTNP
250 260 270 280 290 300
S.cerivisae 141 SLQELNDNNLKYTKMIDVLVNIPELLQIPEKIPENIRKENFHQVQILLERGFILMNNKSL
C.albicans 134 VLGELSSASAKYSEMIEVLDAMPEMNEIPGKIDQLVIDKKIHEVYDVISEGYKTAEKYNL
A.nidulans 239 ELKELATSSQKYDDIIQLFSQIQEIQSIPEKLESRLSDKRFLGAVEVLHDALRLLRRSEL
N.crassa 189 ELKQLHATSRMYDGVLQTTNELDDLRTVEDQLEARISEKRFLTAVEVLQNALRKLRKPEL
M.oryzae 216 ELKKLYNTSQMYDEILQTTNELEELRQVEDQLEARISEKRFLTAVEVLQTAMRKLMKPEL
310 320 330 340 350 360
S.cerivisae 201 KTVEILKPINQQLELQEHLLFNNLIEEIHDIMYSKSNKTNFT----RVTNNDIFKIISIS
C.albicans 194 WSLPAMNGIKTYLEEQSNKLFDMIIDELQNEIYLKYNRNPQEGAIAWQNIIHSSNPQLTS
A.nidulans 299 ENIGALADIRAYFENQESSITDIIVEELHDHLYLKSPYGVDR----WKPPAPETESNGVN
N.crassa 249 DNIGALSDLRSYLANQETALMDIIVEELHEHLYLKSPYCQER----WQNLA---KVQGIS
M.oryzae 276 DNIGALGDLRSYLANQETALMDILIEELHEHLYLKSPYCQER----WQYLA---KTQGHS
370 380 390 400 410 420
S.cerivisae 257 HNGFTSLENYLYNIVNIDIMEHSKTINKNLEQFI-----HDQSLNKGNIMLQENAATQAP
C.albicans 254 FVTLLDSKNLEQIIFNSANLDISEVVDFLTSPVKNFIVNQLPDLHAHNSKNDGVIDYKIL
A.nidulans 355 GAGAGASSWERPVYGFLARLDASKPMVE----------
N.crassa 302 HETYGDAPGVAPPHGILDTIDWEKSVAE----------
M.oryzae 329 NESFGETSTMAPPHAVLDVMDLEKAVQE----------
430 440 450 460 470 480
S.cerivisae 312 LAESRNQENEGFNRIGPILKTINNINKLPVAFNIITERAKEEIHNIIVKSTESIRSKHPS
C.albicans 314 LDSTSNPNTESFYYIYMILLTASKLNRLNQAVEVLLDTNQSELHGLINRTTEAVKSRNGH
A.nidulans 382 -DASRNPEADTFSYLQLLIEALNKMGHLDIAVDRIEQRLPVELFTVVDKTNAELDARYP-
N.crassa 329 -DPQKNPEADTFYYVTLIVEALNRLGRLETAVDMLKQRLPVELFAVVNETINDVDQKHPS
M.oryzae 356 -DPARNPEADTFYYISLVTESLNKLGRLETAMDTLKQRLPVELFAIVNETVNEVDQKHPS
490 500 510 520 530 540
S.cerivisae 372 LLKMATSLKND-NHFGLPVQDI------LSIILRECFWEIFLKLLYAIQCHRAIFEMSNI
C.albicans 374 ALSKLSKMQHLDHGSLFDVIVHGSFSDSAVVLMQDLFGSIFIRCLATFQRHKVITQIVTL
A.nidulans 440 -LPRCFMAQDGKTDSPTEMIQK------RGHVLSEFLWTLYAKFEAIAEGHRVVHDVIAA
N.crassa 389 SLRCGASGSHGLNIYGHRETRM------RADVIHDLLSTLYGKFEAIAEGHRVLHEAIKA
M.oryzae 416 SLRCGSSSSNGLHVYGSRETQL------RAEVIYDLLWTLYGKFEAIAEGQRVLHEYIKA
550 560 570 580 590 600
S.cerivisae 425 LQP----TSSAKPAF----------KFNKIWGKLLDEIELLLVRVINDPEL
C.albicans 434 LQEGKAPSTPKAVAESTPTFDSPQMGRPDTFHARNLFTIWKTIQKELKALMLNYIYDDHN
A.nidulans 494 IVEREGIPKSSSLAG----------GFKELWKLYQSEIRSLMHDVLATDGD
N.crassa 443 LIRREGAGNNSVLLG----------GFKELWNLYQNEIRALLHNVVTTDAD
M.oryzae 470 LIRREGAGNNSALLG----------SFKELWNLYQNEIRSLLHSVVTTDAD
610 620 630 640 650 660
S.cerivisae 462 IS----------SNNGSIKPINGATNNAPTLPKRKNPKIFSLEYNIEDNSSVKDQAFE
C.albicans 493 ----------YKLHSLADTTGATNRNKISNALGKKELFKEEDVTYNPSNKTTK--E
A.nidulans 535 SSIRPDEEADARRQFYSGYRDKNKARLPPLEKWSVSQK--LFKLSDAG-RTTQMKAEQNE
N.crassa 483 ----------VYQFSRTRPRGMGMNGRADSARDN--LFKESEVDAKSAEMASEYEA
M.oryzae 510 ----------VYQYN-QPKAGATANG--KALRQD--LFKEAETDAKAAEIVTEYEE
670 680 690 700 710 720
S.cerivisae 510 LKALLKDIFPGFSVSSN----------MDLDSIYVKDESFEQDEPLVPPS
C.albicans 538 ILDVLADVEPGYSISDD----------NNNGAIIETATEYVKHESFNATVEVLVPK
A.nidulans 592 LDEILRSSVPGLISKSE----------QKSDEDGPTDSRQGTG-HKILIEPS
N.crassa 528 LDSIIRAAVPGLTDSTRRDNKKGSLIIPRSEPITSRKSAGYGSGSSQQNSGTYKSLVEPS
M.oryzae 552 LDGIIRAAVPGLSDKTG-DKKSSAAAGGRVQ--QEKRNNGQGPDSGRQNGEIHKSLVEPS
730 740 750 760 770 780
S.cerivisae 549 -VFNMKVILDPFFLFTQSTSTIVESVLTQNTI-----SSLTFFDDYMNKSFLFKIQMTMD
C.albicans 584 NLFNMRIILEFFTLIPIDGSQRIFFDFEDEKTRGVHARTSFHFFEDFMKISFLSYLRNTIE
A.nidulans 632 -VFNMSLLLPPSLSFIQRLKDIVEVDSDMFTG-----SLTSFLDDFLVNVFLPQLDETVT
N.crassa 587 -VFNMSLLLPPTLTFLQRLKSIVEPGSDLATS-----TLTSFLDNFLVNVFQPQLDETLG
M.oryzae 608 -VFNMSLLLPPTLVFLQRLKGIVEPGSDLATS-----TLTSFLDNFLVNVFQPQLDETLG
790 800 810 820 830 840
S.cerivisae 604 YLFTVEVESNNPYALELSD----------ENHN---IFKTALD

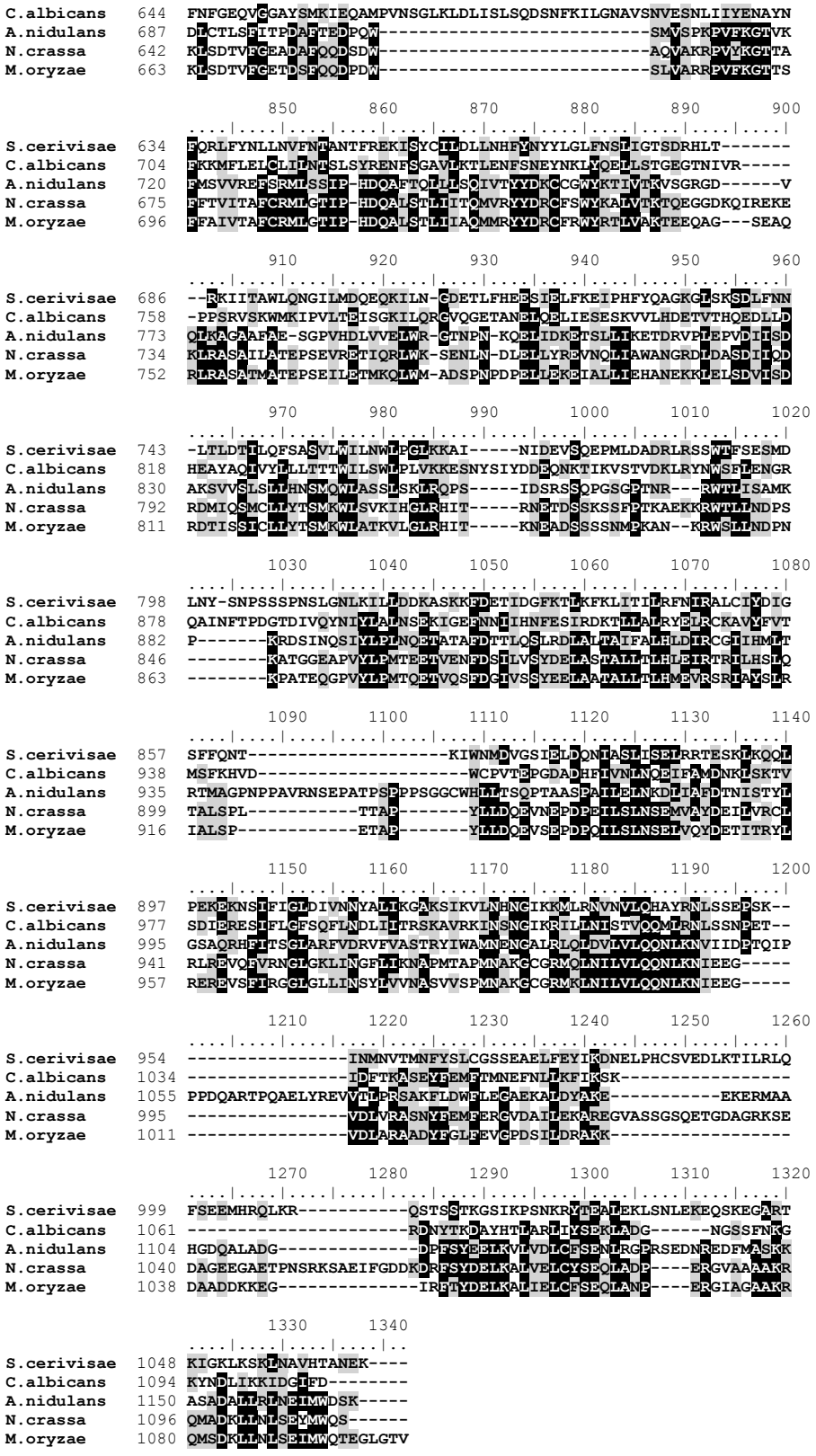

D. Sec3 protein sequence alignment

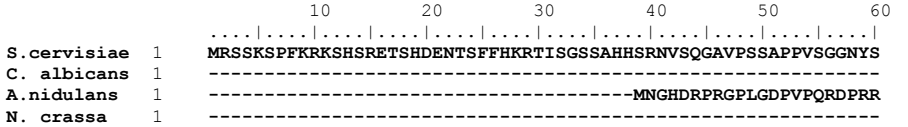

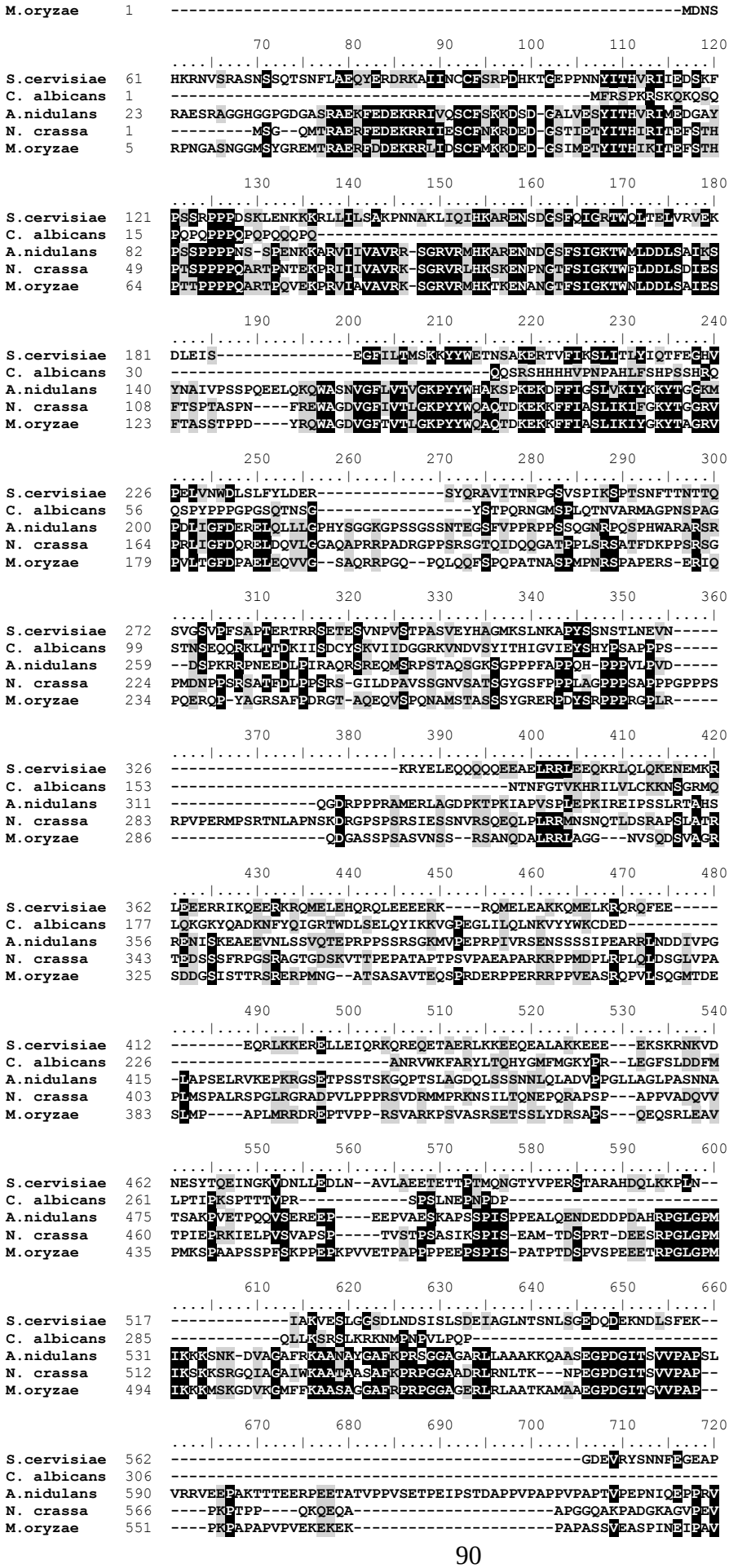
M.oryzae 1 ----------MDNS
70 80 90 100 110 120
S.cervisiae 61 HKRNVSRASNSSQTSNFLAEQYPRDRKAIINCCFSRPDHKTGEPPNNYITHVRIIEDSKF
C. albicans 1 ----------MFRSPKRSKQKQSQ
A.nidulans 23 RAESRAGGHGGPGDGASRAEKFEDEKRRIVQSCFSKKDSD-GALVESYITHVRIMEDGAY
N. crassa 1 ---------MSG--QMTRAERFEDEKRRIIESCFNKRDED-GSTIETYITHIRITEFSTH
M.oryzae 5 RPNGASNGGMSYGREMTRAERFDDEKRRLIDSCFMKKDED-GSIMETYITHIKITEFSTH
130 140 150 160 170 180
S.cervisiae 121 PSSRPPPPDSKLENKKKRLLILSAKPNNAKLIQIHKARENSDGSFQIGRTWQLTELVRVGK
C. albicans 15 PQPQPPPQPQPQQQPQ----------
A.nidulans 82 PSSPPPPNS-SPENKKARVIIVAVRR-SGRVRMHKARENNDGSFSIGKTWMLDDLSAIKS
N. crassa 49 PTSPPPPQARTPNTEKPRIIIVAVRK-SGRVRLHKSKENPNGTFSIGKTWFLDDLSDIES
M.oryzae 64 PTTPPPPQARTPQVEKPRVIAVAVRK-SGRVRMHKTKENANGTFSIGKTWNLDDLSAIES
190 200 210 220 230 240
S.cervisiae 181 DLEIS----------EGEILTMSKKYYWETNSAKERTVPIKSLITLYIQTFEGHV
C. albicans 30 ----------QQSRSHHHHVPNPAHLFSHPSSHRQ
A.nidulans 140 YNAIVPSSPQEELQKQWASNVGETVTVGKPYYWHAKSPKEKDFFIGSLVKIYKKYTGGKM
N. crassa 108 FTSPTASPN----FREWAGDVGPIVTLGKPYYWQAQTDKEKKFFIASLIKIFGKYTGGRV
M.oryzae 123 FTASSTPPD----YRQWAGDVGETVTLGKPYYWQAQTDKEKKFFIASLIKIYGKYTAGRV
250 260 270 280 290 300
S.cervisiae 226 PEIVNWDLSLFYLDER----------SYQRAVITNRPGSVSPIKSPTSNFTTNTTQ
C. albicans 56 QSPYPPPGPGSQTNSG----------YSTPQRNGMSPLQTNVARMAGPNSPAG
A.nidulans 200 PDIIGFDERELQLLLGPHYSGGKGPSSGSSNTEGSFVPPRPPSSQGNRPQSPHWARARSR
N. crassa 164 PRIIGFDQRELDQVLGGAQAPRRPADRGPPSRSGTQIDQQGATPPLSRSATFDKPPSRSG
M.oryzae 179 PVITGFDPAELEQVVG--SAQRRPGQ--PQLQQFSPQPATNASPMPNRSPAPERS-ERIQ
310 320 330 340 350 360
S.cervisiae 272 SVGSVPFSAPTERTRRSETESVNPVSTPASVEYHAGMKSLNKAPYSSNSTLNEVN-----
C. albicans 99 STNSEQQRKLTTDKIISDCYSKVIIDGGRKVNDVSYITHIGVIEYSHYPSAPPPS-----
A.nidulans 259 --DSPKRRPNEEDLDIRAQRSREQMSRPSTAQSGKSGPPPFAPPQH-PPPVLEVD-----
N. crassa 224 PMDNPPSRSATFDLPPSRS-GILDPAVSSGNVSATSGYGSFPPPLAGPPPSAPPPGPPPS
M.oryzae 234 PQERQP-YAGRSAFPDRGT-AQEQVSPQNAMSTASSSYGRERPDYSRPPPRGPLR-----
370 380 390 400 410 420
S.cervisiae 326 ----------KRYELEQQQQQEEAELRRLEEQKRLQLQKENEMKR
C. albicans 153 ----------NTNFGTVKHRILVLCKKNSGRMQ
A.nidulans 311 ----------QGDRPPPRAMERLAGDPKTPKIAPVSPLEPKIREIPSSLRTAHS
N. crassa 283 RPVPERMPSRTNLAPNSKDRGPSPSRSIESSNVRSQEQLPLRRMNSNQTLDSRAPSLAIR
M.oryzae 286 ----------QDGASSPSASVNSS--RSANQDALRRLAGG---NVSQDSVAQR
430 440 450 460 470 480
S.cervisiae 362 LEEERRIKQEERKRQMELEHQRQLEEEERK----RQMELEAKKQMELKRQRQFEE-----
C. albicans 177 LQKGKYQADKNFYQIGRTWDLSELQYIKKVGPEGLILQLNKVYYWKCDED----------
A.nidulans 356 RENISKEAEEVNLSSVQTEPRPPSSRSGKMVPEPRPIVRSENSSSSIPEARRINDDIVPG
N. crassa 343 TEDSSSFRPGSRAGTGDSKVTTPEPATAPTPSVPAEAPARKRPPMDPLRPLQLDSGLVPA
M.oryzae 325 SDDGSISTTRSRERPMNG--ATSASAVTEQSPRDERPPERRRPPVEASRQPVLSQGMTDE
490 500 510 520 530 540
S.cervisiae 412 --------EQRLKKERELLEIQRKQREQETAERLKKEEQEALAKKEEE---EKSKRNKVD
C. albicans 226 ----------ANRVWKFARYLTQHYGMFMGKYPR--LEGFSLDDFM
A.nidulans 415 -LAPSELRVKEPKRGSPTPSSTSKGQPTSLAGDQLSSSNNLQLADVPPGLLAGLPASNNA
N. crassa 403 PLMSPALRSPGLRGRADPVLPPPRSVDRMMPRKNSILTQNEPQRAPSP---APPVADQVV
M.oryzae 383 SLMP----APLMRRDREPTVPP-RSVARKPSVASRSETSSLYDRSAPS---QEQSRLEAV
550 560 570 580 590 600
S.cervisiae 462 NESYTQEINGKVDNLLEDLN--AVLAEETETTPTMQNGTYVPERSTARAHDQLKKPLN--
C. albicans 261 LPTIPKSPTTTVPR----------SPSLNEPNPDP----------
A.nidulans 475 TSAKPVETPQQVSEREEP----EEPVAESKAPSSPISPPEALQENDEDDPDAHRPGLGPM
N. crassa 460 TPIEPRKIELPVSVAPSP-----TVSTPSASIKSPIS-EAM-TDSPRT-DEESRPGLGPM
M.oryzae 435 PMKSPAAPSSPFSKPPEPKPVVETPAPPPEEPSPIS-PATPTDSPVSPEEETRPGLGPM
610 620 630 640 650 660
S.cervisiae 517 ----------IAKVESLGGSDLNDSISLSDEIAGLNTSNLSGEDQDEKNDLSFEK--
C. albicans 285 ----------QLLKSRSLKRKNMPNEVLPQP----------
A.nidulans 531 IKKKSNK-DVAGAFRKAANAYGAEKPRSGGAGARLLAAAKKQAASEGPDGITSVVPAESL
N. crassa 512 IKSKKSRGQIAGAIWKAATAASAEKPRPGGAADRLRNLTK---NPEGPDGITSVVPAP--
M.oryzae 494 IKKKMSKGDVKGMFFKAASAGGAERPRPGGAGERLRLAATKAMAAEGPDGITGVVPAP--
670 680 690 700 710 720
S.cervisiae 562 ----------GDEVRYSNNFEGEAP
C. albicans 306 ----------
A.nidulans 590 VRRVEEPAKTTTEERPEETATVPPVSETPEIPSTDAPPVPAPPVPAPTVPEPNIQEPPRV
N. crassa 566 ----PKPTPP----QKQEQA----------APGGQAKPADGKAGVPEV
M.oryzae 551 ----PKPAPAPVPVEKEKEK----------PAPASSVEASPINEIPAV

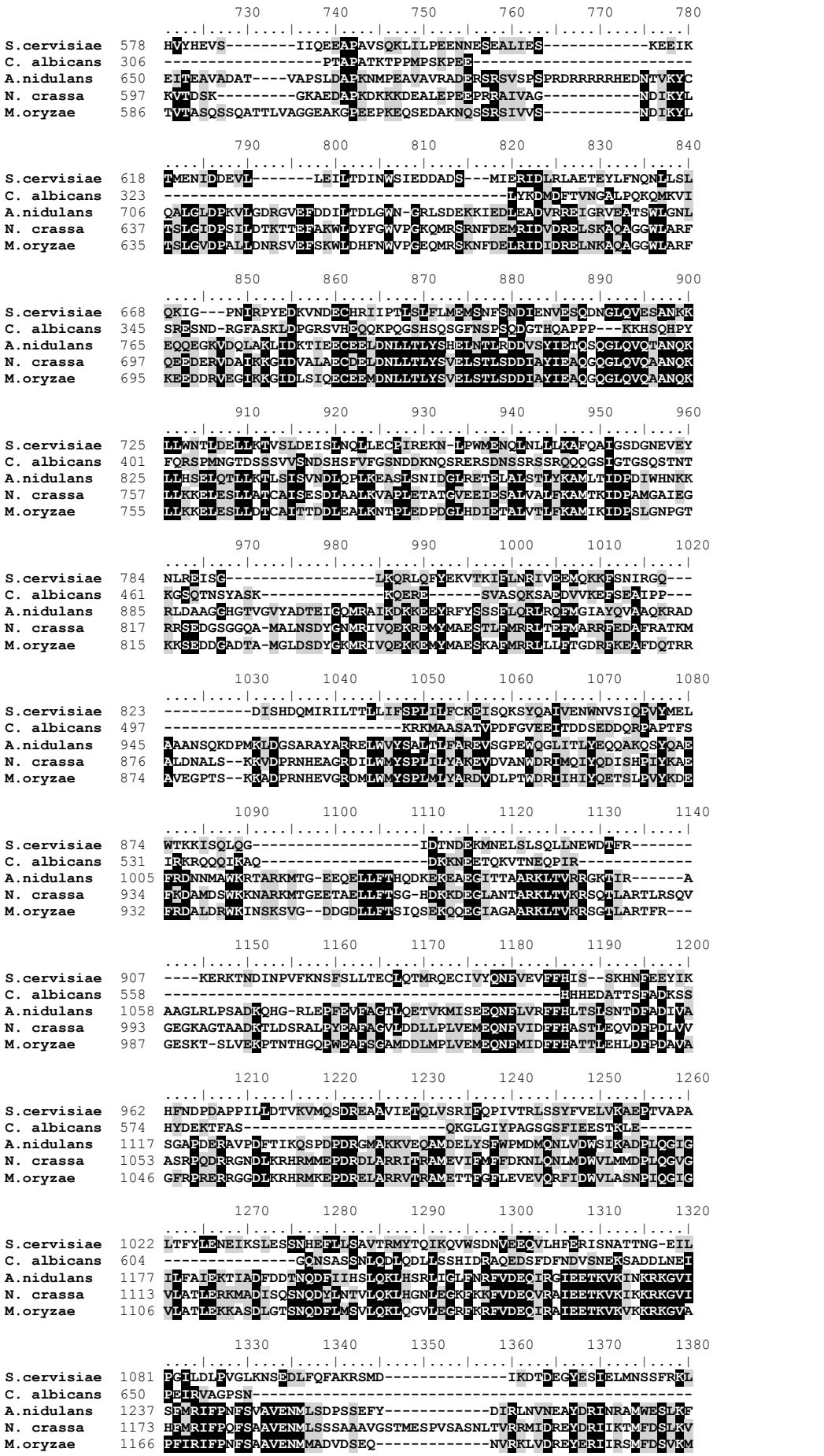
S.cervisiae
C. albicans
A.nidulans
N. crassa
M.oryzae

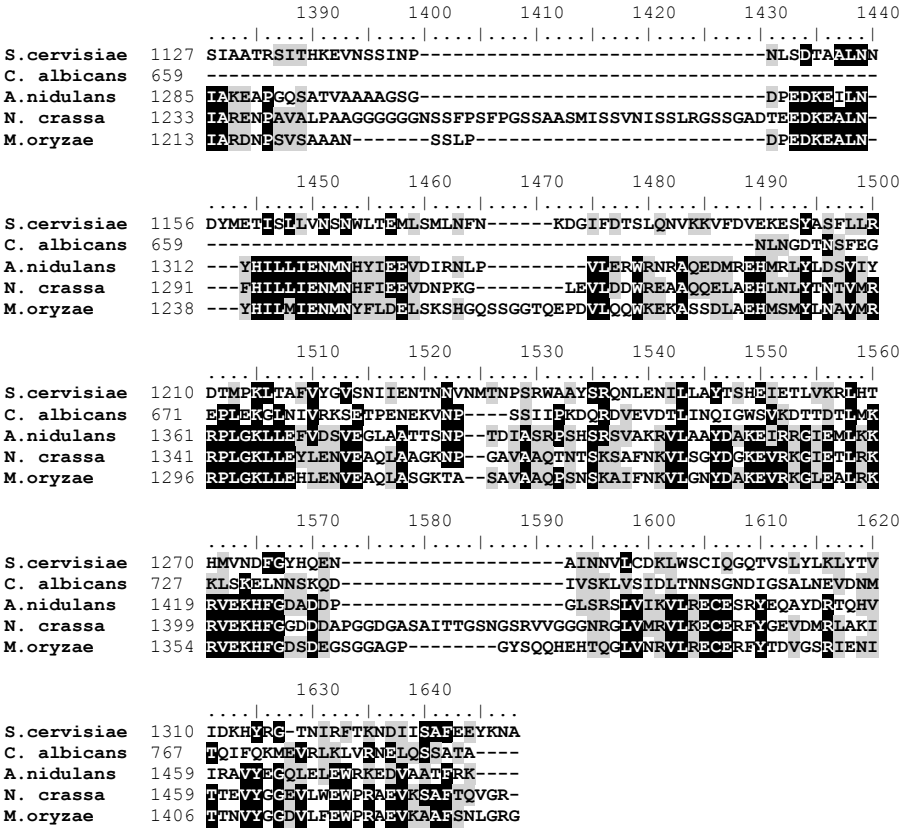

E. Exo84 protein sequence alignment

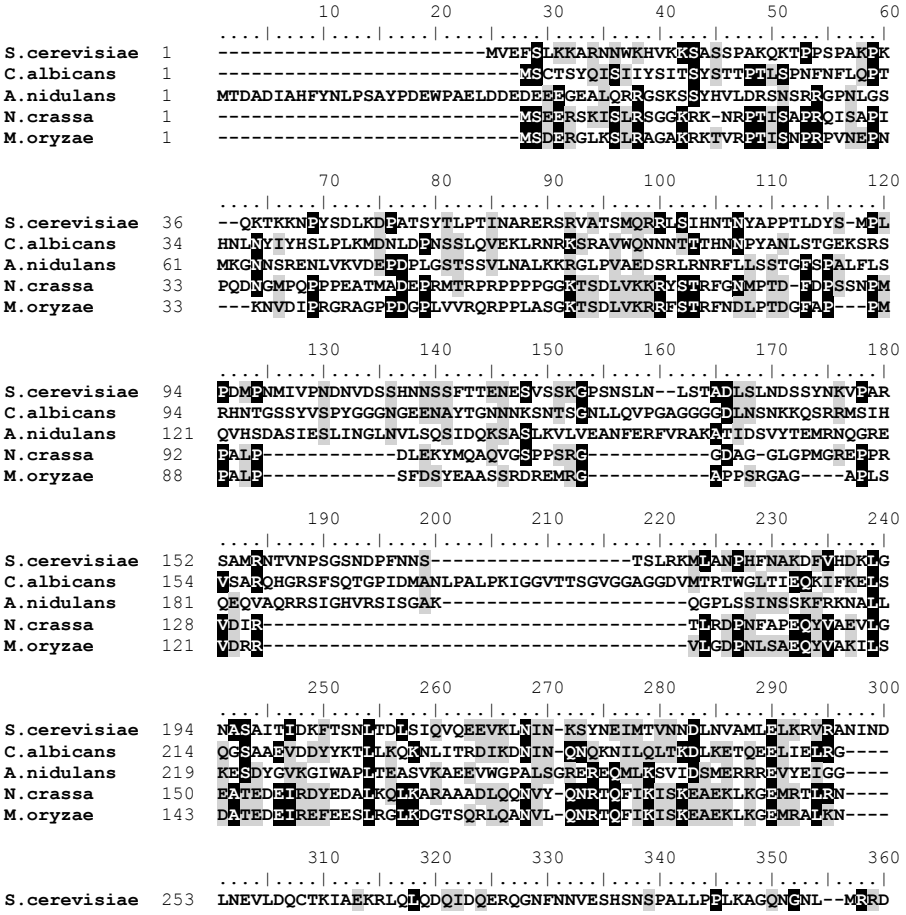

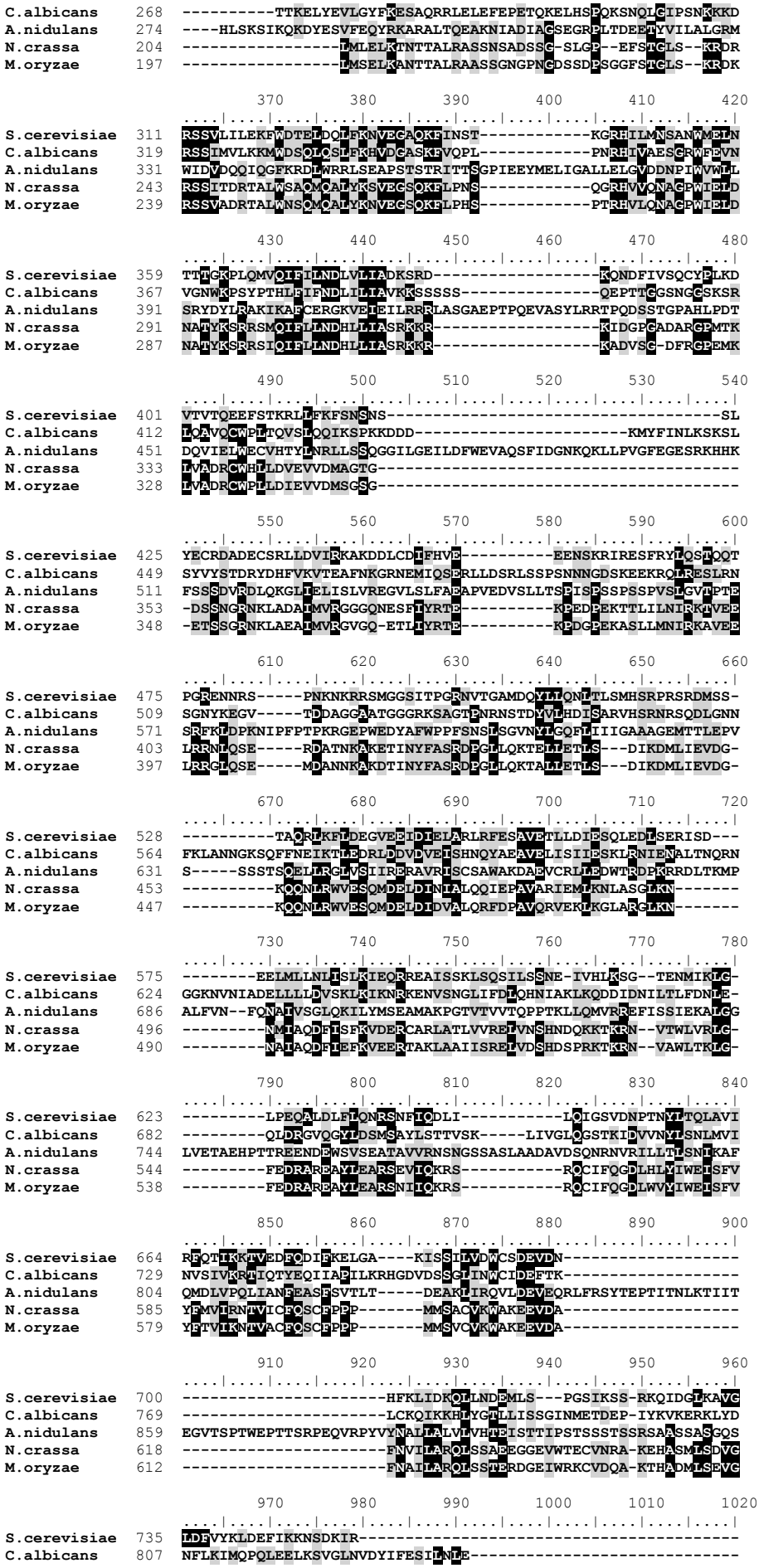
C.albicans 268 ----------TTKELYEVLGYFKESAQRRLELEFEPETQKELHSPQKSNQLGIPSNKKKD
A.nidulans 274 ----HLSKSIKQKDYESVFEQYRKARALTQEAKNIADIACSEGRPLTDEETYVILALGRM
N.crassa 204 ----------LMLELKTNTTALRASSNSADSSG-SLGP--EFSTGLS--KRDR
M.oryzae 197 ----------LMSELKANTTALRAASSGNGPNGDSSDPSGGFSTGLS--KRDK
370 380 390 400 410 420
S.cerevisiae 311 RSSVLILEKFWDTELDQLFKNVEGAQKEINST----------KGRHILMNSANWMELN
C.albicans 319 RSSIMVLKKMWDSQLQSLFKHVDGASKEVQPL----------PNRHIVAESGRWFEVN
A.nidulans 331 WIDVDQQIQGFKRDLWRRLSEAPSTSTRITTSGPIEEYMELIGALLELGVDDNPIWWLL
N.crassa 243 RSSITDRTALWSAQMQALYKSVEGSQKELPNS----------QGRHVVQNAGPWIELD
M.oryzae 239 RSSVADRTALWNSQMQALYKNVEGSQKELPHS----------PTRHVLQNAGPWIELD
430 440 450 460 470 480
S.cerevisiae 359 TTTGKPLQMVQIFILNDLVLIADKSRD----------KQNDFIVSQCYPLKD
C.albicans 367 VGNWKPSYPTHLEIFNDLILIAVKKSSSSS----------QEPTTGSNGGSKSR
A.nidulans 391 SRYDYLRAKIKAFCERGKVEIEILRRRLASGAEPTPQEVASYLRRTPQDSSTGPAHLPDT
N.crassa 291 NATYKSRRSMQIFLLNDHLLIASRKKR----------KIDGPGADARGEMTK
M.oryzae 287 NATYKSRRSIQIFLLNDHLLIASRKKR----------KADVSG-DFRGEEMK
490 500 510 520 530 540
S.cerevisiae 401 VTVTQEEFSTKRLLFKFSNSNS----------SL
C.albicans 412 LQAVQCWPLTQVSLQQIKSPKKDDD----------KMYFINLKSKSL
A.nidulans 451 DQVIELWECVHTYLNRLLSSQGGILGEILDFWEVAQSFIDGNKQKLLPVGFEGESRKHHK
N.crassa 333 LVADRCWHLLDVEVVDMAGTG----------
M.oryzae 328 LVADRCWPLLDIEVVDMSGSG----------
550 560 570 580 590 600
S.cerevisiae 425 YECRDADECSRLLDVIKKADDLCDIFHVE----------EENSKRIRESFRYLQSTQQT
C.albicans 449 SYVYSTDRYDHFVKVTEAFNKGRNEMIQSERLLDSRLSSPSNNNGDSKEEKRQLRESLRN
A.nidulans 511 FSSSDVRDLQKGLIELISLVREGVLSLFAEAPVEDVSLLTSPISPSSPSSPVSLGVTPTE
N.crassa 353 -DSSNGRNKLADAIMVRGGGQNESFIYRTE----------KPEDPEKTTLILNIRKLVEE
M.oryzae 348 -ETSSGRNKLAEAIMVRGVGQ-ETLIYRTE----------KPDGPEKASLLMNIRKAVEE
610 620 630 640 650 660
S.cerevisiae 475 PGRENNRS-----PNKNKRRSMGGSITPGRNVTGAMDQYLLQNLTLSMHSRPRSRDMSS-
C.albicans 509 SGNYKEGV-----TDDAGGAATGGGRKSAGTPNRNSTDYVLHDISARVHSRNRSQDLGNN
A.nidulans 571 SRFKLDPKNIPFPTPKRGEPWEDYAFWPPFSNSLSGVNYLGQFLIIIGAAAGEMTTLEPV
N.crassa 403 LRRNLQSE-----RDATNKAKETINYFASRDPGLLQKTELLETLS---DIKDMLIEVDG-
M.oryzae 397 LRRGLQSE-----MDANNKAKDTINYFASRDPGLLQKTALLETLS---DIKDMLIEVDG-
670 680 690 700 710 720
S.cerevisiae 528 ----------TAQRLKFLDEGVEEIDIELARLRFESAVETLLDIESQLEDLSERISD---
C.albicans 564 FKLANNGKSQFFNEIKTLEDRLDDVDVEISHNQYAEAVELISIIESKLRNIENALTNQRN
A.nidulans 631 S-----SSSTSQELLRGLVSIIRERAVRISCSAWAKDAEVCRLLEDWTRDPKRRDLTKMP
N.crassa 453 ----------KQQNLRWVESQMDELDINIALQQIEPAVARIEMIKNLASGLKN-------
M.oryzae 447 ----------KQQNLRWVESQMDELDIDVALQRFDPAVQRVEKLKGLARGLKN-------
730 740 750 760 770 780
S.cerevisiae 575 --------EELMLLNLISLKIEQRREAISSKLSQSILSSNE-IVHLKSG--TENMIKLG-
C.albicans 624 GGKNVNIADELLLLDVSKLKIKNRKENVSNGLIFDLQHNIAKLKQDDIDNILTLFDNLE-
A.nidulans 686 ALFVN--FQNAIVSGLQKILYMSEAMAKPGTVTVVTQPPTKLLQMVREFISSIEKALGG
N.crassa 496 ---------NMIAQDFISFKVDERCARLATLVVRELVNSHNDQKKTKRN--VTWLVRLG-
M.oryzae 490 ---------NAIAQDFIEFKVEERTAKLAAIISRELVDSHDSPRKTKRN--VAWLTKLG-
790 800 810 820 830 840
S.cerevisiae 623 ---------LPEQALDLFLQNRSNFIQDLI----------LQIGSVDNPTNYLTQLAVI
C.albicans 682 ---------QLDRGVQGYLDSMSAYLSTTVSK-----LIVGLQGSTKIDVVNYLSNLMVI
A.nidulans 744 LVETAEHPTTREENDEWSVSEATAVVRNSNGSSASLAADAVDSQNRNVRILLTLSNIKAF
N.crassa 544 ---------FEDRARFAYLEARSEVIQKRS----------RQCIFQGDLHLVIWEISFV
M.oryzae 538 ---------FEDRARFAYLEARSNIIQKRS----------RQCIFQGDLWVYIWEISFV
850 860 870 880 890 900
S.cerevisiae 664 RLQTIKKTVEDFQDIFKELGA----KISSILVDWCSDEVDN----------
C.albicans 729 NVSIVKRTIQTYEQIIAFILKRHGDVDSSGLINWCIDEFTK----------
A.nidulans 804 QMDLVPQLIANFEASFSVTLT-----DEAKLIRQVLDEVEQRLFRSYTEPTITNLKTIIT
N.crassa 585 YFMVIRNTVICFQSCFPFP-------MMSACVKWAKEEVDA----------
M.oryzae 579 YFTVIKNTVACFQSCFPFP-------MMSVCVKWAKEEVDA----------
910 920 930 940 950 960
S.cerevisiae 700 ----------HFKLIDKQLLNDFMLS---PGSIKSS-RKQIDGLKAVG
C.albicans 769 ----------LCKQIKKHLYGTLLISSGINMETDEP-IYKVKERKLYD
A.nidulans 859 EGVTSPTWEPTTSRPEQVRPYVYNALLALVLVHTFISTTIPSTSSSTSSRSAASSASGQS
N.crassa 618 ----------FNVILARQLSSAEEGGEVWTECVNRA-KEHASMLSDVG
M.oryzae 612 ----------FNAILARQLSSTERDGEIWRKCVDQA-KTHADMLSFVG
970 980 990 1000 1010 1020
S.cerevisiae 735 LDFVYKLDEFIKKNSDKIR----------
C.albicans 807 NFLKIMQPQLEELKSVGLNVDYIFESILNLE----------

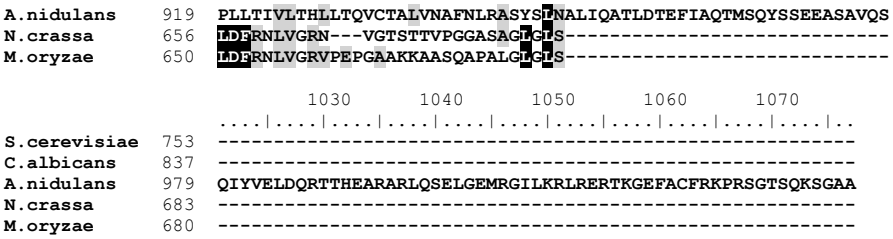

F. Sec5 protein sequence alignment

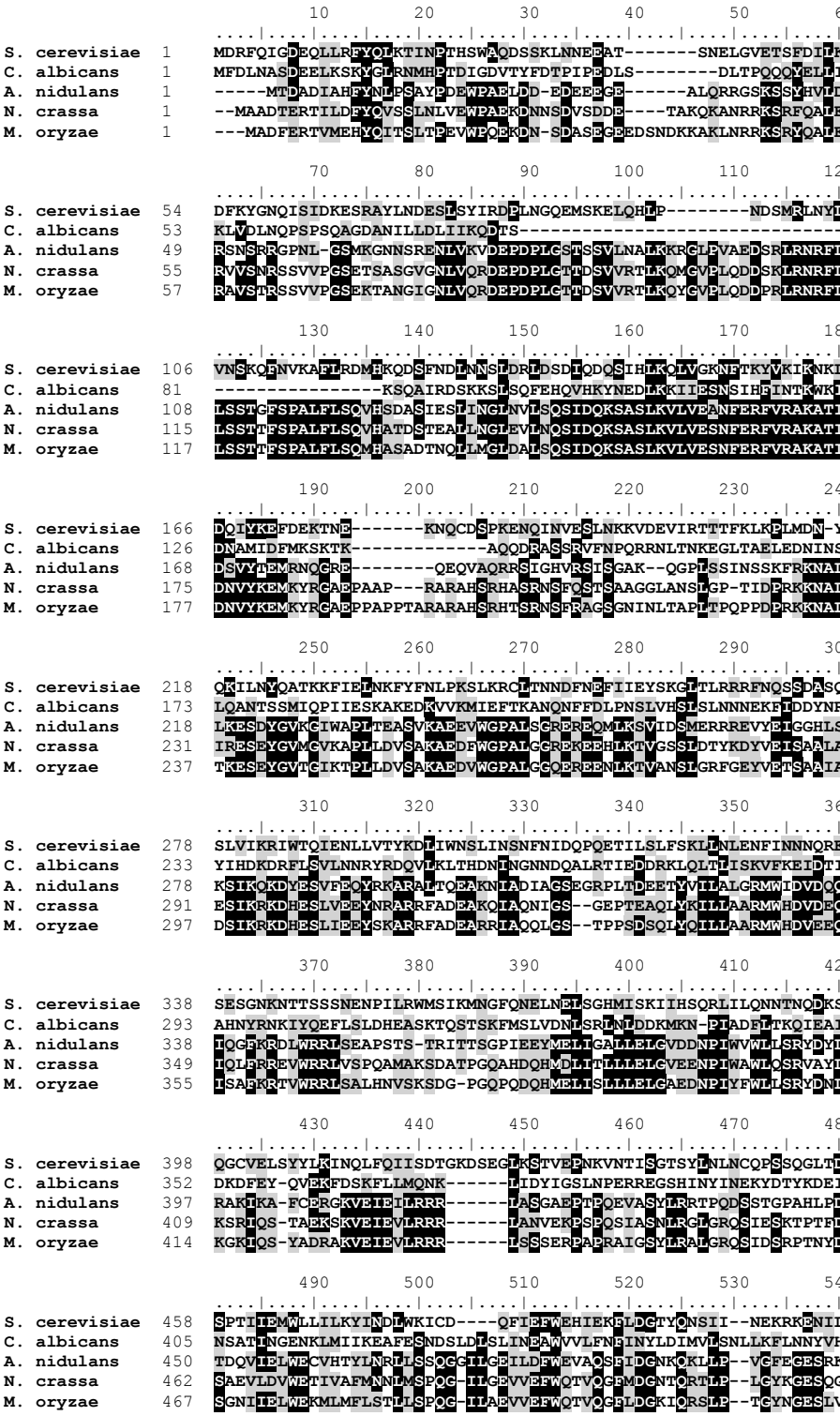

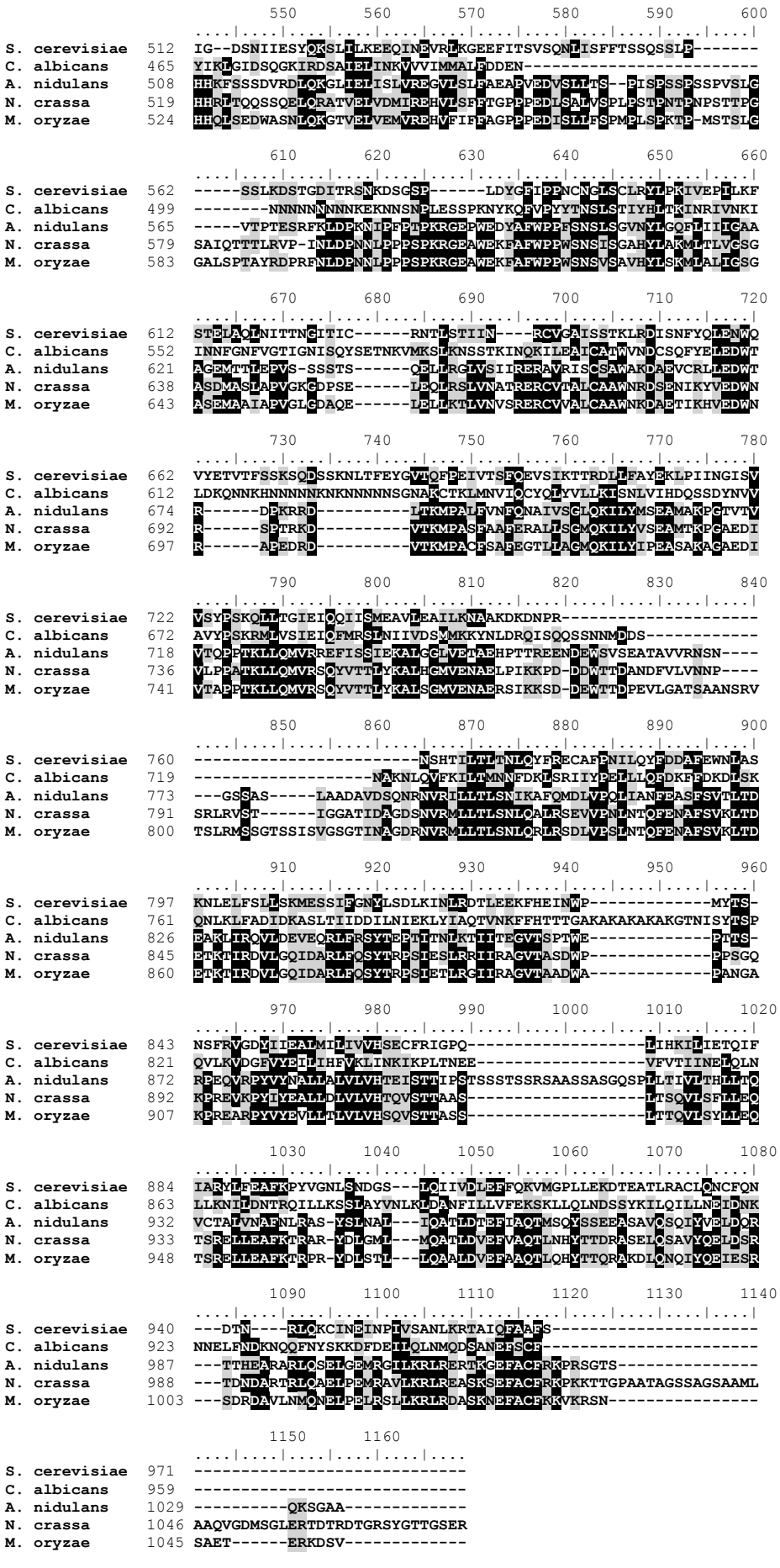
S. cerevisiae
C. albicans
A. nidulans
N. crassa
M. oryzae

G. Sec6 protein sequence alignment

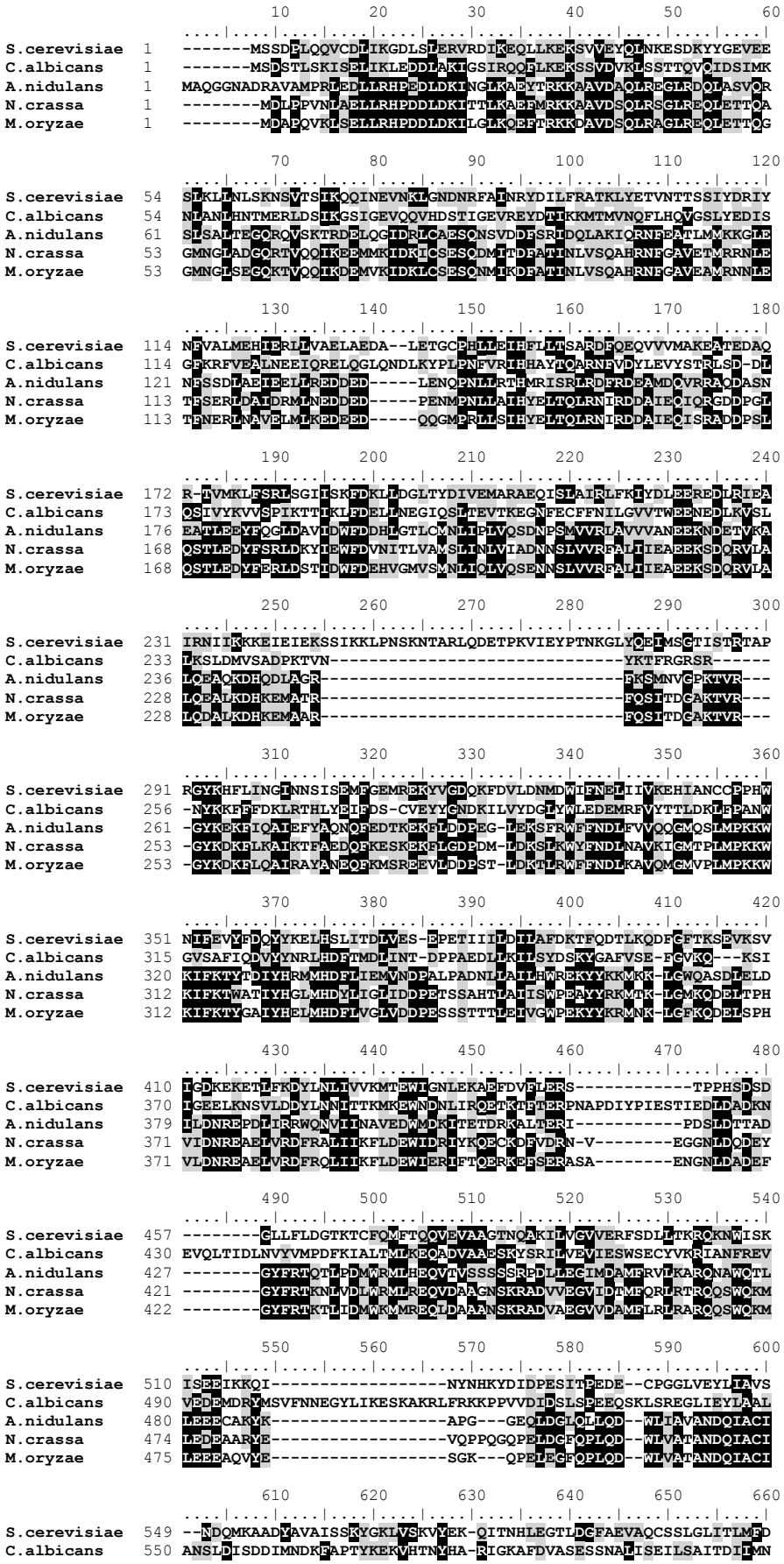

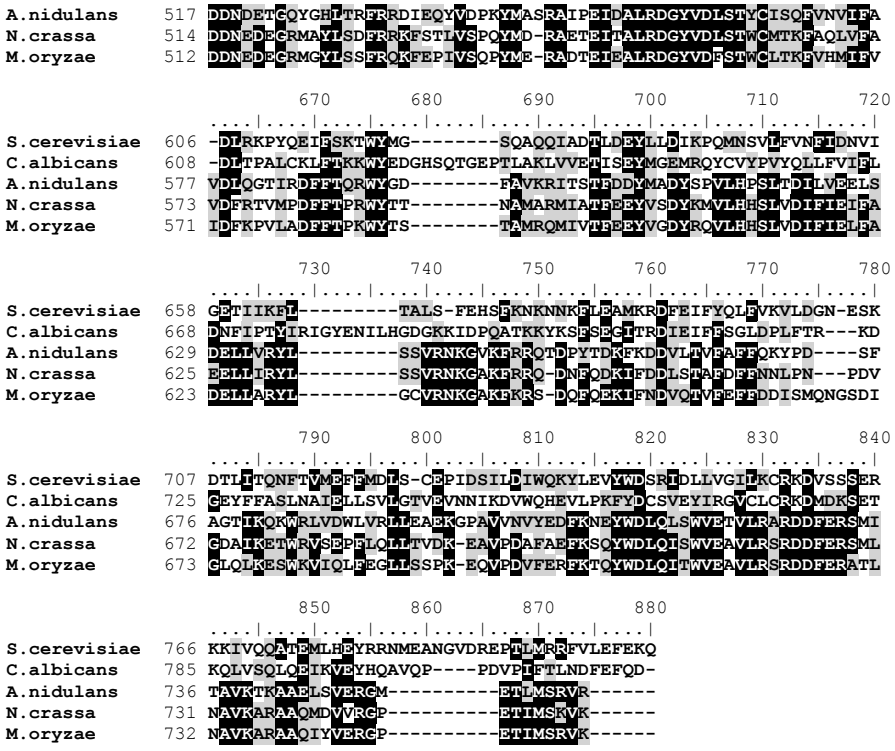

Figure 3.3 Multiple alignment of the predicated amino acid sequences.

Amino acid sequences for proteins involved in the secretory pathways in *M. oryzae* and other fungi were aligned using ClustalW programme (Thompson et al, 1994) in BioEdit sequence alignment editor version *7.1.3.0* software (Hall, 1999). Amino acids highlighted in a black background are identical and amino acids in a light grey background are similar. Gaps in the alignment are indicated by dashes. The putative homologus amino acid sequences are aligned *S. cerevisiae, C. albicans, A. nidulans, N. crassa* and *M. oryzae*, respectively. (A) Exo70 (MGG_01760.6) is aligned with YJL085W, orf19.6512, AN6210 and NCU08012. (B) Sec15 (MGG_00471.6) is aligned with YGL233W, orf19.1418, AN6493 and NCU00117. (C) Sec8 (MGG_03985.6) is aligned with YPR055W, orf19.3647, AN11007 and NCU04190. (D) Sec3 (MGG_03323.6) is aligned with YER008C, orf19.2911, AN0462 and NCU09869. (E) Exo84 (MGG_06098.6) is aligned with YBR102C, orf19.135, AN1002 and NCU06631. (F) Sec5 (MGG_7150.6) is aligned with YDR166C, orf19.74, AN1002 and NCU07698. (G) Sec6 (MGG_03235.6) is aligned with YIL068C, orf19.5463, AN1988 and NCU03341.

3.3.3 Phylogenetic tree of fungal exocyst subunits

Predicated amino acids sequence of all *M. oryzae* exocyst subunits were (Section 3.3.2) aligned with a range of fungi including *Saccharomyces cerevisiae, Candida albicans, Neurospora crassa, Colletotrichum higginsianum, Aspergillus niger, Aspergillus nidulans, Aspergillus fumigatus, Botryotinia fuckeliana, Sclerotinia sclerotiorum, Aspergillus oryzae* and *Zymoseptoria tritici*. Phylogenetic trees were then constructed using the Maximum Likelihood algorithm (Felsenstein, 1981) using the phylogenetic analysis program PhyML (Dereeper et al, 2008), supported by a bootstrap value of 100 resampling of the data (**Figure 3.4**).

Exocyst subunits from *S. cerevisiae* and *C. albicans* always grouped together and different from the filamentous fungi. This is incongruous with the phylogeny but mirrors their morphogenetic separateness. *M. oryzae* exocyst subunits clustered with those of *C. higginsianum* except Sec3, Sec8 and Sec15, which clustered with *N. crassa* (**Figure 3.4**). These results demonstrate that the exocyst subunits in filamentous fungi are conserved and distinct from yeasts.

A) Exo70

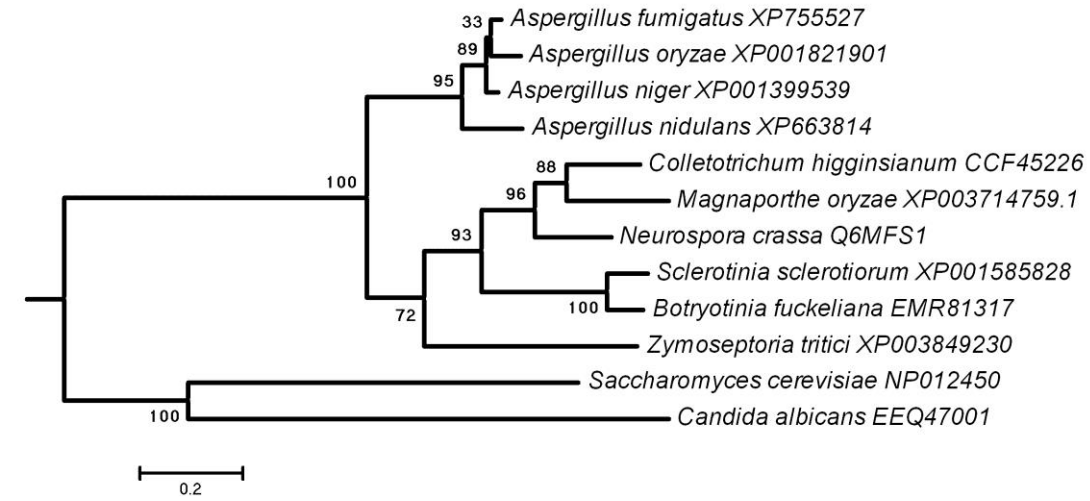

B) Exo84

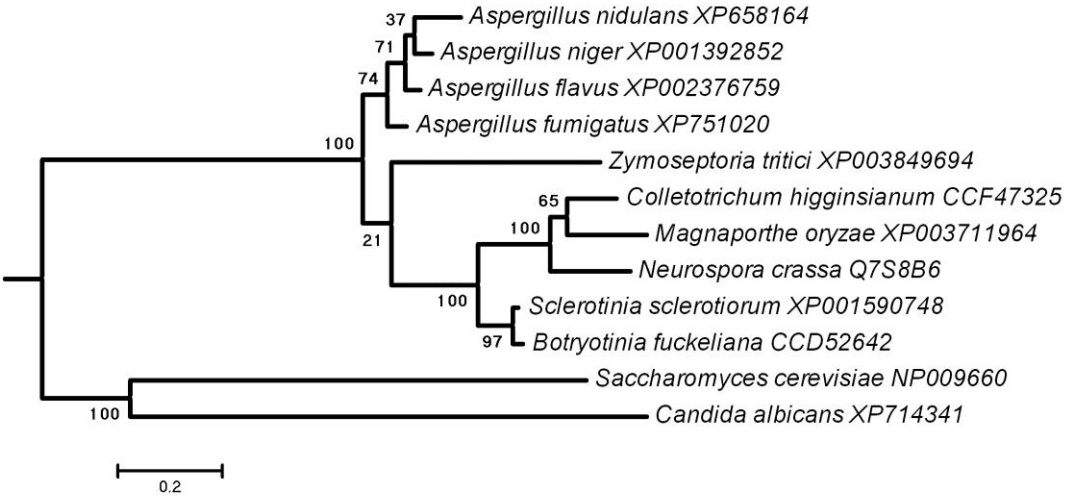

C) Sec3

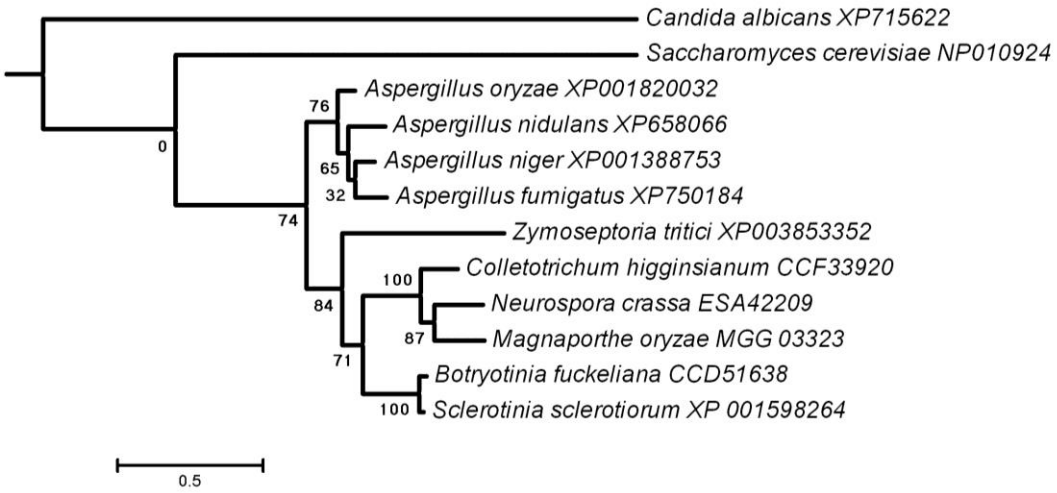
Candida albicans XP715622
Saccharomyces cerevisiae NP010924
Aspergillus oryzae XP001820032
Aspergillus nidulans XP658066
Aspergillus niger XP001388753
Aspergillus fumigatus XP750184
Zymoseptoria tritici XP003853352
Colletotrichum higginsianum CCF33920
Neurospora crassa ESA42209
Magnaporthe oryzae MGG 03323
Botryotinia fuckeliana CCD51638
Sclerotinia sclerotiorum XP 001598264
0
76
65
32
74
100
84
87
71
100
0.5

D) Sec5

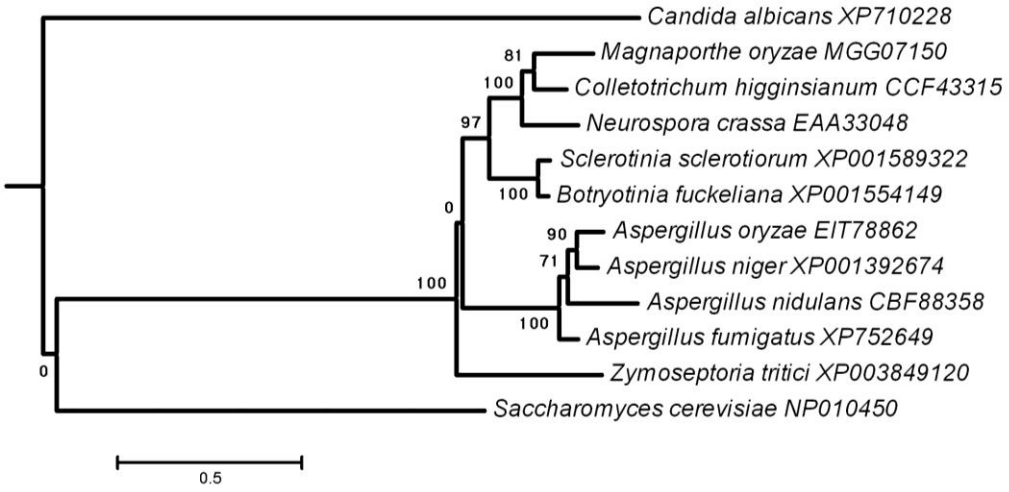
Candida albicans XP710228
Magnaporthe oryzae MGG07150
Colletotrichum higginsianum CCF43315
Neurospora crassa EAA33048
Sclerotinia sclerotiorum XP001589322
Botryotinia fuckeliana XP001554149
Aspergillus oryzae EIT78862
Aspergillus niger XP001392674
Aspergillus nidulans CBF88358
Aspergillus fumigatus XP752649
Zymoseptoria tritici XP003849120
Saccharomyces cerevisiae NP010450
81
100
97
100
0
90
71
100
100
0
0.5

E) Sec6

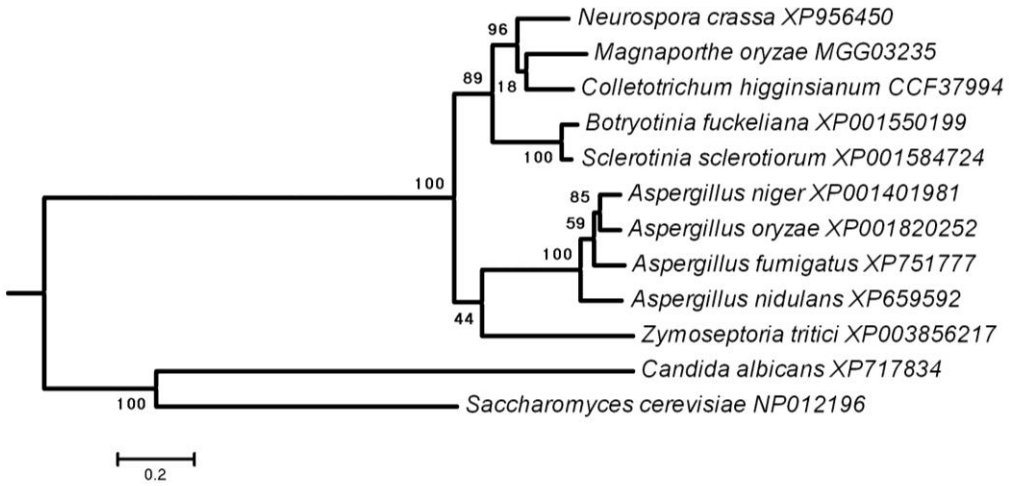
Neurospora crassa XP956450
Magnaporthe oryzae MGG03235
Colletotrichum higginsianum CCF37994
Botryotinia fuckeliana XP001550199
Sclerotinia sclerotiorum XP001584724
Aspergillus niger XP001401981
Aspergillus oryzae XP001820252
Aspergillus fumigatus XP751777
Aspergillus nidulans XP659592
Zymoseptoria tritici XP003856217
Candida albicans XP717834
Saccharomyces cerevisiae NP012196
96
89
18
100
100
85
59
100
44
100
0.2

F) Sec8

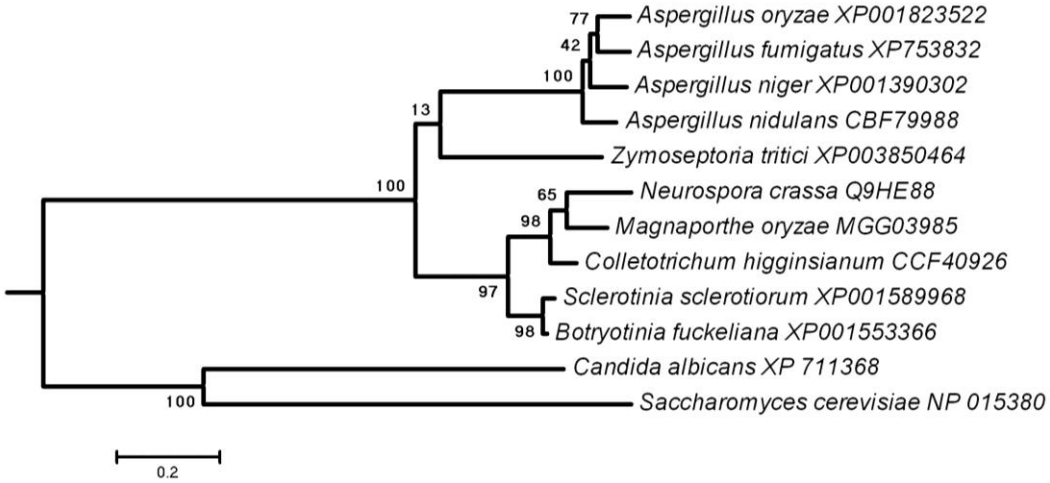
Aspergillus oryzae XP001823522
Aspergillus fumigatus XP753832
Aspergillus niger XP001390302
Aspergillus nidulans CBF79988
Zymoseptoria tritici XP003850464
Neurospora crassa Q9HE88
Magnaporthe oryzae MGG03985
Colletotrichum higginsianum CCF40926
Sclerotinia sclerotiorum XP001589968
Botryotinia fuckeliana XP001553366
Candida albicans XP 711368
Saccharomyces cerevisiae NP 015380
77
42
100
13
100
65
98
97
98
100
0.2

G) Sec10

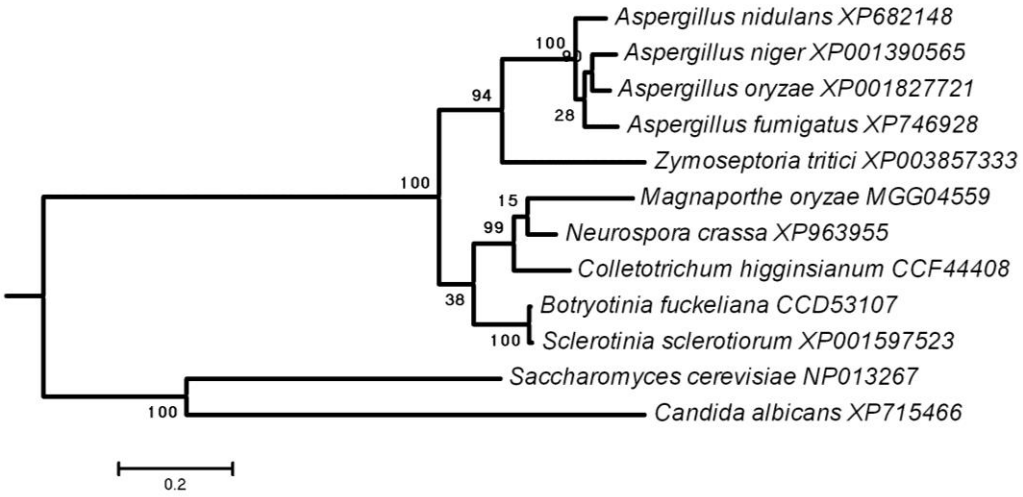

H) Sec15

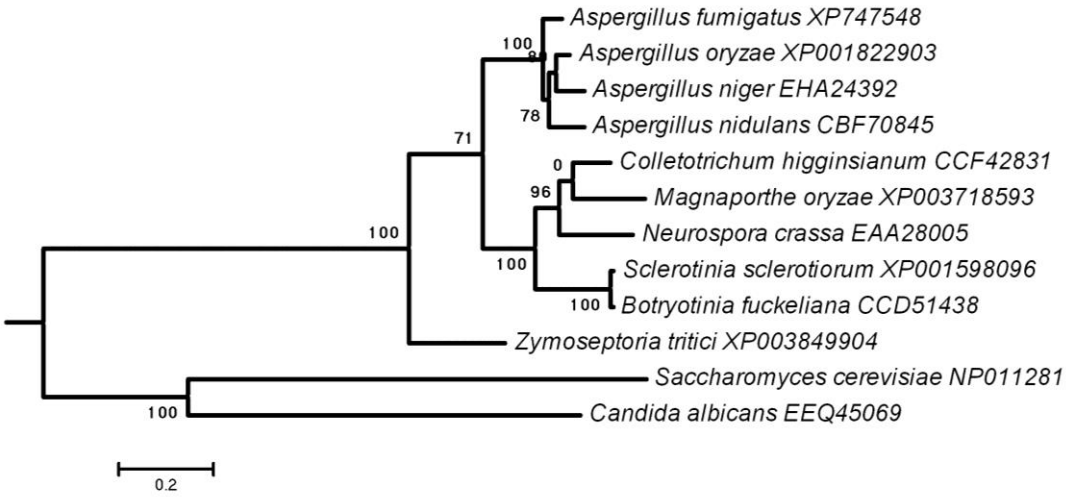

Figure 3.4 Phylogenetic analysis of predicted exocyst sub-units protein from a range of fungi.

Phylogenetic trees were constructed using the maximum likelihood algorithm (Felsenstein, 1981), for exocyst subunits Exo70, Exo84, Sec3, Sec5, Sec6, Sec8, Sec10 and Sec15 are shown **A)** to **H)**, respectively. Amino acid sequences were used from publicly available genome databases at NCBI. Phylogenetic trees were constructed with a re-sampling bootstrap value of 100. Branch strength support is indicated re-smapling values of 100. Accession numbers of the proteins are indicated after the name of the fungal species.

3.3.4 Generation of C-terminal translational fusion vectors

To investigate the sub-cellular localization of the exocyst complex in *M. oryzae*, C-terminal GFP fusion constructs were generated under control of the native promoter of the genes being studied. Fusion constructs for all the exocyst subunits (Sec3, Sec5, Sec6, Sec8, Sec15, Sec10, Exo70 and Exo84) and the t-SNARE Sec9 were constructed through C-terminal translational GFP fusions. For example, the Sec6:GFP construct was generated by amplifying a 3.7 kb fragment from *M. oryzae* genomic DNA, containing the coding region 2.2 kb and 1.5 kb promoter with primer pair Sec6.SUR-F and Sec6.GFP-R (**Table 3.1**). The Sec6.SUR-F primer was designed with 30 bp overhangs complementary in nucleotide sequence to the sulphonylurea resistance gene cassette (Sweigard et al, 1997) while the Sec6-GFP-R primer was designed to exclude the translational stop codon of Sec6 and included a 30 bp overhang complementary to the sequence of the GFP encoding gene. Similarly, the forward primer (Sur.Vec-F) of the sulphonylurea resistance cassette (acetolactate synthase, *ILV1*) (Sweigard et al, 1997), and the reverse primer (TrpC.Vec-R) of the terminator have 30 bp overhangs complementary to the vector sequence (**Table 3.1**). A schematic scheme of the cloning strategy for Sec6:GFP is shown in **Figure 3.6A**. The PCR amplified fragments of Sec6, *ILV1* and GFP-TrpC were then cloned into pNEB-Nat-Yeast cloning vector (**Figure 3.5**), digested with *Hind*III and *Sac*I. Positive clones were confirmed by colony PCR by using specific primers and then verified by DNA sequencing. The Sec6:GFP construct was introduced into the wild type strain Guy11 (Nottegham & Silue, 1992) as described in Section 2.5 and sulphonylurea resistant transformants were selected. Transformants were then screened for GFP using an Olympus IX81 inverted microscope.

Sec6:GFP expressing transformants were than confirm by Southern blot analysis for single copy insertion. Genomic DNA was extracted from seven transformants, digested

with *Eco*RI restriction enzyme and fractionated through gel electrophoresis. Fractionated DNA was transferred to a Hybond-N membrane (Amersham) and probed with 720 bp GFP fragment. Single copy ectopic insertion of Sec6:GFP was observed in two transformants , as shown in **Figure 3.7**.

Constructs for other exocyst subunits (Sec3, Sec5, Sec8, Sec10, Sec15, Exo70 and Exo84) and a t-SNARE Sec9 were designed in the same way as the Sec6:GFP vector.

3.3.5 Generation of N-terminal translational fusion vectors

N-terminal translational fusions were generated for Sec4, Cdc42 and Rac1 genes based on previous analysis in *C. albicans* (Court & Sudbery, 2007; Jones & Sudbery, 2010; Sudbery, 2011). The GFP:Sec4 vector was constructed by first amplifying a 1.7 kb fragment of native promoter with primer pair Sec4.Pro-Sur.F and Sec4.Pro-GFP.R, 1.8 kb fragment, including 844 bp Sec4 coding sequence, was amplified with primer pair Sec4.Orf-GFP.F and Sec4.Ter.R (**Figure 3.6B**). The fragment also includes the native terminator of the Sec4 gene. The PCR-amplified GFP fragment was then cloned between the promoter and the coding region of Sec4 (**Figure 3.6B**). Subsequent selection and verification steps were as described in Section 3.3.4. Constructs for GFP:Cdc42 and GFP:Rac1 were engineered using the same strategy as GFP:Sec4 vector and were then transformed into *M. oryzae* Guy11 strain.

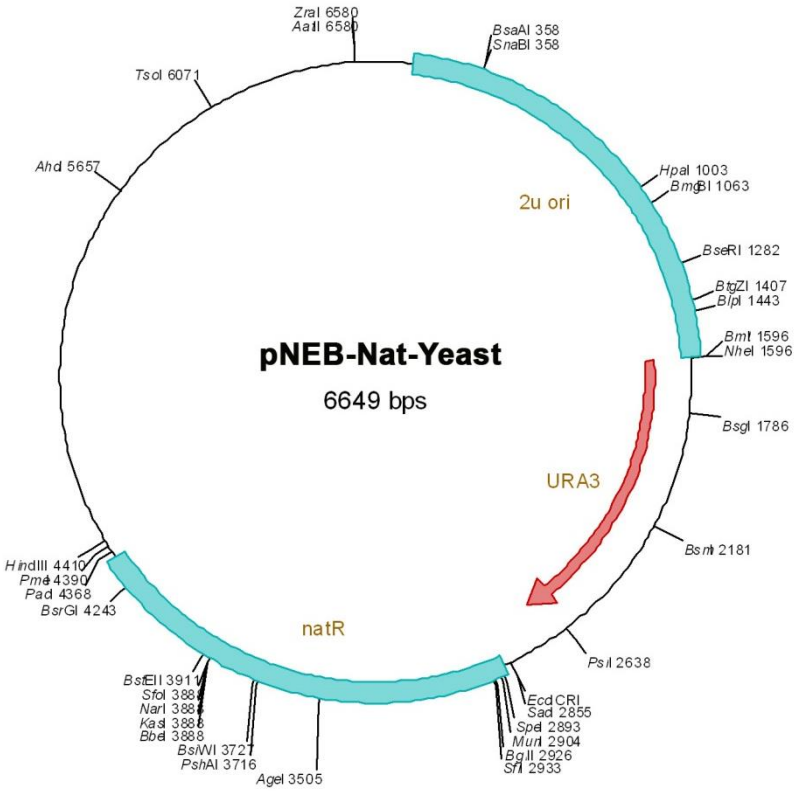

Figure 3.5 Map of the pNEB-Nat-Yeast vector used for the construction of all the GFP translation fusion constructs.

The yeast vector was linearized via restriction digestion with *Hind*III and *Sac*I enzymes. This linearized vector was used for yeast recombination cloning.

A.

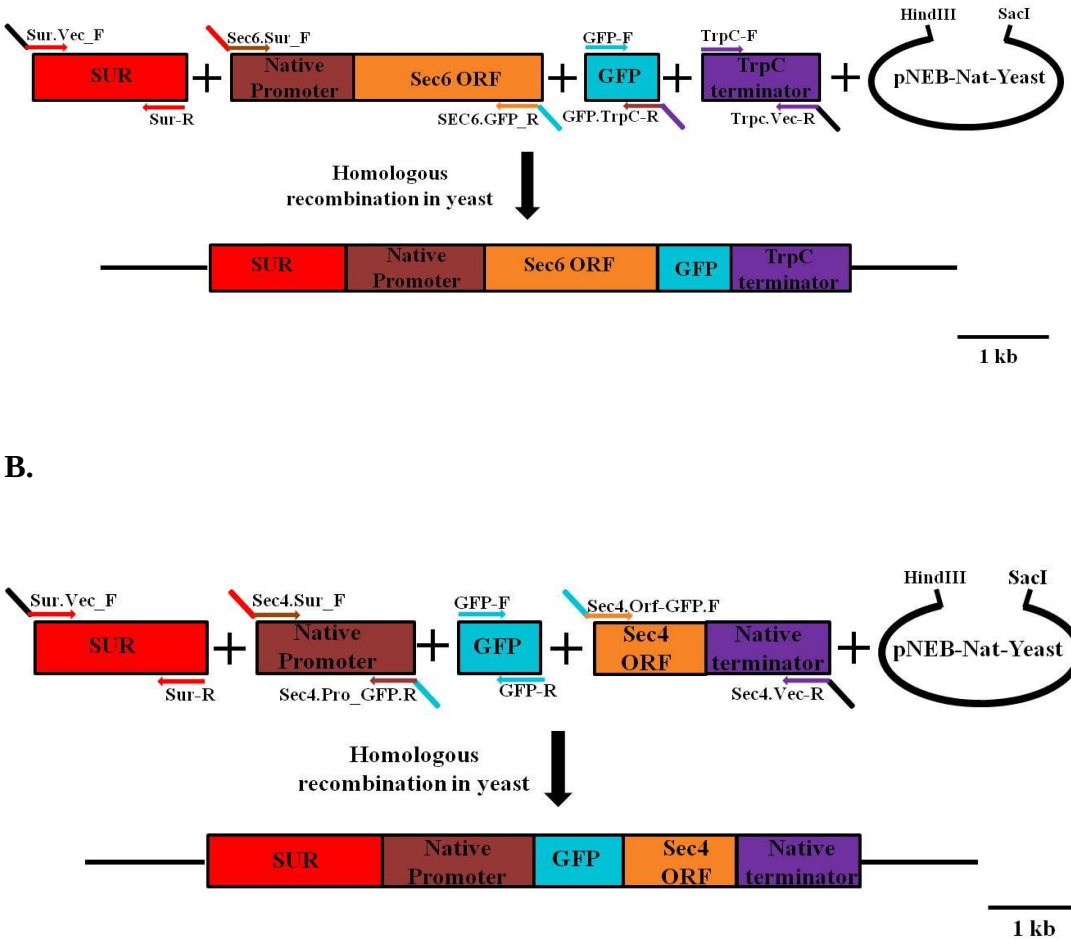

B.

Figure 3.6 Schematic diagrams to show the cloning strategy used for generation of GFP-translational fusions.

A. C-terminal translational fusion constructs were designed so each primer had 30 bp of overlap with the adjacent fragment. The sulphonylurea resistance gene cassette (*ILV1*) (Sweigard et al, 1997), 2 kb of the native promoter of the gene, the Sec6 coding region, the GFP encoding region and a TrpC terminator from *A. nidulans* were separately amplify and cloned in pNEB-Nat-Yeast vector by GAP repair and homologous recombination. **B.** N-terminal translational fusions were constructed through amplifying *ILV1* resistance gene cassette, 2 kb native promoter, the GFP encoding region and 1 kb downstream of the stop codon (terminator) and cloned in pNEB-Nat-Yeast vector.

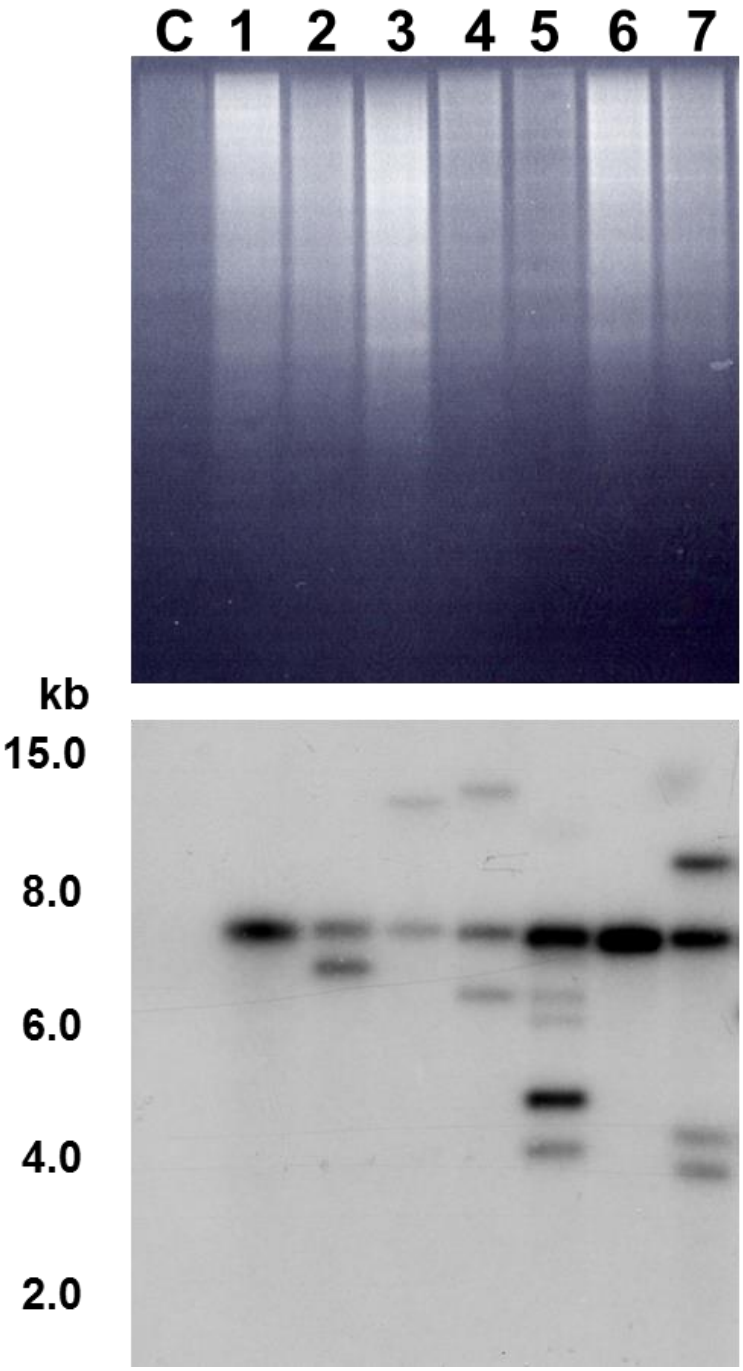

Figure 3.7 Southern blot analysis of Sec6:GFP expressing transformants.

Genomic DNA was extracted from seven putative transfromants, digested with *Eco*RI restriction enzyme before being fractionated through gel electrophoresis and transferred to a Hybond-N membrane (Amersham). The Southern blot was probed with 720 bp of GFP fragment and no hybridisation was observed with the non-transfromed Guy11 (Lane C). Transformant 1 and 6 were selected as single copy insertion and used for further analysis.

3.3.6 Sub-cellular localization of the exocyst components in vegetative hyphae of *M. oryzae*

Localization of exocyst subunits was examined in vegetative hyphae by epifluorescence microscopy. *M. oryzae* strains expressing exocyst subunits were inoculated on a 0.8% (w/v) water agar slide and incubated in a humid chamber overnight at 24°C.After 24 h, a mycelium plug was carefully removed and 20-30 µL distilled water added to the agar slide before placing coverslip on the slide culture. Fluorescence was observed under an Olympus IX81 inverted microscope.

All the exocyst subunits (Sec3, Sec5, Sec6, Sec8, Sec15, Exo84 and Exo70) showed a crescent-like distribution at the growing hyphal tip except Sec10 (**Figure 3.8**). No fluorescence was observed from the Sec10:GFP expressing strain. May be the expression is not enough to observe. Similarly, in *N. crassa* Sec10 is shown as a part of exocyst complex but could not be able to visualize using GFP translational fusion (Riquelme et al, 2014). Organization of the exocyst subunits in growing vegetative hyphae of *M. oryzae* is similar to hyphal tip organization in the pleiomorphic fungus *Candida albicans,* (Jones & Sudbery, 2010). However, Riquelme and colleagues suggested that in *N. crassa* the exocyst components accumulate at two distinct locations; Sec5, Sec6, Sec8 and Sec15, localized as a crescent at the hyphal tip while Exo70 and Exo84 closely associated with the outer layer of the Spitzenkörper (Riquelme et al, 2014). In contrast, we could not able to observe any distinct localisation of *M. oryzae* exocyst components in vegetative hyphae.

3.3.7 Co-localization of the exocyst and Spitzenkörper in growing hyphae

The Spitzenkörper (SPK) is a vesicle dense region which acts as a vesicle supply center and delivers vesicles to the plasma membrane where they fuse to form a new cell wall (Riquelme, 2013) or deliver cargo to the outside of the cell. In *M. oryzae*, the SPK colocalises with Mlc1 in growing vegetative hyphae (Giraldo et al, 2013). In order to understand whether the SPK is also colocalised with the exocyst, FM4-64, a lipophilic styryl dye was used to visualise the SPK in growing hyphae (Fischer-Parton et al, 2000). The SPK was labelled with FM4-64 in growing hyphae of exocyst:GFP expressing strains. The Spitzenkörper clearly localises to the hyphal tip as a bright spot in the centre of the apical dome, while the exocyst components formed a surface crescent at the very tip of cells (**Figure 3.8**). A line scan of fluorescence confirmed the separation. Similar observation have been shown in *Candida albicans* (Jones & Sudbery, 2010). However, in *N. crassa*, Exo70 and Exo84 are associated with the outer layer of the SPK (Riquelme et al, 2014). This suggests that the exocyst subunits localise as a crescent-shaped complex at the apex of the hyphal tip and the exocyst is therefore distinctly situated distal to the SPK.

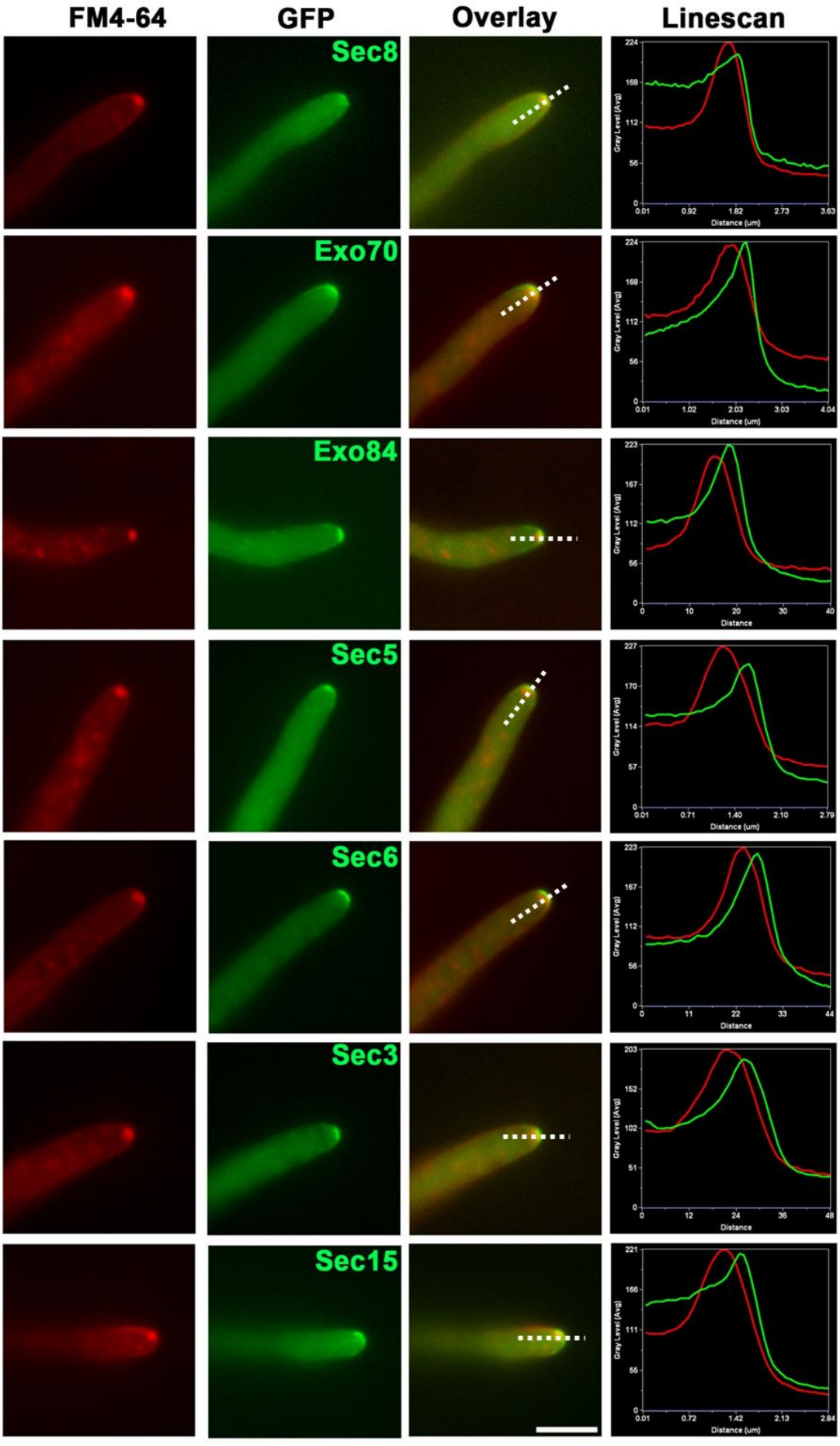
FM4-64
GFP
Overlay
Linescan
Sec8
Exo70
Exo84
Sec5
Sec6
Sec3
Sec15
Gray Level (Avg)
Distance (um)
Distance

Figure 3.8 Co-localisation between the exocyst subunits and the SPK in vegetative hyphae of *M. oryzae*.

Genes encoding the exocyst subunits, Sec8, Exo70, Exo84, Sec5, Sec6, Sec3 and Sec15 were expressed as C-terminal translation fusions in *M. oryzae* under their native promoters. Each strain was inoculated on a 0.8% water agar slide and incubated for overnight at 24°C in humid chamber. Lipophilic dye, FM4-64, was used to label the SPK. Vegetative hyphae were incubated for 5 min before imaged by epifluorescence microscopy. Micrographs of exocyst:GFP and FM4-64 were overlaid to observe the localisation. A linescan graphs of fluorescence showing distinct positions of the exocyst and the SPK at the hyphal tip. Scale bar=10μm.

3.3.8 Sub-cellular localization of other polarity compoments in vegetative hyphae of *M. oryzae*

Other polarity components like Spa2 (a polarisome component), Mlc1 (the regulatory light chain of Myo2), fimbrin (an actin binding protein), Snc1 (a v-SNARE), Sec9 (a t-SNARE), Cdc42 (a small Rho-GTPase), Rac1 (a Rho-GTPase), Sec4 (a Rab-GTPase) and Sec2 (the guanine nucleotide exchange factor (GEF) for Sec4) were observed in vegetative hyphae as fluorescent fusion proteins (**Table 3.2**). Spa2:GFP, Mlc1:GFP and GFP:Snc1 strains were constructed by Dr. Ana lilia Martinez-Rocha (Giraldo et al, 2013). Unpublished Sec2:GFP and Fim1:GFP expressing strains were generated in Prof. Talbot's laboratory by Y. Dagdas and M. Egan, respectively.

The regulatory light chain of Myo2, Mlc1, localised to the hyphal tip (**Figure 3.9 A**) at a region consistent with the position of the Spitzenkörper (Giraldo et al, 2013); polarisome component Spa2 localised as a bright spot at the hyphal tip (**Figure 3.9 B & Supplementary movie 3.1**). The fimbrin Fim1-GFP revealed cortical patches in the sub-apical region of growing vegetative hyphae (**Figure 3.9 C & Supplementary movie 3.2).** Similar results have been shown in *Aspergillus nidulans* (Upadhyay & Shaw, 2008). Other polarity components, Sec2, Sec4, Sec9, Snc1, and Cdc42 preferentially localised to the tips of growing vegetative hyphae (**Figure 3.9 D-F & Supplementary movie 3.3 & 3.4**). It may be concluded, therefore, that the organization of the secretory apparatus in growing vegetative hyphae is similar to the other filamentous fungi observed to-date, mainly *A. nidulans* and *N. crassa* (Harris, 2011; Lichius et al, 2014).

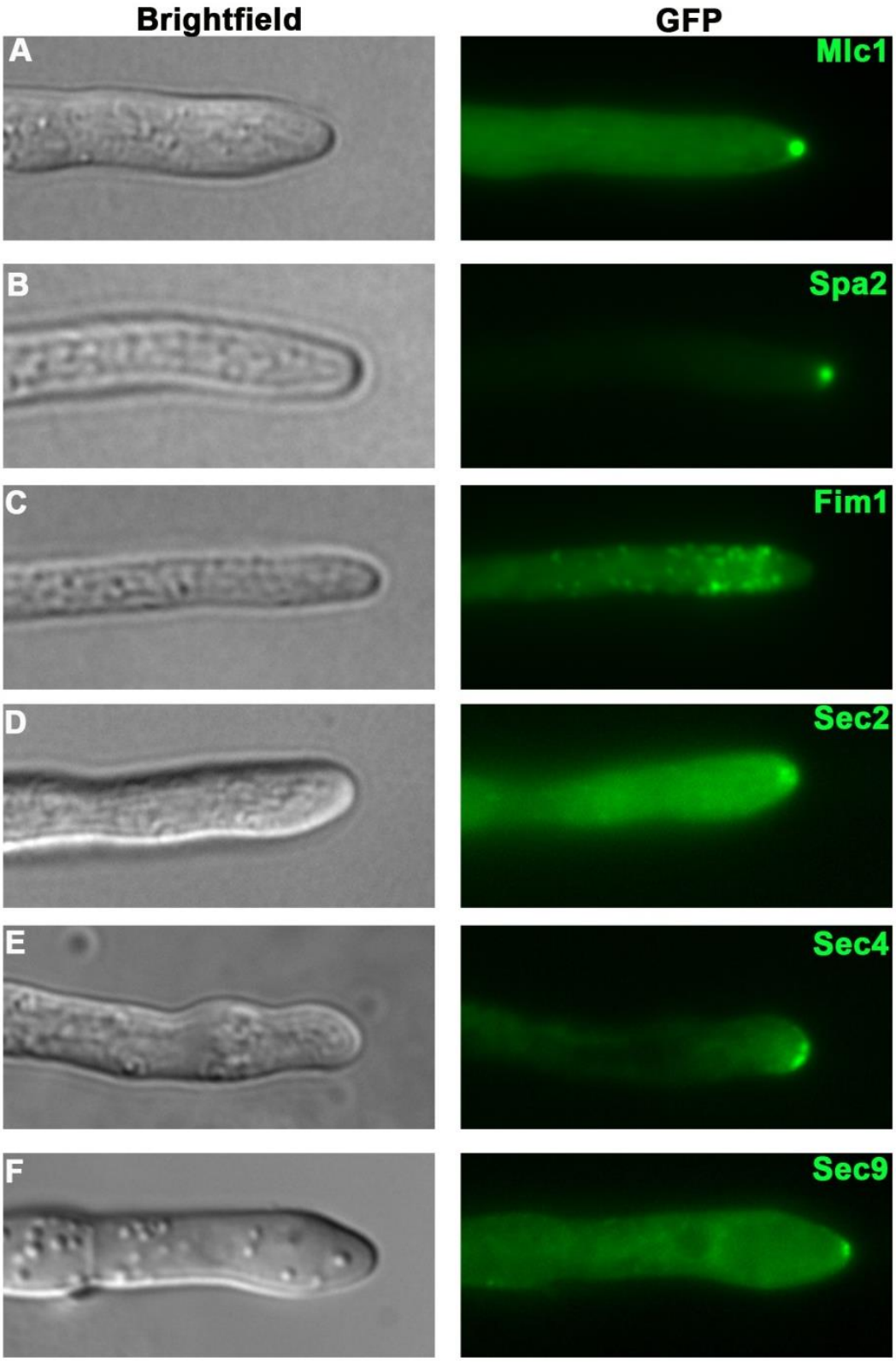
Brightfield
GFP
A
Mlc1
B
Spa2
C
Fim1
D
Sec2
E
Sec4
F
Sec9

Figure 3.9 Localization of polarized secretory apparatus in growing vegetative hyphae.

All the secretory components were tagged with GFP expressed as single insertions under control of their native promoter and visualized in growing vegetative hyphae (A-I). All images are representative of 3 biological replications of the experiment. **(A)** Myosin light chain protein Mlc1:GFP accumulated as a bright spot at the hyphal tip. **(B)** Polarisome component Spa2:GFP localised to the tip of the hyphae. **(C)** Fimbrin is an actin binding protein and Fim1:GFP expressed in the sub-apical region of hyphae. **(D)** Sec2:GFP, GEF for Sec4(**E**), localised to the hyphal tip. **(F)** t-SNARE Sec9:GFP localised to the tip of hyphae. Scale bar=10µm.

3.3.9 Localization of the exocyst during appressorium development in *M. oryzae*

To understand the role of the exocyst complex during infection-related development epifluorescence microscopy was used to visualise localisation of the exocyst components in *M .oryzae* strains expressing GFP-fusion proteins of each exocyst sub-units encoding the gene expressed under control of its native promoter. GFP fused exocyst subunits during a time course of appressorium development were visualized. Sec6:GFP localised to the tip of the germinating conidium and the emerging germ tube, during early stages of appressorium development (2 h) (**Figure 3.10**). The tip of the germ tube starts swelling after 2 h and forms a dome-shaped appressorium after 4 h. Sec6:GFP localised to the cortex of the appressorium at 4 h and by 8 h it was observed as a ring in the appressorium. In the mature appressoium after 24 h, Sec6:GFP localised to the appressorium pore and formed a 4 µm diameter ring (± 0.4 µm, n =50). In three-dimensional construction of the confocal micrographs suggests that Sec6:GFP localise at the base of the appressorium (**Figure 3.12 & Supplementary movie 3.5**). Similar patterns of localisation were observed with other exocyst subunits (Exo70, Exo84, , Sec5, Sec8, Sec15 and Sec3) as presented in **Figures 3.11**. This suggests that prior the emergence of penetration peg, all the exocyst components organised around the appressorium pore and may be involved in active secretion as penetration peg is emerging fungal structure which enters inside the host plant.

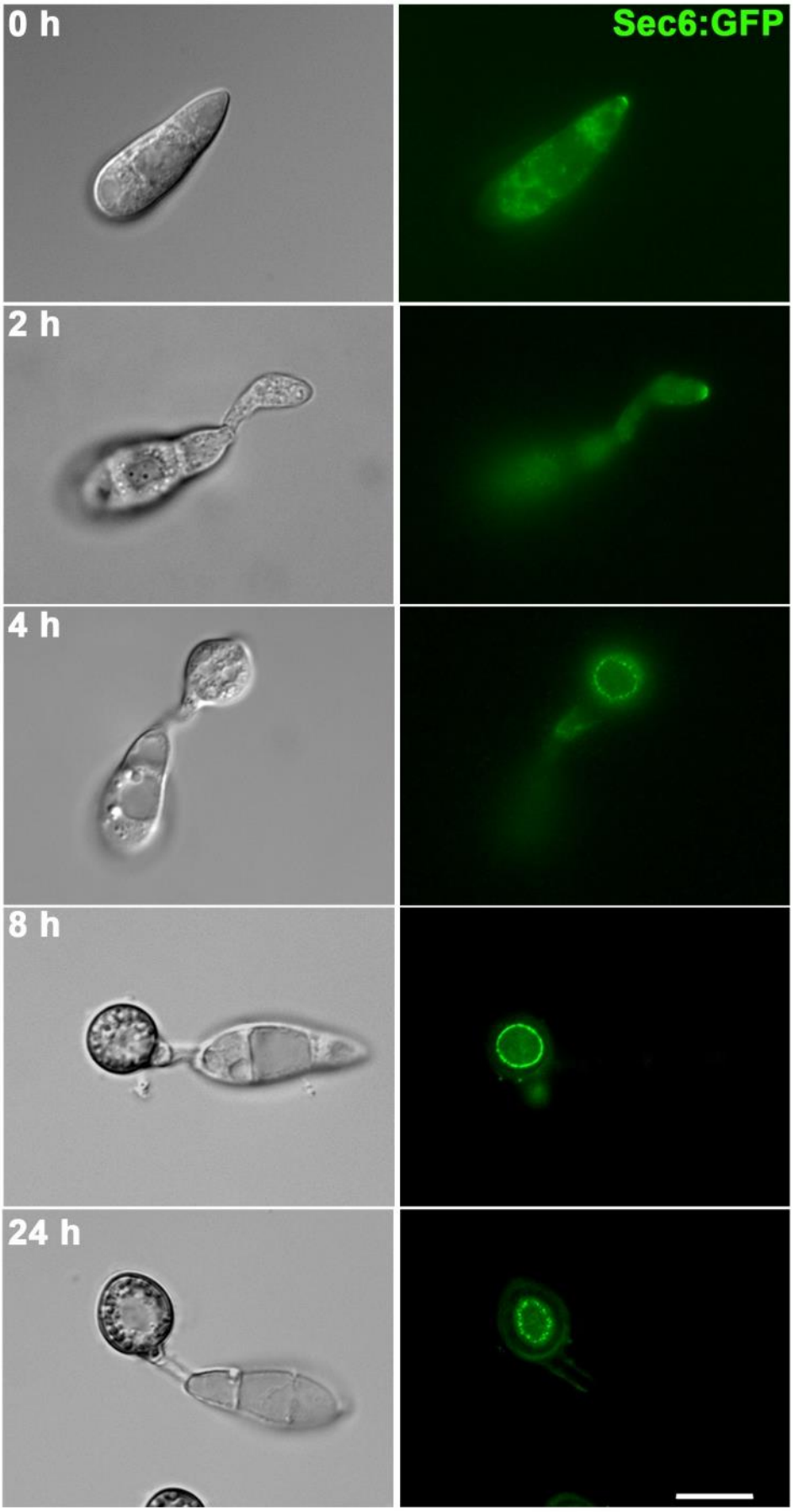
0 h
Sec6:GFP
2 h
4 h
8 h
24 h

Figure 3.10 Expression and localisation of a Sec6:GFP-fusion protein during appressorium development of *M. oryzae*

Conidia were harvested from a Sec6:GFP expressing strain of *M. oryzae*, inoculated onto hydrophobic glass coverslips and observed by epifluorescence microscopy. During initial stages of conidial germination and germ tube formation, Sec6:GFP localised to the tip and during early stages of appressorium formation, Sec6-GFP localised to the periphery of appressoria under the plasma-membrane. After 24 h, Sec6:GFP re-located to the base of the appressorium and formed a ring at the appressorium pore. Scale bar=10 µm.

A.

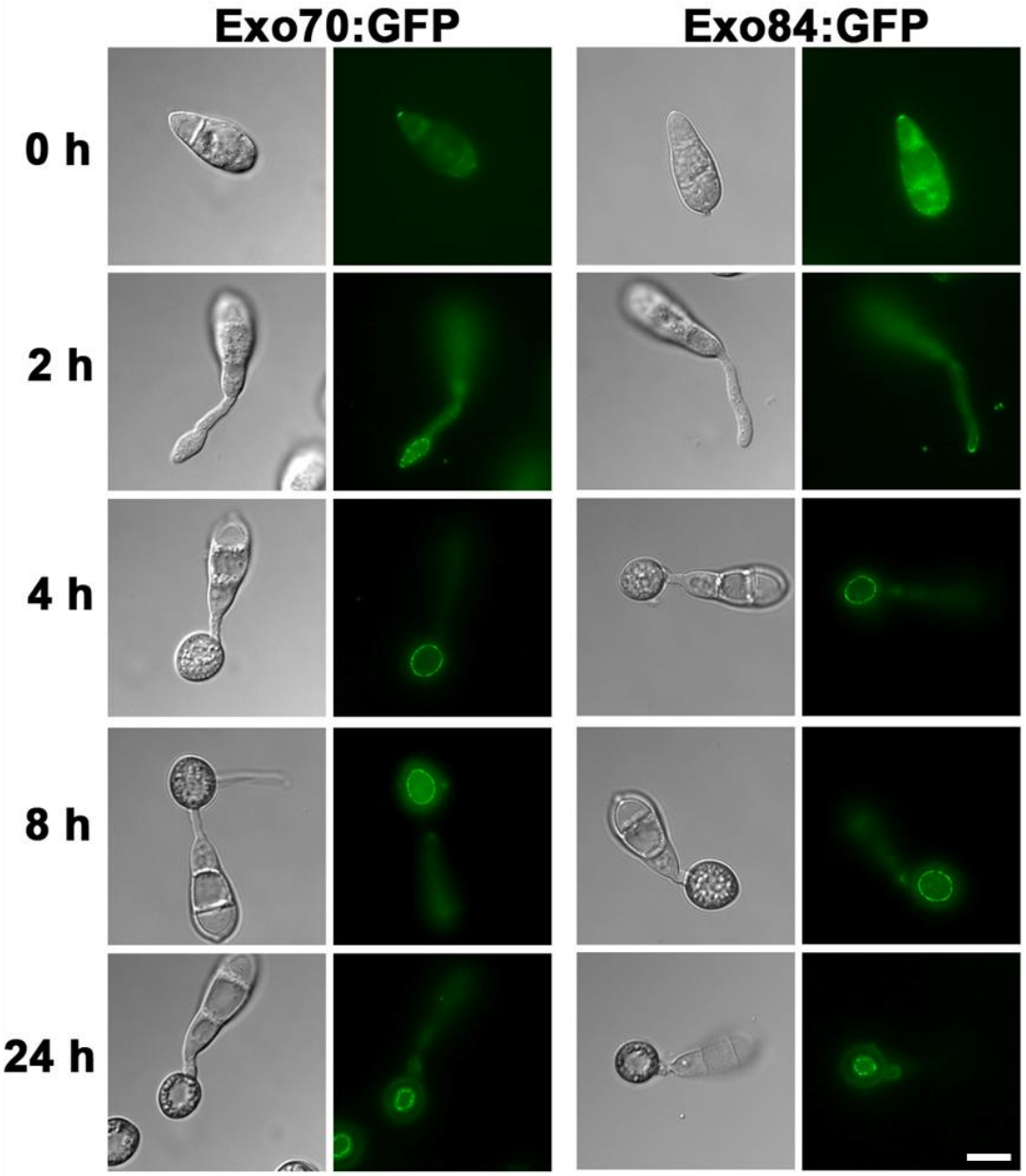

B.

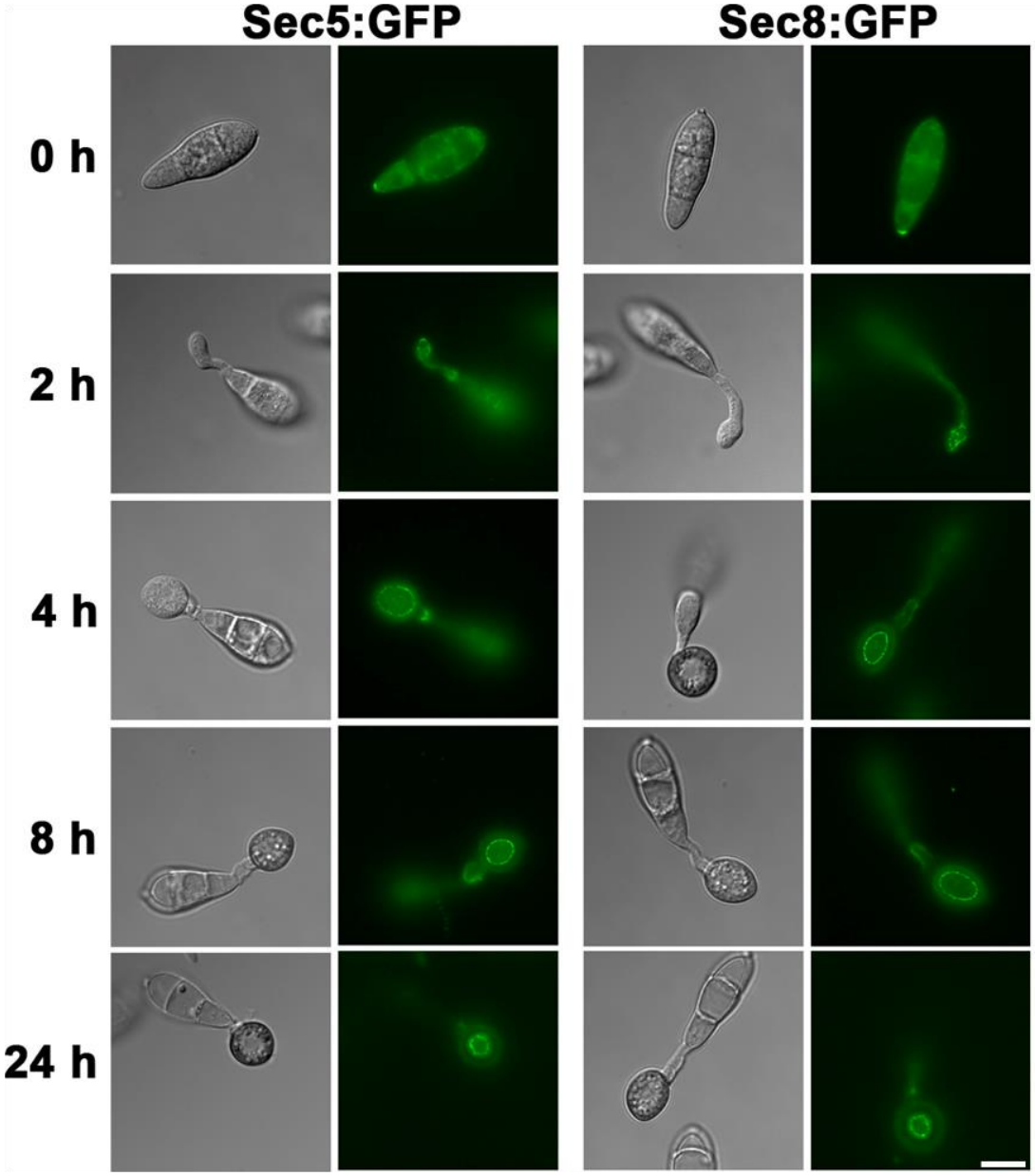

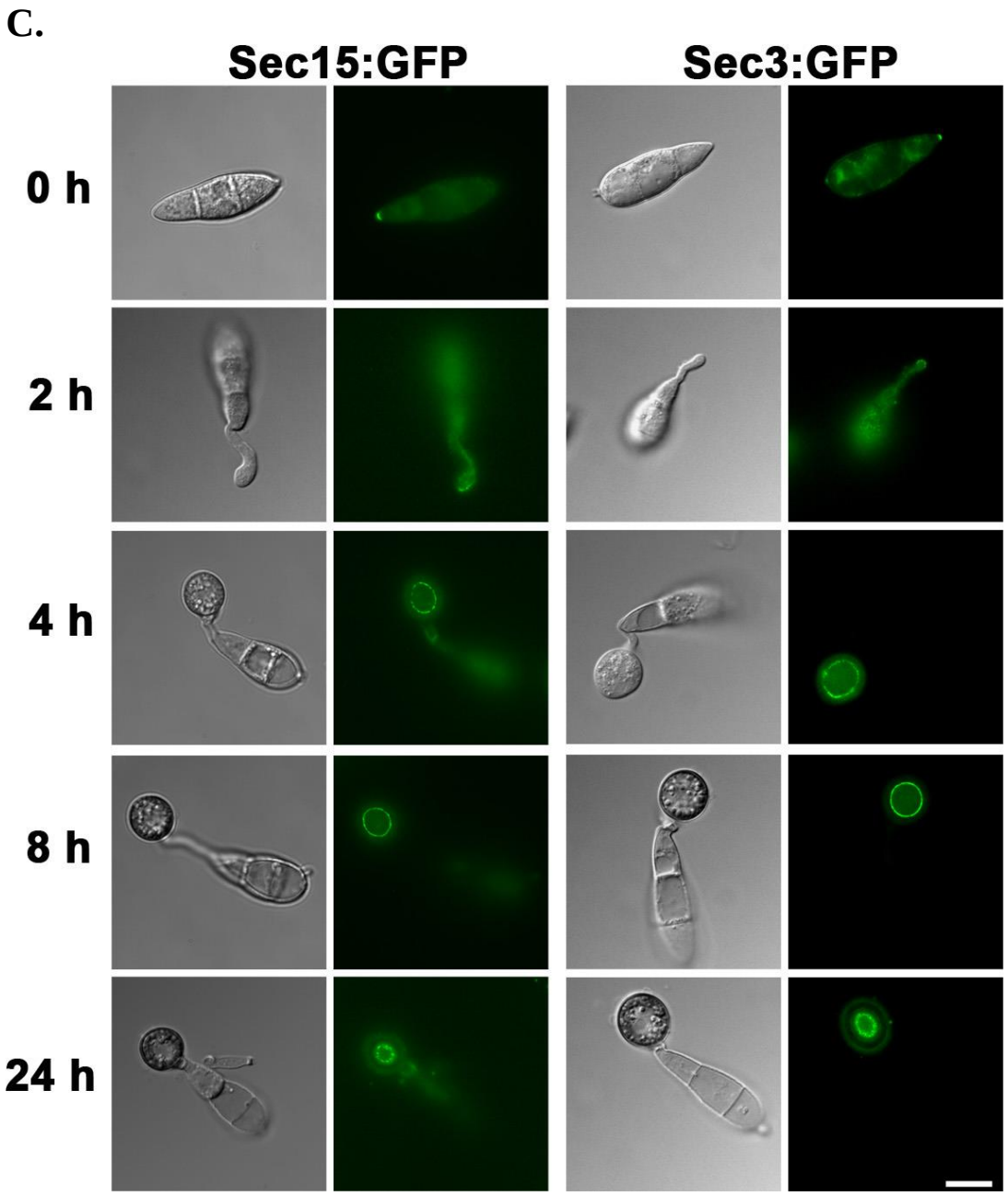

Figure 3.11 Localisation of exocyst encoding genes during appressorium development of *M. oryzae*.

A, B & C. Conidia were harvested from *M. oryzae* Guy11 expressing Exo70:GFP, Exo84:GFP, Sec5:GFP, Sec8:GFP, Sec15:GFP and Sec3:GFP as single copy insertions under control of the native promoters, inoculated on hydrophobic glass coverslips and observed at each time point by epifluorescence microscopy. Localisation of Exo70:GFP, Exo84:GFP, Sec5:GFP, Sec8:GFP, Sec15:GFP and Sec3:GFP is similar to these observed for Sec6:GFP. Scale bar=10 μm.

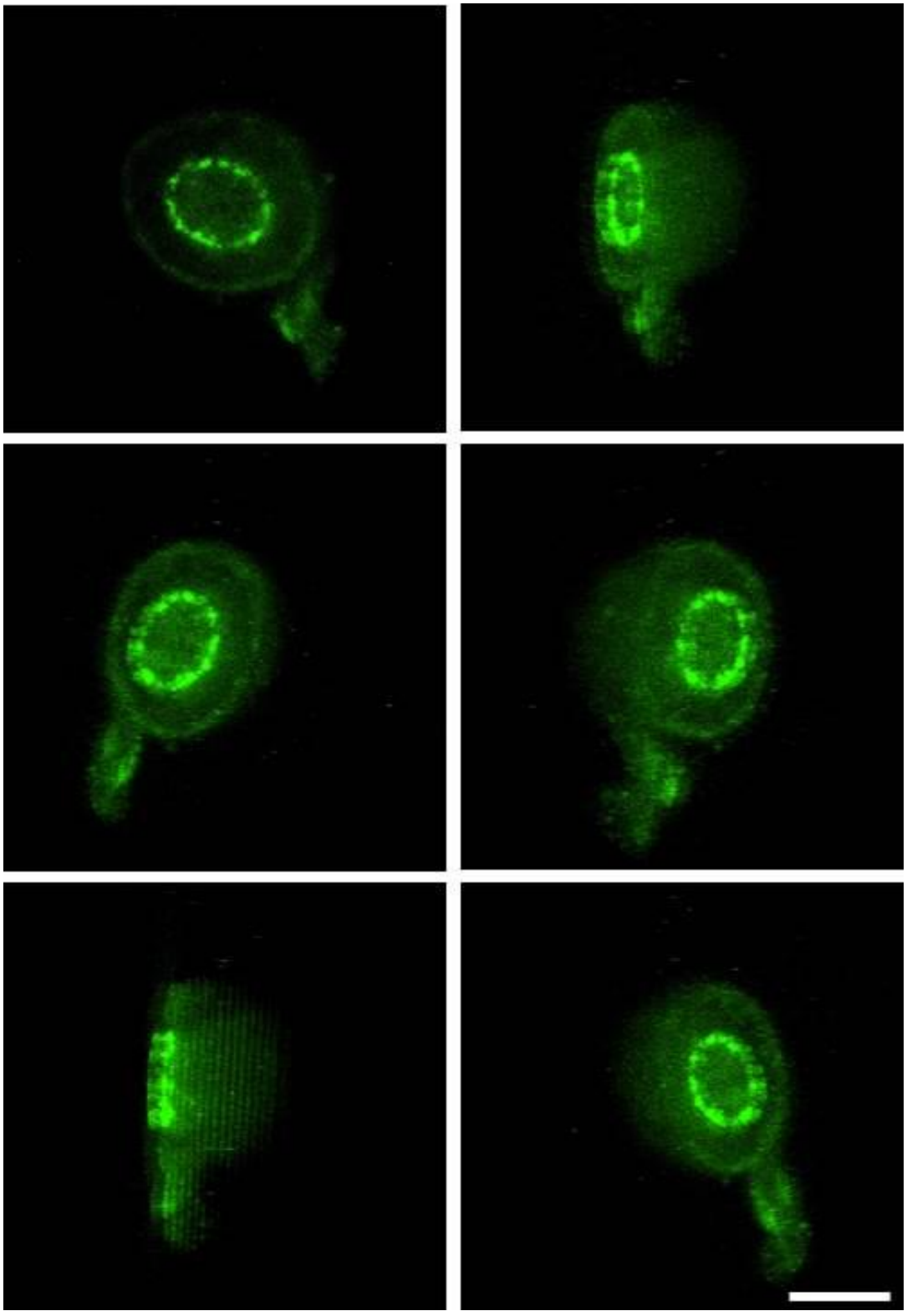

Figure 3.12 Three-dimensional micrographs of the exocyst sub-unit, Sec6.

Confocal imaging and 3-D construction of the Sec6:GFP in appressorium localised at the base of the appressorium. Scale bar=5 µm.

3.3.10 Localisation of the polarity components during appressorium development in *M. oryzae*

SNARE proteins (soluble N-ethylmaleimide-sensitive factor attachment protein receptors) are required for vesicle fusion to the plasma-membrane and membranes of other target compartments (Burri & Lithgow, 2004; Furukawa & Mima, 2014; Kuratsu et al, 2007; Novick et al, 2006). SNAREs are a superfamily of large proteins, subdivided into vesicle or v-SNAREs, on the vesicles and target or t-SNAREs, on the target membranes (Kuratsu et al, 2007).

In budding yeast, 24 SNAREs function in vesicular trafficking (Burri & Lithgow, 2004; Furukawa & Mima, 2014), while in the filamentous fungus *A. oryzae,* Kuratsu and co-workers identified putative 21 SNAREs and localised them using an eGFP fluorescent marker (Kuratsu et al, 2007). In this study, we identified the *M. oryzae* v-SNARE, Snc1 and t-SNARE, Sec9 and observed their expression during appressorium development. GFP:Snc1 and Sec9:GFP localised to the tips of conidia and the germ tube tip (**Figure 3.13A&B**). After 4 h, GFP:Snc1 was associated with vesicles and localised with a punctate distribution in the incipient appressorium (**Figure 3.13A)**. Sec9:GFP was targeted to the plasma membrane and localised at the cortex of the appressorium after 4 h (**Figure 3.13 A**). After 24 h, GFP:Snc1 showed punctate distribution at the centre of the appressorium while Sec9:GFP localised to the appressorium pore, with a punctate distribution in a ring at the pore (**Figure 3.13 A&B**).

Rho-GTPases are involved in the various cellular functions such as polarisation of the F-actin cytoskeleton, cell cycle control and cellular morphogenesis. In the present study, expression of Cdc42 and Rac1 during appressorium development was observed. Expression of N-terminal translational GFP fusions of Cdc42 and Rac1 in *M. oryzae* showed localisation to the tips of the conidia and germ tubes at 2 h (**Figure 3.14A&B**). After 4 h, GFP:Cdc42 and GFP:Rac1 showed a punctate distribution in the

appressorium and Cdc42 also localised at the plasma membrane (**Figure 3.13A&B**). After 24 h, GFP:Cdc42 and GFP:Rac1 localised in a punctate pattern in the centre of the appressorium (**Figure 3.14A&B**).

The actin-binding protein, Fimbrin, is conserved from yeast to humans and required for the development and maintenance of cell polarity (Skau et al, 2011). *M. oryzae* Fimbrin homologue was identified and Fim1:GFP expressing strain was developed by Egan et al (unpublished). During infection-related development, Fim1:GFP localised to the tip of conidia and at 2 h Fim1:GFP, was found at patches around the tip of the germ tube (**Figure 3.15**). After 4 h, Fim1:GFP was cortically distributed under the plasma membrane. In mature appressoria (24 h), Fim1:GFP localised as a patches to the centre of the appressorium pore region (**Figure 3.15**).

A

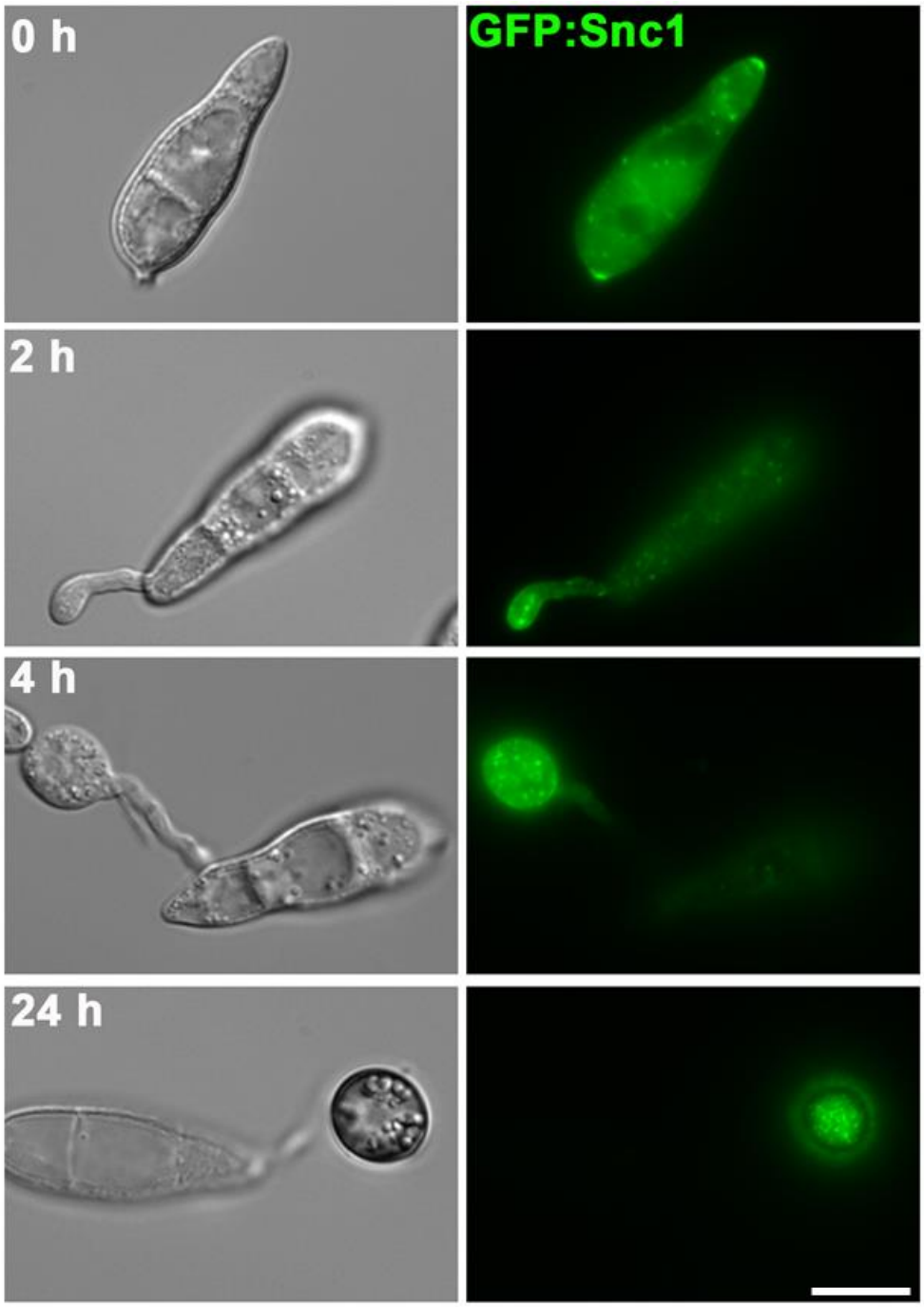

B

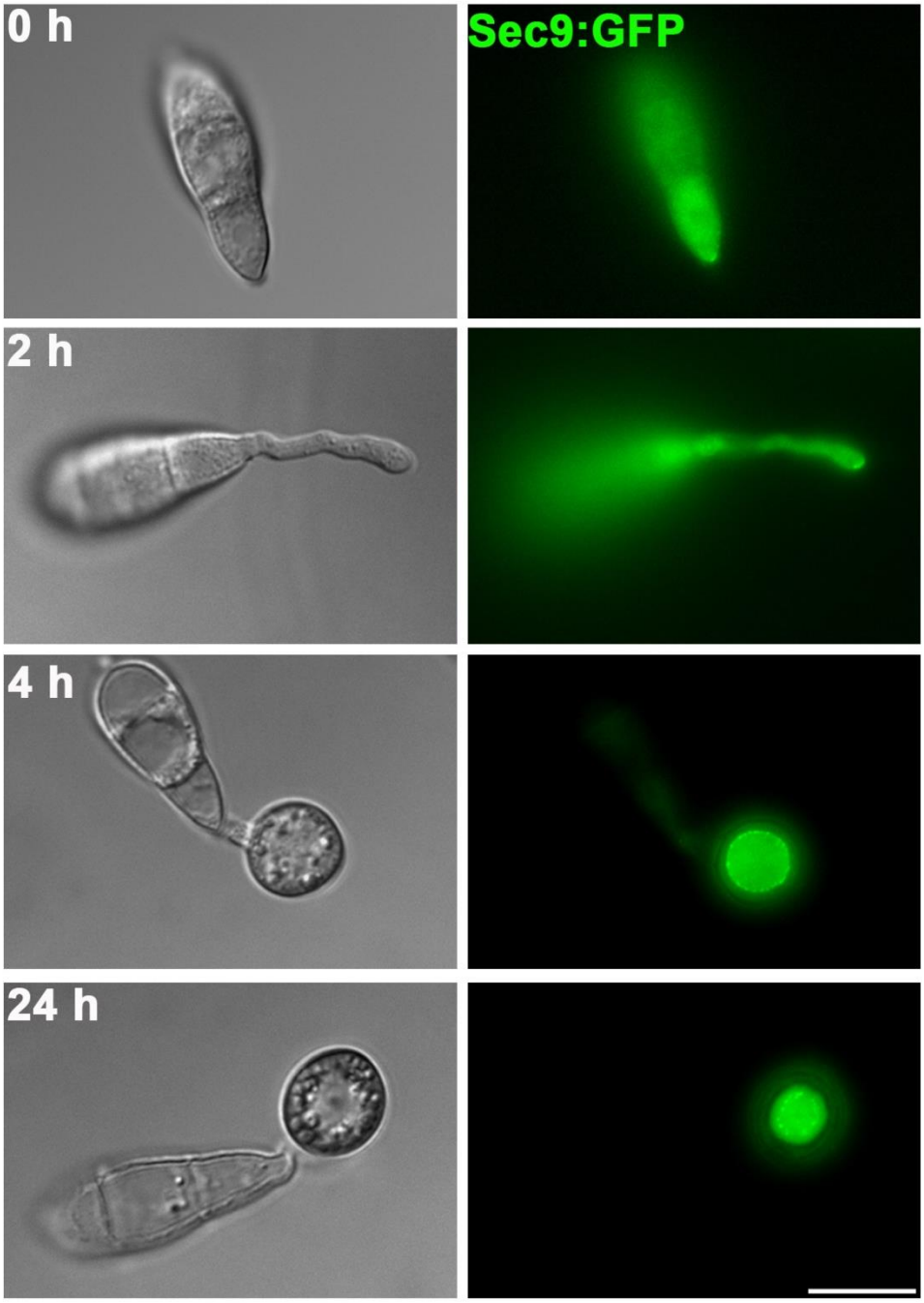

Figure 3.13 Live-cell imaging of *M. oryzae* SNARE proteins during infection-related development.

The v-SNARE, Snc1 (**A**) and t-SNARE Sec9 (**B**) encoding genes were expressed with N- and C- terminal translational GFP fusions. Independent transformants were generated expressing GFP:Snc1 and Sec9:GFP under control of their native promoter. Conidia were harvested from the *M. oryzae* strain expressing single copy insertions, inoculated on hydrophobic glass coverslip and observed at each time point by epifluorescence microscopy. GFP:Snc1 and Sec9:GFP were expressed to the tips of the germinating conidia and germ tubes at 2 h. GFP:Snc1 localised in a punctate distribution to the incipient appressorium after 4 h and 24 h. Sec9:GFP localised to the plasma membrane at 4 h and after 24 h was expressed at the centre of the appressorium. Scale bar=10 μm.

A

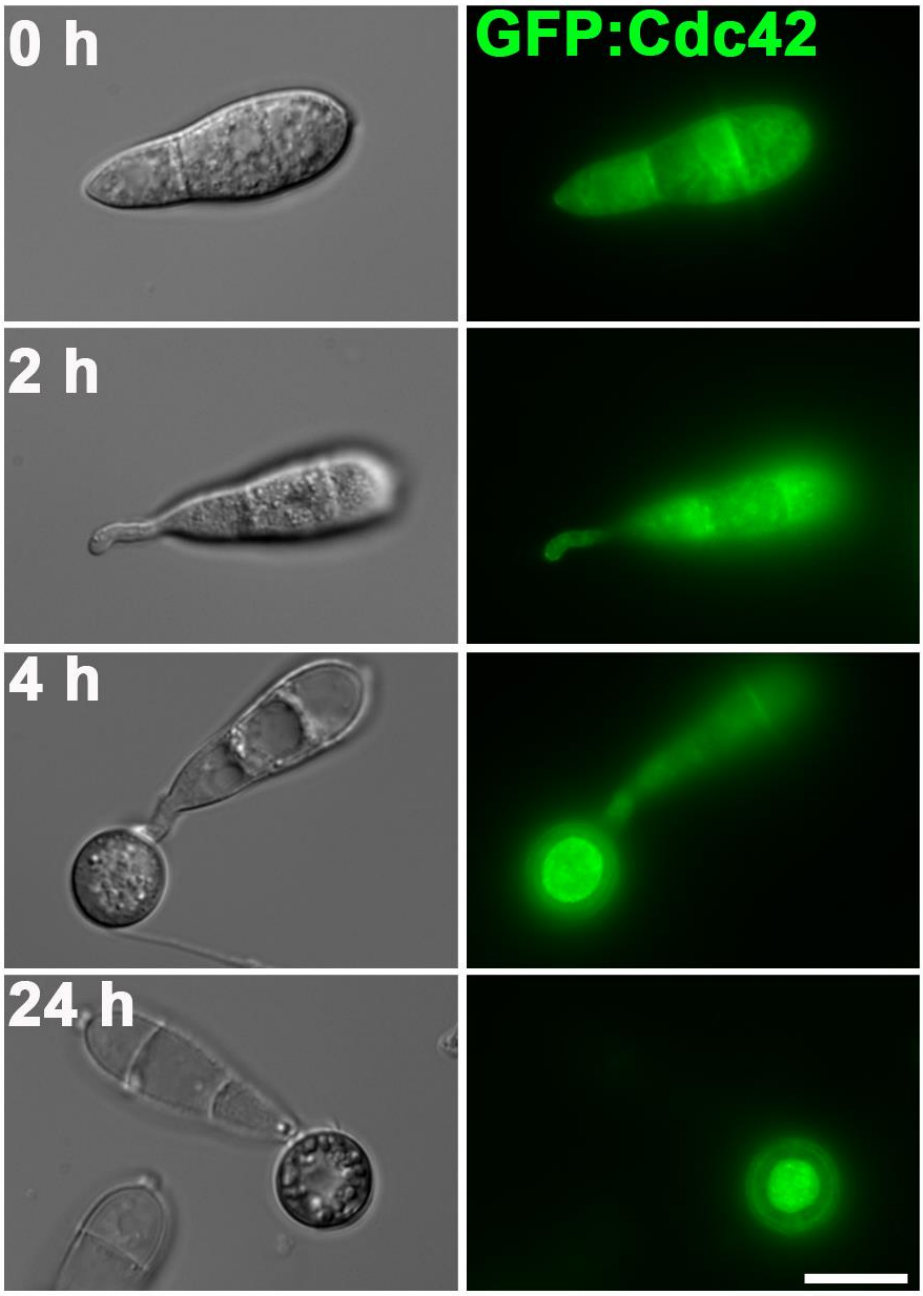

B

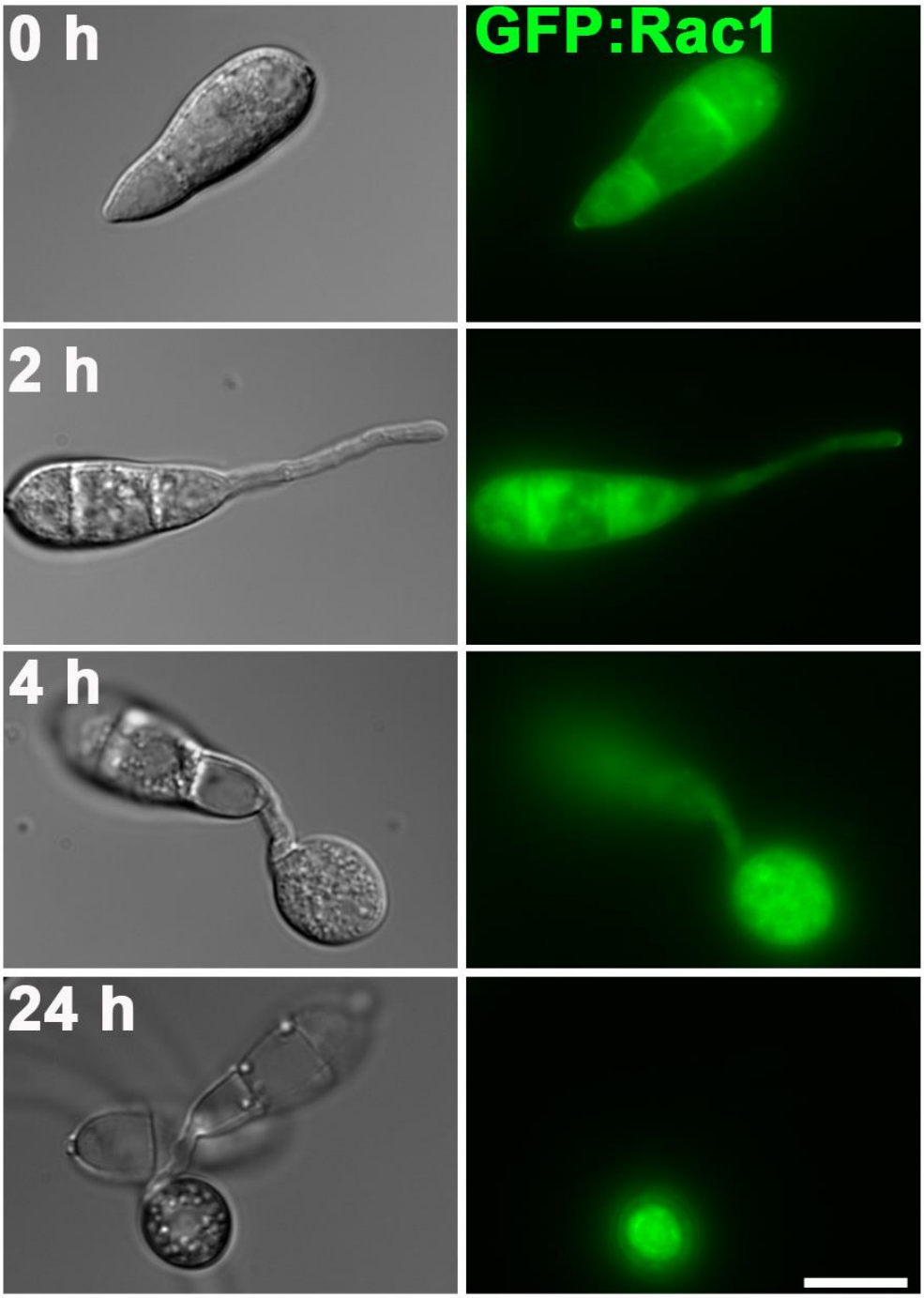

Figure 3.14 Expression of Rho-GTPases during infection related development of *M. oryzae*.

The Rho-GTPases Cdc42 (**A**) and Rac1 (**B**) were expressed as N-terminal translation GFP fusion protein under control of native promoters. Transformants expressing GFP:Cdc42 and GFP:Rac1 were used to harvest conidia and was inoculated onto hydrophobic glass coverslips. Expression of GFP:Cdc42 and GFP:Rac1 was observed at each time point by epifluorescence microscopy. GFP:Cdc42 and GFP:Rac1 were expressed to the tips of germinating conidia and the growing point of the germ tubes after 2 h. After 4 h, GFP:Cdc42 was localised to the plasma membrane and also in the cytoplasm, while at 24 h it was expressed in the appressorium pore region. GFP:Rac1 was expressed in the cytoplasm and by 24 h localised at the centre of the appressorium. Scale bar=10 μm.

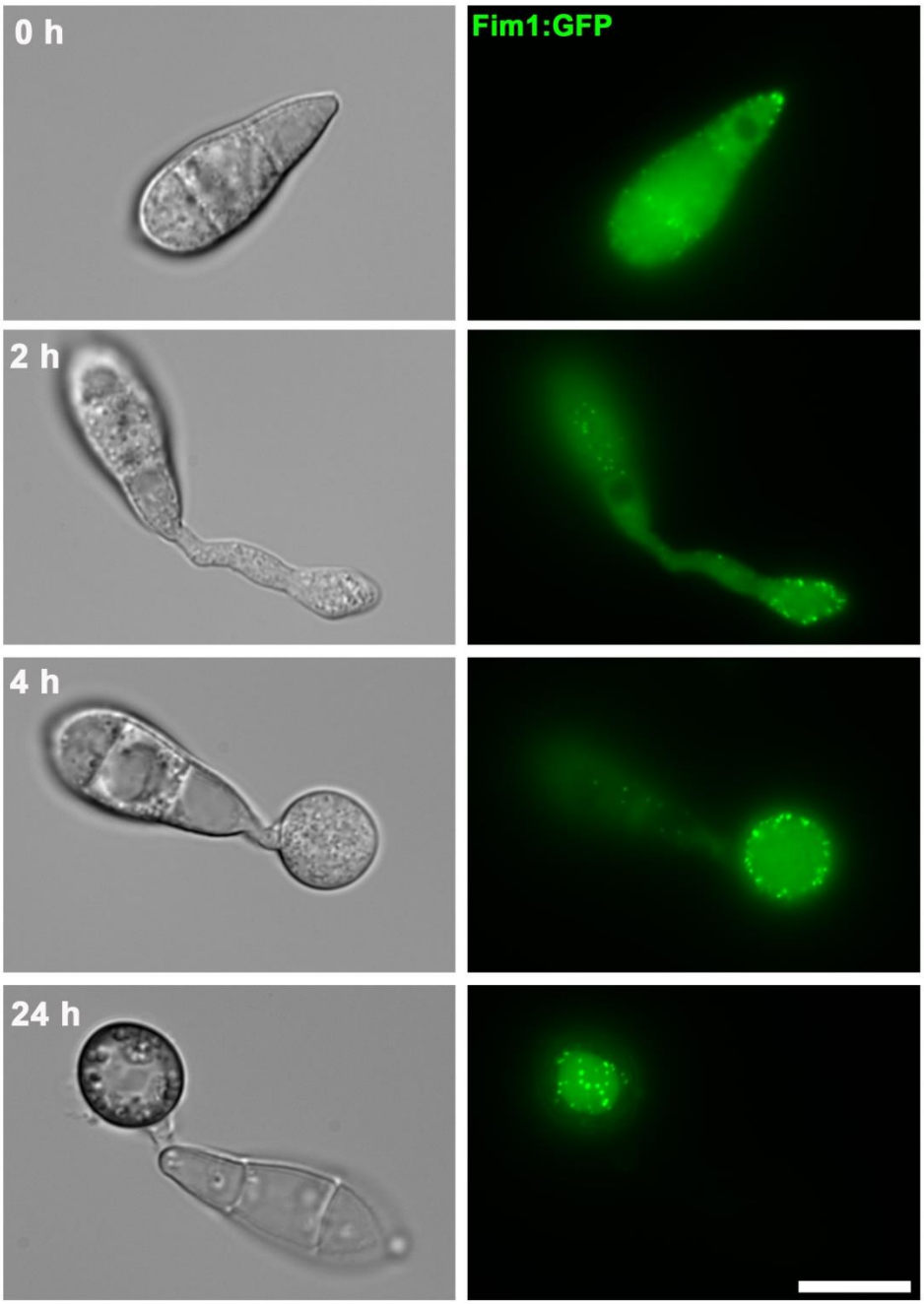

Figure 3.15 Localisation of the actin-binding protein, Fimbrin, during infection-related development of *M. oryzae*.

Conidia were harvested from *M. oryzae* strain expressing Fim1:GFP, inoculated onto glass coverslips and observed by epifluorescence microscopy. Fim1:GFP localised to the apex of germinating conidia. After 2 h, Fim:GFP was observed as a actin patches around the tip of the germ-tube. By 4 h Fim1:GFP localised under the plasma membrane and after 24 h actin patches were observed at the centre of the appressorium. Scale bar=10 µm.

3.3.11 Colocalisation of Sec6:GFP with F-actin network in mature appressorium

In the mature appressorium of *M .oryzae* an F-actin and septin network are generated around the appressorium pore and are essential for repolarization during plant infection (Dagdas et al, 2012). The co-localisation of the exocyst with F-actin was tested. Lifeact:mRFP was transformed to *M. oryzae* strain in the Sec6:GFP expressing strain and used to visualise the F-actin toroidal network. The exocyst ring clearly colocalised with the F-actin network at the base of the appressoium in the pore region (**Figure 3.16**). A linescan of the fluorescence confirm this co-localisation in mature appressorium (**Figure 3.16D**).

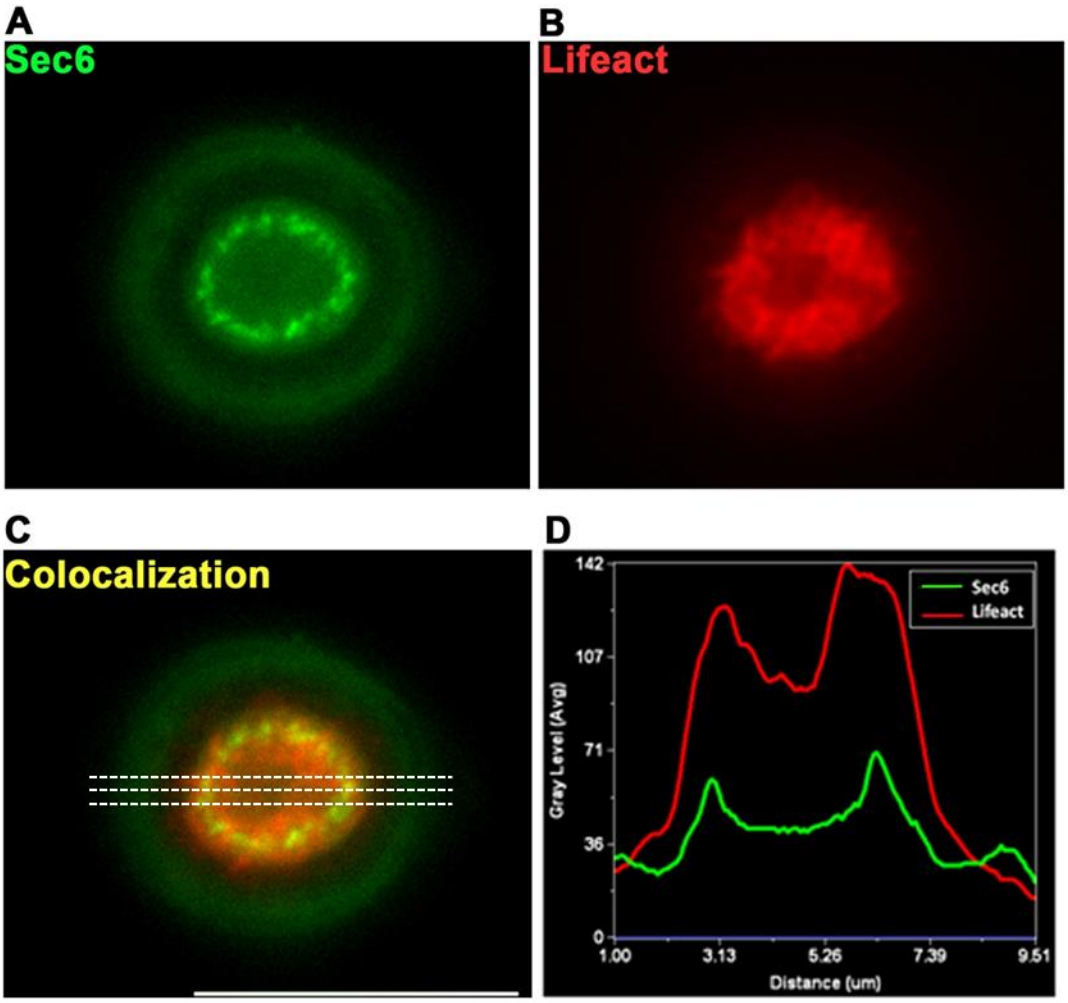

Figure 3.16 Co-localization of Sec6-GFP and LifeAct-RFP in the mature appressorium of *M. oryzae*.

Conidia were harvested from a *M. oryzae* Guy11 strain co-expressing Sec6:GFP and Lifeact-RFP, and inoculated on glass coverslips before observed by epifluorescence microscopy. **A.** Sec6:GFP localised around the appressorium pore, **B.** The F-actin network around the appressorium pore, **C.** Co-localisation of Sec6:GFP and Lifeact:RFP signal and **D.** Linescan showed colocalization of the exocyst ring and actin network around the appressorium pore. Scale bar=10 µm.

3.3.12 Actin cytoskeleton is required for the exocyst localisation in mature appressorium

To test whether exocyst assembly at the pore utilizes the F-actin or microtubule cytoskeleton, chemical inhibitors were used to prevent the polymerisation. Latrunculin A is widely used as an actin depolymerisation agent (Spector et al, 1983) before it binds to actin monomers thereby preventing them from polymerising. Benomyl is a member of the benzimidazole class of compounds and is used as a well-known microtubule depolymerising agent (Jacobs et al, 1988). Conidia were harvested from the Sec6:GFP strain of *M. oryzae* and incubated on coverslips for appressorium development. After 12 h appressorium development, 10 µM latrunculin A, 30 µM benomyl or 0.1 % (v/v) DMSO (control) was added to the conidal suspension (as described by Czymmek et al, 2005). The exocyst ring was observed at 24 h of appressorium development but was significantly disrupted ($P < 0.01$) by latrunculin A treatment compared to the benomyl and DMSO treatments (**Figure 3.17**). These results show that actin polymerisation is required for exocyst localization to the appressorium pore. This suggests that F-actin filaments are required for the exocyst localisation organisation at the appressorium pore.

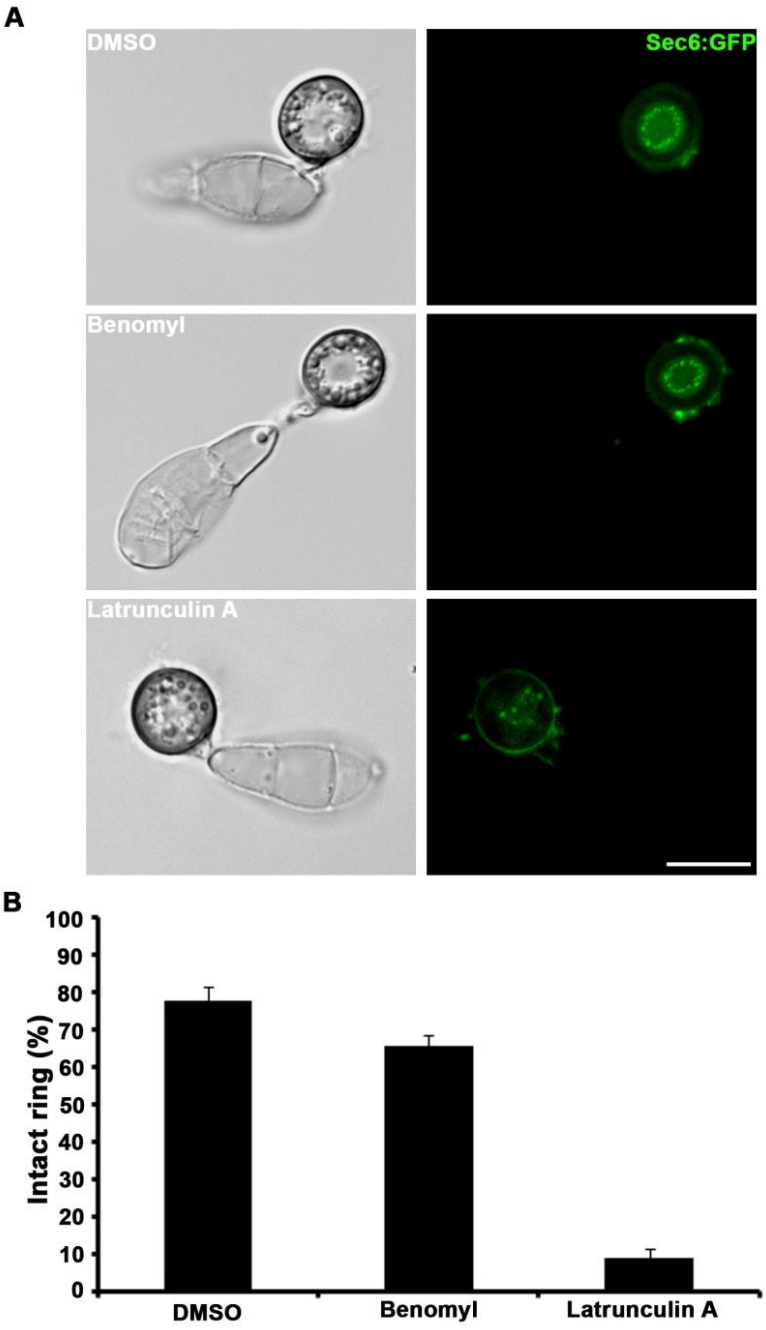

Figure 3.17 The F-actin cytoskeleton is required for exocyst ring formation at the appressorium pore in *M. oryzae*.

A. In mature appressoria, Sec6:GFP localises to the appressorium pore. Treatment with 10 µM latrunculin A led to disorganization of exocyst ring after 24 h while there were not effect of 30 µM benomyl or 0.1 % DMSO (control). Scale bar=10µm. **B.** Bar chart to show disruption of the exocyst ring ($P<0.01$) by latrunculin A compared with benomyl and DMSO treatment. (Values are mean ± S.E., three experiments, n=100).

3.3.13 Exocyst complex is an octameric protein complex in *M. oryzae*

In order to understand the interactions of the exocyst subunits, total protein was extracted from mycelium of *M. oryzae* Guy11 strains expressing Sec6:GFP, Exo84:GFP and ToxA:GFP (expressed in cytoplasm and used as a control). Co-immunoprecipitation was performed using GFP-trap as described in Section 3.2.5.2, followed by liquid chromatography–tandem mass spectrometry (LC-MS/MS) in order to identify unique peptides (Section 3.2.5.3). Mass-spectrometry data were aligned with *M. oryzae* protein database and parameterised setting 95% confidence for protein match and minimum of two unique peptide, matches with 95% confidence. Raw data obtained from LC-MS/MS were filtered against a control data set obtained from purifications with ToxA:GFP and precipitates of Sec6:GFP, and Exo84:GFP. All the exocyst subunits were identified in the precipitates of the *SEC6* and *EXO84* suggest that all the octameric exocyst complex physically interacts during vesicle trafficking (**Table 3.3**). Physical interaction of the exocyst subunits have been shown in *N. crassa* during vesicle trafficking during vegetative growth (Riquelme *et al*, 2014). Unique peptides of septins, actin-binding proteins, Rho-GTPase and MAPK (Mitogen-activated protein kinase) proteins were identified in the precipitates, suggesting their role in polarity establishment and regulation of exocyst subunits (**Table 3.3**). Ypt1 (involved in ER-Golgi pathway), Hex1 (woronin body protein), Sec14 (phosphatidylinositol/ phosphatidylcholine transfer protein) and Arb1 (ABC transporter) were also co-precipitated with Sec6 and Exo84 in LC-MS/MS (**Table 3.3**). Co- immunoprecipitation results suggest that in *M. oryzae* exocyst exists as an octameric complex and all the sub-units physically interact during polarised secretion. Physical interaction of exocyst with septins, actin-binding proteins, Rho-GTPase and other proteins implies the role of exocyst in different cellular activities.

Table 3.3. Exocyst interacting proteins are identified by co-immunoprecipitation with *SEC6* and *EXO84*.

***M. oryzae* proteins identified by Co-IP**		**Total Spectral Count/ Total protein coverage (%)**		
		Sec6:GFP	**Exo84:GFP**	**Control**
Exocyst	Sec3 (MGG_03323)	164/35	69/25	0/0
	Sec5 (MGG_07150)	35/29	57/48	0/0
	Sec6 (MGG_03235)	100/55	27/34	0/0
	Sec8 (MGG_03985)	153/61	48/42	0/0
	Sec10 (MGG_04559)	9/13	119/64	0/0
	Sec15 (MGG_00471)	7/11	77/54	0/0
	Exo70 (MGG_01760)	11/14	163/83	0/0
	Exo84 (MGG_06098)	10/13	191/86	0/0
Septins	Cdc12 (MGG_07466)	2/12	1/2	0/0
	Cdc10 (MGG_06726)	0/0	10/27	0/0
	Cdc3 (MGG_01521)	2/3	0/0	0/0
	Cdc11 (MGG_03087)	0/0	2/5	0/0
Actin binding	Fim1 (MGG_04478)	2/5	3/5	0/0
	Vps1/Dynamin (MGG_09517)	2/3	0/0	1/0
Rho-GTPase	Rho1 (MGG_07176)	8/22	2/16	0/0
	Rac1 (MGG_02731)	3/19	0/0	0/0
MAPK signalling pathway	Mst7 (MGG_06482)	6/3	8/3	1/0
	Pmk1 (MGG_09565)	2/5	6/19	0/0
	Mps1 (MGG_04943)	3/10	0/0	0/0
Others	Sec14 (MGG_00905)	2/17	4/12	0/0
	Sec26 (MGG_06860)	4/6	1/1	1/0
	Ypt1 (MGG_06962)	6/37	1/6	0/0
	Sec24 (MGG_09564)	3/3	1/1	0/0
	Sec63 (MGG_05320)	2/2	0/0	0/0
	Arb1(ABC transporter) (MGG_11862)	5/5	2/1	0/0
	Hex1 (Woronin body protein) (MGG_02696)	9/75	2/5	0/0

3.4 Discussion

In this present study we set out to investigate organisation of the polarised secretory machinery in infection related development of the rice blast fungus. It has been shown that re-orientation of the F-actin cytoskeleton is regulated by a hetero-oligomeric septin complex, which localises at the base of the appressorium (Dagdas et al, 2012). Septin ring formation is tightly regulated by the Nox2/NoxR NADPH oxidase complex and controls F-actin polymerization at the point of plant infection (Ryder et al, 2013). Re-polarisation of the cytoskeleton is required for emergence of the penetration hypha, but how the proteins necessary for polarized growth establish and organise at the point of infection, is unknown. The appressorium pore is a site for emergence of the penetration peg, and is therefore the site at which the fungus is likely to assemble polarity components to repolarize and rupture the outer layer of the rice cuticle and epidermis to allow colonisation of rice cells.

M. oryzae polarity determinants showed very low amino acid identity to the *S. cerevisiae* homologues (**Table 3.2**). However, *M. oryzae* exocyst components showed higher homology to *N. crassa* and *C. higginsianum* in phylogenetic tree than to *S. cerevisiae* and *C. albicans* (**Figure 3.4**). This suggests that there might be some conserved domains in exocyst components of filamentous fungi required for vesicle trafficking. We have shown that components of the octameric exocyst are located at the hyphal tip in a crescent structure, distal to the Spitzenkörper (SPK) (**Figure 3.8**). In *C. albicans*, exocyst components also localise as a crescent at the hyphal tip (Jones & Sudbery, 2010) and in *N. crassa* it has been shown that there are two distinct localization patterns, Exo70/Exo84 localise to the peripheral part of the Spitzenkörper, while Sec5, Sec6, Sec8 and Sec15 localised as a crescent at the hyphal tip (Riquelme et al, 2014). The localisation of the exocyst in *Ashbya gossypii* is furthermore correlated with speed of growth of the hyphae (Kohli et al, 2008). In slow-growing hyphae,

excoyst subunits localise as a cortical cap at the tip, while in fast-growing hyphae the exocyst localises as a bright spot and forms a spheroid shape at the hyphal tip (Kohli et al, 2008). In *Aspergillus oryzae*, AoSec3 localised at the very end of the hyphal tip in a crescent pattern distinct from the SPK (Hayakawa et al, 2011). This suggests that although the exocyst components are conserved in eukaryotes and they may regulate polarized secretion differentially depends upon the cell type. Vegetative hyphae of *M. oryzae* are thinner than *N. crassa* hyphae and the exocyst components might not be easily distinguished. So, high resolution imaging of vegetative hyphae may provide some evidence about the exocyst differentiation.

The *M. oryzae* polarisome component Spa2 localised to the tip of the growing hyphae which is consistent with the localisation observed in *C. albicans* (**Figure 3.9**) (Jones & Sudbery, 2010) Localisation of *M. oryzae* v-SNARE, Snc1 on vesicles and t-SNARE, Sec9, at the plasma membrane which is similar as shown in other filamentous fungi (**Figure 3.9**) (Furukawa & Mima, 2014). *M. oryzae* Rho-GTPase Cdc42, Rab-GTPase Sec4 and Sec2 (GEF for Sec4) localise to the plasma membrane of growing hyphae and shows similar localisations as in other fungi (**Figure 3.9**) (Jones & Sudbery, 2010; Nobes & Hall, 1995).

During appressorium morphogenesis, the exocyst localises at the cortex of the appressorium and this might be involved in the deposition of material for cell wall biogenesis and melanin layer formation, at the early stage of appressorium development (**Figure 3.10**). However, in mature appressoria the exocyst distributes around the appressorium pore at the base of appressorium (**Figure 3.12**) suggesting that the appressorium pore might be involved in active secretion and this was further confirmed by showing other polarity determinants such as v-SNARE (Snc1), t-SNARE (Sec9), Rho-GTPase (Cdc42 and Rac1) and Fimbrin, are expressed at the centre of the

appressorium (**Figure 3.13-3.15**). Earlier, Dagdas and colleagues in our lab showed that *M. oryzae* septins form a hetero-oligomeric ring around the appressorium pore. Septins organize and scaffold the F-actin network around the appressorium pore (Dagdas et al, 2012). This suggests that repolarisation happens from the appressorium pore in a septin-dependent manner. Here, I also observe that *M. oryzae* exocyst subunits also co-localise with the toroidal F-actin network around the appressorium pore and disruption of F-actin cytoskeleton (but not tubulin) causes complete loss of the exocyst ring (**Figure 3.16**). In yeast, the delivery of exocyst-associated secretory vesicles to the plasma membrane is an actin-dependent process (Finger et al, 1998; Pruyne et al, 1998). By contrast, *N. crassa* require both actin and microtubules for delivery of exocyst-associated vesicles (Riquelme et al, 2014). This suggest that in appressorium, which shows isotropic growth, might not requires microtubules for repolarisation as F-actin network is required for the exocyst organisation at the appressorium pore.

Co- immunoprecipitation and fluorescence localisation of the exocyst components Sec6 and Exo84 suggest that *M. oryzae* has a functional exocyst complex involved in vesicle trafficking (**Table 3.3**). Physical interactions of the exocyst components with septins and actin binding proteins during vegetative growth suggest that the exocyst might be established in a septin-dependent manner. Furthermore, interaction of the exocyst with MAPK cascade protein such as Mst7, Pmk1 and Mps1, suggest that MAPK genes might regulate polarised growth through direct interaction with the exocyst components. Recently, it was suggested in human cells that the exocyst component, Exo70, directly interacts with ERK1/2 (Extracellular signal-regulated kinase 1 and 2), and promotes its interaction with other exocyst components, Sec8 and Exo84 and regulates vesicle tethering to the plasma membrane (Ren & Guo, 2012). It has been shown that in *S. cerevisiae*, Rho1-GTPase, maintains cell wall integrity pathway by regulating the cell

wall synthesizing enzyme 1,3-beta-glucan synthase (Qadota et al, 1996). Moreover, Rho1-GTPase regulates the polarised secretion through direct binding with the exocyst component, Sec3 (Guo et al, 2001). Co- immunoprecipitation of Rho1 with Exo84 and Sec6 suggests that Rho1 might regulate polarised secretion in *M. oryzae.*

When considered together, the results presented in this chapter suggest that *M. oryzae* has functional exocyst complex which is involved in polarised secretion from the appressorium pore which suggest that pore act as ‘‘a hub’’ for protein secretion. The exocyst subunit Sec6, co-localises with F-actin network around the appressorium pore and actin polymerisation is required for exocyst assembly at the appressroium pore. In the next chapter I will describe the role of exocyst complex in infection-related development.

Chapter 4. Molecular characterization of exocyst complex in *M. oryzae*

4.1 Introduction

The exocyst complex is an evolutionarliy conserved octameric complex required for polarised growth and secretion (Cvrckova et al, 2012; He & Guo, 2009; Heider & Munson, 2012). Most of the exocyst-encoding genes are essential for viability. In *S. cerevisiae*, deletion of all exocyst subunits is lethal, except for *SEC3* where conditional mutants show accumulation of secretory cargos in the cytoplasm and decreased exocytosis (Finger & Novick, 1997). Deletion mutants of *SEC3* in *C. albicans* and *SEC5* in *N. crassa* remained viable, showed severe growth defects and accumulation of exocytic vesicles under the plasma membrane whereas deletion strains of all other exocyst components were non-viable (Li et al, 2007; Riquelme et al, 2014).

To determine molecular organization of the exocyst complex, protein-protein interactions between exocyst subunits have been widely-studied using yeast two-hybrid assays and protein binding assays (**Figure 4.1**) (Liu & Guo, 2012; Munson & Novick, 2006). These interactions are severally affected in yeast conditional mutants, including *sec3-2*, *sec5-24*, *sec6-4*, *sec10-2* and *sec15-1* mutants (TerBush & Novick, 1995). Structural studies of individual exocyst subunits provide the clue about the molecular function of the complex (Munson & Novick, 2006). All the exocyst subunits are predicted for helical compositions (40%-60%) with several helical bundles and these bundles are packed together to form rod-like structure (Munson & Novick, 2006). Structure-based mutational analysis of yeast Sec6 revealed two patches of highly conserved amino acid residues present on the surface of the Sec6. Mutations in these patches resulted in secretion defects and mis-localization of the exocyst complex (Songer & Munson, 2009).

Fusion of the secretory cargo with the exocyst complex is regulated by the Rab GTPase, Sec4 and its GEF, Sec2 (**Figure 3.1**). Rab-GTPase are small GTP binding proteins required for vesicle fusion and docking to the plasma membrane, which play a central role in vesicle trafficking (Novick & Zerial, 1997; Salminen & Novick, 1987). The active GTP-bound form of Sec4 mediates fusion of secretory cargo to the exocyst subunit Sec15 (Guo et al, 1999b). Conversion of GDP-bound (inactive) to GTP-bound (active) Sec4 is mediated through its GEF, Sec2, which is recruited by an upstream GTPase, *YPT31/32* (Ortiz et al, 2002). It has been shown that Sec4 is completely mislocalised in *sec2* temperature sensitive mutants at non-permissive temperature. The transport of secretory cargo is therefore dependent on activation of Sec4 by Sec2 (Walch-Solimena et al, 1997). In filamentous fungi Sec4 homologues are required for pathogenesis and targeted gene deletion of *SEC4* showed severe growth and secretion defects in *A. nidulans*, *B. cinerea* and *C. lindemuthianum* (Punt et al, 2001; Siriputthaiwan et al, 2005; Zhang et al, 2014b).

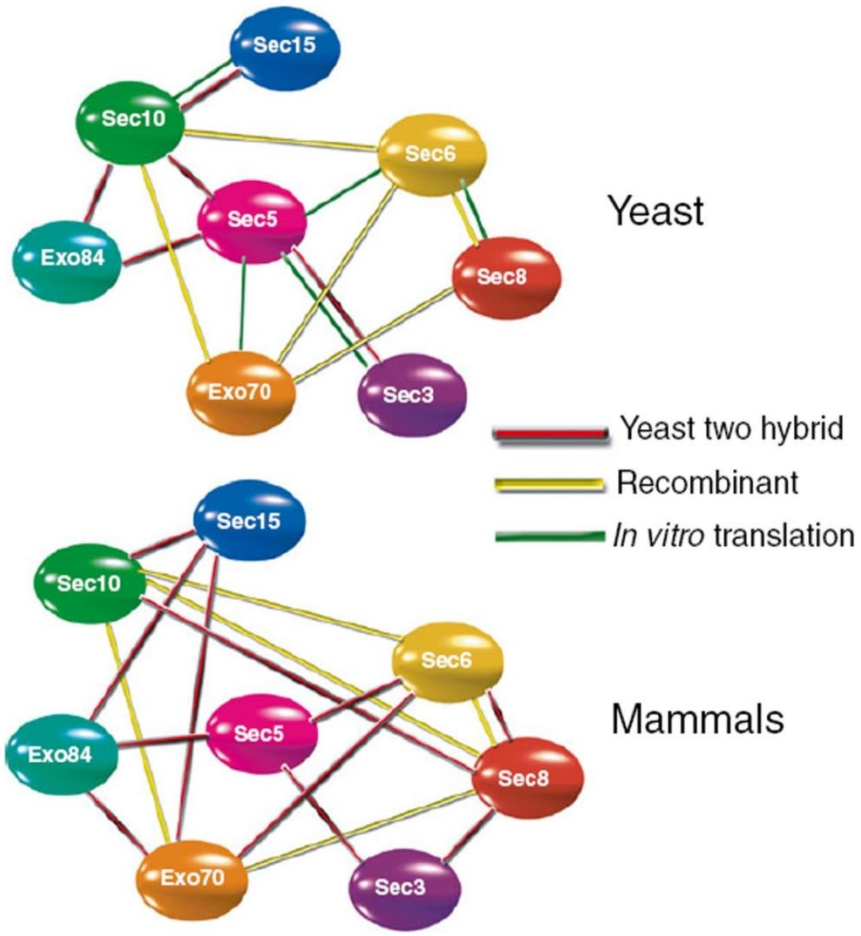

Figure 4.1 Protein-Protein interactions between exocyst subunit. (Taken from Liu & Guo, *Protoplasma* 2012, 249:587-597).

An interaction map suggesting that individual exocyst components interact with multiple exocyst subunits. These interactions have been reported using (1) yeast two-hybrid assay (red lines), (2) protein binding assay with *in vitro* translated proteins (green lines) and (3) protein binding assay with recombinant proteins purified from *E.coli* (yellow lines).

Small GTPases, such as Cdc42, Rac1 and Rho3 are important for the infection-related development in *M. oryzae* and targeted gene deletion mutants of *CDC42, RAC1* and *RHO3* showed severe defect in virulence (Chen et al, 2008; Zheng et al, 2007; Zheng et al 2009). Moreover, Cdc42 regulates septin network around the appressorium pore (Dagdas et al, 2012). In *M. oryzae*, re-polarisation of the cytoskeleton is required for penetration peg emergence and this process is regulated through septin GTPase (Dagdas et al, 2012). Septins are small GTP-binding proteins that are highly conserved from fungi to humans, but interestingly are absent from plants (Pan et al, 2007). Septins form higher-order structures, which include filaments and rings, and act as scaffolds for proteins involved in cell division and polarised growth (Caudron & Barral, 2009; Gladfelter et al, 2001; Momany, 2002; Spiliotis & Gladfelter, 2012). Septins are involved in re-orientation of the cytoskeleton and form diffusion barriers to retain specific proteins at discrete subcellular locations. Septins thereby play key roles in diverse cellular functions such as mitosis, cytokinesis, exocytosis, apoptosis and cellular differentiation (Dagdas et al, 2012; Gladfelter et al, 2001; Longtine & Bi, 2003; Ryder et al, 2013; Weirich et al, 2008).

In *M. oryzae*, appressorium morphogenesis is regulated by cell cycle progression and entry to DNA replication S-phase is a pre-requisite for initiation of appressorium development (Saunders et al, 2010a; Veneault-Fourrey et al, 2006). Appressorium development in *M. oryzae* exhibits both polarised and isotropic growth phases. At the initial stage of conidial germination and germ tube extension, *M. oryzae* shows polarised growth of the germ tube, while at a later stage the tip of the germ tube expands isotropically and forms an appressorium. In the mature appressorium, re-orientation of the F-actin cytoskeleton occurs at the site of penetration peg emergence and this is

meditated through the action of septins. The organisation of septins is controlled by the NADPH oxidase, Nox2-NoxR complex (Dagdas et al, 2012; Ryder et al, 2013).

This chapter addresses the organisation of the exocyst during appressorium-mediated plant infection and reports the results of experiments designed to investigate the role of the exocyst in appressorium-mediated plant infection. The null mutant of *M. oryzae* exocyst *EXO70* and *SEC5* are viable and showed defect in protein secretion and are required for complete virulence. Rab-GTPase, *SEC4* and its GEF, *SEC2* are involved in the plant infection process. On the other hand, *SEC6* played an important role to assemble exocyst subunits at the appressorium pore. The organization of the exocyst subunits at the appressorium pore is mediated through the diffusion barrier formed by heteromeric septin-GTPases.

4.2 Materials and methods

4.2.1 Targeting gene replacement using the split marker method

Targeted gene deletions were carried out using the split marker strategy based on the polymerase chain reaction (PCR), as described by Kershaw & Talbot, (2009). Gene sequences were retrieved from the *M. oryzae* genome database (http://www.broadinstitute.org/annotation/genome/magnaporthecomparative/MultiHome.html) including 2 kb flanking regions of the coding sequence. Gene specific primers were designed to amplify 1-1.5 kb fragments from the flanking sequence of the coding region of the gene of interest. The primer pair LF5' and LF3', and RF5' and RF3' were used to amplify Left and right flank (LF and RF), respectively (**Figure 4.2A**). Reverse complementary sequences of the M13 forward and reverse primers were added to 5' end of the LF3' and RF5' primers. The hygromycin phosphotransferase gene cassette (*HYG*) was amplified from the vector hph-pBLUESCRIPT (Kershaw & Talbot, 2009). The *HYG* gene was first amplified in two fragments HY and YG with primer pairs of M13F and HYsplit, and M13R and YGsplit (**Figure 4.2A**). Initially, the left and right flanks of the gene (LF & RF), and HY and YG fragment from *HYG* resistance cassette were amplified from the first round of PCR amplification (Section 2.2.4) (**Figure 4.2A**). A second round of PCR amplification was then performed using primer pairs LF5' and HYsplit on LF and HY template, and YGspilt and RF3'on YG and RF template which gave the fusion PCR product LF-HY and RF-YG as shown in **Figure 4.2B**. The fragments were then transformed in Wild type Guy11 strain of *M. oryzae*. A full list of the primers used in the present study is shown in **Table 4.1**. The PCR and gel purification of PCR products were both carried out as described in Section 2.2.4 and Section 2.2.5, respectively.

Following transformation, *M. oryzae* transformants appeared after 12-16 days and were selected by resistance to hygromycin. Genomic DNA was extracted from transformants using the protocol described in the Section 2.2.1, and mutants were confirmed by Southern bolt analysis, as described in Section 2.6.

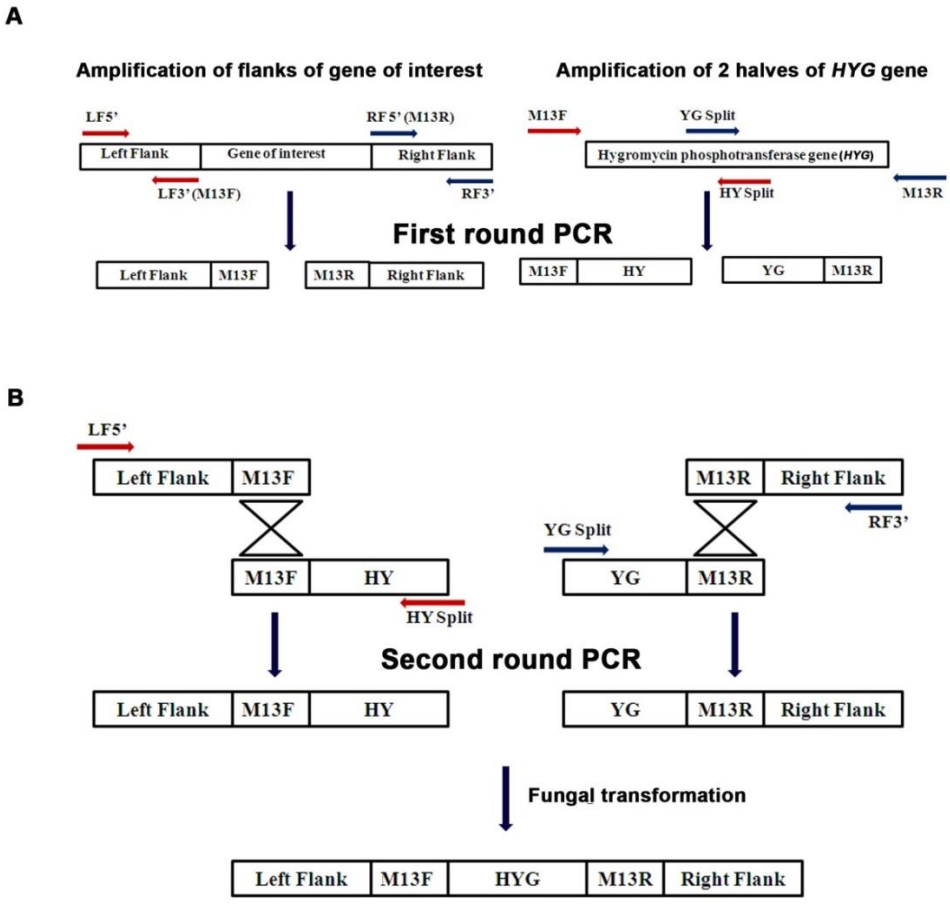

Figure 4.2 Split marker strategy for targeted gene deletion in *M. oryzae* (Modified form Kershaw & Talbot, *PNAS* 2009, 37:15967-15972).

A. First round PCR amplification was carried out using primer pairs, LF5' and LF3', and, RF5' and RF3' in order to generate left flank (LF) and right flank (RF), respectively. The two halves (HY and YG) of hygromycin gene (*HYG*) was generated using primer pairs, M13F and HY split, and, YG split and M13R, respectively. **B.** Second round PCR amplification was performed to fuse LF to HY and RF to YG. LF-HY fragment was generated by using primer pair LF5' and HY split on LF and HY template. Similarly, RF and YG template were fused by primer pair YG split and RF3' to generate RF-YG fragment. Fusion products were then transformed in the appropriate *M. oryzae* strain.

Table 4.1 List of the primers used in this study.

Primer name	Primer sequence 5'---3'
Sec5.50.1	TTGAACTTTGAAGCGATCTCGTCC
Sec5.M13F	GTCGTGACTGGGAAAACCCTGGCGGAACTAATCAACGAGCAGCCAAGA
Sec5.M13R	TCCTGTGTGAAATTGTTATCCGCTAAAAAGGTCAAGCGGTCAAACTCG
Sec5.30.1	CTTACGGTTTTGAATGCTTGTGTG
Sec5.ORF.F	GACTCCAATGACAAAAAGGCAA
Sec5.ORF.R	CTGCGTATGACTGAATCTTTCC
Exo70 50.1	GCTTCGGGCATTTTGGTCATCTGA
Exo70.M13f	GTCGTGACTGGGAAAACCCTGGCGAGACCCCAGATGATTGTAGCTCGT
Exo70.M13r	TCCTGTGTGAAATTGTTATCCGCTCAAGGGCAAGGGCAAGTATGTCAA
EX070.30.1	ATTACTTACCACGCTGCACATGGG
Exo70.5.1	CACTACATACCGCATTTTAACCAA
Exo70.3.1	TTCTTGATACTTTCCTTGTCCTTG
Sec4.50.1	CGGTATGCTTTGTCAGTCAGGTAT
Sec4.M13F	GTCGTGACTGGGAAAACCCTGGCGAGTGGTAATAGTGTGGTTTTGTGA
Sec4.M13R	TCCTGTGTGAAATTGTTATCCGCTCCGTCCTTCTAATCGTAACTCTTT
Sec4.30.1	ACATCTGCTAACCTTCAACCGTCT
M13F	CGCCAGGGTTTTCCCAGTCACGAC
M13R	AGCGGATAACAATTTCACACAGGA
HYsplit	GGATGCCTCCGCTCGAAGTA
YGsplit	CGTTGCAAGACCTGCCTGAA
SEC6.TS.1F	AACTGTTGGGAAGGGCGATCGGTGCGGGCCGGATCCAGCAGGAGTTCACACGCAAG
SEC6.TS.1R	TCGCCGACAGGTTCTTCGAACGTGACAATCATCTGTCGCATGGCTGTTGA
SEC6.TS.2F	GATTGTCACGTTCGAAGAACCTGTCGGCGACTATCGCCAGGTGCTGCACCACTC
SEC6.TS.2R	GCCAAGCCCAAAAATGCTCCTTCAATATCATCACTTGACTCTACTCATAATAGT
SEC6.HYG.F	CCCGAGACTATTATGAGTAGAGTCAAGTGATGATATTGAAGGAGCATTTTT
Sec6.30.1	CTGGCGTTGGTTTTGAGTTTGTCG
HygR	GGTCGGCATCTACTCTATTCC
SEC6.TER.F	GAGGGCAAAGGAATAGAGTAGATGCCGACCGAGATACCAACCAAAGGCACAATC
SEC6.TER.R	TTCACACAGGAAACAGCTATGACCATGATTAAGCTTCTATATACAGATGGGCGCTGAGGT

4.2.2 Construction of a temperature sensitive allele of *SEC6*

An *M. oryzae,* temperature sensitive (TS) mutant of *SEC6* was generated by the GAP repair cloning method, based on homologous recombination in yeast (Kevin et al, 1997). The yeast vector pNEB-Nat-Yeast (**Figure 3.5**) was used to construct a *SEC6* TS allele. Previously, it was reported that a point mutation at L633P in the *S. cerevisiae* Sec6 coding sequence caused temperature sensitive phenotype and a secretion defect at the restrictive temperature at 37°C (Lamping et al, 2005). The conserved region of *M. oryzae SEC6* was identified to generate a TS allele. A Tyrosine amino acid residue at position 601 was mutated to Proline by exchanging TAC to CCT nucleotides. Primers were designed and a 3 bp mutation introduced the overhang of primer pair SEC6.TS.1R and SEC6.TS.2F. The *SEC6* coding region was amplified in two parts and hygromycin resistance gene cassette (Carroll et al, 1994) was inserted between the coding and terminator of *SEC6.* Restriction sites for *BamH*I and *Hind*III were introduced at the 5' end of the primer pair Sec6.TS.1F and Sec6.Ter.R, respectively and 30 bp overhangs incorporated at the 5' end of primers to allow recombination of the fragments. The mutation was confirmed by DNA sequencing and insertion of the *HYG* gene was verified through PCR amplification. Finally, *BamH*I and *Hind*III digested fragments used for transformation of the wild type strain Guy11.

4.2.3 Protein secretion Assay

M. oryzae strains were grown on CM agar plates. After 12 days a 2.5 cm^2 section of mycelium was excised from the growing edge of the colony, homogenised in 150 mL of liquid CM and incubated with shaking for 48 h. Mycelium was harvested by filtration and an equal amount of mycelium transferred to liquid GMM (consisting 10 g L^{-1} glucose, 0.1% (v/v) trace elements (zinc sulphate heptahydrate 22 mg L^{-1}, boric acid 11

mg L^{-1}, manganese(II) chloride tetrahydrate 5 mg L^{-1}, iron sulphate heptahydrate 5 mg L^{-1}, cobalt chloride hexahydrate 1.7 mg L^{-1}, copper sulphate pentahydrate 1.6 mg L^{-1}, sodium molybdate dehydrate 1.5 mg L^{-1}, ethylenediaminetetraacetic acid 50 mg L^{-1}), 0.01% (v/v) thiamine, 0.00025% (w/v) biotin, nitrate salts (sodium nitrate 6 g L^{-1}, potassium chloride 0.5 g L^{-1}, magnesium sulfate heptahydrate 0.5 g L^{-1}, potassium dihydrogen phosphate 1.5 g L^{-1}), pH adjusted to 6.5) for 24 h. Culture filtrates were collected and subsequently lyophilized. The lyophilized culture filtrate was diluted and assayed for total protein concentration using the Bradford method (Bradford, 1976). Protocols and reagents were obtained from Bio-Rad (Quick Start™ Bradford Kit 2 (500-0207)).

Protein quantification was performed using 1 x dye reagent (at room temperature). A standard curve was obtained using known concentrations of BSA (Bovine Serum Albumin) at 0.125, 0.25, 0.5, 0.75, 1.0, 1.5 and 2.0 mg mL^{-1}. A 20 µL aliquot of culture filtrate from each sample and BSA standard were dispensed into a clean test tube and 1 x dye reagent was added to the each sample and BSA standard, followed by rigorous vortexing. Samples were then incubated for 5 min. Absorbance was recorded for all standards and samples. Protein concentration was estimated from the standard curve (Bradford, 1976).

4.3 Results

4.3.1 Generation of targeted gene deletion mutant of Δ*exo70* and Δ*sec5*

To understand the role of the exocyst subunits in infection-related development, targeted gene deletion mutants for exocyst subunit encoding genes were generated. All the exocyst subunits except *SEC3* are known to be essential in budding yeast (Finger & Novick, 1997; Novick et al, 1981), while in *N. crassa* all the exocyst-encoding genes except *SEC5* are crucial for fungal growth (Riquelme et al, 2014). Targeted gene deletions were carried out for *SEC5* and *EXO70*, genes of *M. oryzae*. The *SEC5* and *EXO70* gene deletion constructs were made as described in Section 4.2.1 and are shown in **Figure 4.3A & B**. Putative Δ*sec5* and Δ*exo70* transformants were selected on the basis of their resistance to hygromycin B at concentration of 200 µg mL^{-1}.

Genomic DNA was extracted from putative Δ*sec5* transformants and digested with *Hind*III restriction enzymes. Digested genomic DNA was fractionated by agarose gel electrophoresis and transferred to Hybond-N membrane (Amersham). The membrane was probed with a 1.2 kb fragment of the hygromycin resistance gene cassette and a 1 kb fragment of the *SEC5* coding region. Insertion of the hygromycin resistance gene was observed in 10 independent transformants as hybridizing fragment of 2.1 kb. The wild type strain Guy11 showed a 3.8 kb hybridizing fragment of *SEC5* ORF as shown in **Figure 4.4B**. The *SEC5* deletion mutants were confirmed through a size difference, a 1 kb upstream fragment of *SEC5* gene was used to probe the membrane (**Figure 4.4C**). Southern bot analysis showed a 2.0 kb size difference between wild type strain Guy11 and three putative Δ*sec5* deletion mutants.

Putative transformants for targeted gene deletion of *EXO70* were selected, genomic DNA was extracted and digested with *Xho*I restriction enzyme. Digested genomic DNA

was transferred to Hybond-N membrane (Amersham) after fractionated by agarose gel electrophoresis. The membrane was probed with a 1 kb fragment upstream of the *EXO70* coding region to observe a size difference as an indication of deletion (**Figure 4.5**). The wild type strain Guy11 and putative Δ*exo70* transformants showed a 1.9 kb size difference as shown in **Figure 4.5**.

Targeted gene deletion for other exocyst subunits, *EXO84*, *SEC3*, *SEC6*, *SEC8*, *SEC10* and *SEC15* were failed appear failed after screening more than 100 transformants for each gene from three independent transformation experiments. This suggests that remaining *M. oryzae* exocyst components are essential for viability.

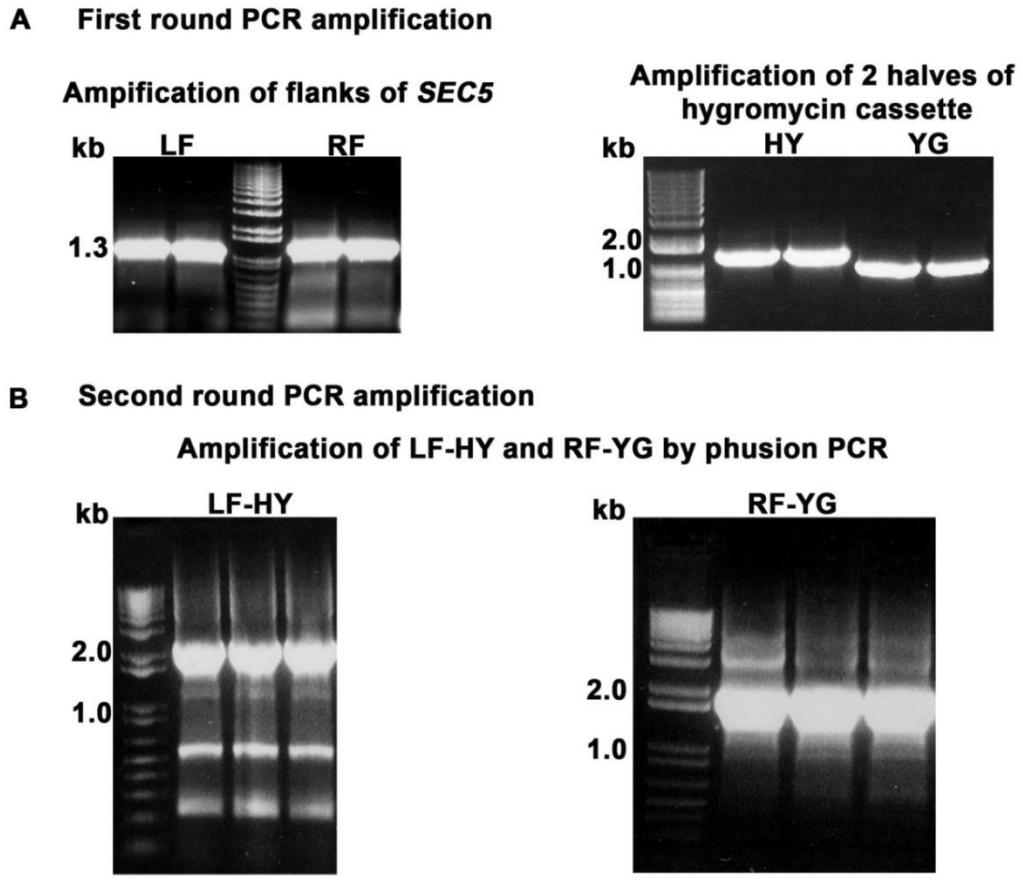

Figure 4.3 PCR amplification of the fragments required for the targeted gene deletion of *SEC5.*

A. First round PCR amplification of the left and right flank of the *SEC5* coding region with primer pairs Sec5.LF5' and Sec5.LF3', and Sec5.RF5' and Sec5.RF3', respectively. Hygromycin cassette, *HYG*, was amplified in two halves HY and YG with primer pairs M13F and HYsplit, and M13R and YGsplit, respectively. **B.** Second round fusion PCR was performed to fuse LF with HY fragment and RF with YG fragment. Fusion fragements (LF-HY and RF-YG) were obtained by PCR amplification with Sec5.LF5' and HYspilt, and YGsplit and Sec5.RF3', primer pairs.

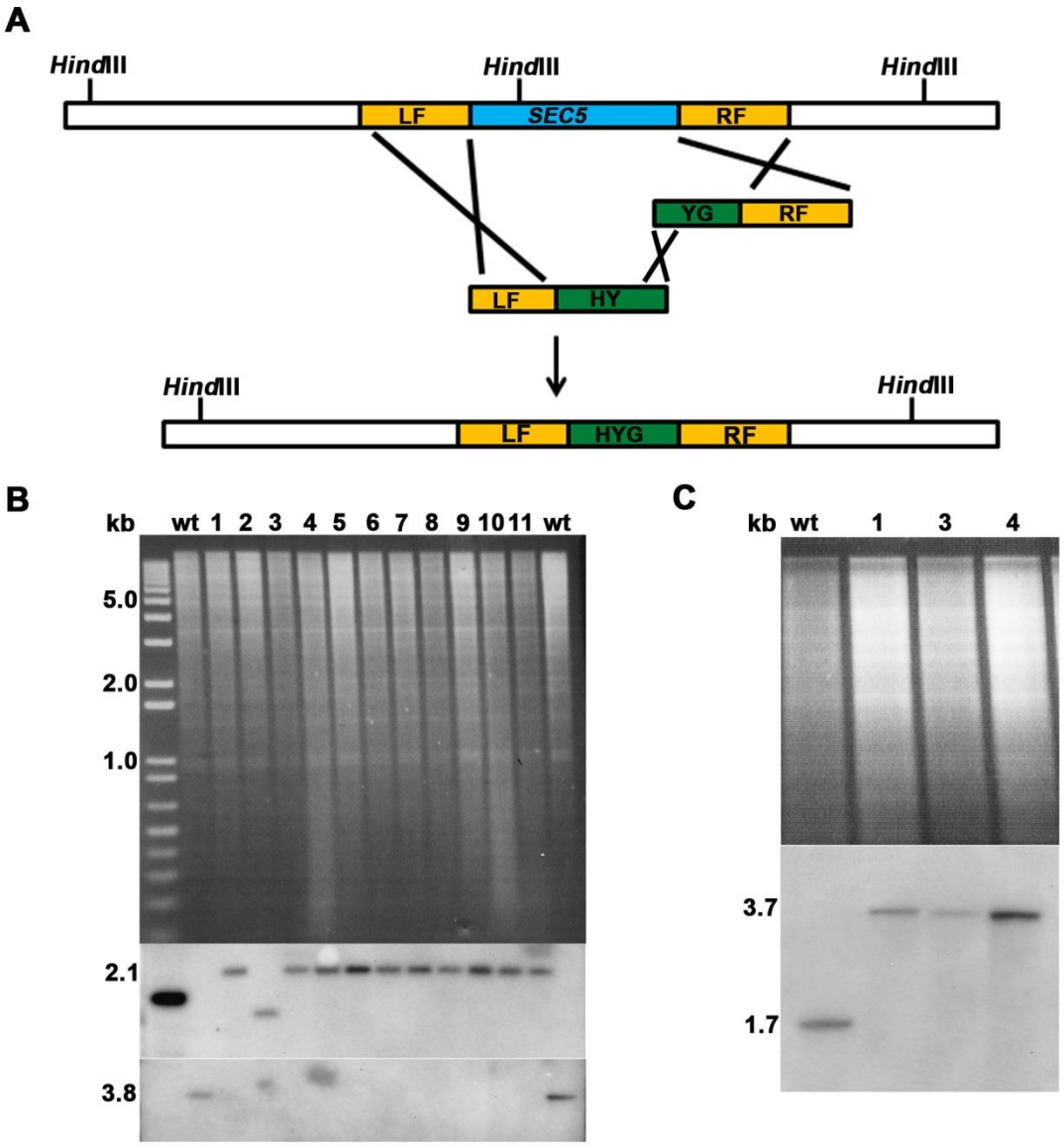
A
HindIII
HindIII
HindIII
LF
SEC5
RF
YG
RF
LF
HY
HindIII
HindIII
LF
HYG
RF
B
kb
wt 1 2 3 4 5 6 7 8 9 10 11 wt
5.0
2.0
1.0
2.1
3.8
C
kb wt
1
3
4
3.7
1.7

Figure 4.4 Targeted gene deletion of *SEC5* and confirmation with the Southern blot analysis.

A. Schematic diagram to show targeted gene replacement strategy for *M. oryzae SEC5* (Kershaw & Talbot, 2009). Hygromycin gene (*HYG*) was used to replace *SEC5* coding region. *Hind*III restriction site was used to confirm Δ*sec5* deletion mutants using Southern bolt analysis. **B.** Southern blot assay to identify Δ*sec5* null mutants. The wild type strain Guy11 and 11 putative transformants were selected. Genomic DNA was isolated and digested with *Hind*III before being fractionated by agarose gel electrophoresis. Fractionated DNA was transferred to Hybond-N and probed with a 1.2 kb fragment of the hygromycin resistance cassette. The same blot was probed again with a 1 kb fragment of *SEC5* coding region. All putative transformants showed the deletion of the *SEC5* gene. **C.** Three independent transformants were further confirmed by a size difference when probed with a 1 kb fragment upstream of *SEC5* gene. A 2 kb size difference was observed consistent with successful replacement of *SEC5* with the hygromycin resistance gene cassette.

A

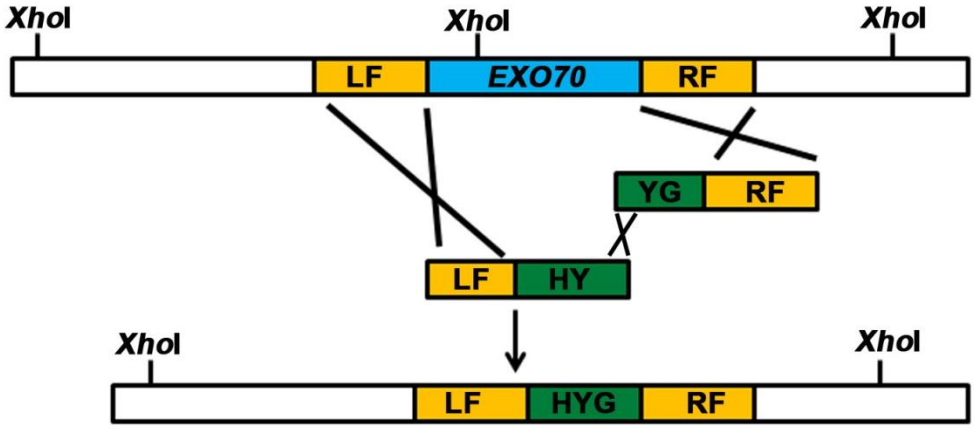
XhoI
XhoI
XhoI
LF
EXO70
RF
YG
RF
LF
HY
XhoI
XhoI
LF
HYG
RF

B

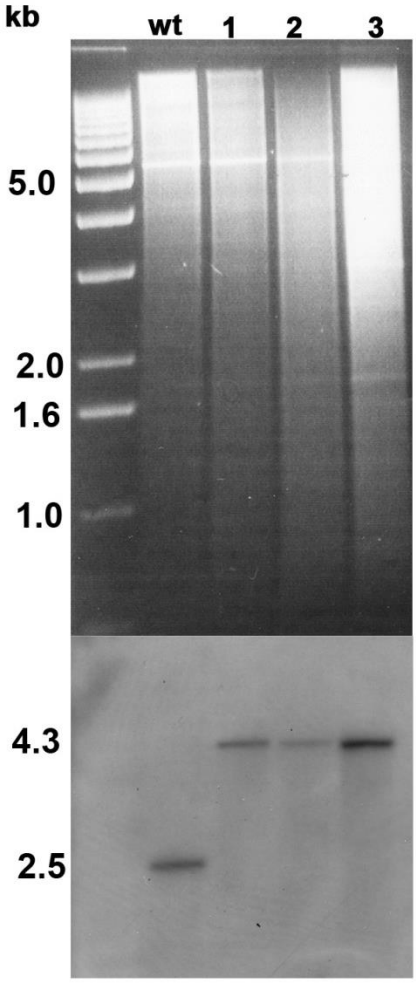
kb
wt
1
2
3
5.0
2.0
1.6
1.0
4.3
2.5

Figure 4.5 Targeted gene deletion of *EXO70* and confirmation by Southern bolt analysis.

A. A schematic diagram to show the split marker strategy for targeted gene deletion of *M. oryzae EXO70*. The *EXO70* gene was replaced with the hygromycin gene (*HYG*) which was confirmed with Southern blot assay. To confirm Δ*exo70* deletion *Xho*1 restriction site was used. **B.** Genomic DNA was extracted from three putative transformants and Guy11, and digested with *Xho*I before being fractionated by agarose gel electrophoresis. Fractionated DNA was transferred to Hybond-N and probed with a 1 kb fragment upstream of *EXO70* gene. After being probed 1.8 kb size difference was revealed consistent with the *EXO70* replacement.

4.3.2 Targeted gene deletion mutant of *SEC4*

SEC4 is a Rab-GTPase required for the vesicle tethering to the plasma membrane (Walworth et al, 1992). The closest homologue of yeast *SEC4* in *M. oryzae* is MGG_06135 (**Table 3.2**). Targeted gene deletion of *SEC4* was carried by amplifying 1 kb flanks of *SEC4* coding region and fusing these with (HY and YG) of the hygromycin resistance gene. The resulting gene fragments LF-HY and RF-YG were mixed simultaneously and transformed the Guy11. Transformants were screened for hygromycin resistance and confirmed by Southern blot. Genomic DNA of Guy11 and six putative transformants was extracted, digested with *Hind*III, fractionated by agarose gel electrophoresis and transferred to hybond-N. Southern blot was hybridised with a 1 kb fragment downstream of *SEC4* coding region as a probe to confirm the *SEC4* deletion. A 6.4 kb size difference was observed between Guy11 and Δ*sec4* mutants **Figure 4.6**.

A

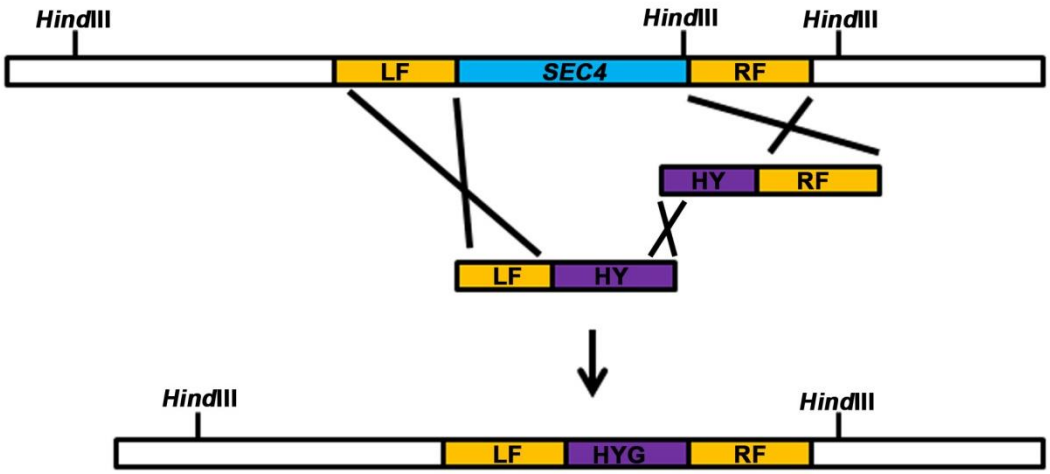
HindIII
HindIII
HindIII
LF
SEC4
RF
HY
RF
LF
HY
HindIII
HindIII
LF
HYG
RF

B

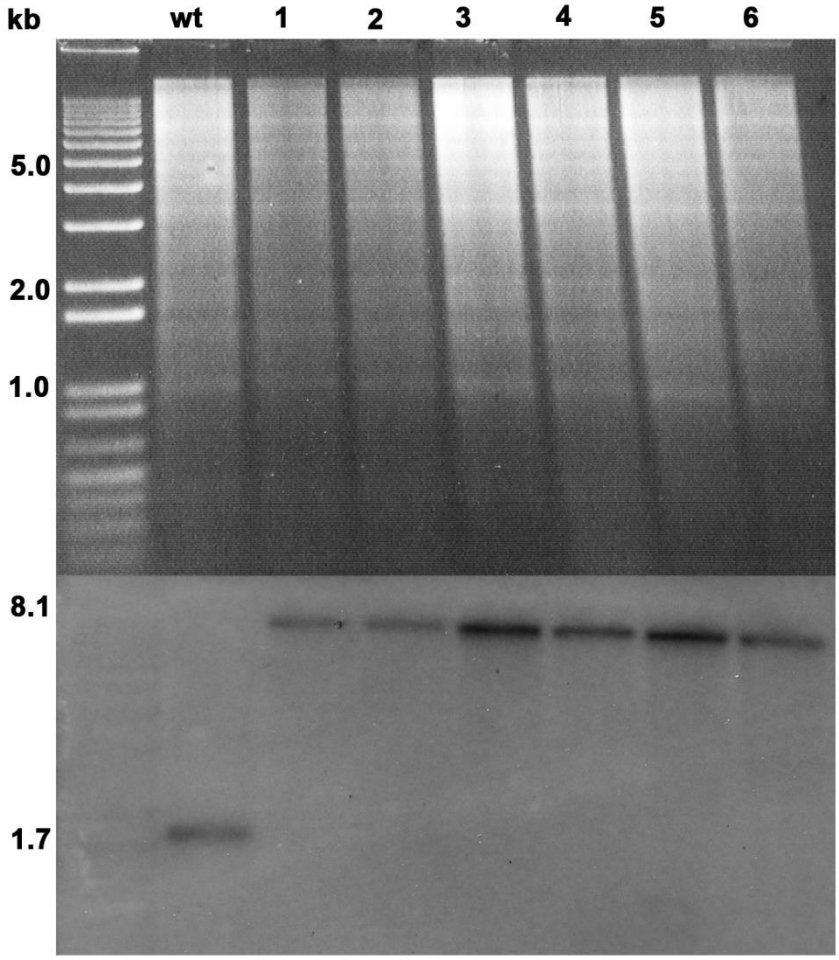
kb
wt
1
2
3
4
5
6
5.0
2.0
1.0
8.1
1.7

Figure 4.6 Targeted gene deletion of *SEC4* and confirmed with the southern blot analysis.

A. Schematic diagram showing targeted gene deletion of *M. oryzae SEC4*. The coding region of *SEC4* was replaced with hygromycin resistance gene cassette (*HYG*). **B.** Six putative *M. oryzae* transformants were selected and genomic DNA extracted. *Hind*III was used to digest genomic DNA of Guy11 and six putative transformants. A Southern blot was probed with a 1 kb fragment downstream of the *SEC4* coding region after being fractionated and transferred to Hybond-N. The Southern blot showed hybridizing fragments of 1.7 kb and 8.1 kb size in Guy11 and putative transformants respectively consistent with *SEC4* gene replacement.

4.3.3 Analysis of vegetative growth and conidiation of Δ*sec5,* Δ*exo70,* Δ*sec2* and Δ*sec4* mutants

Targeted gene deletion mutants *SEC5, EXO70, SEC4,* and *SEC2,* were grown on CM agar plates in order to study colony morphology and vegetative growth. The *SEC2* deletion mutant was kindly provided by Y.F. Dagdas. *SEC2* encodes the guanine exchange factor (GEF) for *SEC4* (Novick et al, 2006; Stalder et al, 2013). A mycelial plug from each mutant and Guy11 were inoculated onto CM agar plates and colony growth measurements recorded over a 14 day period as shown in **Figure 4.7**. All mutants displayed significant reductions in growth compared to the Guy11 strain (two paired t-test, $P < 0.01$). The Δ*sec5,* Δ*sec2* and Δ*sec4* mutants showed a 33%, 25% and 28% reduction in growth compare to the Guy11 strain, respectively. The appearance of colonies of Δ*sec5,* Δ*sec2* and Δ*sec4* mutants was also distinct, with lighter pigmentation as compared to Guy11 (**Figure 4.7A**).

To investigate the role of *SEC5, EXO70, SEC4* and *SEC2* in conidiogenesis, spores were harvested from Δ*sec5,* Δ*exo70,* Δ*sec2* and Δ*sec4* and compared with the Guy11. There was a significant reduction in conidiogenesis in Δ*sec5,* Δ*exo70,* Δ*sec2* and Δ*sec4* mutants compared to Guy11 (two tailed t-test, $P < 0.01$) (**Figure 4.8**). In Δ*sec5* mutant, a 90% reduction was observed while in Δ*exo70,* Δ*sec2* and Δ*sec4* mutants 50%, 70% and 75% reduction was measured, respectively. I conclude that *EXO70, SEC5, SEC4* and *SEC2* are important for vegetative growth and conidiogenesis.

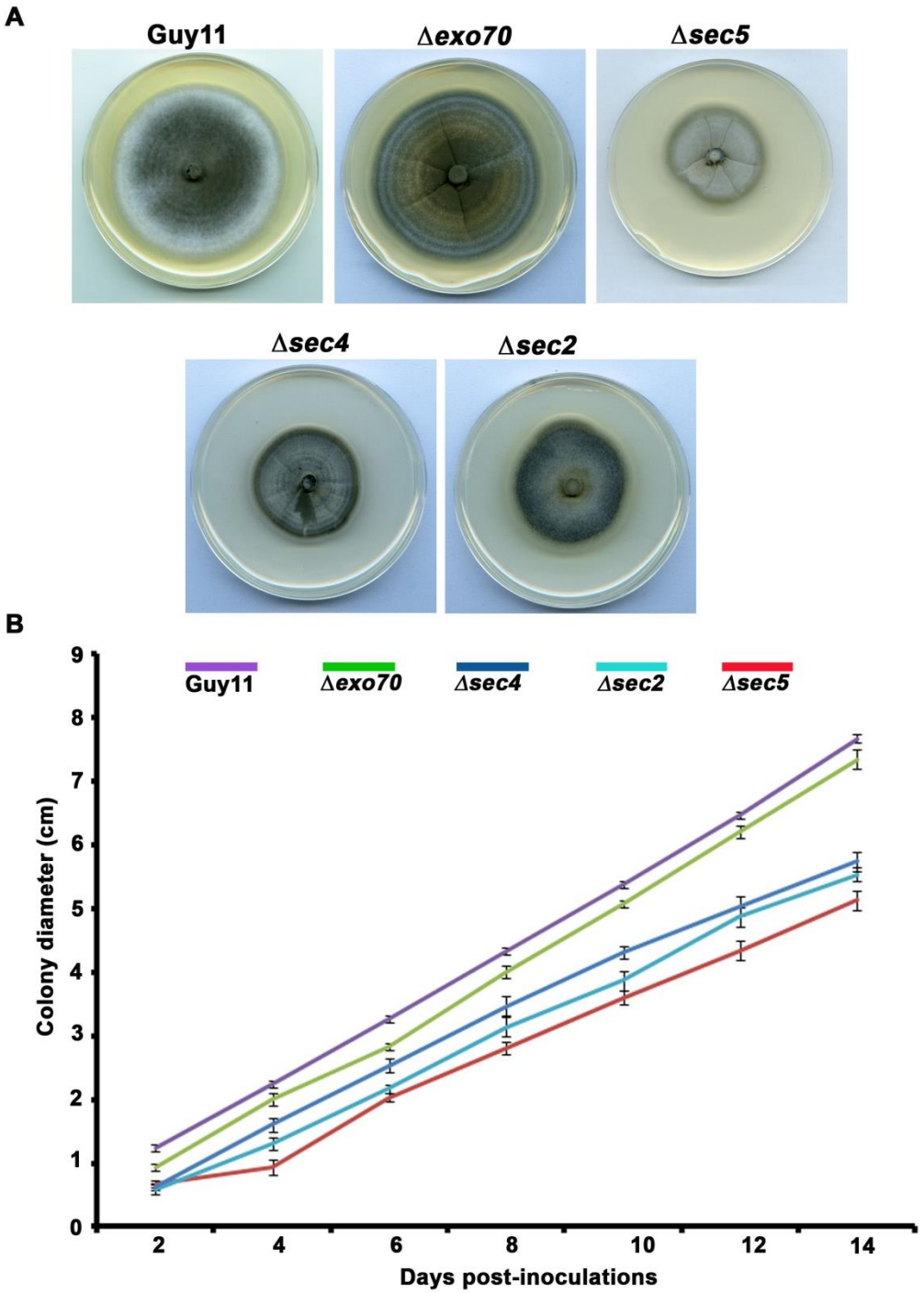

Figure 4.7 Vegetative growth of Δ*sec5*, Δ*exo70*, Δ*sec2* and Δ*sec4* mutants compared to Guy11.

A. Targeted gene deletion mutants Δ*sec5*, Δ*exo70*, Δ*sec2* and Δ*sec4*, and Guy11 strain were inoculated onto CM agar plates and incubated for 12 days at 24°C. **B.** Bar chart to show vegetative growth over a period of 14 days. Measurements were taken from the three independent experiments and the error bar represents the standard deviation ($P < 0.001$).

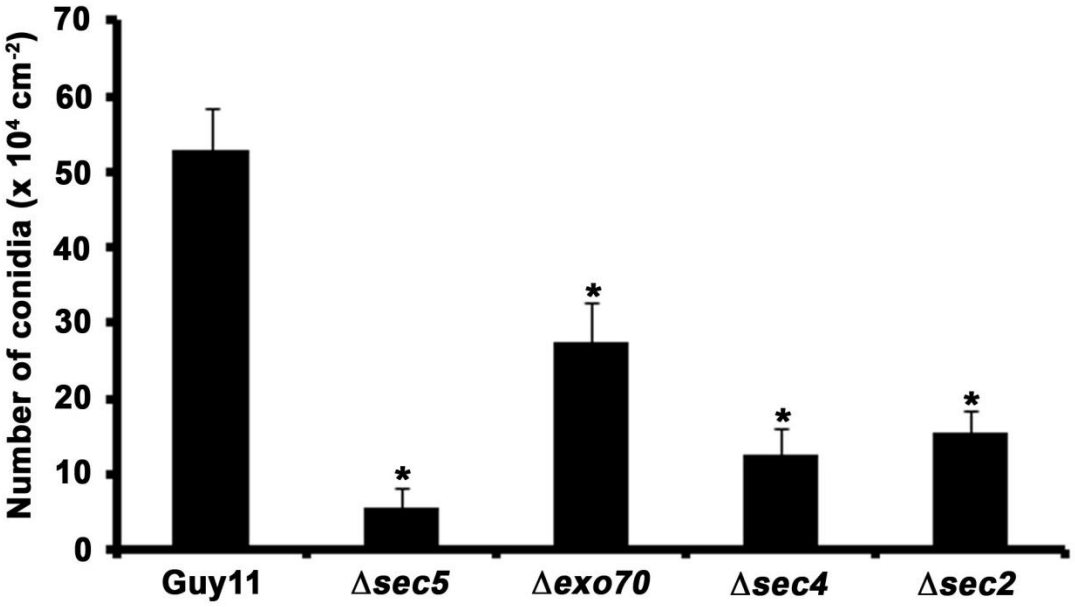

Figure 4.8 Comparison of conidiation between Guy11 strain and Δ*sec5*, Δ*exo70*, Δ*sec2* and Δ*sec4* mutants.

Conidia were harvested from 12 days old plates of *M. oryzae* Δ*sec5*, Δ*exo70*, Δ*sec2* and Δ*sec4* mutants and the Guy11 strain. The number of conidia was significantly reduced compared to Guy11. Observations were taken from three independent replicates and the error bar represents the standard deviation ($P < 0.01$).

4.3.4 Quantification of total secreted protein

Previously, it was reported in *S. cerevisiae* that at the restrictive temperature of 37°C, secretory mutants show a reduction in secretion enzymes (Novick et al, 1981; Novick et al, 1980). We therefore decided to quantify secretion of total protein in culture filtrate. Culture filtrate was collected from each mutant Δ*exo70,* Δ*sec5,* Δ*sec4* and Δ*sec2,* and the wild type Guy11, as described in Section 4.2.3. Secretion of total protein in axenic culture of Δ*exo70,* Δ*sec5,* Δ*sec4* and Δ*sec2* mutants was quantified and compared to Guy11. In Δ*exo70* and Δ*sec4* mutant, a 60% reduction was observed in secretion of protein compared to the Guy11, while in Δ*sec5* and Δ*sec2* the reduction was, 50% as compared to Guy11 (two tailed t-test, $P < 0.01$) (**Figure 4.9**). Results have shown as consistent with the predicated role of *EXO70, SEC5, SEC4* and *SEC2* genes in protein secretion.

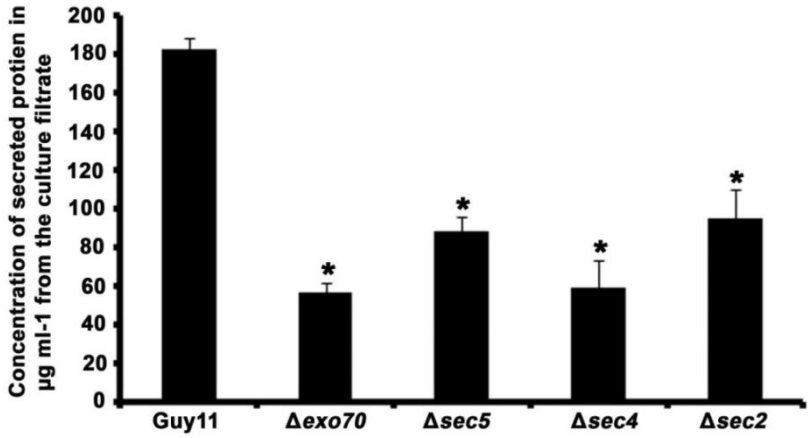

Figure 4.9 Quantification of secreted protein from the culture filtrate.

To estimate the secretion defect in exocyst and Rab mutant, total protein was extracted from Wild type strain Guy11, Δ*exo70,* Δ*sec5,* Δ*sec4* and Δ*sec2* mutant strains. All the strains were grown in liquid CM for 48 h, mycelium was harvested by filtration and an equal amount of mycelia was transferred in liquid GMM to grow further for 24 h. Culture filtrate was collected and subsequently freeze dried. Filtrate for each sample was used to estimate total protein through Bardford method (Bardford, 1976). Values are mean ± S.D. for three repetitions of the experiment.

4.3.5 Plant infection assay with Δ*exo70* and Δ*sec5* mutants

To understand the role of the exocyst in the ability to cause disease on rice plants, targeted gene deletion mutants of exocyst, Δ*exo70* and Δ*sec5* were inoculated onto the susceptible rice cultivar CO-39. Conidia were harvested from 12-day old plates and a uniform concentration of 5 x 10^4 spores mL^{-1} sprayed on 2-3 week old CO-39 rice seedlings. To obtain high humidity, sprayed plants were kept in polythene bags for the first 48 h at 24°C. Plants were then uncovered incubated at 24°C for 3-5 days to develop rice blast symptoms. Rice blast lesions were observed and recorded. The Δ*exo70* and Δ*sec5* mutants were significantly reduced in the ability to cause rice blast disease (two tailed t-test, $P < 0.05$) when compared to Guy11 (**Figure 4.10**).

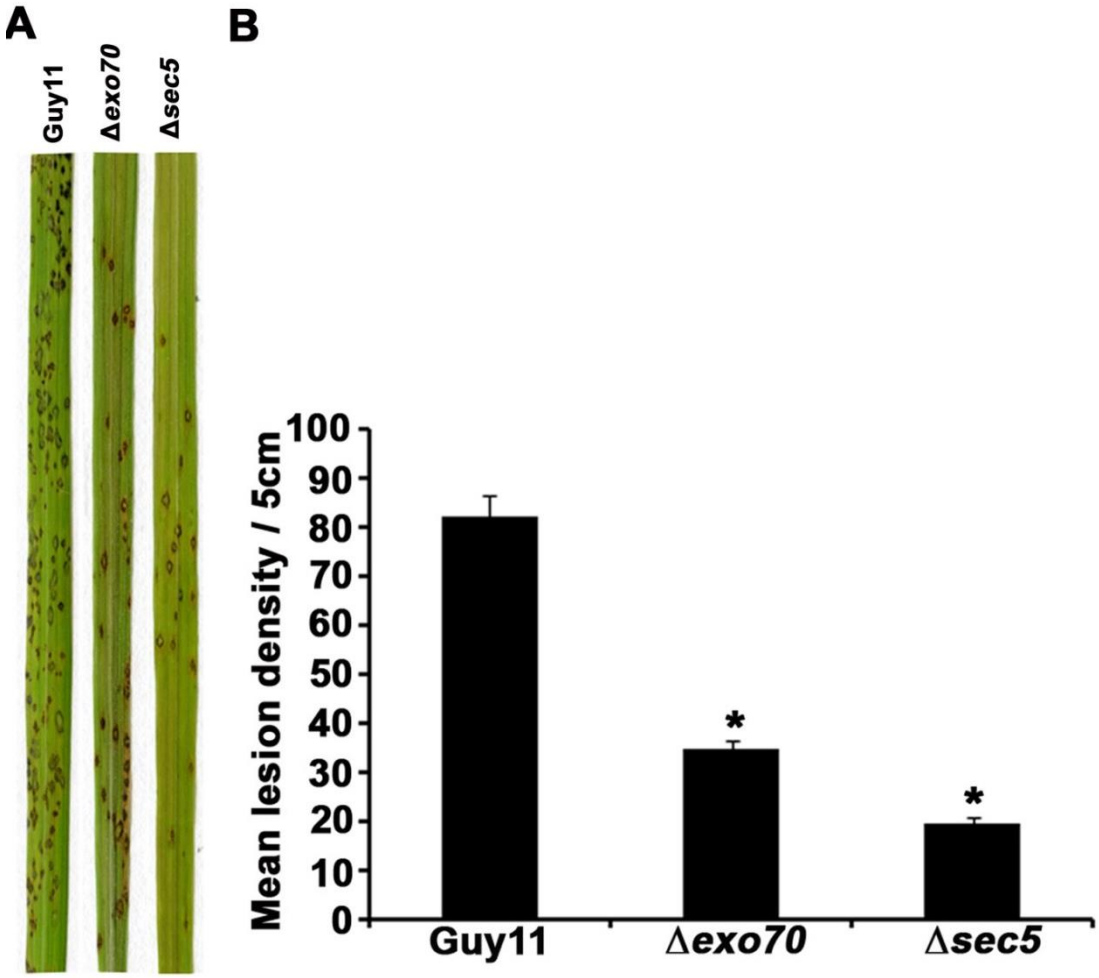

Figure 4.10 The *EXO70* and *SEC5* genes are virulence factors in the rice blast fungus *M. oryzae*.

A. The susceptible rice cultivar CO-39 was used to test the virulence of Δ*exo70* and Δ*sec5* mutants of *M .oryzae*. Eighteen days old seedlings were inoculated with Guy11, Δ*exo70* and Δ*sec5* mutants and Guy11 strain at a spore concentration of 5 x 10^4 spores mL^{-1} and incubated for 5 days. **B.** Bar chart showing the number of lesions per 5 cm on susceptible rice cultivar CO-39 sprayed with Guy11, Δ*exo70* and Δ*sec5* mutant strains ($P < 0.05$ for all mutants, n = 30 for each strain, mean ± S.D., three experiments).

4.3.6 Plant infection assay for Δ*sec4 and* Δ*sec2* mutants

To functionally characterise the role of the Rab-GTPase-encoding gene, *SEC4*, and GEF-encoding gene, *SEC2*, during the plant infection, the Δ*sec4 and* Δ*sec2*, targeted gene deletion mutants, were sprayed on susceptible rice cultivar CO-39. The Δ*sec4 and* Δ*sec2* mutants were significantly reduced in their ability to cause rice blast disease showing only 75% reduction in the ability to cause disease (two tailed t-Test, $P<0.05$) as compare to Guy11 (**Figure 4.11**). I conclude that the Rab-GTPase, Sec4 and its GEF, Sec2 are required for full virulence of *M. oryzae*.

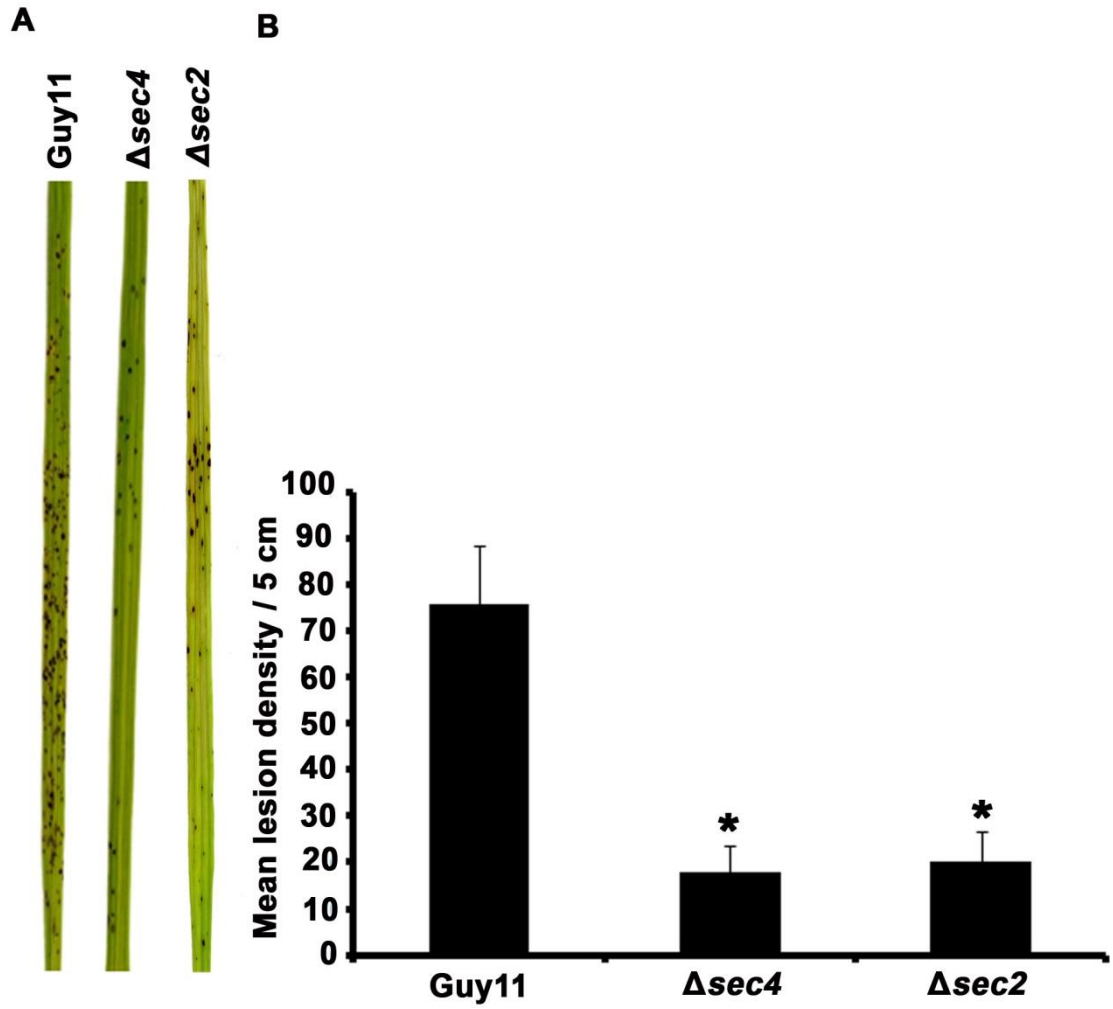

Figure 4.11 The Δ*sec4 and* Δ*sec2* mutants are reduced in their ability to cause rice blast disease.

A. 18 day-old seedlings of susceptible rice cultivar was inoculated with conidial suspensions at concentration of 5 x 10^4 spores mL^{-1} Δ*sec4,* Δ*sec2* and Guy11 and incubated for 5 days. **B.** Bar chart to show the number of disease lesions per 5 cm on susceptible rice cultivar CO-39 sprayed with Guy11, Δ*sec4* and Δ*sec2* mutant strains ($P < 0.05$ for all mutants, n = 30 for each strain after 5 days, Mean ± S.D., three biological replicates of the experiment).

4.3.7 Generation of temperature sensitive allele for *SEC6*

To further characterise the exocyst complex in *M. oryzae*, a temperature sensitive mutant of *SEC6* was generated. In yeast, a point mutation at position 633 in the *SEC6* coding region, L633P, leads to the accumulation of secretory vesicles at non-permissive temperature 37°C (Lamping et al, 2005). The yeast *sec6-4* mutant grows normally at 25°C, but growth is severely impaired at the non-permissive temperature 37°C (Lamping et al, 2005). This suggests that a single point mutation in the *SEC6* coding region is sufficient to cause temperature sensitivity as of the *sec6-4* mutant (Lamping et al, 2005). The same conserved region of the *M. oryzae SEC6* was therefore targeted to generate a temperature-sensitive mutant using allelic replacement. In *M. oryzae*, *SEC6*, encodes a 755 amino acid protein with 20% sequence identity to yeast Sec6 see **Figure 4.12**. The putative amino acid sequence of *M. oryzae* Sec6 was aligned with homologues of *S. cerevisiae* (YIL068C), *C. albicans* (orf19.5463), *A. nidulans* (AN1988), and *N. crassa* (NCU03341) and position 601 of *M. oryzae* was identified as a conserved site to target for generation of a temperature sensitive mutant (**Figure 4.12**). A tyrosine amino acid was substituted with a proline residue at position 601 in *SEC6* gene of *M.oryzae.*

A construct was designed using the yeast recombination gap repair method (Kevin et al, 1997). Primers were designed with complementary over-hangs to the mutated region (**Table 4.1**) (**Figure 4.13A**) and a 3 bp mutation site was introduced by incorporation into the SEC6.TS.1R and SEC6.TS.2F primers (a TAC nucleotide was mutated to CCT) (**Figure 4.13A**). The hygromycin resistance gene cassette (Carroll et al, 1994) was cloned between the coding sequence and terminator of the gene. Restriction sites for *BamH*I and *Hind*III were introduced into the Sec6.TS.1F and Sec6.TER.R primers,

respectively (**Table 4.1**). The resulting plasmid was confirmed by DNA sequencing and the *BamH*I and *Hind*III-digested fragment was used for the transformation of Guy11.

Putative *sec6*^{Y601P} transformants were selected on the basis of their resistance to hygromycin B (200 μg mL^{-1}). Genomic DNA was extracted from putative transformants and a 500 bp region, including the site of mutation in the *SEC6* coding region was amplified and sequenced to confirm the mutation. The sequenced region of *SEC6* was aligned with the sequence from Guy11 and the mutation was confirmed at position 601 (**Figure 4.13B**). Integration of the selectable marker was further confirmed by PCR amplification using primer pair Sec6.TS.2F and Sec6.30.1, which showed a 1.4 kb size difference between Guy11 and *sec6*^{Y601P} mutant consistent with insertion of the hygromycin resistance cassette between the *SEC6* coding region and terminator (**Figure 4.14A**).

Temperature sensitivity was observed at a semi-restrictive temperature of 29°C and *sec6*^{Y601P} mutants showed growth defects compared to Guy11 or ectopic transfromants. Growth was restored by subsequent incubation at 24°C (**Figure 4.14B**).

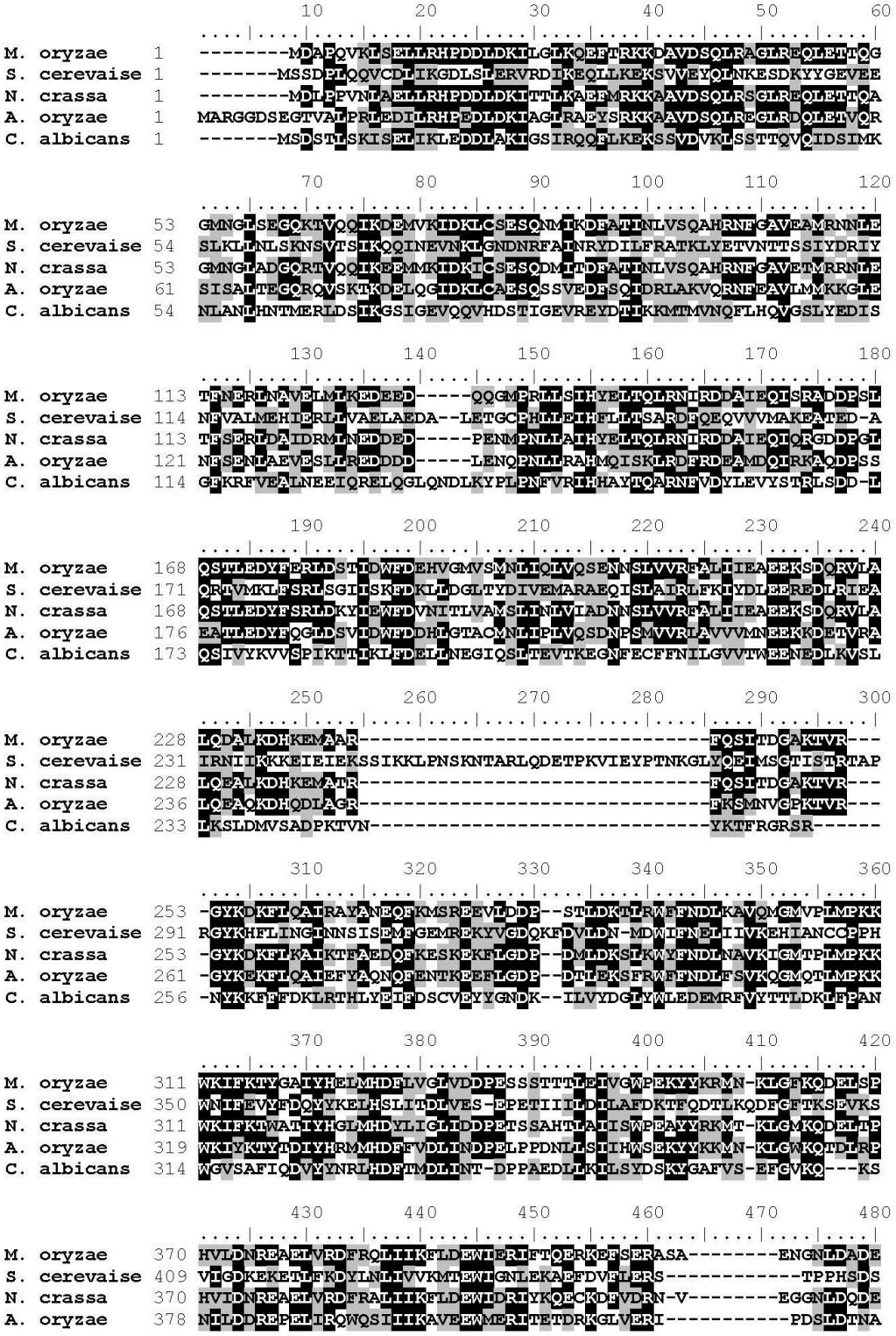
M. oryzae
S. cerevaise
N. crassa
A. oryzae
C. albicans

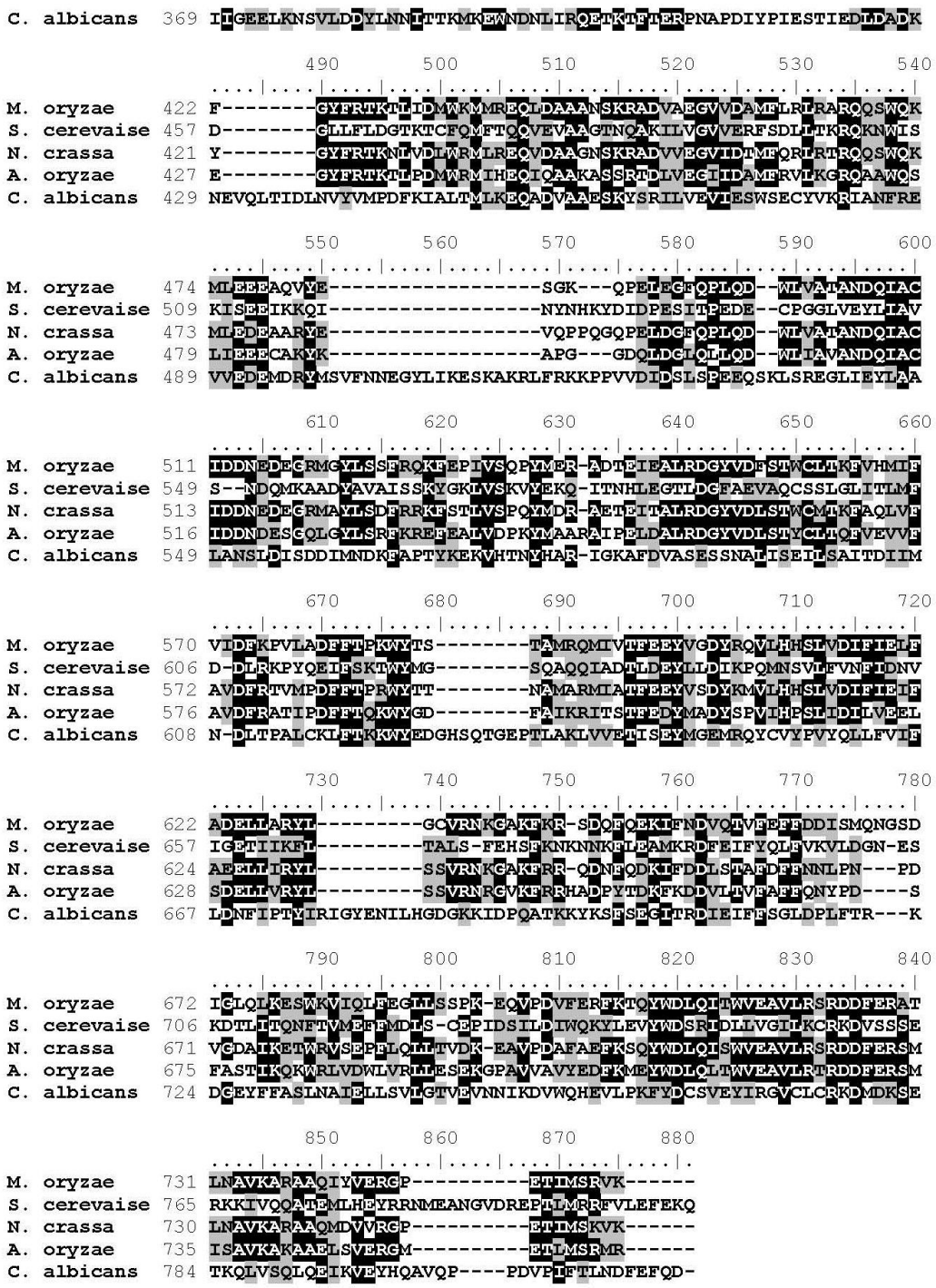

Figure 4.12 Multiple alignment of amino acid sequences of predicted Sec6 coding region from different fungi.

Predicted amino acid sequences of Sec6 protein of *M. oryzae* (MGG_03235.6) aligned with homologues from *S. cerevisiae* (YIL068C), *C. albicans* (orf19.5463), *A. nidulans* (AN1988) and *N. crassa* (NCU03341) using ClustalW (Thompson et al, 1994) in the BioEdit sequence alignment editor version *7.1.3.0* software (Hall, 1999). Amino acids highlighted in a black background are identical and amino acids in a light grey background are similar. Gaps in the alignment are indicated by dashes.

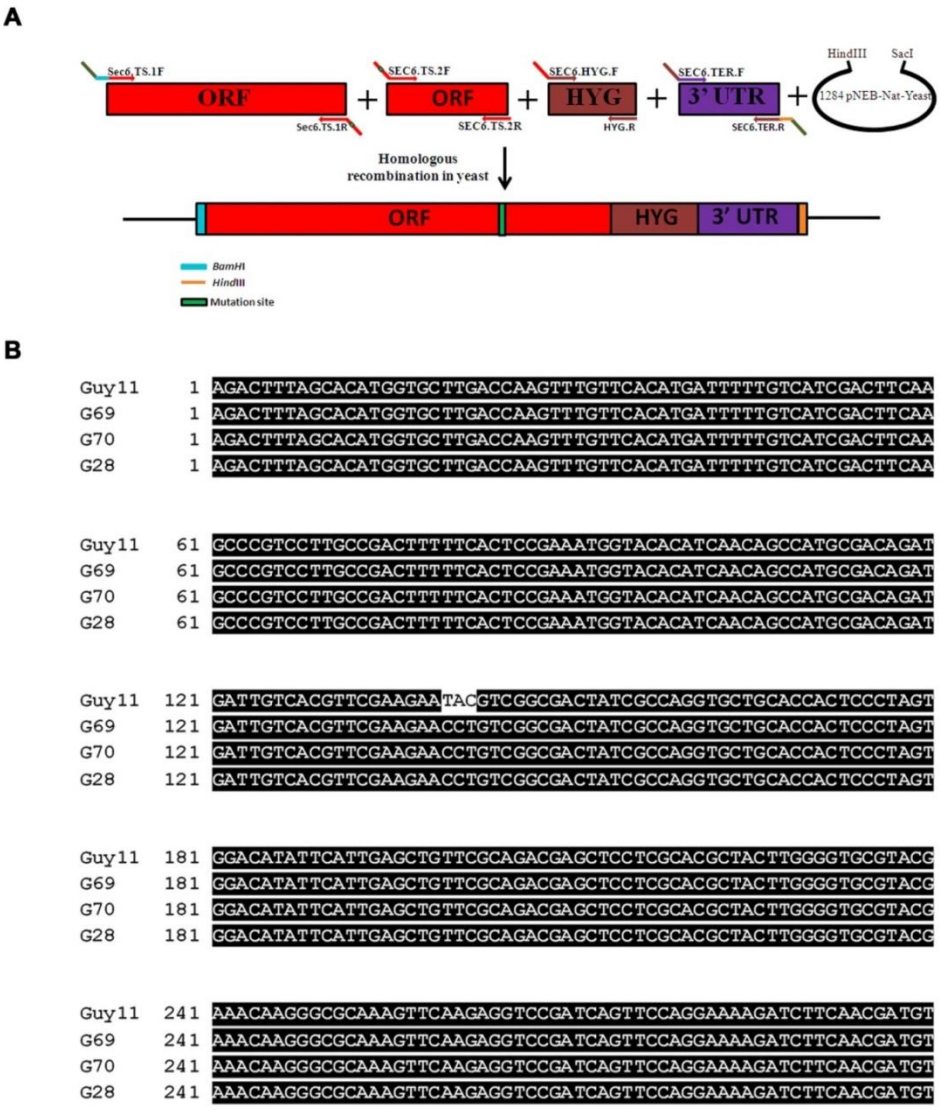

Figure 4.13 Construction of Sec6 TS plasmid and sequencing to confirm the mutation.

A. Schematic diagram to show construction of the Sec6 TS plasmid. The pNEB-Nat yeast vector was used for the cloning and primers were designed with 30 bp complementary over-hangs to the region. A 3 bp mutation was introduced in SEC6.TS.1R and SEC6.TS.2F primers. The hygromycin resistance gene cassette was cloned between the coding region and terminator of the gene. Restriction sites for *BamH*I and *Hind*III were introduced into Sec6.TS.1F and Sec6.TER.R primers, respectively. A *BamH*I/*Hind*III digested fragment was used for transformation of Guy11. **B.** Sequencing of 3 independent transformants and the wild type strain Guy11 was carried out to confirm mutations. Site-directed mutation changed a TAC nucleotide to CCT to obtain a temperature sensitive allele of *M. oryzae SEC6.*

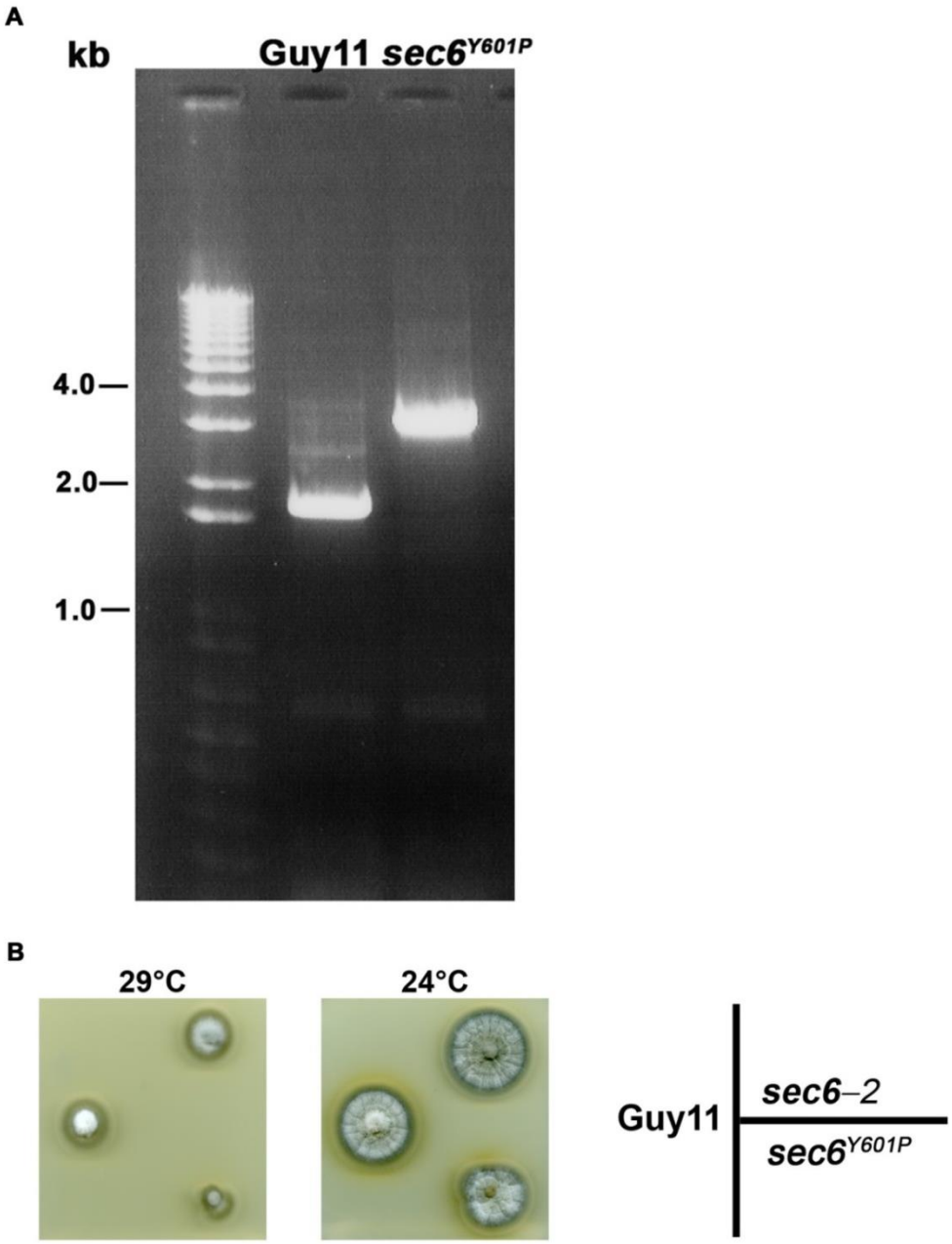

Figure 4.14 PCR confirmation of *sec6*^{Y601P} mutant and test for temperature sensitivity.

A. PCR confirmation to show integration of the selectable marker gene (1.4 kb) between the coding region and terminator, using primers Sec6.TS.2F and Sec6.30.1. A 1.4 kb size difference was observed between *sec6*^{Y601P} mutant and Guy11. **B.** Temperature sensitivity of the *sec6*^{Y601P} mutant was tested by comparision of hyphal growth of the ectopic transformant (*sec6-2*) and wild type Guy11 after incubation at a semi-restrictive temperature of 29°C for 4 days. Restoration of hyphal growth was observed by incubation for a further 3 days at 24°C.

4.3.8 Localization of exocyst subunits in *sec6*^{Y601P} mutant

In budding yeast, conditional mutation of *SEC6* causes disassembly of the exocyst complex at the non-permissive temperature of 37°C (Songer & Munson). To test whether *M. oryzae SEC6* is essential to maintain the exocyst complex at the appressorium pore, translational GFP fusion of each of the exocyst subunits were transformed into the *sec6*^{Y601P} mutant. Sec5-GFP and Sec8-GFP was observed in the *sec6*^{Y601P} mutant and the ring confirmation of the exocyst complex was significantly mis-localized at the semi-restrictive temperature of 29°C ($P < 0.01$) but normal ring formation was observed at 24°C (**Figure 4.15A & B**). Other exocyst subunits were also mis-localised in the mature appressorium when observed in the *sec6*^{Y601P} mutant (**Figure 4.16**). These results suggest that *SEC6* is required for core assembly of the exocyst complex at the appressorium pore of *M. oryzae*.

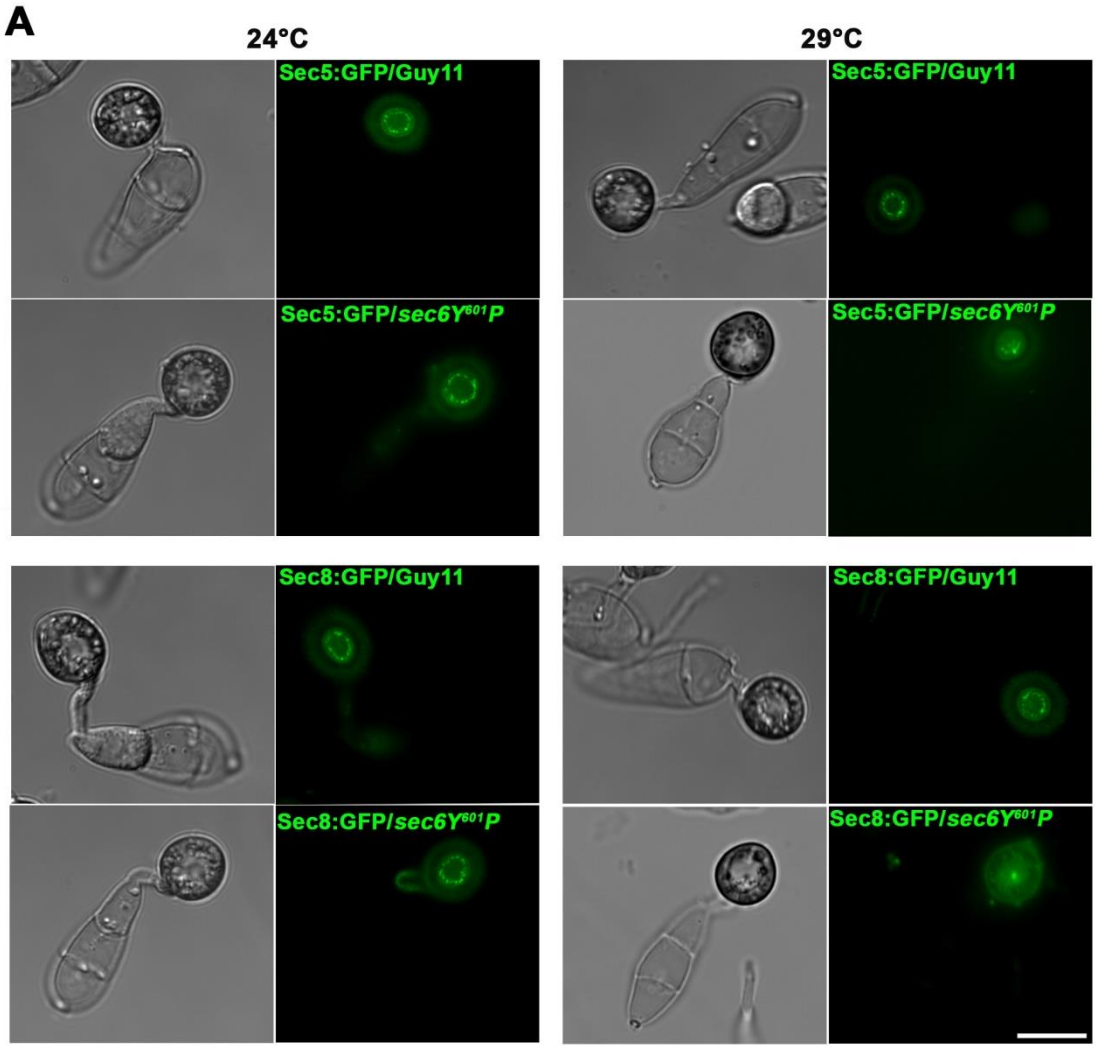
A
24°C
29°C
Sec5:GFP/Guy11
Sec5:GFP/sec6Y601P
Sec8:GFP/Guy11
Sec8:GFP/sec6Y601P
B
24°C
29°C
Intact ring (%)
100
90
80
70
60
50
40
30
20
10
0
*
*
Sec5:GFP Guy11
Sec5:GFP sec6Y601P
Sec8:GFP Guy11
Sec8:GFP sec6Y601P

Figure 4.15 *SEC6* is required for recruitment of the exocyst sub-unit.

A. Micrograph showing localization of Sec5:GFP and Sec8:GFP exocyst subunits in Wild type Guy11 strain and temperature sensitive mutant *sec6*^{Y601P} at a permissive temperature of 24°C and the semi restrictive temperature of 29°C. The exocyst ring was completely mislocalized at the semi restrictive temperature 29°C in *sec6*^{Y601P} mutant. Scale bar=10 µm. **B.** Bar charts showing appressorium pore localisation of exocyst subunit Sec5:GFP and Sec8:GFP at the permissive temperature 24°C (black bars) and the semi restrictive temperature 29°C (grey bars). Values are mean ± S.D., the experiment was repeated three times, n = 300.

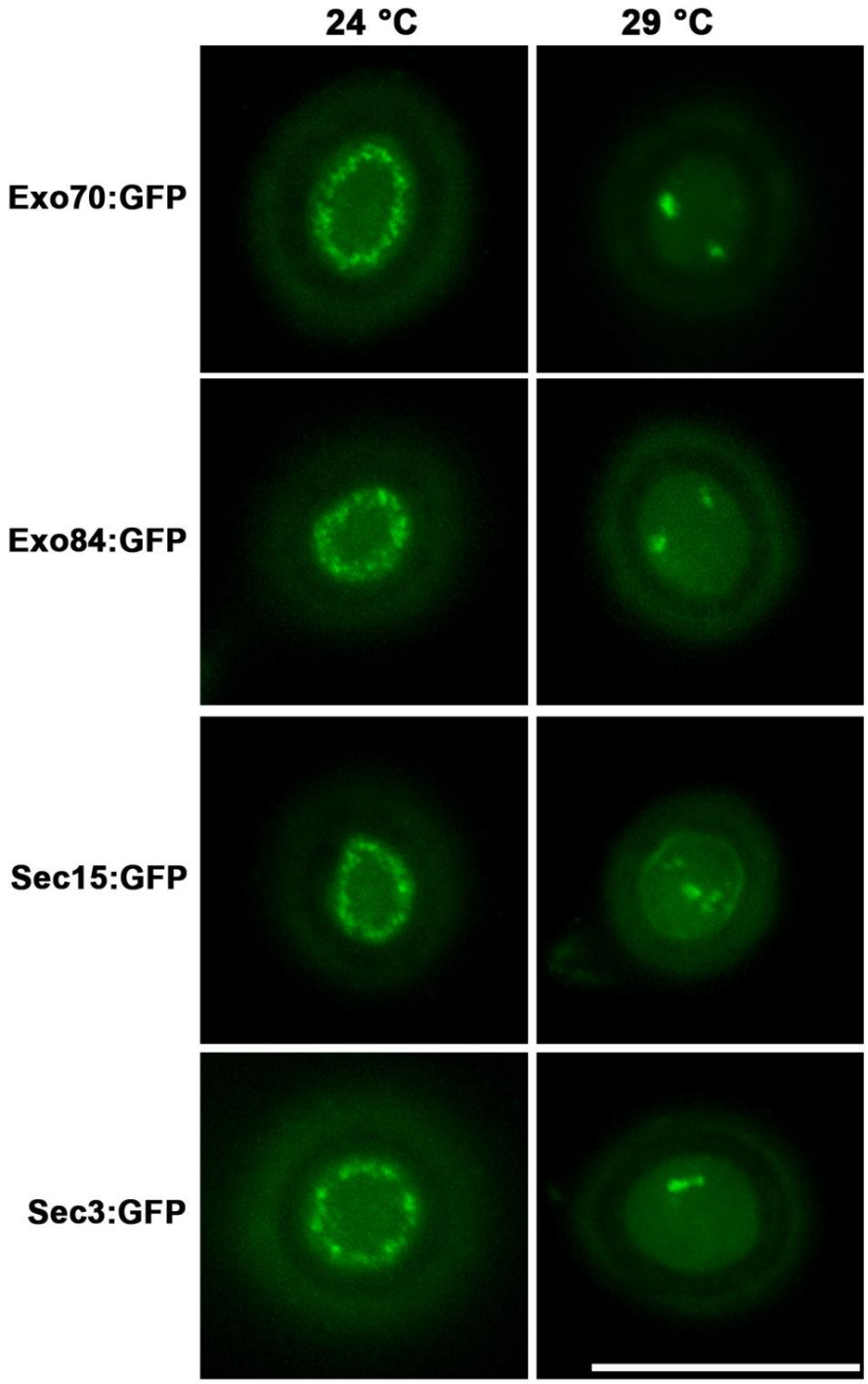

Figure 4.16 Expression and localization of Exo70:GFP, Exo84:GFP, Sec15:GFP and Sec3:GFP in a *sec6*^{Y601P} mutant.

Independent transformants expressing Exo70:GFP, Exo84:GFP, Sec15:GFP and Sec3:GFP in the *sec6*^{Y601P} mutant background were selected, inoculated onto glass coverslips, and observed by epifluorescence microscopy. At the permissive temperature 24°C Exo70, Exo84, Sec15 and Sec3 all formed rings at the appressorium pore, but at the semi-restrictive temperature they all were mislocalized. Scale bar=10µm.

4.3.9 Plant infection assay with *sec6*^{Y601P} mutant

To understand whether *SEC6* is also required for complete virulence on rice plants, *sec6*^{Y601P} mutant and Guy11 were inoculated on susceptible rice cultivar CO-39. Conidia were harvested and CO-39 plants were sprayed with uniform concentration of 5 x 10^4 spores mL^{-1}. Sprayed plants were incubated at the normal temperature 24°C and the semi-restrictive temperature 29°C for 5 day to develop rice blast symptoms. Consistent with loss of exocyst organisation, the *sec6*^{Y601P} mutant was significantly reduced in its ability to cause rice blast disease at the 29°C ($P<0.05$), but showed normal virulence at the 24°C as compared to Guy11 (**Figure 4.17A & B**). The *sec6*^{Y601P} mutant was complemented with the functional Sec6-GFP fusion and loss of virulence was restored (**Figure 4.18**). Leaf sheath assay was performed to check growth of invasive hyphae on susceptible rice cultivar CO-39. At the semi-restrictive temperature the growth of *sec6*^{Y601P} mutant was restricted in first rice cell after 45 hpi while Guy11 and complemented strain infection hyphae invaded up to 3 rice cells over the same period (**Figure 4.18**). More than 50 infection sites were observed for each strain and representative images was shown in **Figure 4.18**. Here, I conclude that the *SEC6* is required for the successful infection of rice plants.

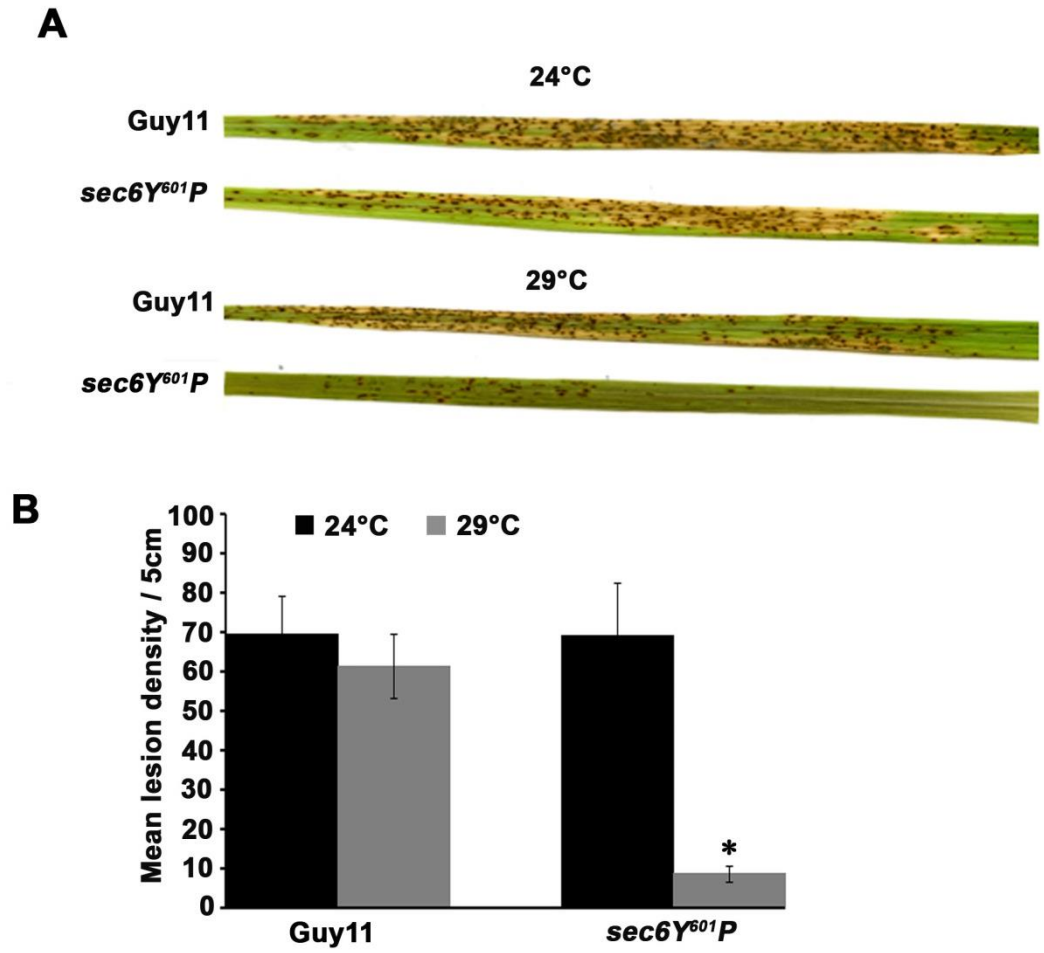

Figure 4.17 The role of *SEC6* in plant infection by *M. oryzae*.

A. Conidia of the *sec6*^{Y601P} mutant and Guy11 were sprayed onto seedlings of the susceptible rice cultivar CO-39 at concentration of 5×10^4 spores mL^{-1} and incubated for 5 days at the permissive temperature 24°C and the semi restrictive temperature 29°C. **B.** Bar charts to show the number of lesions per 5 cm on susceptible rice cultivar CO-39 sprayed with Guy11 and temperature sensitive mutant *sec6*^{Y601P} at a permissive temperature 24°C (black bars) and a semi restrictive temperature 29°C (grey bars) ($P<0.05$) n = 30 for each strain, Mean ± S.D., from three independent experiment.

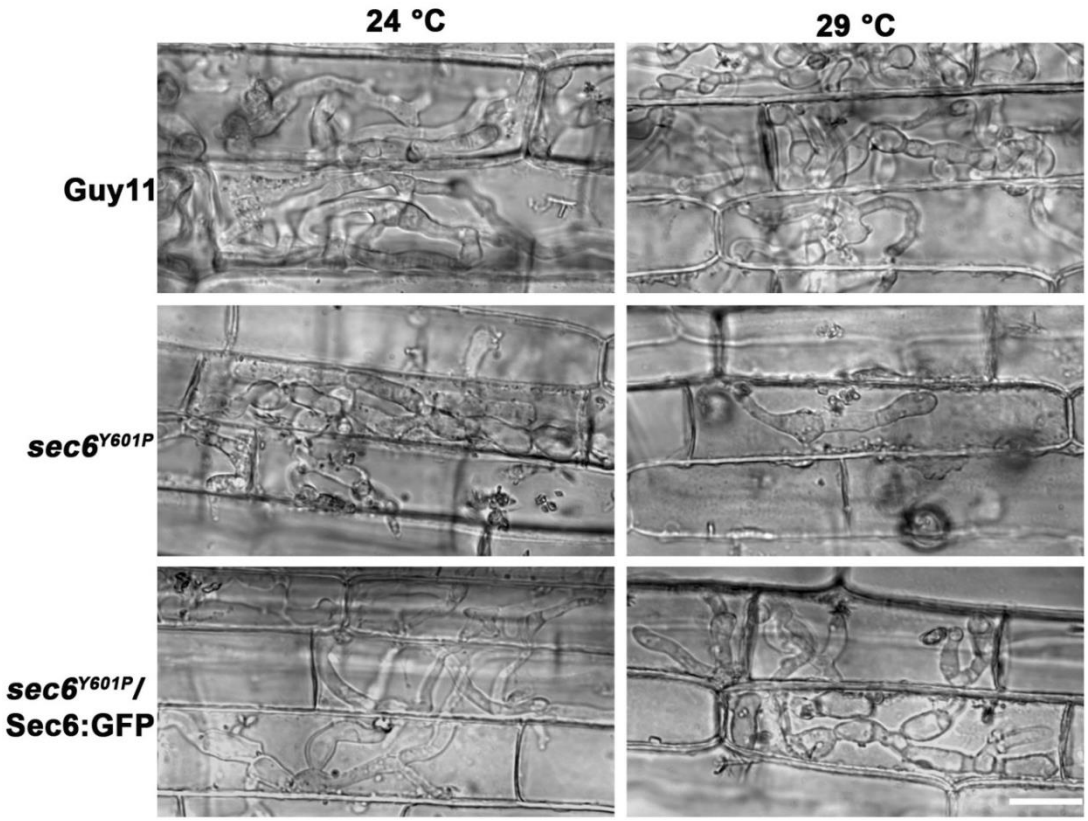

Figure 4.18 Functional complementation of the *sec6*^{Y601P} mutant with Sec6:GFP.

A leaf sheath assay was performed to observe host tissue invasion of susceptible rice cultivar CO-39. Conidia were harvested from each strain and inoculated onto leaf sheath tissue for 45 h. Inoculation were performed at 24°C and 29°C. At 24°C, the wild type strain Guy11, *sec6*^{Y601P} mutant and the complemented strain (*sec6*^{Y601P} mutant::Sec6:GFP) infected rice epidermis normally. At the semi-restrictive temperature 29°C, the *sec6*^{Y601P} mutant infection hyphae remained in first rice cell while the complemented strain and Guy11 infection hyphae invaded up to 3 rice cells over the same period. Scale bar=10µm.

4.3.10 Septin dependent localization of the exocyst subunit at the appressorium pore

M. oryzae exocyst components localise at the cortex of the appressorium during early stage of the appressorium formation however in mature appressorium exocyst ring organise at the appressorium pore (**Figure 3.9**). Transition of the exocyst ring from cortex to the appressorium pore was followed under confocal microscope. It was observed that the exocyst ring moved from the cortex to the appressorium pore after 11 h of the appressorium development (**Figure 4.19 & Supplementary movie 4.1**). In the previous section 3.3.12 we obsereved that the F-actin network is required for the exocyst organisation around the appressorium pore. This suggests that the exocyst transition may be regulated by the cytoskeleton in the mature appressorium. Dagdas and colleagues have shown that the septin GTPases expressed after 8 h of appressorium development, regulate F-actin network and form diffusion barrier around the appressorium pore (Dagdas et al, 2012). To test whether septin-mediated diffusion barrier is required for assembly and organisation of the exocyst complex at the appressorium pore, Sec6-GFP was expressed in a Δ*sep3* septin mutant. During the early stages of appressorium formation (4 h), Sec6p showed cortical localization in the Δ*sep3* mutant in the same way as in Guy11 (**Figure 4.20 & 4.21**). However, after 8 h during appressorium maturation Sec6p was completely mislocalized in the Δ*sep3* mutant (**Figure 4.20 & 4.21**). *M. oryzae* septins are only expressed after 8 h of appressorium development (Dagdas et al, 2012) and the organisation and maintenance of the exocyst complex at the appressorium pore is therefore dependent upon septin ring formation.

CHM1 is a Cla4 homologue of yeast in *M. oryzae,* which is a member of PAK (p21-activated kinase) family and it phosphorylates septins (Chen et al, 2008; Dagdas et al, 2012). In *M. oryzae*, a Δ*chm1* mutant is not able to form the septin and F-actin network

in the appressorium (Dagdas et al, 2012). Sec6:GFP was observed in a Δ*chm1* mutant and also localized to the cortex of appressorium at 4 h, while in a mature appressorium, Sec6 was completely mislocalized (**Figure 4.20 & 4.21**).

Septin-mediated plant infection depends on the regulated synthesis of reactive oxygen species by NADPH oxidases which regulate septin organization in the mature appressorium (Ryder et al, 2013). To test whether organization of the exocyst complex is dependent upon NADPH oxidase activity, we expressed Sec6-GFP in a Δ*noxR* mutant. In mature appressoria of Δ*noxR* mutants, Sec6-GFP was not able to localise normally at the appressorium pore (**Figure 4.20 & 4.21**). A Similar result was observed when Sec6-GFP was expressed in a *Δmst12* mutant (**Figure 4.20 & 4.21**). The *MST12* transcription factor is necessary for septin ring formation and plant infection (Dagdas et al, 2012; Park et al, 2002). We conclude that the hetero-oligomeric septin complex is required for the exocyst assembly at the base of the mature appressorium during plant infection by *M. oryzae*.

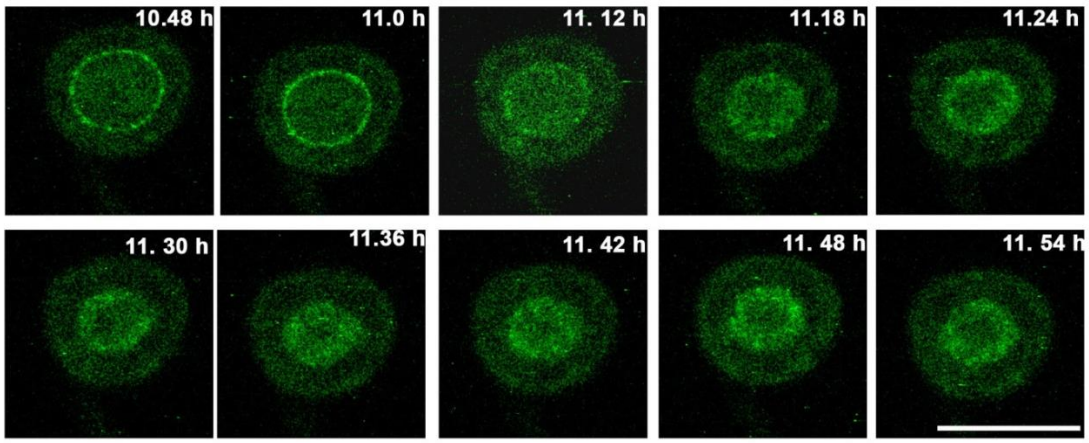

Figure 4.19 Transition of exocyst ring from cortex to the appressorium pore of *M. oryzae*.

Conidia were harvested from the *M. oryzae* strain expressing Exo70:GFP expressing strain, inoculated onto glass coverslip and observed under confocal microscope. After 10 h Exo70:GFP was observed as a ring in the appressorium. However, after 11 h Exo70:GFP quickly re-localise at the centre of the appressorium. Scale bar =10 µm.

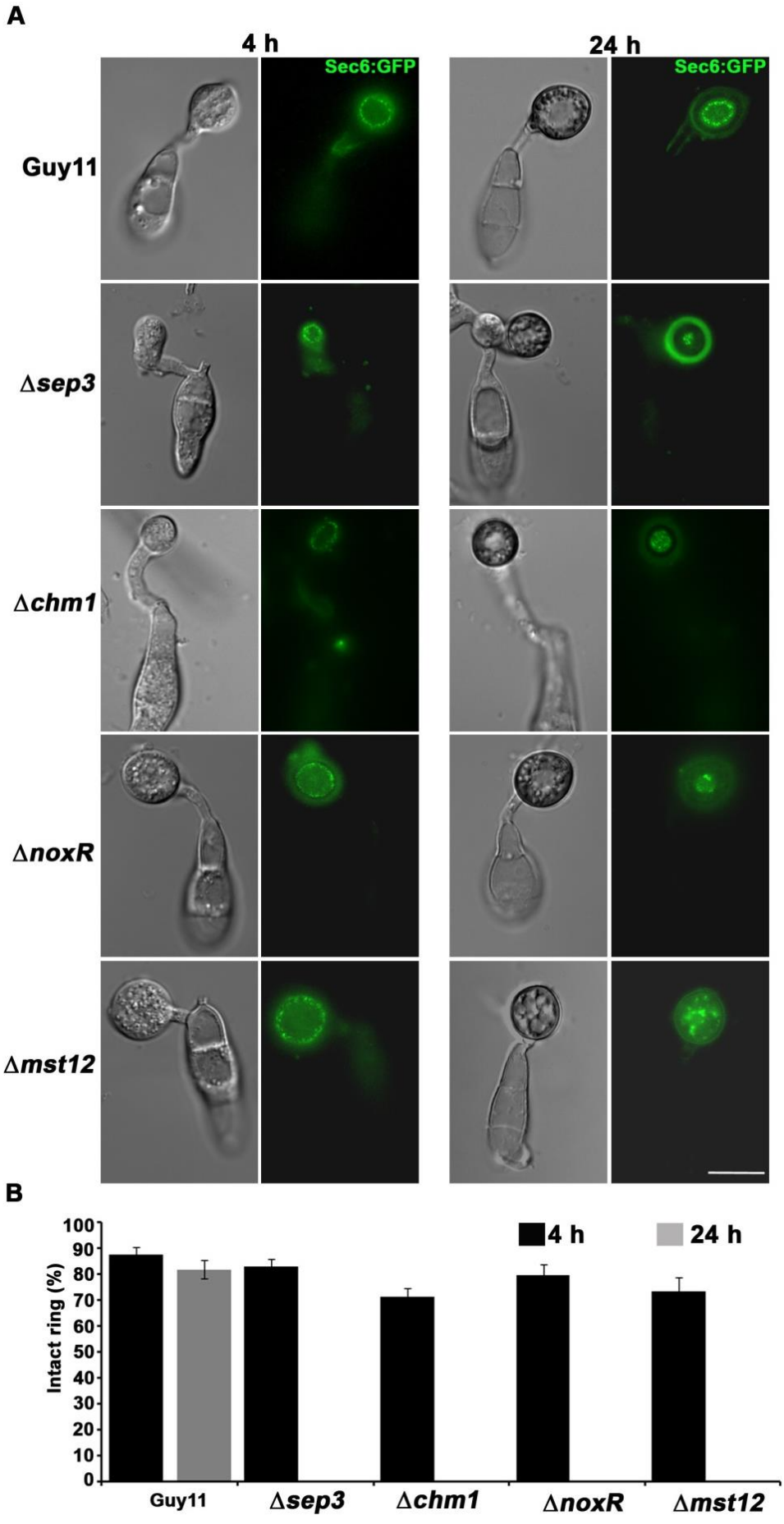
A
4 h
24 h
Sec6:GFP
Sec6:GFP
Guy11
Δsep3
Δchm1
ΔnoxR
Δmst12
B
4 h
24 h
Intact ring (%)
100
90
80
70
60
50
40
30
20
10
0
Guy11
Δsep3
Δchm1
ΔnoxR
Δmst12

Figure 4.20 Recruitment of the exocyst complex to the appressorium pore is septin-dependent in *M. oryzae*.

A. Micrographs showing exocyst sub-unit Sec6:GFP expressed in Guy11, Δ*sep3*, Δ*chm1*, Δ*noxR* and Δ*mst12* mutants. Conidial suspensions at 5×10^4 spores mL^{-1} were inoculated onto glass coverslips and the expression of Sec6:GFP was observed at 4 h and 24 h after inoculation. Scale bar=10 μm. **B.** Bar charts to show percentage of appressoria localising Sec6:GFP correctly at 4 h (black bars) and 24 h (grey bars) after inoculation. Values are Mean ± S.D., the experiment was repeated three times, n = 300.

A

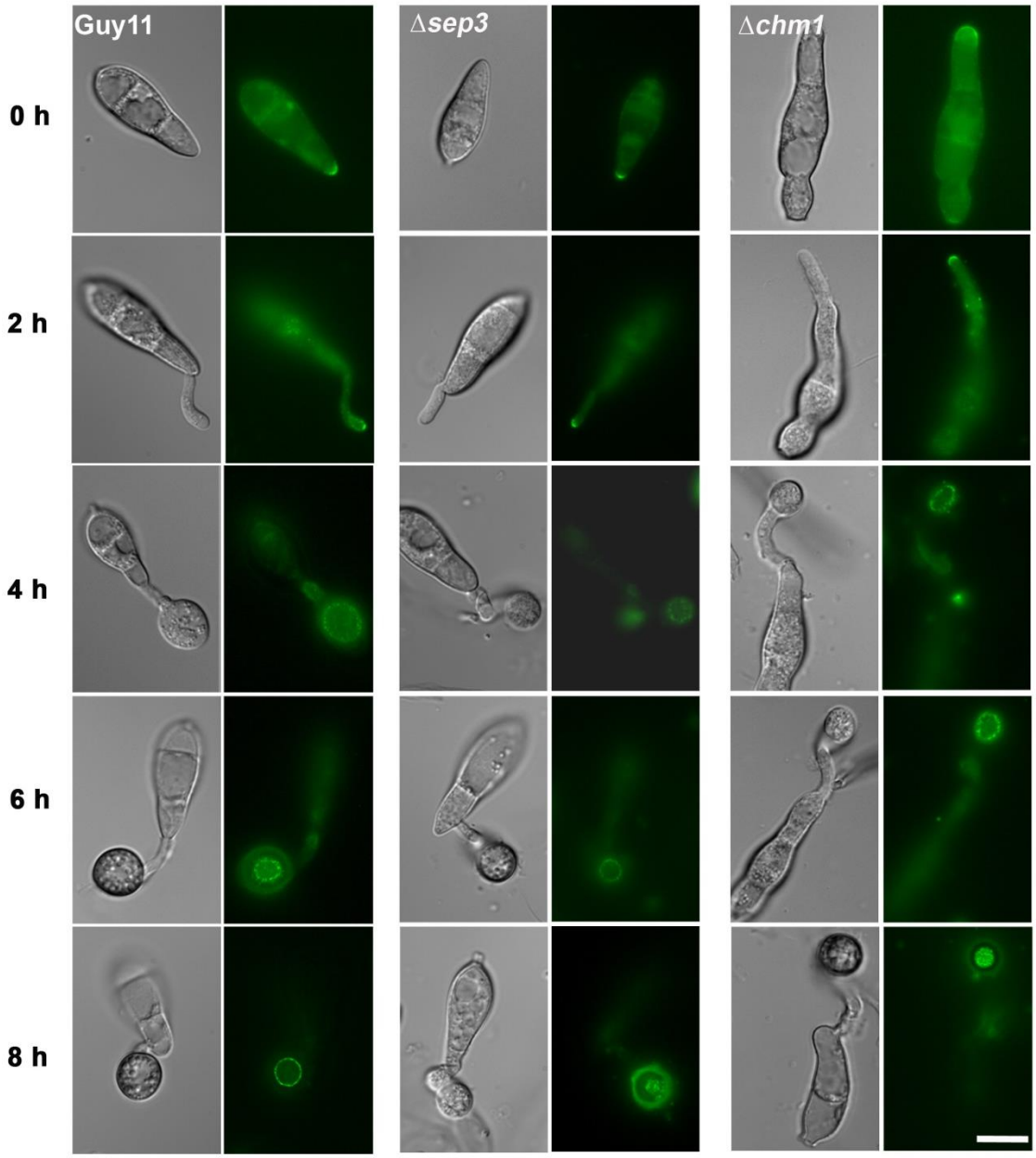

B

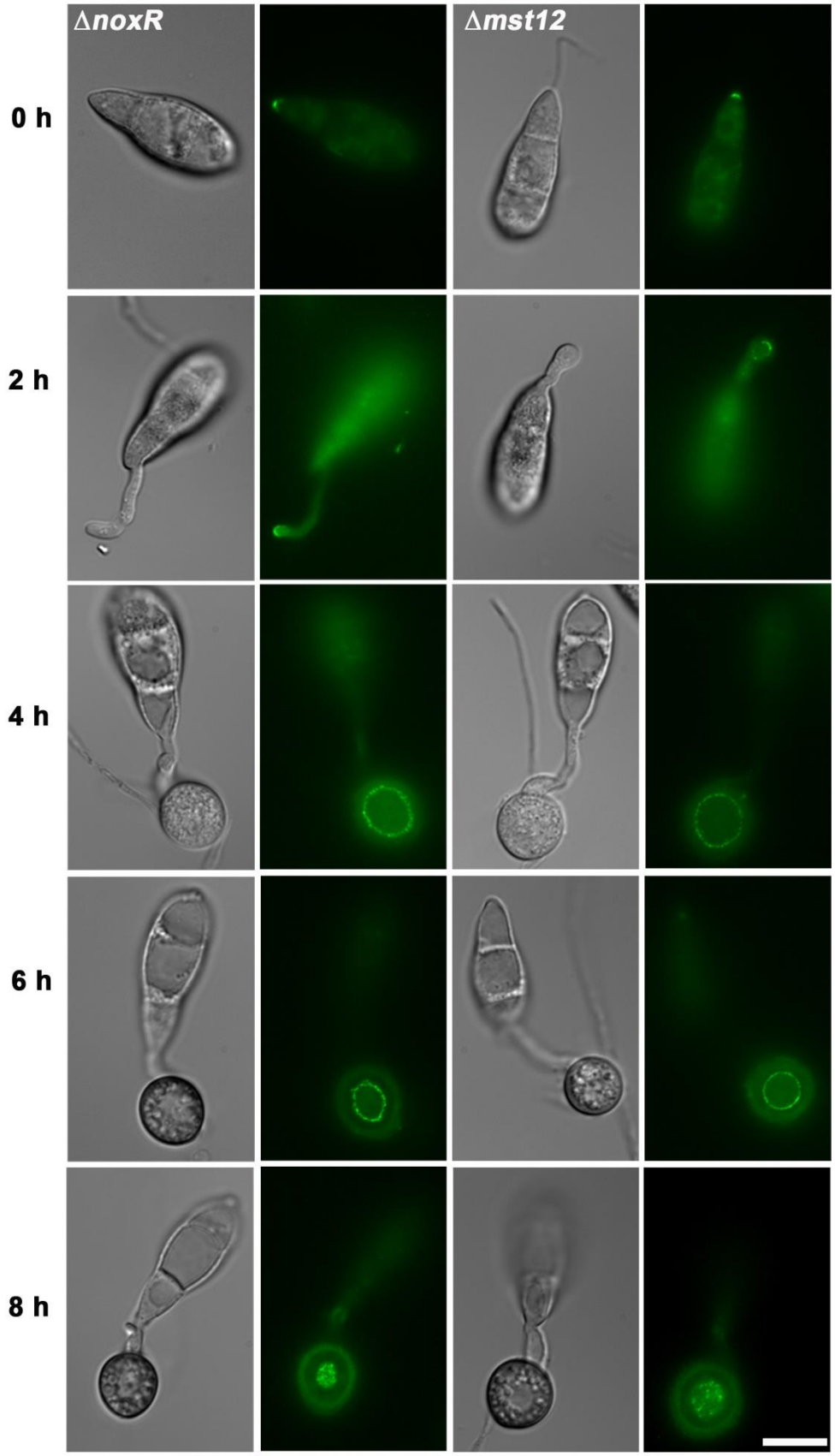

Figure 4.21 Sec6:GFP localization in Δ*sep3*, Δ*chm1*, Δ*noxR* and Δ*mst12* mutants of *M. oryzae*.

A. & B. Micrographs to show the expression of Sec6:GFP in WT, Δ*sep3*, Δ*chm1*, Δ*noxR* and Δ*mst12* mutants during a time course of appressorium development. Conidia were harvested from each strain and inoculated onto glass coverslips and observed by epifluorescence microscopy. Localization of Sec6:GFP was identical in all the strains up to 6 h. At 8 h, there was a ring at the pore of Guy11 and Sec6:GFP was completely mislocalized in Δ*sep3*, Δ*chm1*, Δ*noxR* and Δ*mst12* mutants. Scale bar=10µm.

4.4 Disussion

M. oryzae colonise inside the host through appressorium-mediated infection which shows three symmetry breaking events, i) Germination of conidia and germ tube extension shows polarised growth, ii) Development of the appressorium shows isotropic growth, iii) Emergence of penetration hyphae from the appressorium pore displays polarised growth. We observed these growth events in previous Chapter 3, by localising exocyst complex and other polarity determinants with fluorescence protein, during vegetative growth and appressorium development. In the current study, we set out to investigate the role and the regulation of the exocyst complex in infection-related development.

The secretory components are well conserved from yeast to filamentous fungi and play diverse roles in different fungi. The exocyst complex is essential for polarised growth and null mutants of exocyst subunits are predominantly lethal except *SEC3* in *S. cerevasie* and *C. albicans* (Li et al, 2007; Finger & Novick, 1997). Temperature sensitive mutants of the exocyst subunits showed growth and secretion defects in yeast (Novick et al, 1981; Novick et al, 1980; Novick & Schekman, 1979). Until now there is no report about the role and function of the exocyst in plant pathogenic fungi. Null mutants of *M. oryzae SEC5* and *EXO70* are viable (**Figure 4.4 & 4.5**) and showed similar phenotypes to the *N. crassa sec5* deletion mutant (Riquelme et al, 2014). This suggests some functional similarity of exocyst components in filamentous fungi.

M. oryzae, Rho-GTPases, Rho3, Rac1 and Cdc42 play crucial role in polarity establishment and infection-related development as targeted deletion mutants of *RAC1* and *RHO3* failed to form appressoria and completely non-pathogenic on susceptible rice cultivar (Chen et al, 2008; Zheng et al, 2007; Zheng et al, 2009). However, null mutants

of *CDC42* can form an appressorium but failed to penetrate the host cuticle layer. I show here that exocyst components, *EXO70* and *SEC5* are required for protein secretion and complete virulence (**Figure 4.9, 4.10**). This suggests that establishment of the polarity is critical for the plant infection and exocyst components are required for the polarised secretion during host invasion.

Rab-GTPases have been involved in different steps of vesicle transport, such as vesicle budding, delivery, tethering and fusion to the target compartments (Grosshans et al, 2006). The Sec4 Rab-GTPase has been extensively studied in different organisms and involved in a post-Golgi secretion pathway (Guo et al, 1999b). Homologues of Sec4, Rab8 in mammalian cells, and Sec4 in yeast are essential for viability and temperature sensitive mutation in yeast Sec4 caused severe growth and secretion defects (Huber et al, 1993; Salminen & Novick, 1987). In contrast, deletion of *sec4* in *M. oryzae* is not lethal and showed defects in vegetative growth and conidiation. It has been shown that the deletion of *SEC4* counterpart in *Botrytis cinerea, Bcsas1* is viable and influenced hyphal growth (Zhang et al, 2014b). The *Bcsas1* deletion mutant showed significant reduction of the extracellular activity of polygalacturonases and xylanases (Zhang et al, 2014b). Targeted gene deletion of *M. oryzae SEC4* caused a significant reduction in virulence and protein secretion when compared to the wild type strain (**Figure 4.6, 4.7, 4.8 & 4.11**). Mutants in Clpt1, the Sec4 homologue in *Colletotrichum lindemuthianum* and *Bcsas1* also exhibited severe reductions in pathogenesis and were unable to infect their hosts (Siriputthaiwan et al, 2005; Zhang et al, 2014b). Moreover, *srgA*, a Sec4 homologue in *Aspergillus niger* showed 58% identity to yeast Sec4, was unable to complement the yeast *sec4* temperature-sensitive mutant (Punt et al, 2001). However, SrgA deletion mutants display severe hyphal growth defect and significant reduction in protein secretion (Punt et al, 2001). Altogether, this suggests that in filamentous fungi

Sec4 plays important role in hyphal growth and protein secretion. Even in plant pathogenic fungi Sec4 also act as a virulence determinant for successful infection.

Rab-GTPases are activated by guanine nucleotide exchange factors (GEFs) and Sec2 is a GEF for Rab-GTPase Sec4, is critical for its activity at the later stage of vesicle docking to the plasma membrane (Walch-Solimena et al, 1997). Temperature sensitive mutants of yeast Sec2 showed mis-localisation of Sec4 and abnormal vesicle accumulation to the plasma membrane (Walch-Solimena et al, 1997). In *C. albicans* mutational analysis of *SEC2* revealed that phosphorylation of serine at position 584 is essential for hyphal growth (Bishop et al, 2010). Furthermore, Bishop et al, 2010 reported that Sec2 physically interacts with Cdc28 and serine at position 584 was phosphorylated by Cdc28-Ccn1/Hgc1 kinase (Bishop et al, 2010). In *M. oryzae*, Sec2 is required for hyphal growth and the null mutant was significantly reduced in virulence (**Figure 4.7, 4.8, 4.9 & 4.11**). Targeted gene deletion mutants of *SEC2* and *SEC4* showed similar phenotypes and this suggests that they might act together in protein secretion, involved in vesicle fusion and infection-related development.

In the present study, exocyst components were further characterised in *M. oryzae* by generating a temperature sensitive allele for Sec6 encoding region. In budding yeast, single point mutation at position 633, L633P, in the Sec6 encoding region, showed similar growth phenotype as *sec6-4* temperature sensitive mutants (Lamping et al, 2005). When a similar conserved region of *M. oryzae SEC6* was targeted, hyphal growth of the mutant was reduced at the semi-restrictive temperature (**Figure 4.12-4.14**). Localisation of the exocyst components in a $sec6^{Y601P}$ mutant suggests that Sec6 is critical for the organisation of the exocyst components at the appressorium pore (**Figure 4.15 & 4.16**). This mutation caused a severe virulence effect at the semi-restrictive temperature when sprayed on the susceptible rice cultivar CO-39 (**Figure**

4.17 & 4.18). Sec6 is important for exocyst assembly in yeast and mutation in *SEC6* coding region causes serious growth and secretion defects and perturbation of exocyst assembly at the bud site (Lamping et al, 2005; Songer & Munson, 2009).

Recently, it has been shown in budding yeast that deployment of septins to the polarised site is dependent on Cdc42 and that the septin ring is confined by polarized exocytosis at the bud site (Okada et al, 2013). In *M. oryzae*, septins form a hetero-oligomeric ring around the appressorium pore and Cdc42 is required for septin ring formation (Dagdas et al, 2012). Here, we suggest that first septins form a diffusion barrier around the appressorium pore and this diffusion barrier is required for exocyst assembly at the pore. Sec6:GFP was able to form a cortical ring under the plasma membrane before the septins are expressed in appressorium and in mature appressorium septin-mediated diffusion barrier concentrate the exocyst around the appressorium pore (**Figure 4.20 & 4.21**). Dagdas and colleagues have reported that formation of the septin ring at appressorium pore is regulated by cell cycle checkpoints (Dagdas et al, 2012). The transition of the exocyst ring from the plasma membrane to the appressorium pore might depend on cell cycle checkpoints. In budding yeast, septins are required to compartmentalize the cortex around the cleavage site and maintained both exocyst and polarisome at that site by forming a diffusion barrier (Barral et al, 2000; Dobbelaere & Barral, 2004). This suggests that the diffusion barrier confined the exocystic site in mature appressorium and this site is maintained by septin-GTPases.

In summary, I have shown here that the exocyst components and Rab-GTPase are required for the polarised growth and secretion. The exocyst components, Exo70, Sec5 and Sec6 act as virulence determinants and are involved in infection-related development. The exocyst component, Sec6, is required for the exocyst organisation at the appressorium pore. Finally, I suggest that septin-mediated diffusion barrier is

required for the transition of the exocyst from cortex to the appressorium pore. The exocyst components are further characterised for their role in polarised secretion during host colonisation in following chapter.

Chapter 5. Polarised secretion of effector proteins during host colonisation

5.1 Introduction

Plant pathogens have evolved diverse strategies to enter and colonise inside host plants. Biotrophic plant pathogens create a close association with living host cells through infection hyphae or specialised haustoria, which allow them to utilize plant nutrients (Mendgen & Hahn, 2002) and suppress host immunity (Dodds & Rathjen, 2010). On the other hand, necrotrophic pathogens release toxins and a diverse range of enzymes including proteinases, glucanases, cellulases and xylanases, that can kill host cells and subsequently utilize the nutrients released from dead tissue (Horbach et al, 2011). Hemibiotrophic pathogens initially employ a biotrophic, strategic phase in which the host immune system is suppressed, thereby allowing invasive growth. This phase is followed by a switch to necrotrophic growth when the pathogen secretes toxins to induce host cell death (Horbach et al, 2011).

Plant pathogens secrete a battery of small molecules such as metabolites, sRNA and peptides, called effectors, to suppress host immune responses and alter host gene expression, metabolism and physiology (Win et al, 2012). These effectors are under extreme evolutionary selection, specifically expressed during host invasion, and lack similarity to know proteins (Bozkurt et al, 2012; Djamei & Kahmann, 2012; Yi & Valent, 2013). In response to pathogens, plants have evolved a multi-layered immune system (Jones & Dangl, 2006). Basal defence responses, triggered through conserved microbial elicitors called pathogen- or microbial- associated molecular patterns (PAMPs or MAMPs) (Liu et al, 2014) are recognized by receptor proteins called pattern recognition receptors (Boller & Felix, 2009), such as transmembrane receptor kinases or transmembrane receptor like proteins. PAMP-triggered immunity (PTI) involves the

recognition of PAMPs, include lipopolysaccharides, bacterial flagellin and fungal cell wall components (chitin and glucans), through PRRs. These, in turn, activate downstream components by intracellular signalling and provide basal immunity (Boller & Felix, 2009; Thomma et al, 2011). A second line of defence involves recognition of effectors as avirulence factors by direct binding or through indirect detection called effector-triggered immunity (ETI) (Dodds & Rathjen, 2010; Jones & Dangl, 2006; van der Hoorn & Kamoun, 2008). These avirulence factors are recognised by specific cytoplasmic resistance (R) proteins which are characterised by the presence of nucleotide-binding leucine-rich repeats (NBS-LRR) (Dangl et al, 2013). The interaction between avirulence factors and resistance proteins triggers the hypersensitive response (HR) and limits pathogen growth (Giraldo & Valent, 2013). Evolutionarily, ETI is more dynamic than PTI and effectors are typically more variable and dispensable than PAMPs (Dodds & Rathjen, 2010). PRR functions are quite conserved between species while ETI receptors and pathogen effectors are highly variable as they are continuously under selection pressure (Dodds & Rathjen, 2010). Generally, PTI is effective against non-adapted pathogens and can also be manifested as non-host resistance (NHR), while ETI is effective against pathogens adapted to particular host cultivar defined by major R genes (Dodds & Rathjen, 2010).

Magnaporthe oryzae is a hemibiotrophic pathogen, as biotrophic and necrotrophic infection phases are successively established during host colonisation. *M. oryzae* makes a three-celled conidium, which will germinate when it contacts a hard, hydrophobic surface such as a rice leaf (Howard & Valent, 1996). In mature appressoria, a melanin layer is deposited between the plasma membrane and cell wall and facilitates generation of turgor sufficient to breach the leaf cuticle by retarding the efflux of osmotically active solutes such as glycerol (de Jong et al, 1997; Howard & Valent, 1996; Wilson &

Talbot, 2009). At the base of the appressorium, where cell wall and melanin layer are absent, the fungus forms a penetration peg which emerges at the point of infection (Howard & Valent, 1996; Yi & Valent, 2013). This penetration peg subsequently develops into a primary invasive hypha (IH), which further differentiates into bulbous secondary IH (Giraldo & Valent, 2013).

During the infection process, *M. oryzae* secretes a repertoire of effector proteins and some of these effectors are secreted from the appressorium pore (Collemare et al, 2008). Broadly, two classes of effectors are found in *M. oryzae*. Apoplastic effectors such as Slp1 (secreted LysM protein 1) and Bas4 (biotrophy-associated secreted protein), localise around invasive hyphae and remain in the extra-invasive hyphal compartment bounded by the extra-invasive hyphal membrane (EIHM) (Khang et al, 2010; Mentlak et al, 2012). The second class of effector constitute cytoplasmic effectors such as Pwl2, AvrPita, AvrPiz-t and Bas1 which localise at a host derived structure called the biotrophic interfacial complex (BIC) and within host cytoplasm (Giraldo et al, 2013; Khang et al, 2010; Mosquera et al, 2009; Park et al, 2012). Live-cell imaging of rice blast infections allows the observation of direct secretion of GFP or mRFP-labelled effector proteins in rice cells (Khang et al, 2010; Mosquera et al, 2009).

The *M. oryzae*, apoplastic effector, Slp1, suppresses chitin-induced plant defence responses via direct binding to chitin oligosaccharides and prevents the chitin elicitor binding protein (CEBiP) interacting with chitin oligosaccharide (Mentlak et al, 2012). Slp1 acts as a virulence determinant and the Δ*slp1* mutant is reduced in virulence but this is putatively recognised on a *CEBiP* silenced rice line (Mentlak et al, 2012).

Cytoplasmic effectors, such as Pwl2, Bas1, AvrPita, AvrPizt, AvrPia and AvrPii are host delivered effectors and localise to the BIC (Khang et al, 2010; Park et al, 2012; Yoshida et al, 2009). In response to fungal infections, the plant cell elaborates

membrane cisternae or stacks around the tip of the primary IH which subsequently becomes the subapical region of IH localised into close association with the bulbous IH and is known as the BIC (Giraldo & Valent, 2013; Khang et al, 2010; Mentlak, 2012). To understand the nature of BICs, transgenic rice lines labelled with fluorescence markers for plasma membrane (Lti6B-GFP) and endoplasmic-reticulum (ER) (HDEL-GFP) revealed that the BIC associates with plant plasma membrane and ER (Giraldo et al, 2013; Mentlak, 2012). Accumulation of fluorescently labelled cytoplasmic effectors at the BIC is only observed in compatible interactions and not in incompatible interactions (Mosquera et al, 2009).

The majority of AVRs cloned from *M. oryzae* are cytoplasmic effectors and are recognised by a NB-LRR protein (nucleotide-binding leucine-rich repeat) or a pair of CC-NB-LRR proteins. The cytoplasmic effector Avr-Pita is recognised by the LRR domain of its R protein *Pita* (Jia et al, 2000). On the other hand Avr-Pizt is translocated to host cytoplasm and interacts with rice Avr-Pizt-interacting protein (APIP6), a RING finger ubiquitin E3 ligase, and suppresses PAMP-triggered immunity in rice (Park et al, 2012). Recently, it has been shown that two adjacent NB-LRR resistance genes, *RGA4* and *RGA5,* are required for the recognition of two distinct avriulence genes, *AVR-PIA* and *AVR1-CO39* (Cesari et al, 2014; Cesari et al, 2013). In rice cells RGA4 activates the cell death response while RGA5 represses RGA4 and acts as a receptor for *AVR-PIA* and *AVR1-CO39* (Cesari et al, 2014; Cesari et al, 2013). All cloned rice blast resistance genes are functionally dominant except *pi21*, which encodes a cytoplasmic proline-rich protein consisting of a putative heavy metal-binding domain and a domain for protein-protein interactions which confers non-race-specific durable resistance (Fukuoka et al, 2009).

The mechanism of effector secretion during host colonisation is largely unknown in *M. oryzae.* This study was designed to explore the role of the exocyst complex in plant tissue invasion. Specially, I set out to investigate whether effecor secretion to either the apoplast or the cytoplasm of the rice cells is exocyst-dependent. Futhermore, I analysed the characteristic and role of the BIC as a potential route of effector delivery and set out to explore its relationship to exocyst activity. This research project was carried out in collaboration with the research groups of Prof. Barbara Valent, Department of Plant Pathology, Kansas State University, Manhattan, Kansas, USA and Prof. Ryohei Terauchi, Iwate Biotechnology Center, Kitakami, Iwate, Japan. It showed that apoplastic effectors, but not cytoplasmic effectors are secreted through the conventional ER-Golgi-plasma membrane pathway. The exocyst subunits, *EXO70* and *SEC5,* are required for the secretion of cytoplasmic effectors and *SEC6* is essential for the secretion of the *MEP1* effector which is secreted from the appressorium pore.

5.2 Materials and methods

5.2.1 Chemical inhibition

Rice leaf sheaths were inoculated with *M. oryzae* strains expressing cytoplasmic and apoplastic effectors with fluorescence markers as described in section 2.7.3. Brefeldin A (BFA) (Sigma), inhibits secretion from ER to Golgi pathway and was used to check effector secretion *in planta*. A 10 mg mL^{-1} BFA stock solution was prepared in dimethyl sulphoxide (DMSO, Sigma) (Bourett & Howard, 1996). Rice leaf sheath was inoculated with fungal strains and incubated at 24°C in high humidity sealed containers for 26 h before 50 µg mL^{-1} BFA was added and incubation continued for a further 5 h before microscopy was performed. The microtubule inhibitor methyl 1-(butylcarbamoyl)-2-benzimidazolecarbamate (Sigma) (MBC, the active ingredient in the fungicide benomyl) and the actin depolymerising agent latrunculin A (Sigma), were used to examine the relative contribution of actin and tubulin on effector secretion. Stock solutions of 10 mg mL^{-1} for each inhibitor was prepared and 50 µg mL^{-1} working solution was used to added to leaf sheath for 5 h following 26 h incubation post-inoculation with *M. oryzae* (Czymmek et al, 2005).

5.2.1 Fluorescence recovery after photobleaching (FRAP)

FRAP experiments were performed in Prof. Barbara Valent's lab using a Zeiss LSM 510 confocal microscope with a 488-nm argon laser and a C-Apochromat x 40/1.2 NA water immersion objective at x 2 optical zoom. A region of interest (ROI) covering the entire area of fluorescence in the BIC was selected for photo bleaching. Twenty different sites were selected and photo bleached at 100% laser power. Images were recorded with the acousto-optic tuneable filter attenuated to 5% laser power immediately before and after photo bleaching. Recovery for each experiment was

recorded up to 3 h after bleaching of the BIC associated region. The recovery during this time period was observed from 70% to complete recovery. The GFP fluorescence recovery curves were measured for quantitative analyses as the mean intensity of ROI pixels using the LSM software (version 4.2 SP1).

5.3 Results

5.3.1 Localisation of known *M. oryzae* effectors

In the current study, a range of cytoplasmic and apoplastic effectors were used to understand the general mechanism of effector secretion. Strains expressing effector proteins translationally fused with fluorescence proteins were adapted from previously published studies by Khang et al (2010) and Mentlak et al (2012). Strains expressing the cytoplasmic effectors, Pwl2:mCherry, and apoplastic effector, Bas4:GFP, were kindly provided by Prof. Barbara Valent (Khang et al, 2010). Slp1:GFP, apoplastic effector was characterised by Prof. Talbot's group and used in the present study (Mentlak et al, 2012). Cytoplasmic effectors, Avr-Pia and Avr-Pii, were cloned by Prof. Ryohei Terauchi's group (Yoshida et al, 2009) and C-terminal translationally fused GFP strains were developed by Dr. Xia Yan (Talbot group). To define the general secretion pathway, localisation of cytoplasmic (Pwl2, AvrPia and AvrPii) and apoplastic effectors (Bas4 and Slp1) were observed during host invasion. Strains expressing C-terminal translationally fused FPs (fluorescence proteins) with effector proteins were used for the leaf sheath inoculation to observe intracellular growth of the fungus. Apoplastic effectors, Bas4 and Slp1 localised around the invasive hyphae (IH) while host translocated cytoplasmic effectors, Pwl2, AvrPia and AvrPii, were observed at the BIC (**Figure 5.1 & 5.2**). During biotrophic infection, fungal IH fill the rice epidermal cell without losing its integrity, consistent with previously reported data in *M. oryzae* (Khang et al, 2010; Mosquera et al, 2009).

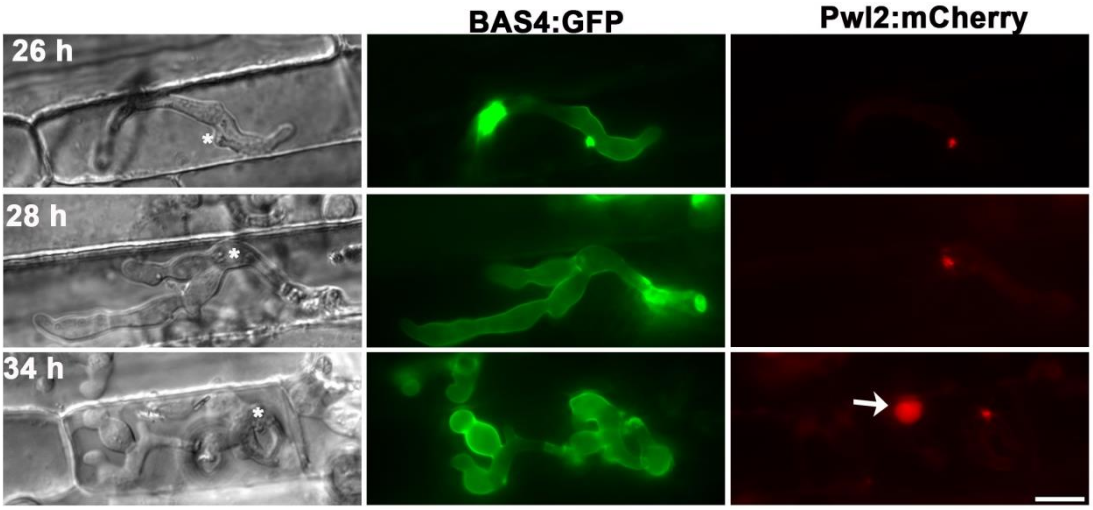

Figure 5.1. Localisation of *M. oryzae* cytoplasmic Pwl2 and apoplastic Bas4 effector proteins in rice cells.

Rice leaf sheath was inoculated with *M. oryzae* strains expressing Bas4:GFP and Pwl2:mCherry. The cytoplasmic effector Pwl2:mCherry was localised at the BIC while the apoplastic effector Bas4:GFP showed apoplastic localisation around the IH. Images of three different time points (26 h, 28 h and 34 h) show the effector localisation during host invasion. Images from left to right for each time point: brightfield, Bas4:GFP (green) and Pwl2:mCherry (red). White asterisks show BIC. Translocation of Pwl2:mCherry to the rice nucleus is shown by arrowhead. All images are representative of more than five different biological replicates. Scale bar=10 µm.

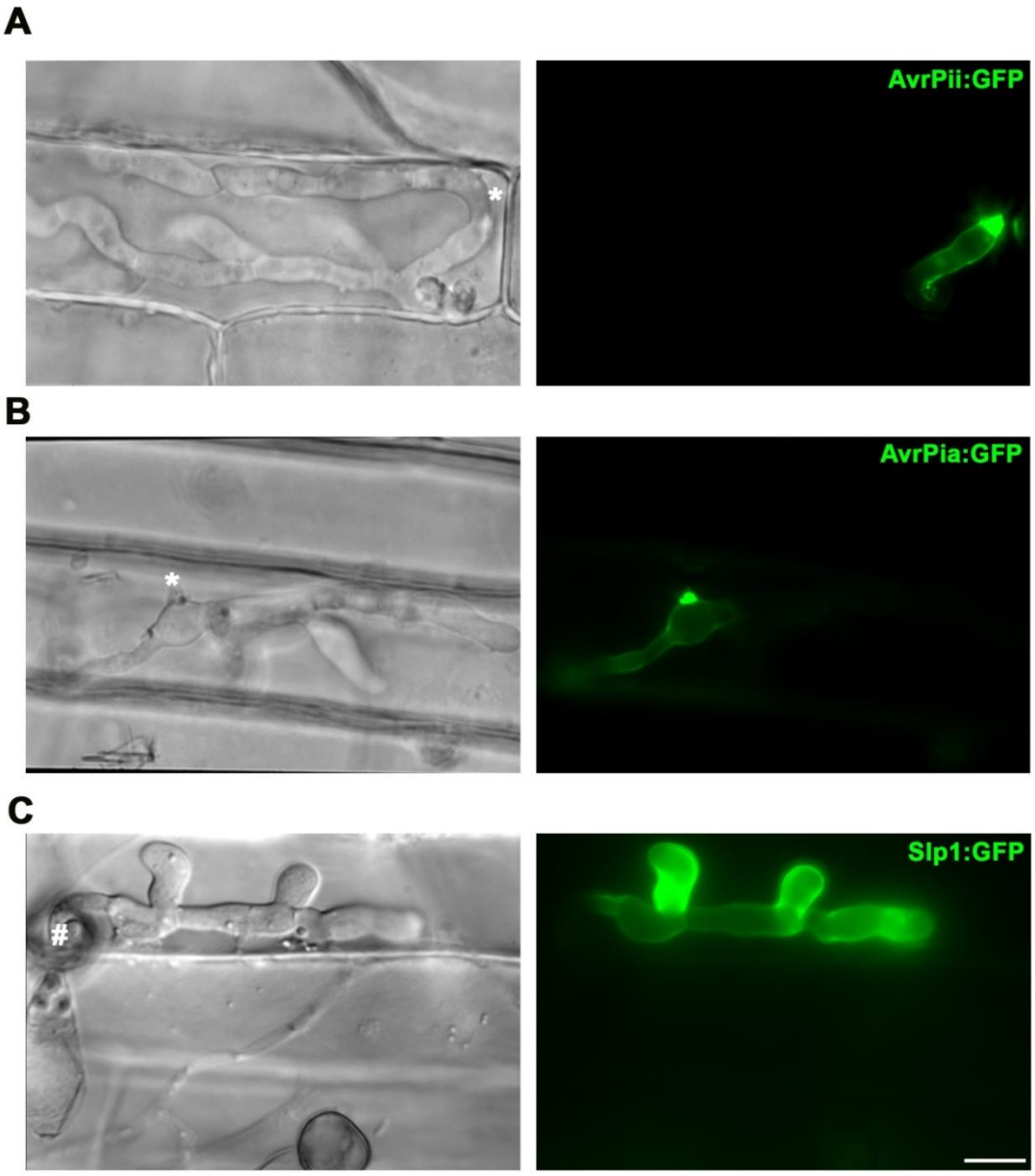

Figure 5.2. **Expression of AvrPia and AvrPii, cytoplasmic and Slp1, apoplastic effectors *in planta*.**

Rice leaf sheath was inoculated with *M. oryzae* strains expressing AvrPii:GFP, AvrPia:GFP and Slp1:GFP. 26 h post inoculation samples were observed for each strain. All images are representative of more than five different biological replicates. Scale=10 µm. **A. & B**. AvrPii:GFP and AvrPia:GFP was observed at BIC. White asterisks show BIC localisation. **C.** Slp1, an apoplastic effector, was localised around the IH. White hash shows point of infection.

5.3.2 Organization of secretory components during host tissue invasion

In order to investigate the secretory mechanism of effector proteins during host colonisation, genes involved in polarised growth and secretion were expressed with translational GFP fusions (Section 3.3.4 & 3.3.5). Each secretory component was localised in vegetative hyphae and most were concentrated at the tip of vegetative hyphae (Section 3.3.6 & 3.3.7). Mlc1, a myosin motor regulatory protein, was localised at the tip of primary IH *in planta* while in bulbous IH, Mlc1:GFP was observed as a spot near each septum and the BIC-associated cell (**Figure 5.3A**). The Polarisome component, Spa2:GFP was localised at the tip of the primary and bulbous IH (**Figure 5.3B**). Vesicle bound v-SNARE, Snc1, largely accumulated at the tip of primary IH (**Figure 5.3C**). In bulbous IH it was observed as a bright spot in the BIC-associated cell and also at the tip of the IH (**Figure 5.3C**). Membrane bound t-SNARE, Sso1, was observed at the BIC associated cell and also at the tip of primary hyphae in secondarily invaded cells (**Figure 5.3D**). *In planta* localisation of Mlc1, Spa2, Snc1 and Sso1 was performed by Dr. Martha C. Giraldo from Prof. Barbara Valent's lab. This suggests that BIC-associated fungal cell might repolarise secretory components to be able to secrete effector proteins directly to the BIC.

Fim1, an actin bundling protein, was found to be localised under the plasma membrane as small punctation in the IH (**Figure 5.4A**). The myosin motor protein, Myo2, was observed as a bright spot at the tip of the bulbous IH (**Figure 5.4B**). Cdc42, a Rab-GTPase, was concentrated as a faint spot at the tip and septum in the bulbous IH (**Figure 5.4C**). Tea1 (tip elongation aberrant protein 1) is known as a cell polarity marker (Mata & Nurse, 1997) and Chm1, the Cla4 kinase homologue in *M. oryzae*, are involved in repolarisation of the cytoskeleton at the appressorium pore (Dagdas et al, 2012). Chm1:GFP and Tea1:GFP were transformed into a Pwl2:mRFP expressing

Guy11 strain and were observed at the septum and tip of the bulbous IH in the rice leaf sheath (**Figure 5.5A&B**). The exocyst subunits, Sec15, Sec6 and Sec3, also co-localised with Pwl2:mRFP and were only observed at the tip of the bulbous IH, with no fluorescence was detected in the BIC associated cell (**Figure 5.5C-E**).

Exocyst subunits, Exo70, Sec8 and Sec5 were observed as faint spots at the tip of bulbous IH, while in the later infections in secondary invaded cells, exocyst components were found in brighter spot at the tip of the IH (**Figure 5.6A-C**). GFP fluorescence signals were weak during the initial stage of infection and as plant cell walls is also produce auto-fluorescence, such that it was difficult to observe exocyst derived signals from the IH.

Results presented here suggest that the primary IH to be more similar to vegetative hyphae than the bulbous secondary IH. Several secretory components such as, v-SNARE Snc1, t-SNARE SSo1 and the myosin regulatory light chain Mlc1 were, however, found to be associated with the fungal cell attached to the BIC. This provides evidence that the BIC is an active site for secretion. Differentiation of bulbous IH and localisation of exocyst, polarisome and other polarity markers at the tip and septum suggest that conventional secretion is also active during early infection. The exocyst localisation signal in secondary invaded cell is also brighter than seen in the first invaded cell, which implies increased secretion and faster growth in second invaded cells.

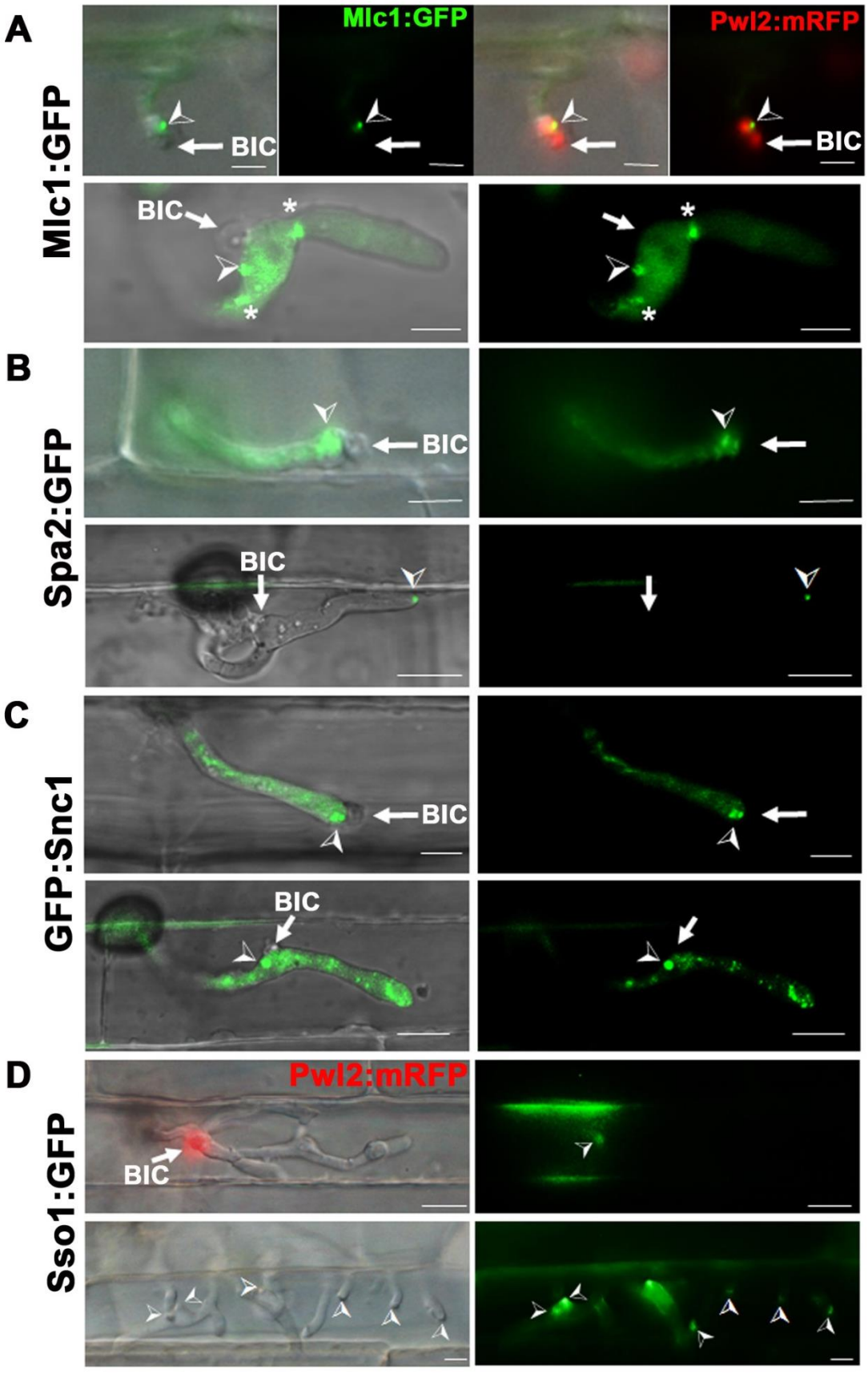
A
Mlc1:GFP
Mlc1:GFP
Pwl2:mRFP
BIC
BIC
BIC
B
Spa2:GFP
BIC
BIC
C
GFP:Snc1
BIC
BIC
D
Sso1:GFP
Pwl2:mRFP
BIC

Figure 5.3. Localisation of the secretory components during host invasion.

Rice leaf sheath was inoculated with conidia of strains expressing labelled secretory components. Expression of each gene was observed at two time points. Images shown here are representatives of at least three different replicates. Scale bar=10 µm. **A.** Mlc1:GFP was localised to the tip of the primary IH (➢) after 24 h and Pwl2:mRFP secreted from the tip (arrow). In bulbous IH after 27 h Mlc1:GFP was observed as a large punct in the BIC associated cell and at the septum. **B.** Spa2:GFP accumulates at the tip of primary and bulbous IH (➢) after 24 h and 27 h post inoculation. The BIC is indicated with an arrow. **C.** v-SNARE, GFP:Snc1 was observed at the tip of the primary IH at 24 h (➢) and in bulbous IH at 27 h showing localisation at the BIC associated cell and smaller vesicles at the growing tip. The BIC is indicated with an arrow. **D.** t-SNARE, Sso1:GFP was localised in the BIC-associated cell in first invaded rice cell (➢) after 27 h and after 40 h it observed at the tip of the primary IH in second invaded cell (➢). Pwl2:mRFP accumulated at the BIC (arrow).

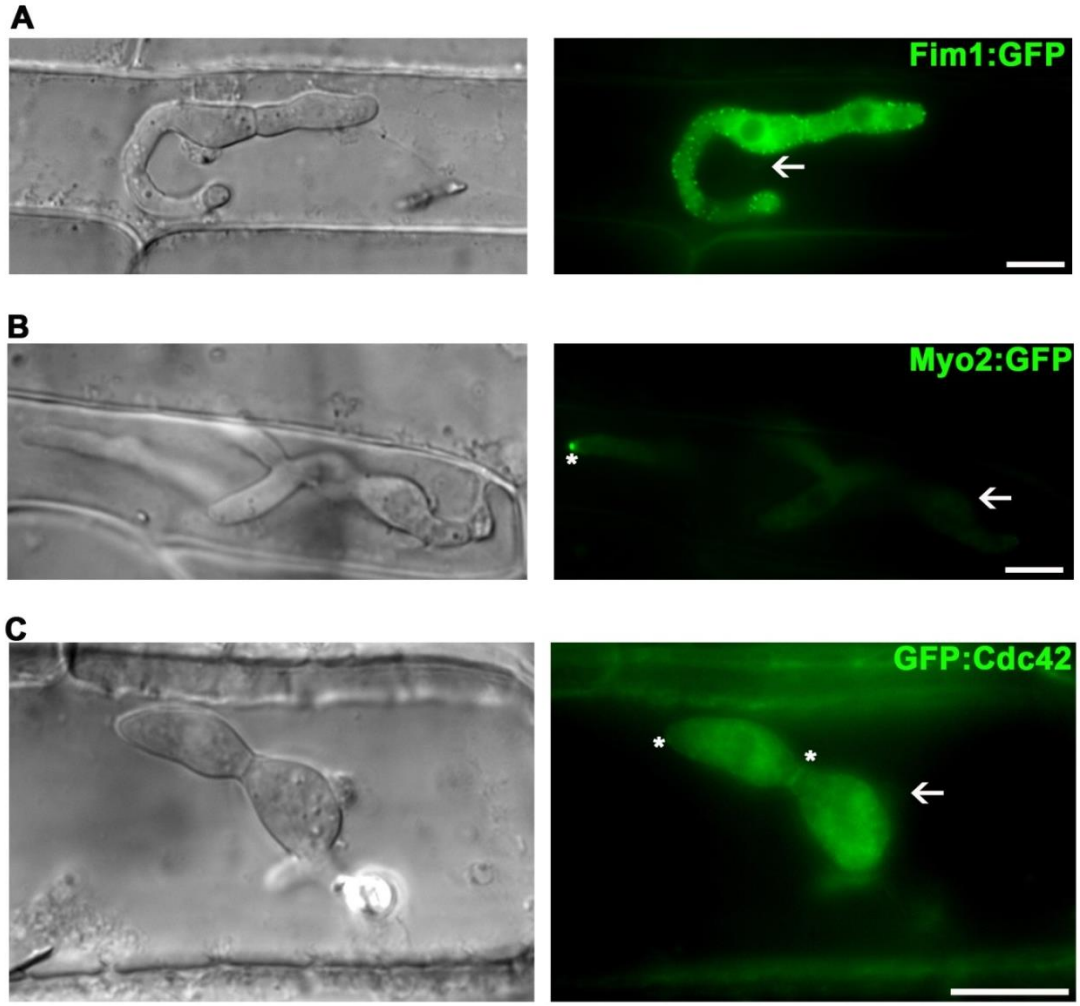

Figure 5.4. Localisation of Fim1:GFP, Myo2:GFP and Cdc42:GFP in rice leaf sheath infection.

Leaf sheath of susceptible rice cultivar CO-39 were inoculated with conidia harvested from strains expressing Myo2:GFP, Fim1:GFP and GFP:Cdc42. Expression was observed 26 h post inoculation. White arrows indicate the BIC. Images shown are representative of at least three different replicates. Scale bar=10 µm. **A.** Fim1:GFP was localised as a actin patches under the plasma membrane of the IH in leaf sheath assay. **B.** MyoII:GFP was observed as a bright spot at the tip of the invasive hyphae (White star). **C.** GFP:Cdc42, a Rho-GTPase was observed at the tip of IH and septum after 26 h in leaf sheath assay (White star).

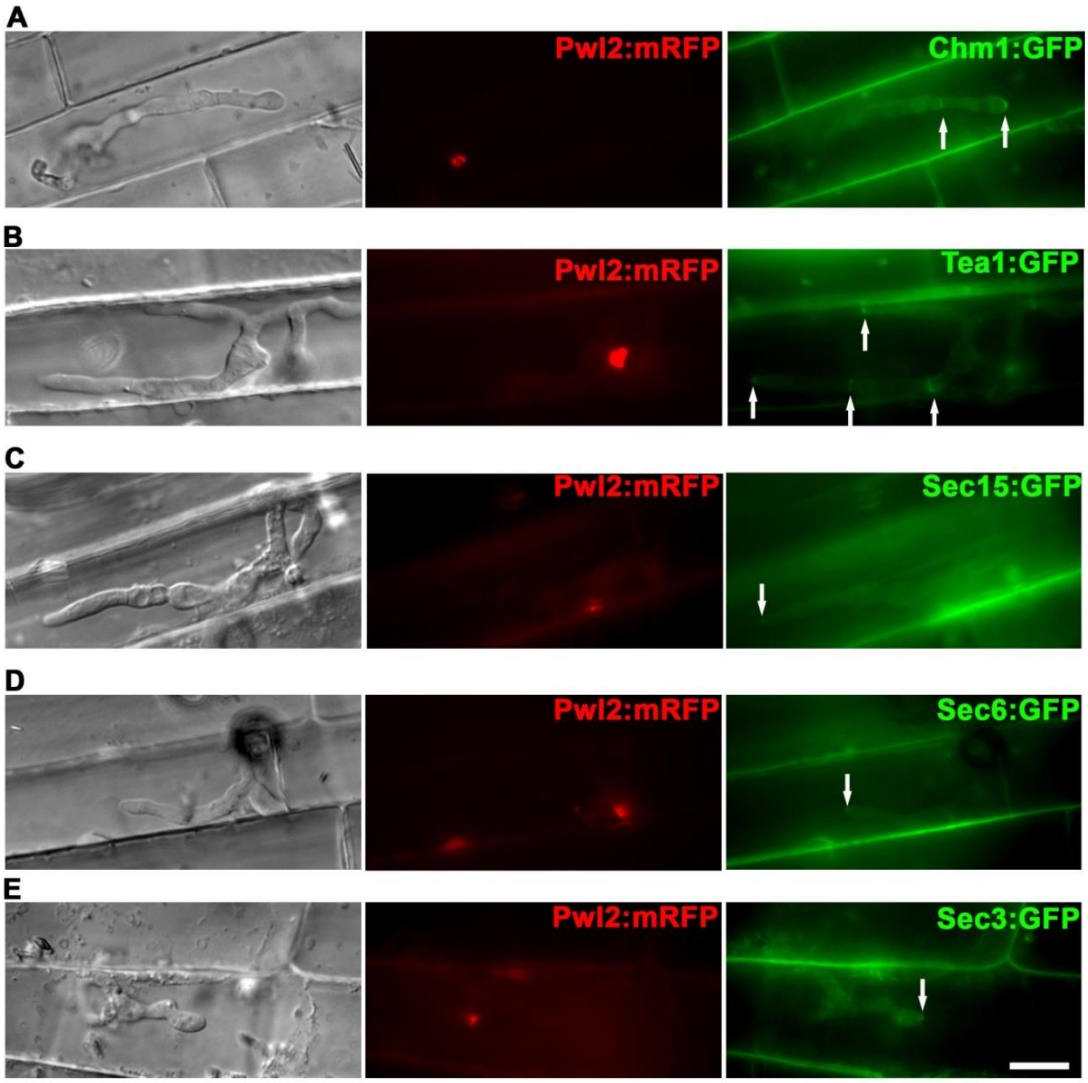

Figure 5.5. Co-localisation of Chm1, Tea1 and exocyst subunits with cytoplasmic effector Pwl2 in rice leaf sheath tissue.

Rice leaf sheath was inoculated with strains expressing Pwl2:mRFP in combination with Chm1:GFP, Tea1:GFP, Sec15:GFP, Sec6:GFP and Sec3:GFP. Scale bar=10 µm. **A.** Chm1, the Cla4 homologue in *M. oryzae*, was observed at the septum and tip (arrow) of the IH after 26 h in rice leaf sheath. **B.** Tea1, a polarity marker was localised at the septum and tip (arrow) of the IH after 26 h in rice leaf sheath. **C. D. & E.** Exocyst subunits Sec15:GFP, Sec6:GFP and Sec3:GFP were observed at the tip of the growing IH and no fluorescence was observed in the BIC associated cell after 26 h in rice leaf sheath.

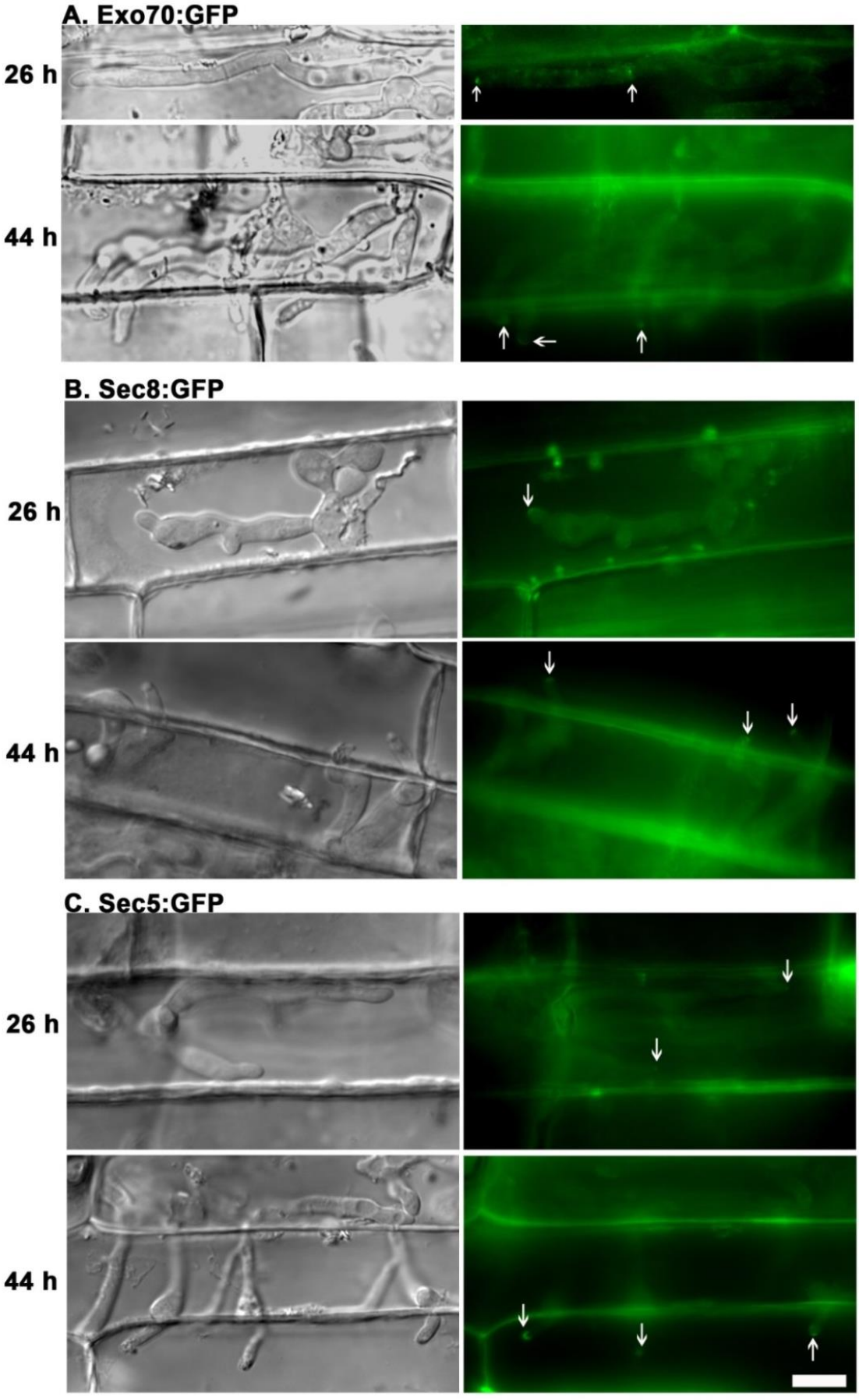
A. Exo70:GFP
26 h
44 h
B. Sec8:GFP
26 h
44 h
C. Sec5:GFP
26 h
44 h

Figure 5.6. Exocyst localisation in rice leaf sheath.

Strains expressing exocyst subunits, *EXO70*, *SEC8* and *SEC5*, with translational C-terminal GFP fusion were observed in rice leaf sheath **A, B & C**, respectively. At the early, 26 h and later stage, 44 h, of the infection *EXO70*, *SEC8* and *SEC5* were observed at the tip of the IH (white arrow head) and no fluorescence was detected in the BIC-associated cells. Scale=10 µm.

5.3.3 Golgi-independent secretion of cytoplasmic effectors in *M. oryzae*

Protein secretion is mainly conducted through the ER-to-Golgi pathway and to understand the mechanism of effector secretion, Brefeldin A (BFA) was used in this study. This experiment was performed by Dr. Martha C. Giraldo as part of a collaborative project to characterise the effector secretion pathway (Giraldo et al, 2013). BFA inhibits conventional ER-to-Golgi transport by preventing the association of ADP-ribosylation factor Arf1 to the Golgi and is therefore widely used in fungi to study mechanisms of secretion (Chardin & McCormick, 1999). A *M. oryzae* strain expressing the apoplastic effector Bas4:GFP and cytoplasmic effector Pwl2:mCherry:NLS was subjected to BFA treatment in order to access the mechanism of secretion of these classes of effectors. Rice leaf sheath sections were inoculated with *M. oryzae* spore suspensions, as detailed in Section 2.7.3 and incubated at 24°C for 24 h before the addition of BFA (10 mg mL^{-1}). Leaf sheath sections were than further incubated for 3 h before checking the localisation of Bas4 and Pwl2. The apoplastic effector Bas4:GFP was retained inside the IH and exhibited a reticulate distribution, typical of ER but Pwl2:mCherry still accumulated at the BIC and no fluorescence was observed inside the IH (**Figure 5.7B**). To confirm this result, the secretion of Avr-Pita, Bas1 and Bas107 cytoplasmic effectors was also tested and no retention was observed inside fungal invasive hyphae in the presence of BFA (**Figure 5.7C & 5.8B**). The retention of apoplastic effectors was further confirmed with additional apoplastic effectors, Slp1:GFP and Bas113:mRFP (**Figure 5.8C**).

To understand whether Pwl2 is actively secreted to the BIC in the presence of BFA, fluorescence recovery after photobleaching (FRAP) analysis was performed using a *M. oryzae* strain expressing both Pwl2:GFP and Bas4:mRFP. Retention of Bas4:mRFP was shown in hyphal-ER like structures in BFA-treated samples before photobleaching with

the Pwl2:GFP signal at the BIC (**Figure 5.7D**). Full recovery of Pwl2:mRFP was observed after 3 h (**Figure 5.7D**), suggesting that *M .oryzae* actively secretes cytoplasmic effectors in the presence of BFA whereas BFA specially blocks the secretion of apoplastic effectors. Results presented here suggest cytoplasmic effectors are secreted via a Golgi-independent pathway and apoplastic effectors are secreted through a Golgi-mediated pathway.

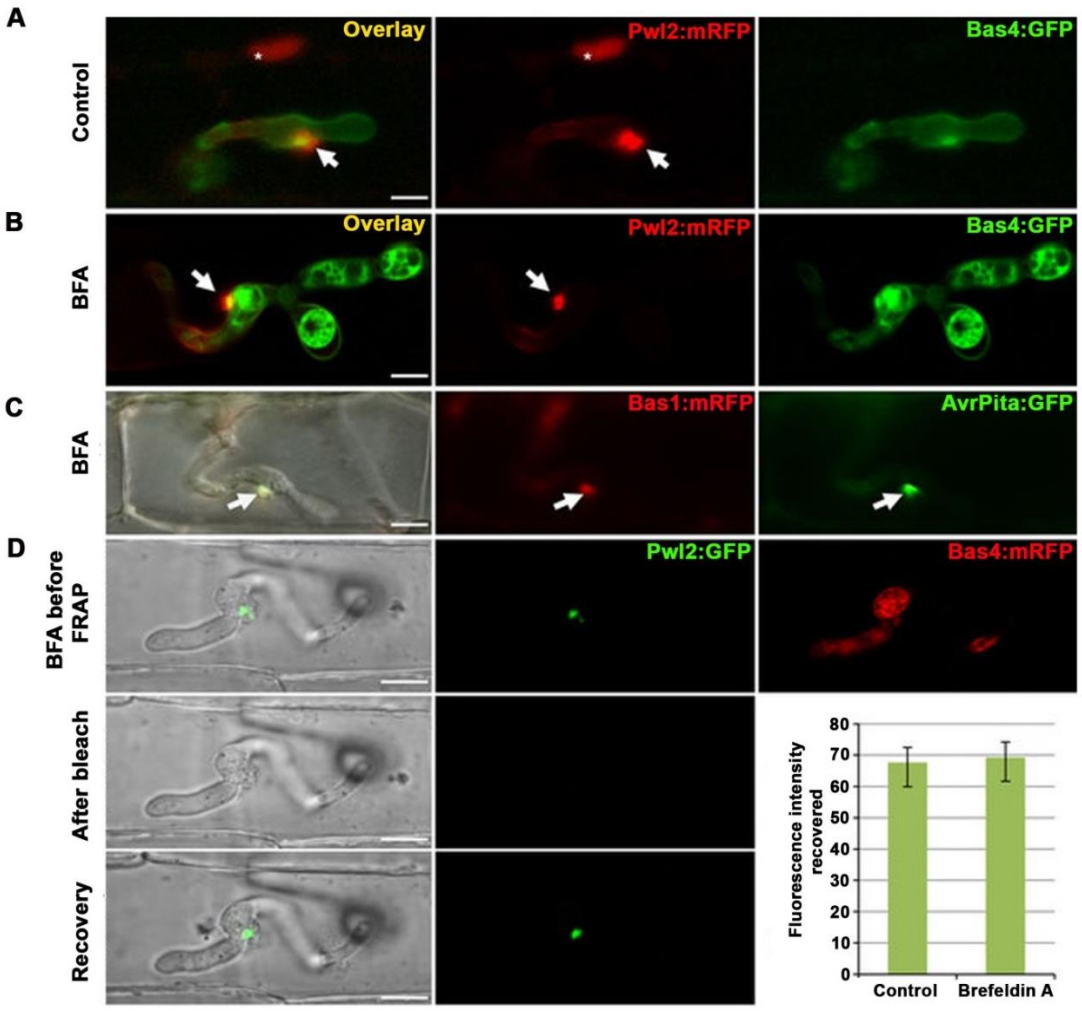

Figure 5.7. *M. oryzae* cytoplasmic effectors are secreted via a Golgi-independent pathway.

Rice leaf sheath was inoculated with strains expressing fluorescently labelled effector proteins. 24 h post inoculation, each leaf sheath was treated with BFA (10 mg mL^{-1}) and further incubated for 3 h unless stated otherwise. Scale bar=10 µm. **A.** Control showing normal apoplastic localisation of Bas4:GFP and BIC localisation of Pwl2:mCherry. **B.** In the presence of BFA, Bas4:GFP was retained in ER-like structures of fungal IH while Pwl2:mRFP still accumulated at the BIC and no retention of Pwl2:mRFP was detectable in fungal hyphae. **C.** *M. oryzae* strains expressing the cytoplasmic effectors Bas1:mRFP (middle) and AvrPita:GFP (right) were incubated in the presence of BFA and no retention was observed after 5 h of exposure. **D.** Rice leaf sheath infected with a *M. oryzae* strain expressing cytoplasmic effector Pwl2:GFP and apoplastic effector Bas4:mRFP was used to assess fluorescence recovery after photobleaching (FRAP) of GFP with 485 nm exicitation. After 3 h incubation in BFA Bas4:mRFP (right) was retained inside fungal hyphae. Pwl2:GFP (middle) was observed at the BIC before photobleaching and signal fully recovered within 3 h in presence of BFA. Bar chart to show mean fluorescence recovery after photobleaching (P=0.019, mean ± s.d., four FRAP experiments).

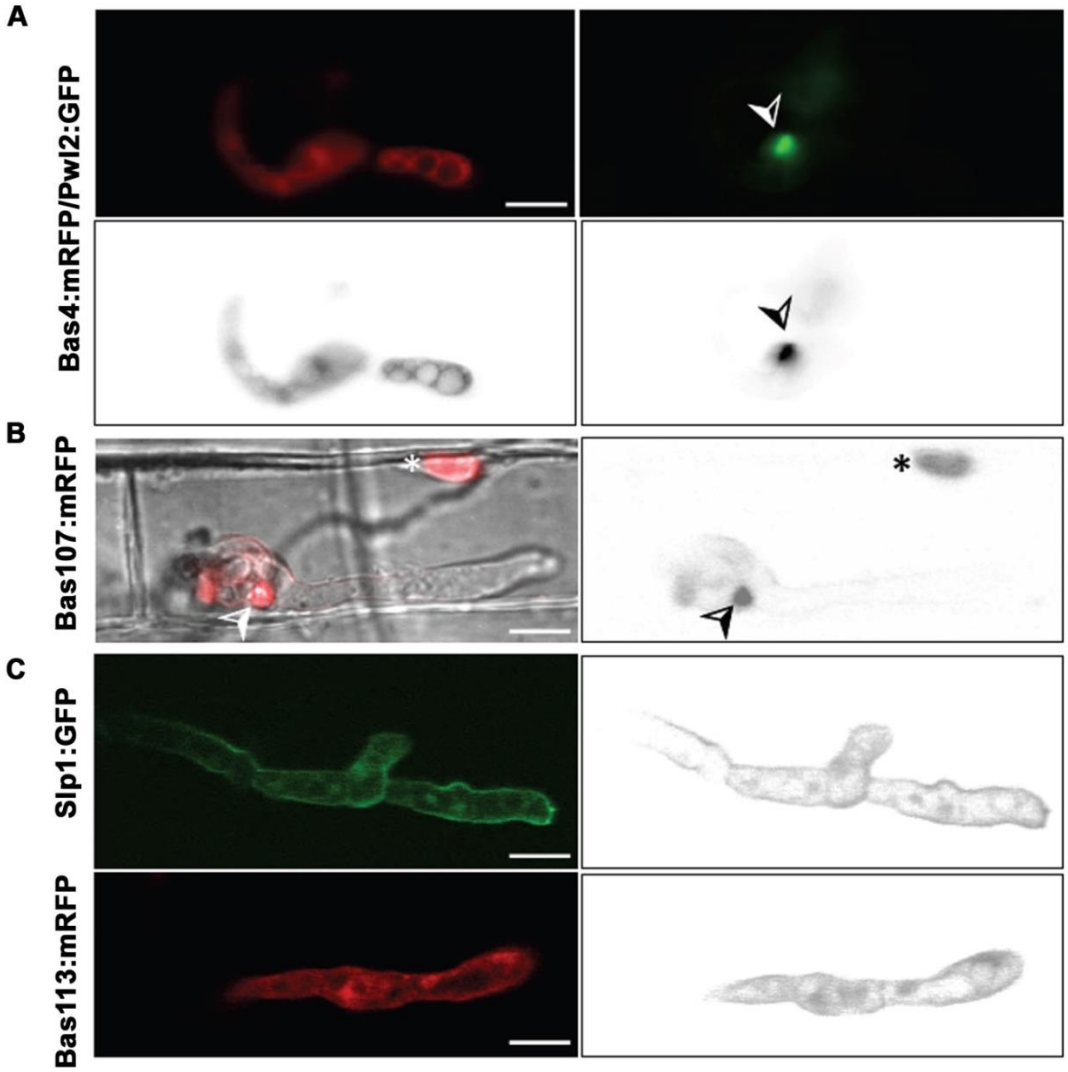

Figure 5.8. *M. oryzae* apoplastic effectors are secreted via a Golgi-dependent pathway.

To analyse the sensitivity of *M. oryzae* cytoplasmic and apoplastic effectors to BFA, multiple fluorescent effectors were tested. Scale bar=10 µm. **A.** Control experiment showing normal expression of Pwl2:GFP at BIC and retention of Bas4:mRFP in invasive hyphae in the presence of BFA, after 6 h of incubation. Corresponding black and white inverse images were used to show fluorescence signal more clearly. **B.** The cytoplasmic effector Bas107:mRFP showed normal secretion after 5 h exposure to BFA and exhibited accumulation in rice nucleus (white asterisk) after translocation without adding artificial NLS. **C.** Additional apoplastic effectors Slp1:GFP and Bas113:GFP showed accumulation with reticulate localisation pattern similar to BAS4.

5.3.4 The role of the cytoskeleton in *M. oryzae* effector secretion

Secretory vesicles are delivered to the site of secretion via the cytoskeleton. This experiment was performed by Dr. Martha C. Giraldo. To test the requirement for the cytoskeleton during effector secretion, the microtubule inhibitor methyl 1-(butylcarbamoyl)-2-benzimidazolecarbamate (MBC, an active ingredient in the fungicide benomyl) and the actin inhibitor latrunculin A (LatA) were used (50 µg mL^{-1} for each inhibitor) to distrupt cytoskeletal components. Rice leaf sheaths were inoculated with a *M. oryzae* strain expressing Bas4mRFP and Pwl2:GFP and incubated at 24°C. After 24 h incubation, 50 µg mL^{-1} inhibitor was added to leaf sheaths, which were then further incubated for 3 h before being subjected to microscopic analysis. Bas4:mRFP localisation was impaired in the presence of both inhibitors and retention was observed inside hyhae suggesting both actin and microtubules are important in Bas4:mRFP localisation (**Figure 5.9A-C**). No effect was observed on Pwl2:GFP secretion and accumulation at the BIC (**Figure 5.9A-C**) which suggests that Pwl2:GFP localisation is independent of the cytoskeleton. To observe the active secretion of Pwl2:GFP in the presence of inhibitor, FRAP was performed. Recovery of Pwl2:GFP fluorescence was observed 3 h after photobleaching (**Figure 5.9D**), which further confirms that cytoplasmic effectors are actively secreted and accumulated at the BIC even after distruption of microtubules or the F-actin cytoskeleton.

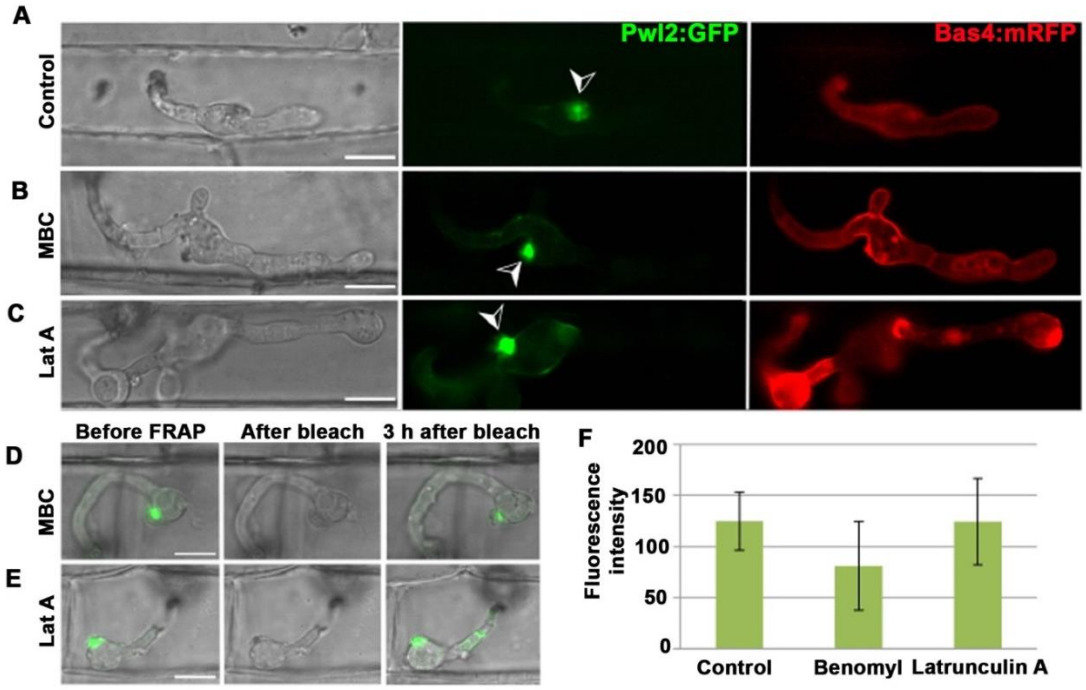

Figure 5.9. Integrity of the cytoskeleton is not required for secretion of cytoplasmic effectors by *M. oryzae* to the BIC.

Rice leaf sheath was inoculated with a *M. oryzae* strain expressing Pwl2:GFP & Bas4:mRFP and incubated for 24 h. Images shown here are representative of four different FRAP experiments. **A.** Localisation of cytoplasmic effector Pwl2:GFP at BIC and Bas4:mRFP in the apoplastic space in the absence of inhibitors. **B.** Rice leaf sheath inoculated for 24 h was subsequently exposed to MBC (50 µg mL^{-1}) for 3 h, which inhibits microtubule formation in fungus, but no effect was observed in Pwl2:GFP BIC accumulation while Bas4:mRFP was partially retained inside the hyphae. **C.** Rice leaf sheath inoculated for 24 h was subsequently incubated with Latrunculin A (Lat A) (50 µg mL^{-1}) for 3 h, which inhibits actin polymerisation in fungi. No effect was observed in localisation of Pwl2:GFP to the BIC, but Bas4:mRFP localisation varied greatly from control. **D & E.** FRAP analysis of Pwl2:GFP secretion and accumulation at the BIC in the presence of inhibitors, MCB and Lat A, which suggests continuous secretion of Pwl2. Recovery of photobleached Pwl2 was seen after 3 additional hours in presence of inhibitors. **F.** The bar chart shows mean recovery of fluorescence intensity and results were identical in the presence or absence of MBC (P=0.014) and in the presence or absence of Lat A(P=0.015) (mean ± s.d., four FRAP experiments). Scale bar=10 µm.

5.3.5 *EXO70* and *SEC5* are required for the secretion of spore tip mucilage (STM)

To investigate the role of the appressorium pore in polarized exocytosis, we set out to determine whether known pathogenicity determinants are secreted in an exocyst-dependent manner during plant infection. The initiation of plant infection by *M. oryzae* occurs when a conidium lands on the rice leaf surface and immediately releases spore tip mucilage (STM) to attach itself to the leaf surface (Hamer et al, 1988). This mucilage acts as an adhesive and is also secreted from the appressorium during its maturation in order to stick tightly to the hydrophobic cuticle during turgor generation and infection. STM can be detected using a lectin concanavalin A conjugated to fluorescein isothiocyanate (FITC) (Hamer et al, 1988). STM secretion was therefore monitored in Δ*sec5* and Δ*exo70* exocyst mutants. Spores from Δ*sec5* and Δ*exo70* mutants were harvested in water and appressoria allowed to form on hydrophobic boroslicate glass coverslips. The secretion of STM was observed by FITC-ConA labeling and epifluorescence microscopy (**Figure 5.10**). After 30 min, conidia were checked for mucilage secretion during initial attachment to the surface. The wild type strain Guy11 showed a very strong signal for STM when compared to Δ*sec5* and Δ*exo70* exocyst mutants both at the tips of germinating conidia and at the base of appressorium (**Figure 5.10A**). Δ*sec5* and Δ*exo70* mutants respectively showed 83% and 71% lower STM stained spores than Guy11 wild type (**Figure 5.10B**). Similarly, the fluorescence signal from mature appressoria in exocyst mutants was also significantly reduced ($P<0.05$) with 80% and 66% of appressorium showing less fluorescence in Δ*sec5* and Δ*exo70* mutants, respectively, than Guy11. Taken together, this suggests that the appressorium pore is an active site of secretion during appressorium maturation and that STM secretion is an exocyst dependent process.

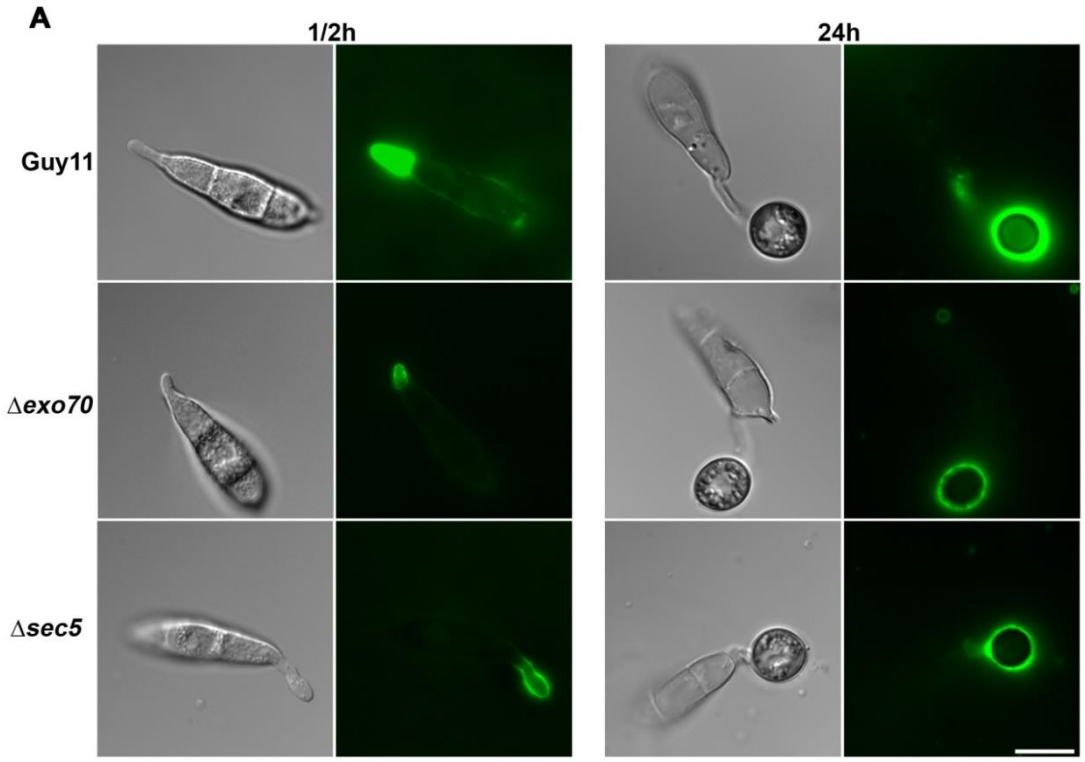
A
1/2h
24h
Guy11
Δexo70
Δsec5

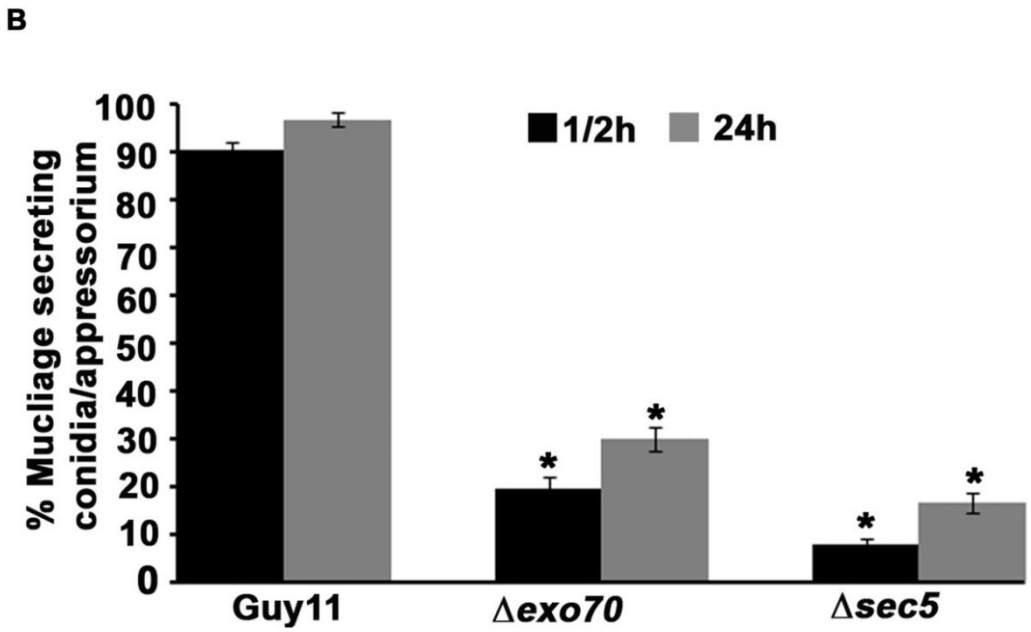
B
% Mucliage secreting conidia/appressorium
100
90
80
70
60
50
40
30
20
10
0
1/2h
24h
*
*
*
*
Guy11
Δexo70
Δsec5

Figure 5.10. Exocyst sub-units required for the mucilage secretion.

A. Mucilage secreted form conidia stained with FITC-ConA. The conidial suspension of 5×10^4 mL^{-1} from wild type Guy11, Δ*exo70* and Δ*sec5* mutant strains were inoculated onto glass coverslips. Conidia from all the strains were stained with FITC-ConA after ½ h and 24 h of inoculation. Scale bar=10 µm. **B.** Bar chart showing percentage of conidia/ appressorium strongly labelled with FITC-ConA after 1/2 h (black bars) and 24 h (grey bars). Values are mean ± S.E. for three repetitions of the experiment, n = 300.

5.3.6 The role of exocyst subunits, *EXO70* and *SEC5*, in effector secretion

It has been shown in the previous chapter that exocyst components are required for protein secretion and also needed for full virulence of *M. oryzae* on rice plants (Section 4.3.4 and 4.3.5). To understand the role of the exocyst in effector secretion, fluorescently-tagged effector proteins were observed in Δ*exo70* and Δ*sec5* mutants. The exocyst mutants formed normal IH in the first invaded rice cells, compared to the wild type strain, but showed significant accumulation of two different cytoplasmic effectors, Pwl2 and Bas1, inside BIC-associated cells (**Figure 5.11**). The cytoplasmic effector Pwl2:mCherry:NLS showed impaired secretion in 60 out of 65 random infection sites in the Δ*exo70* mutant (**Figure 5.11B**) and in 37 out of 40 randomly imaged infection sites in the Δ*sec5* mutant (**Figure 5.11C**). Signal inside hyphae were never observed in Pwl2:mCherry or Bas1:mRFP expressing WT strains (**Figure 5.11A**). The retention of cytoplasmic effectors inside hyphae was confirmed by measuring pixel intensity through a transect across micrographs, as denoted by white arrows in **Figure 5.11**. The distribution of fluorescence intensity showed that a significant amount of the fluorescent signal was retained inside IH (**Figure 5.11**). Interestingly, no retention was observed with the apoplastic effector BAS4:GFP in Δ*exo70* and Δ*sec5* mutants, which was also confirmed using line scans (**Figure 5.11B & C**). The retention was only observed in the BIC associated cell, not in the subsequently formed IH cells. Similar results were observed when another cytoplasmic effector, Bas1:mRFP was localised in Δ*exo70* and Δ*sec5* mutants. In an Δ*exo70* mutant, Bas1:mRFP was retained inside the BIC-associated cell in 22 out of 28 infection sites, while in Δ*sec5* mutant 23 out of 27 infection sites showed retention (**Figure 5.11D-F**).

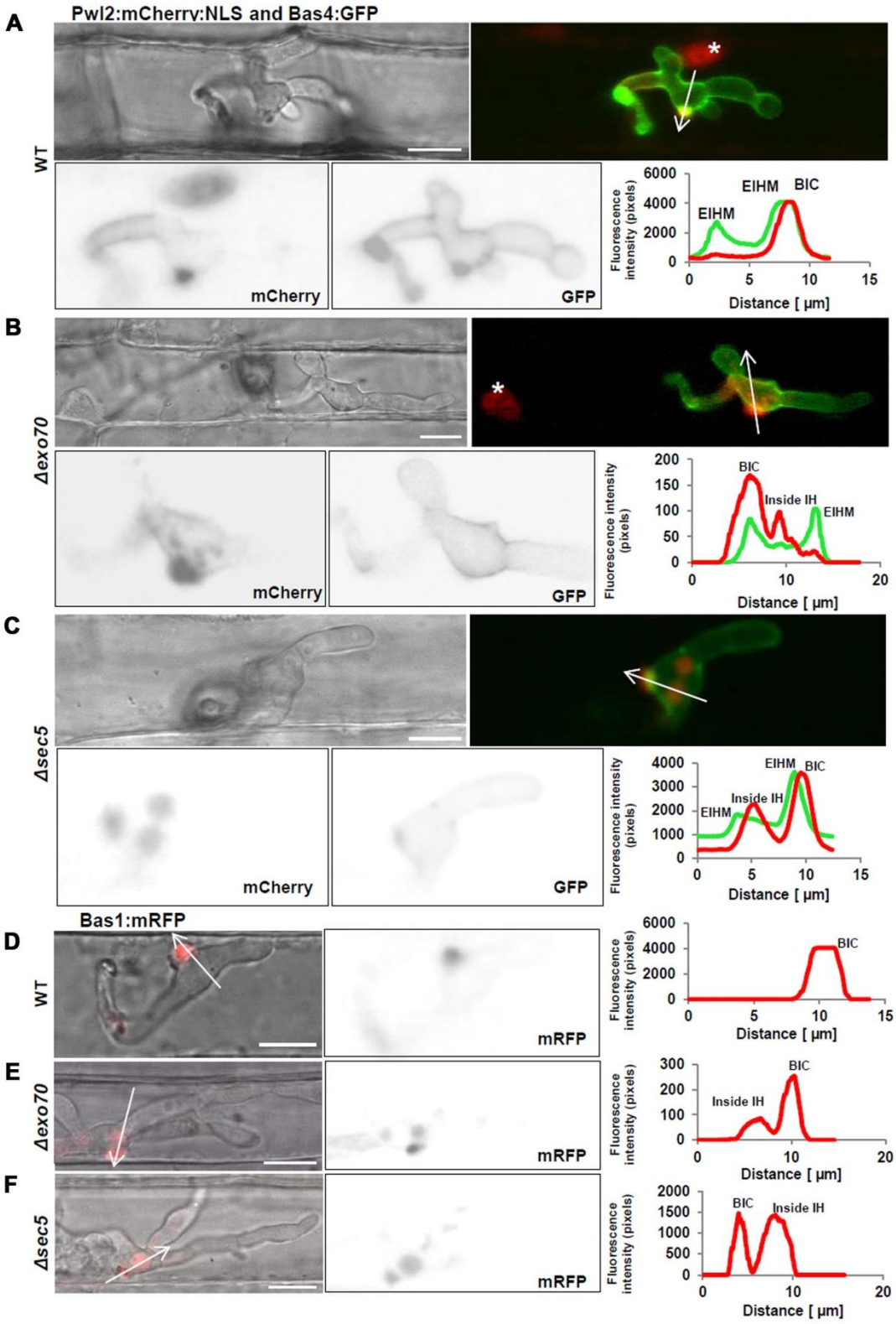
A
Pwl2:mCherry:NLS and Bas4:GFP
WT
mCherry
GFP
Fluorescence intensity (pixels)
EIHM
BIC
Distance [µm]
B
Δexo70
Inside IH
C
Δsec5
D
Bas1:mRFP
mRFP
E
F

Figure 5.11. Exocyst subunits, *EXO70* and *SEC5* are required for the secretion of cytoplasmic effectors.

A *M. oryzae* strain expressing Pwl2:mcherry:NLS and Bas4:GFP was used to study effector secretion. Targeted gene deletions of the exocyst subunit, *EXO70* and *SEC5* were confirmed in Pwl2:mcherry:NLS::Bas4:GFP and Bas1:mRFP strains. All the strains were imaged in the rice leaf sheath and infections were observed after 26 h. Scale bar=10 µm. **A.** Cytoplasmic effector Pwl2:mCherry:NLS showed normal localisation and accumulation at the BIC. Translocation of Pwl2 was observed in the rice nucleus (white asterisk) and no fluorescence was detected in BIC associated invasive hyphal cell. Bas4:GFP was localised to around the IH. **B. & C.** Δ*exo70* and Δ*sec5* mutants showed partial retention of Pwl2:mCherry, predominately inside the BIC associated cells and normal secretion of Bas4:GFP in the apoplastic region. Internal fluorescence in BIC-associated cells was further verified by a black and white inverse image (lower left) and fluorescence intensity linescans (lower right). **D.** Cytoplasmic Bas1:mRFP fluorescence was seen predominately at the BIC and no fluorescence was observed in the BIC-associated cells. **E. & F.** Bas1:mRFP expressed in Δ*exo70* and Δ*sec5* mutants showed significant retention inside the BIC associated invasive hyphal cell. No signal was observed in the non-BIC associated cells. Fluorescence intensity linescans and black and white inverse image were further confirmed the retention of Bas1:mRFP inside BIC-associated cells.

5.3.7 Targeted gene deletion of t-SNARE, *SSO1* and its role in effector secretion

To understand the role of SNAREs in effector secretion, the t-SNARE *SSO1* homologue was identified by sequence homology in *M. oryzae* MGG_04090. A targeted gene deletion mutant of t-SNARE *SSO1* was generated, as described in Section 4.2.1 in which *SSO1* coding region was replaced with the hygromycin resistance gene casette. Genomic DNA of Guy11 and putative transformants was extracted, digested with *Xho*1, fractionated by agarose gel electrophoresis and transferred by Southern blotting to Hybond-N membrane (Amersham). The DNA gel blot was hybridised with the left flank of *SSO1* as a radio-labelled probe to confirm *SSO1* deletion. A 2.8 kb size difference was observed after probing, which is consistent with the successful replacement of *SSO1* gene with hygromycin resistance cassette (**Figure 5.12A**).

A *M. oryzae* strain expressing both Pwl2:mcherry:NLS and Bas4:GFP effectors was used as the genetic background to generate a knockout mutant of Δ*sso1*. This mutant was used to test the secretion of effectors. In the Δ*sso1* mutant, Pwl2:mCherry accumulated at two distinct points of infection. One appeared to be a normal BIC and the second was observed adjacent to the primary hypha before differentiation of bulbous hyphae (**Figure 5.12B & C**). Bas4:GFP was normally secreted to the apoplastic region in an Δ*sso1* mutant (**Figure 5.12B & C**). This double BIC phenotype was detected in 32 out of 40 random infection sites. This abnormal phenotype for cytoplasmic effector secretion was not observed previously in any null mutant of other genes involved in the secretory pathway and also confirmed with the secretion of another cytoplasmic effector Bas1:mRFP (in 25 out of 30 random infection sites). The virulence defect caused by the targeted gene deletion of *SSO1* was around 50%, which suggests that it is required for the efficient secretion of cytoplasmic effectors and potentially other virulence determinants (**Figure 5.12E & F**). The results presented here demonstrate involvement of the SNARE protein *SSO1* in secretion of cytoplasmic effectors.

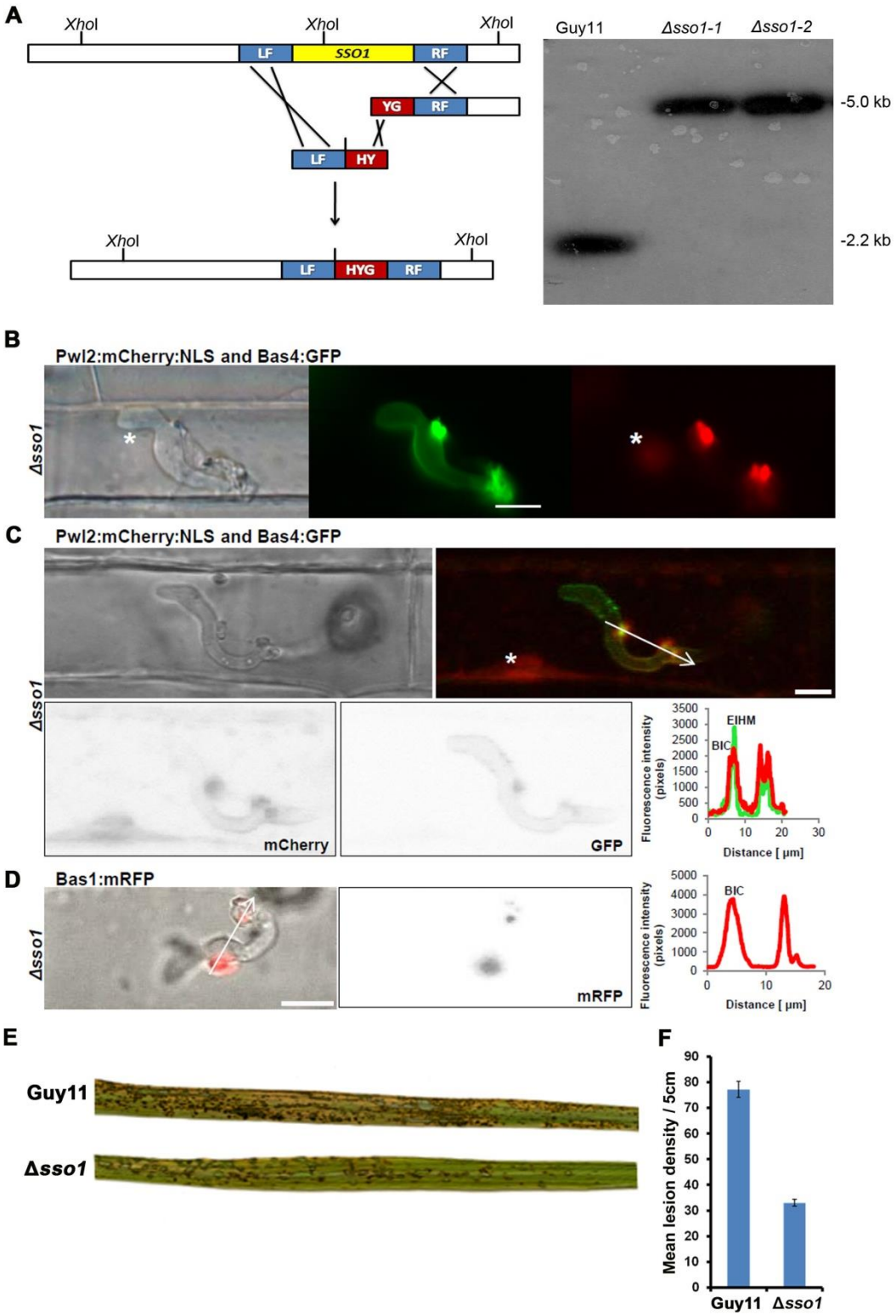
A
XhoI
XhoI
XhoI
LF
SSO1
RF
YG
RF
LF
HY
XhoI
XhoI
LF
HYG
RF
Guy11
Δsso1-1
Δsso1-2
-5.0 kb
-2.2 kb
B
Pwl2:mCherry:NLS and Bas4:GFP
Δsso1
C
Pwl2:mCherry:NLS and Bas4:GFP
Δsso1
mCherry
GFP
Fluorescence intensity (pixels)
EIHM
BIC
Distance [µm]
D
Bas1:mRFP
Δsso1
mRFP
Fluorescence intensity (pixels)
BIC
Distance [µm]
E
Guy11
Δsso1
F
Mean lesion density / 5cm
Guy11
Δsso1

Figure 5.12. t-SNARE *SSO1*¸ is involved in the secretion of cytoplasmic effectors.

A. Schematic to show the split marker strategy for targeted gene deletion of *SSO1*. The coding region of *SSO1* was replaced with hygromycin phosphotransferase resistance cassette (*HPH*) which was confirmed by Southern blot assay. Genomic DNA of putative transformants and wild type strain Guy11 was digested with *Xho*1 restriction enzyme. Southern Blot was probed with the LF fragment upstream of the *SSO1* after being fractionated and transferred to the Hybond-N membrane (Amersham). After being probed with LF, DNA gel bot showed 2.8 kb size difference which is consistent with the *SSO1* ORF replacement with the resistance cassette. **B. & C.** Two different infections of the Δ*sso1* mutant showed accumulation of Pwl2:mCherry at two distinct foci. Apart from the normal localisation of Pwl2:mCherry at the BIC, it also accumulated at the tip of primary invasive hyphae. Images in **B** left to right: brightfield, Bas4:GFP (green) and Pwl2:mCheery (red). Images in **C** clockwise from upper left: brightfield, overlay of Pwl2:mcherry (red) and Bas4:GFP (green), linescan for Pwl2 (red) and Bas4 (green) along the white arrow, black and white inverse images to show GFP and mCherry fluorescence at two distinct locations. **D.** Localisation of the Bas1:mRFP in Δ*sso1* mutant showed accumulation at two different foci. Images Left to right: overlay of brightfield and Bas1:mRFP, mRFP fluorescence shown in black and white inverse image and fluorescence intensity linescan along through the white arrow. Scale Bar=10 µm. **E.** Targeted gene deletion mutants of *SSo1* and Guy11 strains were used to spray susceptible rice cultivar CO-39 to test virulence defect. Spore concentration of 5 x 10^4 spores mL^{-1} were inoculated on 18 days old rice seedlings and incubated for 5 days. **F.** Bar chart to show the number of disease lesions per 5 cm on CO-39 rice cultivar sprayed with Guy11 and Δ*sso1* mutants ($P < 0.05$, $n = 30$ for each strain, mean ± S.D., three experiments).

5.3.8 *SEC6* is required for the secretion of the effector protein Mep1 during host infection

In the previous chapters, it has been shown that the *M. oryzae SEC6* is required for exocyst organisation at the appressorium pore (AP) and that the AP is a hub for protein secretion. Effector proteins are a functionally diverse class of proteins which neutralize host defence responses. It has been shown that some of the effectors are secreted before penetration (Kleemann et al, 2012) and in our lab, Dr. Xia Yan has identified a *M. oryzae* effector, Mep1, through RNA-seq of infected rice tissue that is differentially expressed during plant infection. Mep1 is a highly expressed effector during host infection and is not expressed at all *in vitro*. Mep1:GFP was therefore observed in Guy11 and the $sec6^{Y601P}$ temperature sensitive strain and localised around the appressorium pore in Guy11 and $sec6^{Y601P}$ at 24°C while at the semi-restrictive temperature 29°C, Mep1:GFP was significantly mislocalised in the $sec6^{Y601P}$ strain ($P < 0.05$, paired two-tailed t-test) (**Figure 5.13A & B**). This suggests that the AP is actively involved in protein secretion and that the exocyst component, *SEC6* is required for secretion of Mep1 during host infection.

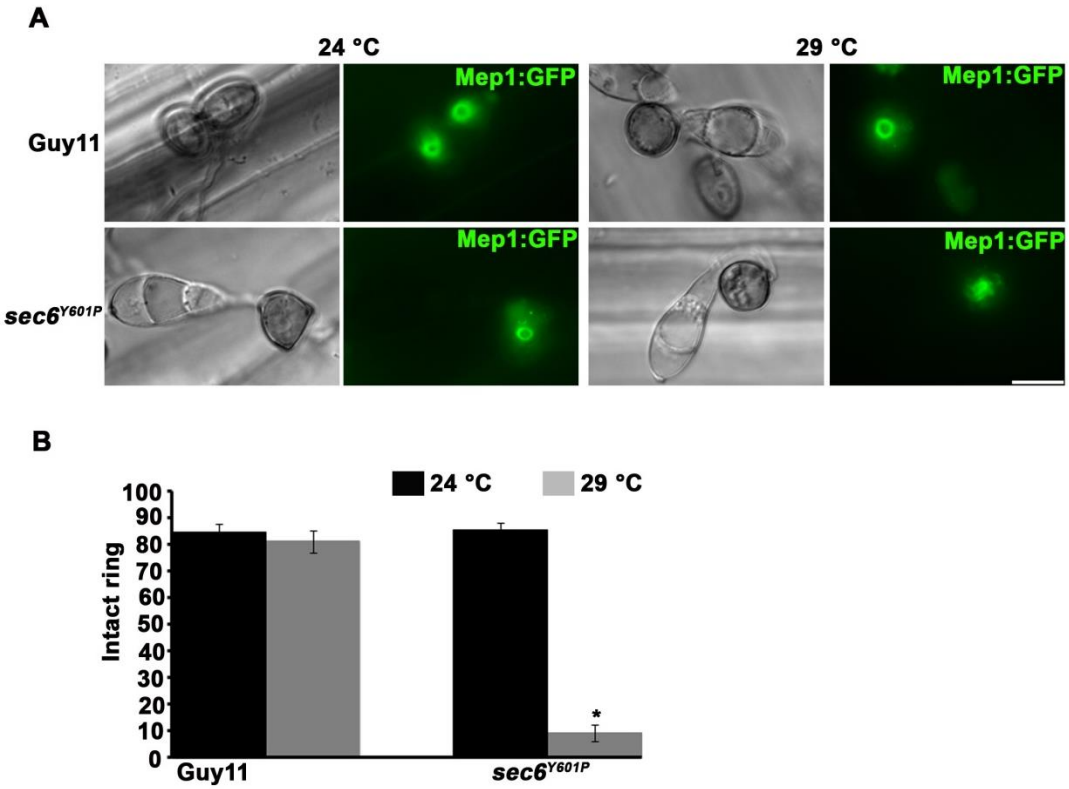

Figure 5.13. *SEC6* is required for secretion of the Mep1 effector protein from the appresorium pore.

A.. Micrograph showing localization Mep1:GFP in Guy11 and temperature sensitivite mutant *sec6*^{Y601P} at the permissive temperature, 24°C and semi restrictive temperature, 29°C. Mep1:GFP was completely mislocalized at the semi restrictive temperature in *sec6*^{Y601P} mutant. **B.** Bar chart showing percentage of appressoria expressing Mep1:GFP at permissive temperature, 24°C (black bars) and semi restrictive temperature, 29°C (grey bars). Values are mean ± S.D. for three repetitions of the experiment, n = 300. Scale bar = 10 µm.

5.4 Discussion

The results presented here provide insight into the mechanism by which effectors are delivered to the host-pathogen interface and strongly implicate exocyst subunits in cytoplasmic effector secretion. Based on their accumulation patterns, *M. oryzae* effectors can be categorised into two different classes, host-delivered cytoplasmic effectors and apoplastic effectors accumulating in the EIHM compartment (Giraldo & Valent, 2013; Khang et al, 2010). Treatment with BFA suggests that apoplastic effectors are secreted through a conventional secretion pathway, while cytoplasmic effectors are actively delivered to the BIC via a Golgi-independent pathway. Targeted gene deletion mutants of the exocyst subunits, *EXO70* and *SEC5*, showed retention of cytoplasmic effectors inside the fungal IH. It was also shown here that exocyst subunits are required for production of spore tip mucilage during appressorium development. In Chapter 4, it was demonstrated that a temperature sensitive (TS) mutation in *SEC6* disrupts exocyst assembly at the appressorium pore and here a *sec6* TS mutant was shown to be involved in secretion of the Mep1 effector protein through the appressorium pore. This suggests that early secretion from the pore is exocyst-dependent.

Localisation of the secretory component such as v-SNARE Snc1, t-SNARE Sso1 and the myosin regulatory light chain Mlc1 in BIC-associated cells provide evidence of direct secretion to the BIC (**Figure 5.3**). However, attempts to localise exocyst components in bulbous IH showed localisation to the tips of these cells (**Figure 5.5 & 5.6**) and fluorescence signal was not clearly observed in BIC-associated cells. This suggests that exocyst activity in invasive hyphae is predominants hyphal tip associated, as in vegetative hyphae. However, previously Giraldo et al, (2013) observed a weak Exo70:GFP signal in the BIC-associated cell. Although we were unable to replicate this observation (in our laboratory) when considered with the results of the FRAP

experiments and exocyst mutants, Δ*exo70* and Δ*sec5*, we can not preclude that an exocyst assembly also operates in these cells providing a route for the direct secretion into the BIC. Clearly this requires further investigation and an ultrastructural study will be required to determine exocyst organisation both at the hyphal tip and in the BIC-associated cell.

Previously, it was shown that a P-type ATPase encoding gene, *APT2*, in *M. oryzae* is required for successful plant infection and is deficient in the secretion of extra-cellular enzymes (Martin et al, 2006). Immunogold labelling of Apt2 showed it to be localised in Golgi like vesicular compartments and showed it to colocalise with *M. oryzae KTR1*, which encodes a 1,2-α-mannosyltransferase (Martin et al, 2006). Targeted gene deletion of *APT2* failed to show a hypersensitive response during incompatible interactions, which suggests the possible involvement of *APT2* in effector secretion (Martin et al, 2006). Yi et al (2009) also provided evidence that the ER localised protein, *LHS1*, is involved in secretion of extracellular enzymes. The *LHS1* deletion mutant, Δ*lhs1*, was not able to form a BIC and showed a defect in secretion of the avirulence gene product, AvrPita (Yi et al, 2009), Additionally, the Δ*lhs1* mutant exhibited a significant reduction in pathogenicity on susceptible rice plants and a gain of virulence on a resistance rice cultivar (Yashiro-mochi) containing the *Pi-ta* resistance gene (Yi et al, 2009). Since exocyst subunits are downstream components of the secretion pathway, it seems reasonable to expect that exocyst mutants would show partial retention of cytoplasmic effector proteins.

Here, I have demonstrated that the t-SNARE, *SSO1* is required for complete virulence and development of invasive hyphae because the Δ*sso1* mutant showed accumulation of cytoplasmic effectors at two distinct locations. It has been shown in *Trichoderma reesei* that two distinct secretion pathways employ different t-SNARE proteins at different

sites in hyphae (Valkonen et al, 2007). *M. oryzae* SNAREs, *SEC22* and *VAM7*, are required for growth, maintenance of cell wall integrity, conidiation, appressorium formation and pathogenicity (Dou et al, 2011; Song et al, 2010). Moreover, these SNAREs have been shown to be essential in secretion of extracellular enzymes, such as peroxidases and laccases (Dou et al, 2011; Song et al, 2010). In other filamentous fungi such as *U. maydis*, the t-SNARE,Yup1, is required for hyphal morphogenesis and pathogencity and has been shown to be involved in endocytic recycling via early endosomes (Wedlich-Soldner et al, 2000). When considered together this suggests that in *M. oryzae* SNAREs are involved in the membrane trafficking between ER–Golgi-plasma membrane.

Recently, it has been reported that fluorescently labelled effectors (NIS1, DN3 and MC69) from *Colletotrichum orbiculare* are actively accumulated in a ring-like structure which encircles the primary invasive hyphae during infection of the host, cucumber (Irieda et al, 2014). This ring signal was observed at the neck region which is an interfacial region outside the fungal cell wall and suggests some similarity to the *M. oryzae* BIC. Irieda et al, 2014 have made observations of *C.orbiculare* secretory components, *SEC4* and *EXO70*, and actin cytoskeleton *ACT1* localisation during host invasion and found that all the components are localised to the cavity of the effector ring at the neck of biotrophic hyphae, supporting their role in effector secretion (Irieda et al, 2014). The v-SNARE homologue, *SEC22*, was shown to be predominantly located in the peri-nuclear ER network in the biotrophic hyphae and targeted gene deletions of *SEC4* and *SEC22* showed that effectors are retained inside the fungal cell which also leads to a defect in virulence (Irieda et al, 2014). Both hemi-biotrophic pathogens, *C.orbiculare* and *M. oryzae* show some similarity in the delivery and accumulation of effector proteins during host colonisation.

Altogether, the results shown here provide evidence that distinctly localised fungal effectors are likely to be secreted through different pathways and also demonstrate that the secretory pathway may be conserved in pathogens which use a similar strategy to infect plants.

Chapter 6. General discussion and future directions

This study aimed to unravel the underlying mechanism of protein secretion and to understand how the rice blast fungus *Magnaporthe oryzae* orchestrates protein secretion during plant infection. To achieve this, three objectives were set out. The first objective was to define the localisation of the secretory machinery during vegetative growth and appressorium development in *M. oryzae*. The second objective focused on the role of the exocyst complex in infection-related development and in appressorium development. The final objective addressed the role of the exocyst complex in effector secretion during host colonisation.

6.1 Establishment of cell polarity during vegetative growth in *M. oryzae*

Polarised growth in the model yeast *S. cervesiae* is characterised by a continuous supply of secretory vesicles to the site of cell expansion (Novick et al, 1981). Secretory vesicles are delivered to the site of polarised growth via F-actin cables, where they fuse to the plasma membrane and release enzymes and cell wall synthesising components (Esmon et al, 1981; Klis et al, 2006; Lesage & Bussey, 2006; Pruyne et al, 1998). In budding yeast, the polarisome complex, which consists of Bni1, Spa2, Bud6 and Pea1, nucleates actin cables and Mlc1, an essential light chain for the type V myosin Myo2, provides motive force for vesicle transport (Evangelista et al, 2003; Pruyne et al, 2002; Schott et al, 1999; Sheu et al, 1998). Secretory vesicles fuse to the plasma membrane via an octameric complex called the exocyst, which is composed of Sec3, Sec5, Sec6, Sec8, Sec10, Sec15, Exo70 and Exo84 (Guo et al, 1999a; He & Guo, 2009; TerBush et al, 1996). Vesicle fusion with the exocyst is mediated through the Rab-GTPase Sec4, which is activated by its guanine nucleotide exchange factor (GEF), Sec2 (Novick et al, 2006; Stalder et al, 2013). In fungi, the Spitzenkörper (SPK), a vesicle dense region

proximal to the tip of growing hyphae, acts as a vesicle supply centre (VSC) and from there, vesicles migrate toward the cell apex (Bartnicki-Garcia et al, 1995; Read, 2011; Riquelme, 2013; Riquelme & Sanchez-Leon, 2014; Steinberg, 2007; Sudbery, 2011). Transmission electron microscopy reveals that the SPK is mainly composed of vesicles, ribosomes and actin microfilaments (Bourett & Howard, 1991; Girbardt, 1969; Grove & Bracker, 1970; Howard, 1981; Riquelme & Sanchez-Leon, 2014; Roberson & Vargas, 1994).

In the current study, we decided to investigate polarised growth in *M. oryzae* using live-cell imaging and, initially, localised each component of the octameric exocyst complex in both vegetative hyphal growth and during infection-related development by expression of translational fusions with GFP (Green Fluorescence Protein). We found that all the known exocyst components except Sec10 were localised to the hyphal tip ahead of the SPK in *M. oryzae* (**Figure 3.7**). This follows a similar distribution pattern seen in *C. albicans*, where exocyst subunits localise as a crescent at the hyphal tip (Jones & Sudbery, 2010). This contrast with *N. crassa*, where Riquelme *et al* (2014) suggest that the exocyst components primarily accumulate at two locations; Sec5, Sec6, Sec8 and Sec15 localized as a crescent at the hyphal tip, while Exo70 and Exo84 are closely associated with the outer layer of the Spitzenkörper (Riquelme et al, 2014). Localisation of the exocyst complex is also dependent upon hyphal growth in *A. gossypii*. Fast growing hyphae show cortical distribution of the exocyst to the tip while exocyst components in slow growing hyphae are found in a spheroid region at the hyphal tip (Kohli et al, 2008). Differential localisation of the exocyst components in *M. oryzae* was not observed in growing vegetative hyphae as shown in *N. crassa*. One possible explanation is that vegetative hyphae in *M. oryzae* are thinner than those of *N. crassa* hyphae and these structures might not be easily distinguished. High resolution

microscopy of hyphal tips may provide some clues to these differences and their underlying reasons.

We could not detect GFP fluorescence in Sec10:GFP transformants of *M. oryzae* strain, which may be a result of low expression levels but we believe Sec10 is a part of this octameric exocyst complex in *M. oryzae* because we co-purified Sec10 with Sec6 and Exo84 immuno-precipitates from protein extracts of fungal mycelium (**Table 3.3**). Similar results have been shown in *N. crassa* where Sec10 is part of the exocyst complex, but could not be visualised in GFP translational fusions in growing hyphae (Riquelme et al, 2014).

These observations suggest that *M. oryzae* has functional exocyst complex in which all components physically interact during vesicle trafficking. Localisation of exocyst components during vegetative growth is was therefore expected, based on the observations made in other fungal species.

6.2 Establishment and maintenance of cell polarity during appressorium development in *M. oryzae*

Appressorium-mediated tissue invasion by the rice blast fungus *M. oryzae* is an excellent model to study pre-penetration process (Dean et al, 2012). Rice blast infection starts when a three celled conidium lands on the hydrophobic leaf surface and in response to the leaf surface, begins to germinate, exhibiting polarised growth to generate a germ tube. The tip of the germ tube hooks expands isotropically and develops into a melanised structure called an appressorium. During maturation of the dome-shaped appressorium, a septum forms at the base of the cell between the appressorium and germ tube. This septation event is followed by generation of an appressorium pore at the base of the appressorium, where the cell wall and melanin

layer is not present (**Figure 6.1**). In mature appressoria, a repolarisation event results in formation of a narrow penetration peg which emerges below the appressorium pore and breaches the cuticle to colonise plant tissue. In this infection process, polarisation requires re-orientation of polarity determinants to the appressorium pore (Dagdas et al, 2012). In this present study, I have shown that exocyst components re-orient around the appressorium pore prior to infection and subsequently localise to the growing tip of invasive hyhae. This reorientation of exocyst components is mediated through the interlaced F-actin and septin networks (**Figure 6.1**). Septins are evolutionarily conserved hetero-oligomeric GTP binding proteins localised to the mother-bud neck or shmoo neck in budding yeast (Caudron & Barral, 2009; Spiliotis & Gladfelter, 2012). Septins are crucial for recruitment of proteins required for the assembly of a contractile actomyosin ring (CAR), such as MyoII and polarity establishment proteins such as Spa2 (Barral et al, 2000; Dobbelaere & Barral, 2004; Orlando et al, 2011). The Septin ring acts as a diffusion barrier at the site of cleavage and maintains diffusible exocyst and polarisome proteins at this site (Barral et al, 2000; Dobbelaere & Barral, 2004).

In *M. oryzae,* septins form a hetero-oligomeric ring around the appressorium pore which acts as a diffusion barrier to corral proteins involved in membrane curvature such as Rvs167 and Las17 (**Figure 6.1**) (Dagdas et al, 2012). Ryder et al (2013) showed that NADPH oxidases (Nox) are required for septin mediated-reorientation of F-actin network around the appressorium pore which is necessary for successful plant invasion (Ryder et al, 2013). Here, we argue that the septin-mediated diffusion barrier maintains exocyst components around the appressorium pore and consistent with this idea, in the mature appressorium exocyst ring is completely mis-localised in Δ*sep3*, Δ*chm1*, Δ*noxR* and Δ*mst12* mutants (**Figure 4.18 & 4.19**). Co-immunoprecipitation with either Sec6 or Exo84 shows physical interaction of exocyst components with septins during polarised

growth in hyphae (**Table 3.3**) and it would be interesting to see when this interaction happens during appressorium development because septins are expressed in the appressorium after 8 h of appressorium development. In *M. oryzae*, Rac1 GTPase plays an important role in conidiogenesis and appressorium formation (Chen *et al*, 2008), while Cdc42 is required for repolarization of the cytoskeleton in the appressorium (Dagdas et al, 2012; Zheng et al, 2009) and we can assume that the organisation of the exocyst complex in the appressorium is therefore dependent on the presence of Cdc42 and Rac1 GTPase. We can test this hypothesis by localising the exocyst in Δ*cdc42* and Δ*rac1* mutants during infection-related development in due course.

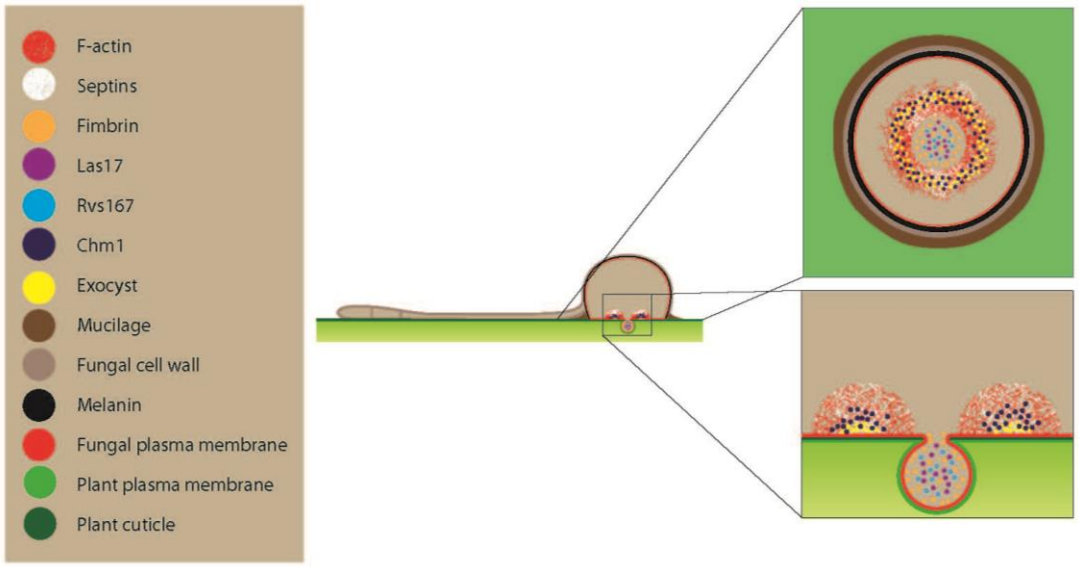

Figure 6.1 Model to show localisation of polarity determinants in the mature appressorium of *M. oryzae*.

Recently, it has been shown that the exocyst component, Exo70, serves as a direct substrate for ERK1/2, which is an important component of the Ras (Small GTPase) - MEK (Mitogen-activated protein kinases) - ERK (Extracellular signal-regulated kinase 1 and 2) cascade and activated through receptor-linked tyrosine kinases, such as the epidermal growth factor receptor (EGFR) (Ren & Guo, 2012). Phosphorylation of Exo70 by ERK1/2 promotes its interaction with other exocyst components, Sec8 and Exo84, and regulates vesicle tethering to the plasma membrane (Ren & Guo, 2012). Co-immunoprecipitation from *M. oryzae* mycelial protein extracts with either Sec6 or Exo84 identifies physical interactions of the exocyst with MAPK signalling components such as Mst7 and Pmk1 (**Table 3.3**). Mst7 and Pmk1 are important components of the mating and pheromone response pathways and deletion mutants of *Mst7* and *Pmk1* fail to form appressoria or produce lesions on a susceptible rice cultivar (**Figure 6.2**) (Xu & Hamer, 1996; Zhao et al, 2005). Interactions between the exocyst and MAPK signalling cascade might therefore be specific and it would be interesting to see how MAPK genes coordinate organisation of the exocyst and regulate exocytosis. This could be achieved by testing individual interactions *in vitro* via a yeast two-hybrid assay and localising the exocyst components in MAPK mutants. Physical interactions between exocyst components and Rho1 (a small GTPase which is involved in establishment of cell polarity and regulates protein kinase C (Pkc1)) were also observed in pull-down experiments using Sec6 and Exo84 (**Table 3.3**). In *S. cerevisiae*, the Rho1 GTPase regulates the cell wall synthesizing enzyme 1,3-beta-glucan synthase and maintains the cell wall integrity pathway (Qadota et al, 1996). In addition, the exocyst component, Sec3, directly interacts with GTP-bound Rho1 (Guo et al, 2001). It would be interesting to explore how Rho1 regulates exocyst components to maintain cell polarity in appressorium mediated infection. This could be explained by localising exocyst components in targeted gene deletion mutants of *RHO1*. The Rho1 GTPase might for

instance be expected to interact with specific components of the exocyst complex and this may be tested via yeast-two hybrid interaction.

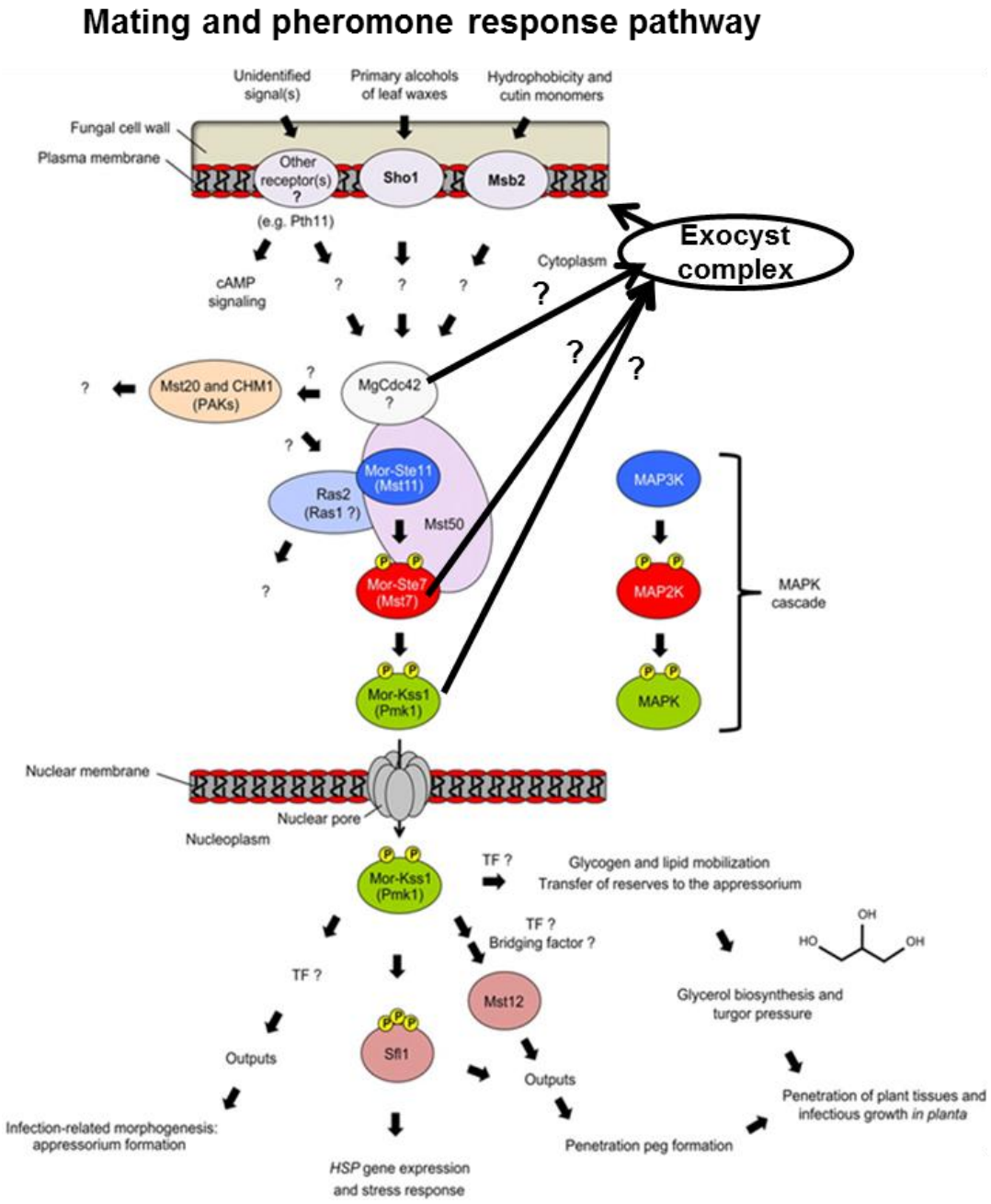

Figure 6.2 Cross talk between the exocyst complex and MAPK cascade in *M. oryzae* (modified from Hamel et al, 2012).

The mating and pheromone response pathway is activated by sensing host signals and transducing the signal to the downstream components including Mst50 and MAPK signalling components. The Kss1 MAPK (Pmk1) is activated by Mor-Ste7 (Mst7) which stimulates formation of appressoria. The downstream components, Kss1, Mst12 and Sfl1 are involved in appressorium-mediated tissue invasion and are required for complete virulence. MAPK signalling components might regulate exocyst organisation during vesicle trafficking.

6.3 The role of exocyst components in protein secretion

Exocyst components are crucial for survival (TerBush et al, 1996). Gene deletion and temperature-sensitive mutants in exocyst-encoding genes accumulate vesicles, which fail to fuse with the plasma membrane, resulting in severe growth and secretion defects in *S. cerevisae* (Novick *et al*, 1981; Novick *et al*, 1980). In *S. cerevisae* all exocyst-encoding genes, except *SEC3*, are essential (Finger & Novick, 1997; Novick *et al*, 1980). In *M. oryzae* targeted deletion of only two exocyst encoding genes, *EXO70* and *SEC5*, was possible. Gene knockout experiments carried out in this study targeting other exocyst components all failed to yield null mutants, suggesting that they are likely to be essential genes. Likewise, in *N. crassa* only the *SEC5* homokaryotic deletion mutant was available (Riquelme et al, 2014). In contrast, mammalian and plant deletions have been generated in all the exocyst-encoding genes. Extensive bioinformatic and genetic analysis in *Arabidopsis* and rice has uncovered huge expansion of Exo70 homologues, which suggests diverse roles of the exocyst components in different cellular activities such as autophagic transport, cargo specific delivery to the plasma membrane (Synek et al, 2006; Wang et al, 2004; Zarsky et al, 2013).

The exocyst components were initially identified in budding yeast through a genetic screen for secretion and mutations in these genes showed intra-cellular accumulation of secreted enzymes, such as invertase (Novick et al, 1980). The *M. oryzae* exocyst components are involved in secretion of spore tip mucilage, which is required for attachment to the leaf surface (Hamer et al, 1988) and proteins secreted from appressorium pore during host invasion. The *M. oryzae* avirulence gene product, *ACE1,* has been shown to be secreted from the appressorium and recognized by rice cultivars carrying, the *Pi33* resistance gene (Fudal *et al*, 2007). Similarly, another plant pathogen, *Colletotrichum higginsianum* forms appressorium and it has been revealed that effectors

are focally secreted from the appressorium pore before infection (Kleemann *et al*, 2012). In the related species, *C. orbiculare*, effectors have been seen to accumulate around the neck of the biotrophic primary hyphae under the appressoria and are secreted via Sec4, a Rab GTPase and Sec22, a v-SNARE-dependent pathway (Irieda et al, 2014). Assembly of the exocyst sub-units around the appressorium pore suggests its active involvement in protein secretion and as this region lacks a fungal cell wall, it might act as a signal hub during establishment of the host-pathogen interaction (**Figure 6.1**). Further characterisation of the exocyst complex was carried out by generation of a temperature-sensitive mutant of Sec6 through a single point mutation in the conserved region Y601P. The exocyst sub-units, Sec3, Sec5, Sec8, Sec15, Exo70 and Exo84 were not able to form a ring at the semi-restrictive temperature in the resultant *sec6*^{Y601P} mutant (**Figure 4.15 & 4.16**). This mutation caused a severe virulence effect at the semi-restrictive temperature when sprayed on the susceptible rice cultivar CO-39. In *S. cerevisiae* it has been shown that mutation of the Sec6 gene leads to serious growth and secretion defects, and causes disruption of exocyst assembly at the bud site (Lamping *et al*, 2005; Songer & Munson, 2009). This suggests that there are some conserved interactions between yeast and *M. oryzae* exocyst components.

6.4 The role of the exocyst in other cellular activities

The exocyst complex is regulated through cell cycle components and in *S. cerevisiae*, where mitotic-phosphorylation of Exo84 at its C-terminal region is mediated by Cdk1-Clb2, which inhibits assembly of the exocyst complex, thereby preventing docking of secretory vesicles to the plasma membrane and halting expansion of the cell surface (Luo *et al*, 2013). In *C. albicans*, phosphorylation of the Exo84 PH domain is mediated through Cdk1-Hgc1 (a hyphal-specific G1 cyclin) and is required for polarised growth of hyphae (Caballero-Lima & Sudbery, 2014). The regulation of Exo84 is under

developmental control and varies with cell type. In *M. oryzae*, appressorium-development is tightly regulated through cell-cycle checkpoints (Saunders et al, 2010a; Veneault-Fourrey et al, 2006). During infection-related development, the transition to appressorium development is regulated by the S-phase check point while G2-M phase check point controls later appressorium maturation (Saunders et al, 2010a). In *M. oryzae*, cytokinesis is also required for the development of the functional appressorium (Saunders et al, 2010b). We argue here that the transition of exocyst components from the periphery to the appressorium pore might be regulated through cell-cycle check points in *M. oryzae*. This idea could be tested by following the transition of the exocyst in the presence of the DNA replication inhibitor, hydroxyurea (HU), and this may be further confirmed by expressing exocyst components in cell-cycle conditional mutants.

Recently, it has emerged that the exocyst also scaffolds autophagosomes in animal cells (Bodemann *et al*, 2011). The Ras-like small GTPase, RalB directly binds with Sec5 and Exo84. During starvation conditions, RalB GTPase binds with Exo84 and induces phosphorylation of Ulk1 (an autophagy associated kinase) and activates other regulators of autophagosome formation, such as Beclin1, Atg14L and Vps34. In nutrient-rich conditions, Sec5 replaces Exo84 and forms an autophagy-inactive complex (Bodemann *et al*, 2011). In *Arabidopsis thaliana* meanwhile, the Exo70 paralogue, EXO70B1, co-localises with the autophagosomal marker ATG8f and interacts with SEC5 and EXO84, which leads to the Golgi-independent transport to the vacuole (Kulich *et al*, 2013). Autophagic cell-death is required for appressorium function in *M. oryzae* (Veneault-Fourrey et al, 2006) and targeted deletion of genes-encoding autophagy proteins showed that non-selective macroautophagy is required for rice blast disease (Kershaw & Talbot, 2009). Therefore, it would be interesting to check the association of exocyst

components and the autophagy machinery of *M. oryzae* during appressorium maturation.

6.5 Delivery of effector proteins during host colonisation

Although there is growing information regarding the signalling cascade that controls appressorium morphogenesis (Wilson & Talbot, 2009), the process that controls morphogenetic changes during plant tissue invasion in *M. oryzae* is largely unknown. Gaining more insight into this control would be very helpful in combating this devastating disease. One of the major objectives of this study is to understand how the rice blast fungus proliferates and secretes effector proteins during host tissue invasion. After gaining entry to the host cytoplasm, *M. oryzae* forms tubular primary invasive hyphae (IH) and then switches to bulbous secondary IH, enclosed inside the host derived extra-invasive hyphal membrane (EIHM) (Kankanala et al, 2007; Khang et al, 2010). In response to fungal infection, rice cells position membranes around the tip of the growing primary IH and subsequently this membranous structure, known as the Biotrophic Interfacial Complex (BIC), is located to a sub-apical region of the bulbous secondary IH (Giraldo & Valent, 2013; Kankanala et al, 2007; Khang et al, 2010; Yi & Valent, 2013). The BIC might represent a focal immune response from the plant into which, cytoplasmic effectors are actively secreted (Khang et al, 2010). Labelling the plant plasma membrane and ER with fluorescent protein tags suggest that the BIC is a plant-derived structure, rich in plant plasma membrane (Giraldo et al, 2013). Active secretion from the BIC-associated fungal cell suggests that there is re-orientation of the secretory apparatus during infection which was also confirmed by showing secretory components, Mlc1 and Snc1, inside the IH (**Figure 5.3**). In this study, we found that the polarisome, exocyst and other polarity determinants are localised to the tip and septum

of IH (**Figure 5.3-5.6**), which suggests the possibility that effector specific secretion or secretion might occurr at both sites.

The presence of effector-specific secretion was confirmed by showing apoplastic effectors (which label the apoplastic space and the IH) such as Slp1 and Bas4, to be are secreted from BrefeldinA-sensitive pathway suggesting that ER-Golgi pathway is involved. In contrast, the cytoplasmic effectors (host translocated) Pwl2 and Bas1, are secreted via a Golgi-independent pathway (**Figure 5.7 & 5.8**). Cytoplasmic effectors are involved in suppression of host immune responses and have been shown to be localised to BICs (Giraldo & Valent, 2013; Khang et al, 2010; Yi & Valent, 2013). Previously, it has been shown that *M. oryzae* encodes *MgAPT2*, an aminophospholipid translocase (flippase) which is involved in secretion of extracellular proteins. Targeted gene deletion of *MgAPT2* showed complete loss of pathogenicity. However it has been suggested that *MgAPT2* might be involved in effector secretion, becasue Δ*mgapt2* mutants failed to stimulate the hypersensitive response, when used to challenge a resistant cultivar of rice, IR-68 (Gilbert et al, 2006). In another *M. oryzae* study, an ER chaperone, Lhs1, has been shown to be required for the secretion of cytoplasmic effectors in *M. oryzae* and a null mutant of *LHS1* failed to show focal accumulation of cytoplasmic effector (Yi et al, 2009). This suggests that fungal effector proteins are secreted via the ER-Plasma membrane route during host invasion. This study shows that deletion mutants of the exocyst components, *EXO70* and *SEC5*, are impaired in the secretion of cytoplasmic effector and showed significant accumulation of these effectors inside the IH (**Figure 5.11**). This suggests that an effector-specific secretion mechanism, in which subsets of exocyst components are involved, is likely to be unconventional or potentially a novel secretion pathway. In recent years, a number of studies provide supporting evidence for the presence of unconventional secretion mechanism in plants and animals (Ding et al, 2012; Malhotra, 2013; Nickel &

Rabouille, 2009). In Arabidopsis and tobacco, Wang et al, 2010 have provided evidence for the presence of a novel exocytic structure called EXPO (exocyst-positive organelle) by using specific antibodies to Exo70 and immunogold labelling of EXPO. There are spherical double membrane structures similar to autophagosomes, which do not colocalise with Atg8E, an autophagosomal marker, and the numbers of structures are not affected by starvation (Ding et al, 2014; Wang et al, 2010). These structures are shown to be fused with the plasma membrane and are insensitive to BrefeldinA and Wortmannin inhibitors (Wang et al, 2010), suggesting that they may be involved in an unconventional secretion pathway. It will be interesting to test the sensitivity of the *M. oryzae* exocyst to BrefeldinA, as there might be a similar pathway functioning in *M. oryzae.* In yeast, a novel compartment for unconventional protein secretion (CUPS), which has Grh1 (mammalian GRASP55/65 (Golgi-reassembly stacking protein) homologue) rich membranes, forms in the vicinity of ER exit sites has been described (Bruns et al, 2011). *M. oryzae* has a Grh1 homologue and functional characterisation of Grh1 may provide further evidence for unconventional secretion by *M. oryzae*.

It is possible that the exocyst is involved in translocation of sRNA or mRNA effectors, in which the Golgi-mediated network is not required and proteins are secreted from the Endoplasmic reticulum (ER)-Plasma membrane (PM). In budding yeast, Takizawa et al, 2000 identified a plasma membrane protein-encoding mRNA (Ist2) transported to the bud tip via an actomyosin-driven process, which is independent of SEC genes. In addition, higher concentrations of IST2 protein in the bud are maintained by a septin-mediated diffusion barrier around the mother-bud neck region (Takizawa et al, 2000). Translocation of IST2 from the cortical ER to PM required cortical sorting signal which allows interaction with membrane lipids such as phosphatidylinositol-4,5-bisphosphate (Ercan et al, 2009). Interestingly, no such protein sorting signals have been identified in *M. oryzae* effectors. To understand focal secretion of effectors in *M .oryzae*, mRNA

tagged-imaging of effector proteins might be useful to observe focal translation and secretion. To further confirm that the BIC is a portal for cytoplasmic effector secretion, labelling cytoplasmic effectors with photo-activable GFP (paGFP) might prove enlightning. paGFP can be activated by laser illumination at 405 nm and activated GFP can be tracked in the cell using the non-activating 488 nm laser. Activation at specific sites and subsequent observation of the GFP signal may give insights into the mechanism of trafficking of effectors. Activation of cytoplasmic effectors may be tested by targeting lasers to specific region of infected rice cells, such as BIC-associated cell, tip of growing IH and rice cell cytoplasm. Accumulation of cytoplasmic effectors at the BIC may then be measured after the activation of selected region, which may, in turn, confirm or deny that the BIC-associated cell directly delivers effectors to the BIC.

In summary, this study has revealed the molecular mechanism for recruitment of the exocyst complex during infection-related development and also shows septin-dependent regulation of the exocyst in mature appressoria. This study demonstrates that exocyst components are required for protein secretion by *M. oryzae* and Sec6 plays a crucial role in recruitment of the exocyst to the appressorium pore. In addition, I have provided further definition of the role of the exocyst complex in effector secretion during host colonisation and the potential existence of an effector-specific secretion pathway in *M. oryzae*. Further investigation will be required to understand regulation of the exocyst complex by the cell-cycle and how exocyst components interact with the autophagic machinery during infection-related development in *M. oryzae*. Characterisation of the unconventional secretion pathway and immuno-localisation and ultra-structural localisation of *M. oryzae* effectors during biotrophic growth will also help in order to understand effector secretion in *M. oryzae*.

Bibiology

Adachi K, Hamer JE (1998) Divergent cAMP signaling pathways regulate growth and pathogenesis in the rice blast fungus *Magnaporthe grisea*. *The Plant Cell* **10:** 1361-1374

Adamo JE, Rossi G, Brennwald P (1999) The Rho GTPase Rho3 has a direct role in exocytosis that is distinct from its role in actin polarity. *Molecular Biology of Cell* **10:** 4121-4133

Altschul SF, Gish W, Miller W, Myers EW, Lipman DJ (1990) Basic local alignment search tool. *Journal of Molecular Biology* **215:** 403-410

Barral Y, Mermall V, Mooseker MS, Snyder M (2000) Compartmentalization of the cell cortex by septins is required for maintenance of cell polarity in yeast. *Molecular Cell* **5:** 841-851

Bartnicki-Garcia S, Bartnicki DD, Gierz G, Lopez-Franco R, Bracker CE (1995) Evidence that Spitzenkorper behavior determines the shape of a fungal hypha: a test of the hyphoid model. *Experimental Mycology* **19:** 153-159

Bhattacharjee S, Stahelin RV, Speicher KD, Speicher DW, Haldar K (2012) Endoplasmic reticulum PI(3)P lipid binding targets malaria proteins to the host cell. *Cell* **148:** 201-212

Birch PR, Armstrong M, Bos J, Boevink P, Gilroy EM, Taylor RM, Wawra S, Pritchard L, Conti L, Ewan R, Whisson SC, van West P, Sadanandom A, Kamoun S (2009) Towards understanding the virulence functions of RXLR effectors of the oomycete plant pathogen *Phytophthora infestans*. *Journal of Experimental Botany* **60:** 1133-1140

Bishop A, Lane R, Beniston R, Chapa-y-Lazo B, Smythe C, Sudbery P (2010) Hyphal growth in *Candida albicans* requires the phosphorylation of Sec2 by the Cdc28-Ccn1/Hgc1 kinase. *The EMBO Journal* **29:** 2930-2942

Bodemann BO, Orvedahl A, Cheng T, Ram RR, Ou YH, Formstecher E, Maiti M, Hazelett CC, Wauson EM, Balakireva M, Camonis JH, Yeaman C, Levine B, White MA (2011) RalB and the exocyst mediate the cellular starvation response by direct activation of autophagosome assembly. *Cell* **144:** 253-267

Boller T, Felix G (2009) A renaissance of elicitors: perception of microbe-associated molecular patterns and danger signals by pattern-recognition receptors. *Annual Review of Plant Biology* **60:** 379-406

Bolte S, Talbot C, Boutte Y, Catrice O, Read ND, Satiat-Jeunemaitre B (2004) FM-dyes as experimental probes for dissecting vesicle trafficking in living plant cells. *Journal of Microscopy* **214:** 159-173

Bourett TM, Howard RJ (1990) In vitro development of penetration structures in the rice blast fungus *Magnaporthe grisea*. *Canadian Journal of Botany* **68:** 329-342

Bourett TM, Howard RJ (1991) Ultrastructural immunolocalization of actin in a fungus. *Protoplasma* **163:** 199-202

Bourett TM, Howard RJ (1996) Brefeldin A-induced structural changes in the endomembrane system of a filamentous fungus,*Magnaporthe grisea*. *Protoplasma* **190:** 151-163

Boyd C, Hughes T, Pypaert M, Novick P (2004) Vesicles carry most exocyst subunits to exocytic sites marked by the remaining two subunits, Sec3p and Exo70p. *Journal of Cell Biology* **167:** 889-901

Bozkurt TO, Schornack S, Banfield MJ, Kamoun S (2012) Oomycetes, effectors, and all that jazz. *Current Opinion in Plant Biology* **15:** 483-492

Bradford MM (1976) A rapid and sensitive method for the quantitation of microgram quantities of protein utilizing the principle of protein-dye binding. *Analytical Biochemistry* **72:** 248-254

Bruns C, McCaffery JM, Curwin AJ, Duran JM, Malhotra V (2011) Biogenesis of a novel compartment for autophagosome-mediated unconventional protein secretion. *Journal of Cell Biology* **195:** 979-992

Burri L, Lithgow T (2004) A complete set of SNAREs in yeast. *Traffic* **5:** 45-52

Butler D (2013) Fungus threatens top banana. *Nature* **504:** 195-196

Caballero-Lima D, Sudbery PE (2014) In *Candida albicans*, phosphorylation of Exo84 by Cdk1-Hgc1 is necessary for efficient hyphal extension. *Molecular Biology of the Cell* **25:** 1097-1110

Carbo N, Perez-Martin J (2008) Spa2 is required for morphogenesis but it is dispensable for pathogenicity in the phytopathogenic fungus *Ustilago maydis*. *Fungal Genetics and Biology* **45:** 1315-1327

Carroll A, Sweigard J, Valent B (1994) Improved vectors for selecting resistance to hygromycin. *Fungal Genetics Newsletter* **41:** 22

Caudron F, Barral Y (2009) Septins and the lateral compartmentalization of eukaryotic membranes. *Developmental Cell* **16:** 493-506

Cesari S, Kanzaki H, Fujiwara T, Bernoux M, Chalvon V, Kawano Y, Shimamoto K, Dodds P, Terauchi R, Kroj T (2014) The NB-LRR proteins RGA4 and RGA5 interact functionally and physically to confer disease resistance. *The EMBO Journal* **33:** 1941-1959

Cesari S, Thilliez G, Ribot C, Chalvon V, Michel C, Jauneau A, Rivas S, Alaux L, Kanzaki H, Okuyama Y, Morel JB, Fournier E, Tharreau D, Terauchi R, Kroj T (2013) The rice resistance protein pair RGA4/RGA5 recognizes the *Magnaporthe oryzae* effectors AVR-Pia and AVR1-CO39 by direct binding. *The Plant Cell* **25:** 1463-1481

Chardin P, McCormick F (1999) Brefeldin A: the advantage of being uncompetitive. *Cell* **97:** 153-155

Chen J, Zheng W, Zheng S, Zhang D, Sang W, Chen X, Li G, Lu G, Wang Z (2008) Rac1 is required for pathogenicity and Chm1-dependent conidiogenesis in rice fungal pathogen *Magnaporthe grisea*. *PLoS Pathogens* **4:** e1000202

Chen XL, Shi T, Yang J, Shi W, Gao X, Chen D, Xu X, Xu JR, Talbot NJ, Peng YL (2014) N-glycosylation of effector proteins by an alpha-1,3-mannosyltransferase is required for the rice blast fungus to evade host innate immunity. *The Plant Cell* **26:** 1360-1376

Chenna R, Sugawara H, Koike T, Lopez R, Gibson TJ, Higgins DG, Thompson JD (2003) Multiple sequence alignment with the Clustal series of programs. *Nucleic Acids Research* **31:** 3497-3500

Choi W, Dean RA (1997) The adenylate cyclase gene MAC1 of *Magnaporthe grisea* controls appressorium formation and other aspects of growth and development. *The Plant Cell* **9:** 1973-1983

Chuma I, Shinogi T, Hosogi N, Ikeda K-i, Nakayashiki H, Park P, Tosa Y (2009) Cytological characteristics of microconidia of *Magnaporthe oryzae*. *Journal of General Plant Pathology* **75:** 353-358

Chumley FG, Valent B (1990) Genetic analysis of melanin-deficient, non-pathogenic mutants of *Magnaporthe grisea*. *Molecular Plant-Microbe Interactions* **3:** 135-143

Cole RA, Synek L, Zarsky V, Fowler JE (2005) SEC8, a subunit of the putative Arabidopsis exocyst complex, facilitates pollen germination and competitive pollen tube growth. *Plant Physiology* **138:** 2005-2018

Collemare J, Pianfetti M, Houlle AE, Morin D, Camborde L, Gagey MJ, Barbisan C, Fudal I, Lebrun MH, Bohnert HU (2008) *Magnaporthe grisea* avirulence gene ACE1 belongs to an infection-specific gene cluster involved in secondary metabolism. *The New Phytologist* **179:** 196-208

Couch BC, Kohn LM (2002) A multilocus gene genealogy concordant with host preference indicates segregation of a new species, *Magnaporthe oryzae*, from *M. grisea*. *Mycologia* **94:** 683-693

Court H, Sudbery P (2007) Regulation of Cdc42 GTPase activity in the formation of hyphae in *Candida albicans*. *Molecular Biology of Cell* **18:** 265-281

Cruz CD, Bockus WW, Stack JP, Tang X, Valent B, Pedley KF, Peterson GL (2012) Preliminary Assessment of Resistance Among U.S. Wheat Cultivars to the Triticum Pathotype of *Magnaporthe oryzae*. *Plant Disease* **96:** 1501-1505

Cvrckova F, Grunt M, Bezvoda R, Hala M, Kulich I, Rawat A, Zarsky V (2012) Evolution of the land plant Exocyst complexes. *Frontiers in Plant Science* **3**: 159

Czymmek KJ, Bourett TM, Shao Y, DeZwaan TM, Sweigard JA, Howard RJ (2005) Live-cell imaging of tubulin in the filamentous fungus *Magnaporthe grisea* treated with anti-microtubule and anti-microfilament agents. *Protoplasma* **225:** 23-32

Dagdas YF, Yoshino K, Dagdas G, Ryder LS, Bielska E, Steinberg G, Talbot NJ (2012) Septin-mediated plant cell invasion by the rice blast fungus, *Magnaporthe oryzae*. *Science* **336:** 1590-1595

Dangl JL, Horvath DM, Staskawicz BJ (2013) Pivoting the plant immune system from dissection to deployment. *Science* **341:** 746-751

Dawe D (2002) The changing structure of the world rice market, 1950–2000. *Food Policy* **27:** 355-370

de Jong JC, McCormack BJ, Smirnoff N, Talbot NJ (1997) Glycerol generates turgor in rice blast. *Nature* **389:** 244-244

Dean R, Van Kan JAL, Pretorius ZA, Hammond-Kosack KE, Di Pietro A, Spanu PD, Rudd JJ, Dickman M, Kahmann R, Ellis J, Foster GD (2012) The Top 10 fungal pathogens in molecular plant pathology. *Molecular Plant Pathology* **13:** 414-430

Dean RA, Talbot NJ, Ebbole DJ, Farman ML, Mitchell TK, Orbach MJ, Thon M, Kulkarni R, Xu JR, Pan H, Read ND, Lee YH, Carbone I, Brown D, Oh YY, Donofrio N, Jeong JS, Soanes DM, Djonovic S, Kolomiets E, Rehmeyer C, Li W, Harding M, Kim S, Lebrun MH, Bohnert H, Coughlan S, Butler J, Calvo S, Ma LJ, Nicol R, Purcell S, Nusbaum C, Galagan JE, Birren BW (2005) The genome sequence of the rice blast fungus *Magnaporthe grisea*. *Nature* **434:** 980-986

Dereeper A, Guignon V, Blanc G, Audic S, Buffet S, Chevenet F, Dufayard JF, Guindon S, Lefort V, Lescot M, Claverie JM, Gascuel O (2008) Phylogeny.fr: robust phylogenetic analysis for the non-specialist. *Nucleic Acids Research* **36:** W465-469

DeZwaan TM, Carroll AM, Valent B, Sweigard JA (1999) *Magnaporthe grisea* pth11p is a novel plasma membrane protein that mediates appressorium differentiation in response to inductive substrate cues. *The Plant Cell* **11:** 2013-2030

Ding Y, Wang J, Chun Lai JH, Ling Chan VH, Wang X, Cai Y, Tan X, Bao Y, Xia J, Robinson DG, Jiang L (2014) Exo70E2 is essential for exocyst subunit recruitment and EXPO formation in both plants and animals. *Molecular Biology of Cell* **25:** 412-426

Ding Y, Wang J, Wang J, Stierhof YD, Robinson DG, Jiang L (2012) Unconventional protein secretion. *Trends in Plant Science* **17:** 606-615

Dixon KP, Xu JR, Smirnoff N, Talbot NJ (1999) Independent signaling pathways regulate cellular turgor during hyperosmotic stress and appressorium-mediated plant infection by *Magnaporthe grisea*. *The Plant Cell* **11:** 2045-2058

Djamei A, Kahmann R (2012) *Ustilago maydis*: dissecting the molecular interface between pathogen and plant. *PLoS Pathogens* **8:** e1002955

Dobbelaere J, Barral Y (2004) Spatial coordination of cytokinetic events by compartmentalization of the cell cortex. *Science* **305:** 393-396

Dodds PN, Rathjen JP (2010) Plant immunity: towards an integrated view of plant-pathogen interactions. *Nature Reviews Genetics* **11:** 539-548

Dou D, Kale SD, Wang X, Jiang RH, Bruce NA, Arredondo FD, Zhang X, Tyler BM (2008) RXLR-mediated entry of *Phytophthora sojae* effector Avr1b into soybean cells does not require pathogen-encoded machinery. *The Plant Cell* **20:** 1930-1947

Dou X, Wang Q, Qi Z, Song W, Wang W, Guo M, Zhang H, Zhang Z, Wang P, Zheng X (2011) MoVam7, a conserved SNARE involved in vacuole assembly, is required for growth, endocytosis, ROS accumulation, and pathogenesis of *Magnaporthe oryzae*. *PloS One* **6:** e16439

Ebbole DJ (2007) Magnaporthe as a model for understanding host-pathogen interactions. *Annual Review of Phytopathology* **45:** 437-456

Egan MJ, Wang ZY, Jones MA, Smirnoff N, Talbot NJ (2007) Generation of reactive oxygen species by fungal NADPH oxidases is required for rice blast disease. *Proceedings of the National Academy of Sciences of the United States of America* **104:** 11772-11777

Ellis CJ, Coppins BJ, Hollingsworth PM (2012) Tree fungus: Lichens under threat from ash dieback. *Nature* **491:** 672-672

Ercan E, Momburg F, Engel U, Temmerman K, Nickel W, Seedorf M (2009) A conserved, lipid-mediated sorting mechanism of yeast Ist2 and mammalian STIM proteins to the peripheral ER. *Traffic* **10:** 1802-1818

Esmon B, Novick P, Schekman R (1981) Compartmentalized assembly of oligosaccharides on exported glycoproteins in yeast. *Cell* **25:** 451-460

Evangelista M, Zigmond S, Boone C (2003) Formins: signaling effectors for assembly and polarization of actin filaments. *Journal of Cell Science* **116:** 2603-2611

Feinberg AP, Vogelstein B (1983) A technique for radiolabeling DNA restriction endonuclease fragments to high specific activity. *Analytical biochemistry* **132**: 6-13

Felsenstein J (1981) Evolutionary trees from DNA sequences: a maximum likelihood approach. *Journal of Molecular Evolution* **17:** 368-376

Finger FP, Hughes TE, Novick P (1998) Sec3p is a spatial landmark for polarized secretion in budding yeast. *Cell* **92:** 559-571

Finger FP, Novick P (1997) Sec3p is involved in secretion and morphogenesis in *Saccharomyces cerevisiae*. *Molecular Biology of the Cell* **8:** 647-662

Fischer-Parton S, Parton RM, Hickey PC, Dijksterhuis J, Atkinson HA, Read ND (2000) Confocal microscopy of FM4-64 as a tool for analysing endocytosis and vesicle trafficking in living fungal hyphae. *Journal of Microscopy* **198:** 246-259

Fisher MC, Henk DA, Briggs CJ, Brownstein JS, Madoff LC, McCraw SL, Gurr SJ (2012) Emerging fungal threats to animal, plant and ecosystem health. *Nature* **484:** 186-194

Fudal I, Collemare J, Bohnert HU, Melayah D, Lebrun MH (2007) Expression of *Magnaporthe grisea* avirulence gene ACE1 is connected to the initiation of appressorium-mediated penetration. *Eukaryotic Cell* **6:** 546-554

Fujikawa T, Kuga Y, Yano S, Yoshimi A, Tachiki T, Abe K, Nishimura M (2009) Dynamics of cell wall components of *Magnaporthe grisea* during infectious structure development. *Molecular Microbiology* **73:** 553-570

Fukuoka S, Saka N, Koga H, Ono K, Shimizu T, Ebana K, Hayashi N, Takahashi A, Hirochika H, Okuno K, Yano M (2009) Loss of function of a proline-containing protein confers durable disease resistance in rice. *Science* **325:** 998-1001

Furukawa N, Mima J (2014) Multiple and distinct strategies of yeast SNAREs to confer the specificity of membrane fusion. *Scientific Reports* **4**:4277

Gilbert MJ, Thornton CR, Wakley GE, Talbot NJ (2006) A P-type ATPase required for rice blast disease and induction of host resistance. *Nature* **440:** 535-539

Gilbert RD, Johnson AM, Dean RA (1996) Chemical signals responsible for appressorium formation in the rice blast fungus*Magnaporthe grisea*. *Physiological and Molecular Plant Pathology* **48:** 335-346

Giraldo MC, Dagdas YF, Gupta YK, Mentlak TA, Yi M, Martinez-Rocha AL, Saitoh H, Terauchi R, Talbot NJ, Valent B (2013) Two distinct secretion systems facilitate tissue invasion by the rice blast fungus *Magnaporthe oryzae*. *Nature Communications* **4:** 1996

Giraldo MC, Valent B (2013) Filamentous plant pathogen effectors in action. *Nature Reviews Microbiology* **11:** 800-814

Giraud T, Gladieux P, Gavrilets S (2010) Linking the emergence of fungal plant diseases with ecological speciation. *Trends in Ecology & Evolution* **25:** 387-395

Girbardt M (1969) Ultrastructure of the apical region of fungal hyphae. *Protoplasma* **67:** 413-441

Gladfelter AS, Pringle JR, Lew DJ (2001) The septin cortex at the yeast mother-bud neck. *Current Opinion in Microbiology* **4:** 681-689

Godfray HCJ, Beddington JR, Crute IR, Haddad L, Lawrence D, Muir JF, Pretty J, Robinson S, Thomas SM, Toulmin C (2010) Food Security: The Challenge of Feeding 9 Billion People. *Science* **327:** 812-818

Grosshans BL, Ortiz D, Novick P (2006) Rabs and their effectors: achieving specificity in membrane traffic. *Proceedings of the National Academy of Sciences of the United States of America* **103:** 11821-11827

Grove SN, Bracker CE (1970) Protoplasmic organization of hyphal tips among fungi: vesicles and Spitzenkörper. *Journal of Bacteriology* **104:** 989-1009

Guo W, Grant A, Novick P (1999a) Exo84p is an exocyst protein essential for secretion. *The Journal of Biological Chemistry* **274:** 23558-23564

Guo W, Roth D, Walch-Solimena C, Novick P (1999b) The exocyst is an effector for Sec4p, targeting secretory vesicles to sites of exocytosis. *The EMBO Journal* **18:** 1071-1080

Guo W, Tamanoi F, Novick P (2001) Spatial regulation of the exocyst complex by Rho1 GTPase. *Nature Cell Biology* **3:** 353-360

Hall T (1999) BioEdit: a user-friendly biological sequence alignment editor and analysis program for Windows 95/98/NT. *Nucleic Acids Symposium Series* **41:** 95

Hamel LP, Nicole MC, Duplessis S, Ellis BE (2012) Mitogen-activated protein kinase signaling in plant-interacting fungi: distinct messages from conserved messengers. *The Plant Cell* **24**: 1327-1351

Hamer JE, Howard RJ, Chumley FG, Valent B (1988) A mechanism for surface attachment in spores of a plant pathogenic fungus. *Science* **239:** 288-290

Harris SD (2011) Cdc42/Rho GTPases in fungi: variations on a common theme. *Molecular Microbiology* **79:** 1123-1127

Hayakawa Y, Ishikawa E, Shoji JY, Nakano H, Kitamoto K (2011) Septum-directed secretion in the filamentous fungus *Aspergillus oryzae*. *Molecular Microbiology* **81:** 40-55

He B, Guo W (2009) The exocyst complex in polarized exocytosis. *Current Opinion in Cell Biology* **21:** 537-542

He B, Xi F, Zhang X, Zhang J, Guo W (2007) Exo70 interacts with phospholipids and mediates the targeting of the exocyst to the plasma membrane. *The EMBO Journal* **26:** 4053-4065

Heider MR, Munson M (2012) Exorcising the exocyst complex. *Traffic* **13:** 898-907

Horbach R, Navarro-Quesada AR, Knogge W, Deising HB (2011) When and how to kill a plant cell: infection strategies of plant pathogenic fungi. *Journal of Plant Physiology* **168:** 51-62

Howard RJ (1981) Ultrastructural analysis of hyphal tip cell growth in fungi: Spitzenkorper, cytoskeleton and endomembranes after freeze-substitution. *Journal of Cell Science* **Vol. 48:** 89-103

Howard RJ, Ferrari MA, Roach DH, Money NP (1991) Penetration of hard substrates by a fungus employing enormous turgor pressures. *Proceedings of the National Academy of Sciences of the United States of America* **88:** 11281-11284

Howard RJ, Valent B (1996) Breaking and entering: host penetration by the fungal rice blast pathogen *Magnaporthe grisea*. *Annual Review of Microbiology* **50:** 491-512

Hsu SC, Ting AE, Hazuka CD, Davanger S, Kenny JW, Kee Y, Scheller RH (1996) The mammalian brain rsec6/8 complex. *Neuron* **17:** 1209-1219

Huang J, Si W, Deng Q, Li P, Yang S (2014) Rapid evolution of avirulence genes in rice blast fungus *Magnaporthe oryzae*. *BMC Genetics* **15:** 45

Huber LA, Pimplikar S, Parton RG, Virta H, Zerial M, Simons K (1993) Rab8, a small GTPase involved in vesicular traffic between the TGN and the basolateral plasma membrane. *Journal of Cell Biology* **123:** 35-45

Hutagalung AH, Coleman J, Pypaert M, Novick PJ (2009) An internal domain of Exo70p is required for actin-independent localization and mediates assembly of specific exocyst components. *Molecular Biology of Cell* **20:** 153-163

International Rice Genome Project (2005) The map-based sequence of the rice genome. *Nature* **436:** 793-800

Irieda H, Maeda H, Akiyama K, Hagiwara A, Saitoh H, Uemura A, Terauchi R, Takano Y (2014a) *Colletotrichum orbiculare* secretes virulence effectors to a biotrophic interface at the primary hyphal neck via exocytosis coupled with SEC22-mediated traffic. *The Plant Cell* **26**: 2265-2281

Jacobs CW, Adams AE, Szaniszlo PJ, Pringle JR (1988) Functions of microtubules in the Saccharomyces cerevisiae cell cycle. *The Journal of Cell Biology* **107:** 1409-1426

Jeon J, Goh J, Yoo S, Chi MH, Choi J, Rho HS, Park J, Han SS, Kim BR, Park SY, Kim S, Lee YH (2008) A putative MAP kinase kinase kinase, MCK1, is required for cell wall integrity and pathogenicity of the rice blast fungus, *Magnaporthe oryzae*. *Molecular Plant-Microbe Interactions* **21:** 525-534

Jia Y, McAdams SA, Bryan GT, Hershey HP, Valent B (2000) Direct interaction of resistance gene and avirulence gene products confers rice blast resistance. *The EMBO Journal* **19:** 4004-4014

Jiang RH, Tripathy S, Govers F, Tyler BM (2008) RXLR effector reservoir in two Phytophthora species is dominated by a single rapidly evolving superfamily with more than 700 members. *Proceedings of the National Academy of Sciences of the United States of America* **105:** 4874-4879

Jones JD, Dangl JL (2006) The plant immune system. *Nature* **444:** 323-329

Jones LA, Sudbery PE (2010) Spitzenkorper, exocyst, and polarisome components in *Candida albicans* hyphae show different patterns of localization and have distinct dynamic properties. *Eukaryotic Cell* **9:** 1455-1465

Kale SD, Gu B, Capelluto DG, Dou D, Feldman E, Rumore A, Arredondo FD, Hanlon R, Fudal I, Rouxel T, Lawrence CB, Shan W, Tyler BM (2010) External lipid PI3P

mediates entry of eukaryotic pathogen effectors into plant and animal host cells. *Cell* **142:** 284-295

Kamakura T, Yamaguchi S, Saitoh K, Teraoka T, Yamaguchi I (2002) A novel gene, CBP1, encoding a putative extracellular chitin-binding protein, may play an important role in the hydrophobic surface sensing of *Magnaporthe grisea* during appressorium differentiation. *Molecular Plant-Microbe Interactions* **15:** 437-444

Kankanala P, Czymmek K, Valent B (2007) Roles for rice membrane dynamics and plasmodesmata during biotrophic invasion by the blast fungus. *The Plant Cell* **19:** 706-724

Kato H, Mayama S, Sekine R, Kanazawa E, Izutani Y, Urashima AS, Kunoh H (1994) Microconidim formation in *Magnaporthe grisea*. *Annals of the Phytopathological Society of Japan* **60:** 175-185

Kershaw MJ, Talbot NJ (2009) Genome-wide functional analysis reveals that infection-associated fungal autophagy is necessary for rice blast disease. *Proceedings of the National Academy of Sciences of the United States of America* **106:** 15967-15972

Kershaw MJ, Wakley G, Talbot NJ (1998) Complementation of the mpg1 mutant phenotype in *Magnaporthe grisea* reveals functional relationships between fungal hydrophobins. *The EMBO Journal* **17:** 3838-3849

Kevin R, Oldenburg V, Kham T, Michaelis S, Paddon C (1997) Recombination-mediated PCR-directed plasmid construction in vivo in yeast. *Nucleic Acids Research* **25:** 451-452

Khang CH, Berruyer R, Giraldo MC, Kankanala P, Park SY, Czymmek K, Kang S, Valent B (2010) Translocation of *Magnaporthe oryzae* effectors into rice cells and their subsequent cell-to-cell movement. *The Plant Cell* **22:** 1388-1403

Kleemann J, Rincon-Rivera LJ, Takahara H, Neumann U, Ver Loren van Themaat E, van der Does HC, Hacquard S, Stuber K, Will I, Schmalenbach W, Schmelzer E,

O'Connell RJ (2012) Sequential delivery of host-induced virulence effectors by appressoria and intracellular hyphae of the phytopathogen *Colletotrichum higginsianum*. *PLoS Pathogens* **8:** e1002643

Klis FM, Boorsma A, De Groot PW (2006) Cell wall construction in S*accharomyces cerevisiae*. *Yeast (Chichester, England)* **23:** 185-202

Kohli M, Galati V, Boudier K, Roberson RW, Philippsen P (2008) Growth-speed-correlated localization of exocyst and polarisome components in growth zones of *Ashbya gossypii* hyphal tips. *Journal of Cell Science* **121:** 3878-3889

Kulich I, Cole R, Drdová E, Cvrčková F, Soukup A, Fowler J, Žárský V (2010) Arabidopsis exocyst subunits SEC8 and EXO70A1 and exocyst interactor ROH1 are involved in the localized deposition of seed coat pectin. *New Phytologist* **188:** 615-625

Kulich I, Pečenková T, Sekereš J, Smetana O, Fendrych M, Foissner I, Höftberger M, Žárský V (2013) Arabidopsis exocyst subcomplex containing subunit EXO70B1 is involved in autophagy-related transport to the vacuole. *Traffic* **14:** 1155-1165

Kuratsu M, Taura A, Shoji JY, Kikuchi S, Arioka M, Kitamoto K (2007) Systematic analysis of SNARE localization in the filamentous fungus *Aspergillus oryzae*. *Fungal Genetics and Biology* **44:** 1310-1323

Lamping E, Tanabe K, Niimi M, Uehara Y, Monk BC, Cannon RD (2005) Characterization of the Saccharomyces cerevisiae sec6-4 mutation and tools to create S. cerevisiae strains containing the sec6-4 allele. *Gene* **361:** 57-66

Lee YH, Dean RA (1993) cAMP regulates infection structure formation in the plant pathogenic fungus *Magnaporthe grisea*. *The Plant Cell* **5:** 693-700

Lesage G, Bussey H (2006) Cell wall assembly in *Saccharomyces cerevisiae*. *Microbiology and Molecular Biology Reviews* **70:** 317-343

Li C, Yang J, Zhou W, Chen XL, Huang JG, Cheng ZH, Zhao WS, Zhang Y, Peng YL (2014) A spindle pole antigen gene MoSPA2 is important for polar cell growth of

vegetative hyphae and conidia, but is dispensable for pathogenicity in *Magnaporthe oryzae*. *Current Genetics*. DOI: 10.1007/s00294-014-0431-4

Li CR, Lee RT, Wang YM, Zheng XD, Wang Y (2007) *Candida albicans* hyphal morphogenesis occurs in Sec3p-independent and Sec3p-dependent phases separated by septin ring formation. *Journal of Cell Science* **120:** 1898-1907

Li G, Zhou X, Xu JR (2012) Genetic control of infection-related development in *Magnaporthe oryzae*. *Current Opinion in Microbiology* **15:** 678-684

Li L, Xue C, Bruno K, Nishimura M, Xu JR (2004) Two PAK kinase genes, CHM1 and MST20, have distinct functions in *Magnaporthe grisea*. *Molecular Plant-Microbe Interactions* **17:** 547-556

Li W, Wang B, Wu J, Lu G, Hu Y, Zhang X, Zhang Z, Zhao Q, Feng Q, Zhang H, Wang Z, Wang G, Han B, Wang Z, Zhou B (2009) The *Magnaporthe oryzae* avirulence gene AvrPiz-t encodes a predicted secreted protein that triggers the immunity in rice mediated by the blast resistance gene Piz-t. *Molecular Plant-Microbe Interactions* **22:** 411-420

Li Y, Yan X, Wang H, Liang S, Ma WB, Fang MY, Talbot NJ, Wang ZY (2010) MoRic8 Is a novel component of G-protein signaling during plant infection by the rice blast fungus *Magnaporthe oryzae*. *Molecular Plant-Microbe Interactions* **23:** 317-331

Lichius A, Goryachev AB, Fricker MD, Obara B, Castro-Longoria E, Read ND (2014) CDC-42 and RAC-1 regulate opposite chemotropisms in *Neurospora crassa*. *Journal of Cell Science* **127:** 1953-1965

Lichius A, Yáñez-Gutiérrez ME, Read ND, Castro-Longoria E (2012) Comparative live-cell imaging analyses of SPA-2, BUD-6 and BNI-1 in *Neurospora crassa* reveal novel features of the filamentous fungal polarisome. *PloS One* **7:** e30372

Liu H, Suresh A, Willard FS, Siderovski DP, Lu S, Naqvi NI (2007a) Rgs1 regulates multiple Galpha subunits in Magnaporthe pathogenesis, asexual growth and thigmotropism. *The EMBO Journal* **26:** 690-700

Liu J, Guo W (2012) The exocyst complex in exocytosis and cell migration. *Protoplasma* **249:** 587-597

Liu J, Zuo X, Yue P, Guo W (2007b) Phosphatidylinositol 4,5-bisphosphate mediates the targeting of the exocyst to the plasma membrane for exocytosis in mammalian cells. *Molecular Biology of Cell* **18:** 4483-4492

Liu S, Dean RA (1997) G protein alpha subunit genes control growth, development, and pathogenicity of *Magnaporthe grisea*. *Molecular Plant-Microbe Interactions* **10:** 1075-1086

Liu W, Iliuk A, Tao A, Ding S (2011) Identifying protein complexes by affinity purification and mass spectrometry analysis in the rice blast fungus. *Methods in Molecular Biology (Clifton, NJ)* **722:** 157-166

Liu W, Liu J, Triplett L, Leach JE, Wang G-L (2014) Novel insights into rice innate immunity against bacterial and fungal pathogens. *Annual Review of Phytopathology* **52:** 213-41

Longtine MS, Bi E (2003) Regulation of septin organization and function in yeast. *Trends of Cell Biology* **13:** 403-409

Loo J (2009) Ecological impacts of non-indigenous invasive fungi as forest pathogens. *Biological Invasions* **11:** 81-96

Luo G, Zhang J, Luca FC, Guo W (2013) Mitotic phosphorylation of Exo84 disrupts exocyst assembly and arrests cell growth. *The Journal of Cell Biology* **202:** 97-111

Malhotra V (2013) Unconventional protein secretion: an evolving mechanism. *The EMBO Journal* **32:** 1660-1664

Martin JG, Christopher RT, Gavin EW, Nicholas JT (2006) A P-type ATPase required for rice blast disease and induction of host resistance. *Nature* **440:** 535-539

Mata J, Nurse P (1997) tea1 and the microtubular cytoskeleton are important for generating global spatial order within the fission yeast cell. *Cell* **89:** 939-949

Mehrabi R, Ding S, Xu JR (2008) MADS-box transcription factor mig1 is required for infectious growth in *Magnaporthe grisea*. *Eukaryotic Cell* **7:** 791-799

Mendgen K, Hahn M (2002) Plant infection and the establishment of fungal biotrophy. *Trends in Plant Science* **7:** 352-356

Mentlak TA (2012) Investigating LysM effector function and the biotrophic growth phase of *Magnaporthe oryzae*. *Thesis*

Mentlak TA, Kombrink A, Shinya T, Ryder LS, Otomo I, Saitoh H, Terauchi R, Nishizawa Y, Shibuya N, Thomma BP, Talbot NJ (2012) Effector-mediated suppression of chitin-triggered immunity by *Magnaporthe oryzae* is necessary for rice blast disease. *The Plant Cell* **24:** 322-335

Mitchell TK, Dean RA (1995) The cAMP-dependent protein kinase catalytic subunit is required for appressorium formation and pathogenesis by the rice blast pathogen *Magnaporthe grisea*. *The Plant Cell* **7:** 1869-1878

Mohanty S (2009) Rice and the global financial crisis. *Rice Today* **8**

Momany M (2002) Polarity in filamentous fungi: establishment, maintenance and new axes. *Current Opinion in Microbiology* **5:** 580-585

Moseley JB, Sagot I, Manning AL, Xu Y, Eck MJ, Pellman D, Goode BL (2004) A conserved mechanism for Bni1- and mDia1-induced actin assembly and dual regulation of Bni1 by Bud6 and profilin. *Molecular Biology of Cell* **15:** 896-907

Mosquera G, Giraldo MC, Khang CH, Coughlan S, Valent B (2009) Interaction transcriptome analysis identifies *Magnaporthe oryzae* BAS1-4 as Biotrophy-associated secreted proteins in rice blast disease. *The Plant Cell* **21:** 1273-1290

Munson M, Novick P (2006) The exocyst defrocked, a framework of rods revealed. *Nature Structural & Molecular Biology* **13:** 577-581

Nickel W, Rabouille C (2009) Mechanisms of regulated unconventional protein secretion. *Nature Reviews Molecular Cell Biology* **10:** 148-155

Nobes CD, Hall A (1995) Rho, rac, and cdc42 GTPases regulate the assembly of multimolecular focal complexes associated with actin stress fibers, lamellipodia, and filopodia. *Cell* **81:** 53-62

Nottegham JL, Silue D (1992) Distribution of mating type alleles in *Magnaporthe grisea* populations pathogenic on rice blast. *Phytopathology* **82**

Novick P, Ferro S, Schekman R (1981) Order of events in the yeast secretory pathway. *Cell* **25:** 461-469

Novick P, Field C, Schekman R (1980) Identification of 23 complementation groups required for post-translational events in the yeast secretory pathway. *Cell* **21:** 205-215

Novick P, Medkova M, Dong G, Hutagalung A, Reinisch K, Grosshans B (2006) Interactions between Rabs, tethers, SNAREs and their regulators in exocytosis. *Biochemical Society Transactions* **34:** 683-686

Novick P, Schekman R (1979) Secretion and cell-surface growth are blocked in a temperature-sensitive mutant of Saccharomyces cerevisiae. *Proceedings of the National Academy of Sciences of the United States of America* **76:** 1858-1862

Novick P, Zerial M (1997) The diversity of Rab proteins in vesicle transport. *Current Opinion in Cell Biology* **9:** 496-504

Ntoukakis V, Mucyn TS, Gimenez-Ibanez S, Chapman HC, Gutierrez JR, Balmuth AL, Jones AME, Rathjen JP (2009) Host inhibition of a bacterial virulence effector triggers immunity to infection. *Science* **324:** 784-787

O'Connell RJ, Panstruga R (2006) Tete a tete inside a plant cell: establishing compatibility between plants and biotrophic fungi and oomycetes. *The New Phytologist* **171:** 699-718

Oh S-K, Young C, Lee M, Oliva R, Bozkurt TO, Cano LM, Win J, Bos JIB, Liu H-Y, van Damme M, Morgan W, Choi D, Van der Vossen EAG, Vleeshouwers VGAA, Kamoun S (2009) in planta expression screens of *Phytophthora infestans* RXLR effectors reveal diverse phenotypes, including activation of the *Solanum bulbocastanum* disease resistance protein Rpi-blb2. *The Plant Cell* **21:** 2928-2947

Okada S, Leda M, Hanna J, Savage NS, Bi E, Goryachev AB (2013) Daughter cell identity emerges from the interplay of Cdc42, septins, and exocytosis. *Developmental Cell* **26:** 148-161

Orlando K, Sun X, Zhang J, Lu T, Yokomizo L, Wang P, Guo W (2011) Exo-endocytic trafficking and the septin-based diffusion barrier are required for the maintenance of Cdc42p polarization during budding yeast asymmetric growth. *Molecular Biology of Cell* **22:** 624-633

Ortiz D, Medkova M, Walch-Solimena C, Novick P (2002) Ypt32 recruits the Sec4p guanine nucleotide exchange factor, Sec2p, to secretory vesicles; evidence for a Rab cascade in yeast. *The Journal of Cell Biology* **157:** 1005-1016

Pan F, Malmberg R, Momany M (2007) Analysis of septins across kingdoms reveals orthology and new motifs. *BMC Evolutionary Biology* **7:** 103

Park C-H, Chen S, Shirsekar G, Zhou B, Khang CH, Songkumarn P, Afzal AJ, Ning Y, Wang R, Bellizzi M, Valent B, Wang G-L (2012) The *Magnaporthe oryzae* effector AvrPiz-t targets the RING E3 ubiquitin ligase apip6 to suppress pathogen-associated molecular pattern–triggered immunity in rice. *The Plant Cell* **24**:4748-62

Park G, Xue C, Zhao X, Kim Y, Orbach M, Xu JR (2006) Multiple upstream signals converge on the adaptor protein Mst50 in *Magnaporthe grisea*. *The Plant Cell* **18:** 2822-2835

Park G, Xue C, Zheng L, Lam S, Xu JR (2002) MST12 regulates infectious growth but not appressorium formation in the rice blast fungus *Magnaporthe grisea*. *Molecular Plant-Microbe Interactions* **15:** 183-192

Park H-O, Bi E (2007) Central Roles of Small GTPases in the Development of Cell Polarity in Yeast and Beyond. *Microbiology and Molecular Biology Reviews* **71:** 48-96

Pečenková T, Hála M, Kulich I, Kocourková D, Drdová E, Fendrych M, Toupalová H, Žárský V (2011) The role for the exocyst complex subunits Exo70B2 and Exo70H1 in the plant–pathogen interaction. *Journal of Experimental Botany* **62:** 2107-2116

Pennisi E (2010) Armed and Dangerous. *Science* **327:** 804-805

Pruyne D, Evangelista M, Yang C, Bi E, Zigmond S, Bretscher A, Boone C (2002) Role of formins in actin assembly: nucleation and barbed-end association. *Science* **297:** 612-615

Pruyne DW, Schott DH, Bretscher A (1998) Tropomyosin-containing actin cables direct the Myo2p-dependent polarized delivery of secretory vesicles in budding yeast. *The Journal of Cell Biology* **143:** 1931-1945

Punt PJ, Seiboth B, Weenink XO, van Zeijl C, Lenders M, Konetschny C, Ram AF, Montijn R, Kubicek CP, van den Hondel CA (2001) Identification and characterization of a family of secretion-related small GTPase-encoding genes from the filamentous fungus *Aspergillus niger*: a putative SEC4 homologue is not essential for growth. *Molecular Microbiology* **41:** 513-525

Qadota H, Python CP, Inoue SB, Arisawa M, Anraku Y, Zheng Y, Watanabe T, Levin DE, Ohya Y (1996) Identification of yeast Rho1p GTPase as a regulatory subunit of 1,3-beta-glucan synthase. *Science* **272:** 279-281

Qi Z, Wang Q, Dou X, Wang W, Zhao Q, Lv R, Zhang H, Zheng X, Wang P, Zhang Z (2012) MoSwi6, an APSES family transcription factor, interacts with MoMps1 and is required for hyphal and conidial morphogenesis, appressorial function and pathogenicity of *Magnaporthe oryzae*. *Molecular Plant Pathology* **13:** 677-689

Read ND (2011) Exocytosis and growth do not occur only at hyphal tips. *Molecular Microbiology* **81:** 4-7

Ren J, Guo W (2012) ERK1/2 regulate exocytosis through direct phosphorylation of the exocyst component Exo70. *Developmental Cell* **22:** 967-978

Richthammer C, Enseleit M, Sanchez-Leon E, März S, Heilig Y, Riquelme M, Seiler S (2012) RHO1 and RHO2 share partially overlapping functions in the regulation of cell wall integrity and hyphal polarity in Neurospora crassa. *Molecular Microbiology* **85:** 716-733

Riquelme M (2013) Tip growth in filamentous fungi: a road trip to the apex. *Annual Review of Microbiology* **67:** 587-609

Riquelme M, Bartnicki-García S, González-Prieto JM, Sánchez-León E, Verdín-Ramos JA, Beltrán-Aguilar A, Freitag M (2007) Spitzenkörper localization and intracellular traffic of green fluorescent protein-labeled CHS-3 and CHS-6 chitin synthases in living hyphae of *Neurospora crassa*. *Eukaryotic Cell* **6:** 1853-1864

Riquelme M, Bredeweg EL, Callejas-Negrete O, Roberson RW, Ludwig S, Beltran-Aguilar A, Seiler S, Novick P, Freitag M (2014) The *Neurospora crassa* exocyst complex tethers Spitzenkorper vesicles to the apical plasma membrane during polarized growth. *Molecular Biology of Cell* **25:** 1312-1326

Riquelme M, Sanchez-Leon E (2014) The Spitzenkorper: a choreographer of fungal growth and morphogenesis. *Current Opinion in Microbiology* **20c:** 27-33

Roberson RW, Vargas MM (1994) The tubulin cytoskeleton and its sites of nucleation in hyphal tips of *Allomyces macrogynus*. *Protoplasma* **182:** 19-31

Robinson NG, Guo L, Imai J, Toh EA, Matsui Y, Tamanoi F (1999) Rho3 of *Saccharomyces cerevisiae*, which regulates the actin cytoskeleton and exocytosis, is a GTPase which interacts with Myo2 and Exo70. *Molecular and Cellular Biology* **19:** 3580-3587

Roumanie O, Wu H, Molk JN, Rossi G, Bloom K, Brennwald P (2005) Rho GTPase regulation of exocytosis in yeast is independent of GTP hydrolysis and polarization of the exocyst complex. *Journal of Cell Biology* **170:** 583-594

Ryder LS, Dagdas YF, Mentlak TA, Kershaw MJ, Thornton CR, Schuster M, Chen J, Wang Z, Talbot NJ (2013) NADPH oxidases regulate septin-mediated cytoskeletal remodeling during plant infection by the rice blast fungus. *Proceedings of the National Academy of Sciences of the United States of America* **110:** 3179-3184

Sagot I, Klee SK, Pellman D (2002) Yeast formins regulate cell polarity by controlling the assembly of actin cables. *Nature Cell Biology* **4:** 42-50

Saleh D, Xu P, Shen Y, Li C, Adreit H, Milazzo J, Ravigne V, Bazin E, Notteghem JL, Fournier E, Tharreau D (2012) Sex at the origin: an Asian population of the rice blast fungus *Magnaporthe oryzae* reproduces sexually. *Molecular Ecology* **21:** 1330-1344

Salminen A, Novick PJ (1987) A ras-like protein is required for a post-Golgi event in yeast secretion. *Cell* **49:** 527-538

Salminen A, Novick PJ (1989) The Sec15 protein responds to the function of the GTP binding protein, Sec4, to control vesicular traffic in yeast. *Journal of Cell Biology* **109:** 1023-1036

Sambrook J, Russell DW (2000) Molecular cloning : A Laboratory Manual. Cold Spring Harbour Laboratory Press, New York, USA, **3rd** Edition

Saunders DG, Aves SJ, Talbot NJ (2010a) Cell cycle-mediated regulation of plant infection by the rice blast fungus. *The Plant Cell* **22:** 497-507

Saunders DG, Dagdas YF, Talbot NJ (2010b) Spatial uncoupling of mitosis and cytokinesis during appressorium-mediated plant infection by the rice blast fungus *Magnaporthe oryzae*. *The Plant Cell* **22:** 2417-2428

Schott D, Ho J, Pruyne D, Bretscher A (1999) The Cooh-Terminal Domain of Myo2p, a Yeast Myosin V, Has a Direct Role in Secretory Vesicle Targeting. *The Journal of Cell Biology* **147:** 791-808

Sharpless KE, Harris SD (2002) Functional characterization and localization of the *Aspergillus nidulans* formin SEPA. *Molecular Biology of Cell* **13:** 469-479

Sheu YJ, Santos B, Fortin N, Costigan C, Snyder M (1998) Spa2p interacts with cell polarity proteins and signaling components involved in yeast cell morphogenesis. *Molecular and Cellular Biology* **18:** 4053-4069

Siriputthaiwan P, Jauneau A, Herbert C, Garcin D, Dumas B (2005) Functional analysis of CLPT1, a Rab/GTPase required for protein secretion and pathogenesis in the plant fungal pathogen *Colletotrichum lindemuthianum*. *Journal of Cell Science* **118:** 323-329

Skamnioti P, Gurr SJ (2009) Against the grain: safeguarding rice from rice blast disease. *Trends in Biotechnology* **27:** 141-150

Skau CT, Courson DS, Bestul AJ, Winkelman JD, Rock RS, Sirotkin V, Kovar DR (2011) Actin filament bundling by fimbrin is important for endocytosis, cytokinesis, and polarization in fission yeast. *The Journal of Biological Chemistry* **286:** 26964-26977

Soanes DM, Alam I, Cornell M, Wong HM, Hedeler C, Paton NW, Rattray M, Hubbard SJ, Oliver SG, Talbot NJ (2008) Comparative genome analysis of filamentous fungi reveals gene family expansions associated with fungal pathogenesis. *PloS One* **3:** e2300

Song W, Dou X, Qi Z, Wang Q, Zhang X, Zhang H, Guo M, Dong S, Zhang Z, Wang P, Zheng X (2010) R-SNARE homolog *MoSec22* is required for conidiogenesis, cell wall integrity, and pathogenesis of *Magnaporthe oryzae*. *PloS One* **5:** e13193

Songer JA, Munson M (2009) Sec6p anchors the assembled exocyst complex at sites of secretion. *Molecular Biology of Cell* **20:** 973-982

Southern EM (1975) Detection of specific sequences among DNA fragments separated by gel electrophoresis. *Journal of Molecular Biology* **98:** 503-517

Spector I, Shochet NR, Kashman Y, Groweiss A (1983) Latrunculins: novel marine toxins that disrupt microfilament organization in cultured cells. *Science* **219:** 493-495

Spiliotis ET, Gladfelter AS (2012) Spatial guidance of cell asymmetry: septin GTPases show the way. *Traffic* **13:** 195-203

Stalder D, Mizuno-Yamasaki E, Ghassemian M, Novick PJ (2013) Phosphorylation of the Rab exchange factor Sec2p directs a switch in regulatory binding partners. *Proceedings of the National Academy of Sciences* **110:** 19995-20002

Steinberg G (2007) Hyphal growth: a tale of motors, lipids, and the Spitzenkörper. *Eukaryotic Cell* **6:** 351-360

Strange RN, Scott PR (2005) Plant disease: a threat to global food security. *Annual Review of Phytopathology* **43:** 83-116

Sudbery P (2011) Fluorescent proteins illuminate the structure and function of the hyphal tip apparatus. *Fungal Genetics and Biology* **48:** 849-857

Sweigard J, Chumly, F., Carrol, A., Farrall, L., Valent, B. (1997) A series of vectors for fungal transformation. . *Fungal Genetics Newsletter* **44:** 52-53

Synek L, Schlager N, Eliáš M, Quentin M, Hauser M-T, Žárský V (2006) AtEXO70A1, a member of a family of putative exocyst subunits specifically expanded in land plants, is important for polar growth and plant development. *The Plant Journal* **48:** 54-72

Synek L, Sekeres J, Zarsky V (2014) The exocyst at the interface between cytoskeleton and membranes in eukaryotic cells. *Frontiers in Plant Science* **4:** 543

Taheri-Talesh N, Horio T, Araujo-Bazan L, Dou X, Espeso EA, Penalva MA, Osmani SA, Oakley BR (2008) The tip growth apparatus of *Aspergillus nidulans*. *Molecular Biology of Cell* **19:** 1439-1449

Takizawa PA, DeRisi JL, Wilhelm JE, Vale RD (2000) Plasma membrane compartmentalization in yeast by messenger RNA transport and a septin diffusion barrier. *Science* **290:** 341-344

Talbot NJ (1995) Having a blast: exploring the pathogenicity of *Magnaporthe grisea*. *Trends in Microbiology* **3:** 9-16

Talbot NJ (2003) On the trail of a cereal killer: Exploring the biology of *Magnaporthe grisea*. *Annual Review of Microbiology* **57:** 177-202

Talbot NJ, Ebbole DJ, Hamer JE (1993) Identification and characterization of MPG1, a gene involved in pathogenicity from the rice blast fungus *Magnaporthe grisea*. *The Plant Cell* **5:** 1575-1590

Tang X, Halleck MS, Schlegel RA, Williamson P (1996) A Subfamily of P-Type ATPases with Aminophospholipid Transporting Activity. *Science* **272:** 1495-1497

TerBush DR, Maurice T, Roth D, Novick P (1996) The Exocyst is a multiprotein complex required for exocytosis in *Saccharomyces cerevisiae*. *The EMBO Journal* **15:** 6483-6494

TerBush DR, Novick P (1995) Sec6, Sec8, and Sec15 are components of a multisubunit complex which localizes to small bud tips in *Saccharomyces cerevisiae*. *Journal of Cell Biology* **130:** 299-312

Thinlay, Zeigler RS, Finckh MR (2000) Pathogenic variability of *Pyricularia grisea* from the high- and mid-elevation zones of Bhutan. *Phytopathology* **90:** 621-628

Thomma BP, Nurnberger T, Joosten MH (2011) Of PAMPs and effectors: the blurred PTI-ETI dichotomy. *The Plant Cell* **23:** 4-15

Thompson JD, Higgins DG, Gibson TJ (1994) CLUSTAL W: improving the sensitivity of progressive multiple sequence alignment through sequence weighting, position-specific gap penalties and weight matrix choice. *Nucleic Acids Research* **22:** 4673-4680

Tucker SL, Talbot NJ (2001) Surface attachment and pre-penetration stage development by plant pathogenic fungi. *Annual Review of Phytopathology* **39:** 385-417

Tufan HA, McGrann GR, Magusin A, Morel JB, Miche L, Boyd LA (2009) Wheat blast: histopathology and transcriptome reprogramming in response to adapted and nonadapted Magnaporthe isolates. *The New Phytologist* **184:** 473-484

Tyler BM, Kale SD, Wang Q, Tao K, Clark HR, Drews K, Antignani V, Rumore A, Hayes T, Plett JM, Fudal I, Gu B, Chen Q, Affeldt KJ, Berthier E, Fischer GJ, Dou D, Shan W, Keller NP, Martin F, Rouxel T, Lawrence CB (2013) Microbe-independent entry of oomycete RxLR effectors and fungal RxLR-like effectors into plant and animal cells is specific and reproducible. *Molecular Plant-Microbe Interactions* **26**: 611-616

Upadhyay S, Shaw BD (2008) The role of actin, fimbrin and endocytosis in growth of hyphae in *Aspergillus nidulans*. *Molecular Microbiology* **68:** 690-705

Urashima AS, Lavorent NA, Goulart ACP, Mehta YR (2004) Resistance spectra of wheat cultivars and virulence diversity of *Magnaporthe grisea* isolates in Brazil. *Fitopatologia Brasileira* **29:** 511-518

Valent B, Farrall L, Chumley FG (1991) Magnaporthe-grisea genes for pathogenicity and virulence identified through a series of backcrosses. *Genetics* **127:** 87-101

Valkonen M, Kalkman ER, Saloheimo M, Penttila M, Read ND, Duncan RR (2007) Spatially segregated SNARE protein interactions in living fungal cells. *The Journal of Biological Chemistry* **282:** 22775-22785

van der Hoorn RA, Kamoun S (2008) From Guard to Decoy: a new model for perception of plant pathogen effectors. *The Plant Cell* **20:** 2009-2017

van Drogen F, Peter M (2002) Spa2p functions as a scaffold-like protein to recruit the Mpk1p MAP kinase module to sites of polarized growth. *Current Biology* **12:** 1698-1703

Vaskovicova K, Zarsky V, Rosel D, Nikolic M, Buccione R, Cvrckova F, Brabek J (2013) Invasive cells in animals and plants: searching for LECA machineries in later eukaryotic life. *Biology Direct* **8:** 8

Veneault-Fourrey C, Barooah M, Egan M, Wakley G, Talbot NJ (2006) Autophagic fungal cell death is necessary for infection by the rice blast fungus. *Science* **312:** 580-583

Verdín J, Bartnicki-Garcia S, Riquelme M (2009) Functional stratification of the Spitzenkörper of Neurospora crassa. *Molecular Microbiology* **74:** 1044-1053

Virag A, Harris SD (2006) Functional characterization of *Aspergillus nidulans* homologues of *Saccharomyces cerevisiae* Spa2 and Bud6. *Eukaryotic Cell* **5:** 881-895

Walch-Solimena C, Collins RN, Novick PJ (1997) Sec2p mediates nucleotide exchange on Sec4p and is involved in polarized delivery of post-Golgi vesicles. *Journal of Cell Biology* **137:** 1495-1509

Walworth NC, Brennwald P, Kabcenell AK, Garrett M, Novick P (1992) Hydrolysis of GTP by Sec4 protein plays an important role in vesicular transport and is stimulated by

a GTPase-activating protein in *Saccharomyces cerevisiae*. *Molecular and Cellular Biology* **12:** 2017-2028

Wang J, Ding Y, Wang J, Hillmer S, Miao Y, Lo SW, Wang X, Robinson DG, Jiang L (2010) EXPO, an exocyst-positive organelle distinct from multivesicular endosomes and autophagosomes, mediates cytosol to cell wall exocytosis in Arabidopsis and tobacco cells. *The Plant Cell* **22:** 4009-4030

Wang S, Liu Y, Adamson CL, Valdez G, Guo W, Hsu SC (2004) The mammalian exocyst, a complex required for exocytosis, inhibits tubulin polymerization. *The Journal of Biological Chemistry* **279:** 35958-35966

Wawra S, Djamei A, Albert I, Nurnberger T, Kahmann R, van West P (2013) In vitro translocation experiments with RxLR-reporter fusion proteins of Avr1b from *Phytophthora sojae* and AVR3a from *Phytophthora infestans* fail to demonstrate specific autonomous uptake in plant and animal cells. *Molecular Plant-Microbe Interactions* **26:** 528-536

Wedlich-Soldner R, Bolker M, Kahmann R, Steinberg G (2000) A putative endosomal t-SNARE links exo- and endocytosis in the phytopathogenic fungus *Ustilago maydis*. *The EMBO Journal* **19:** 1974-1986

Weirich CS, Erzberger JP, Barral Y (2008) The septin family of GTPases: architecture and dynamics. *Nature Reviews Molecular Cell Biology* **9:** 478-489

Whisson SC, Boevink PC, Moleleki L, Avrova AO, Morales JG, Gilroy EM, Armstrong MR, Grouffaud S, van West P, Chapman S, Hein I, Toth IK, Pritchard L, Birch PR (2007) A translocation signal for delivery of oomycete effector proteins into host plant cells. *Nature* **450:** 115-118

Wilson RA, Talbot NJ (2009) Under pressure: investigating the biology of plant infection by *Magnaporthe oryzae*. *Nature Reviews Microbiology* **7:** 185-195

Win J, Chaparro-Garcia A, Belhaj K, Saunders DG, Yoshida K, Dong S, Schornack S, Zipfel C, Robatzek S, Hogenhout SA, Kamoun S (2012) Effector biology of plant-associated organisms: concepts and perspectives. *Cold Spring Harbor symposia on quantitative biology* **77:** 235-247

Win J, Morgan W, Bos J, Krasileva KV, Cano LM, Chaparro-Garcia A, Ammar R, Staskawicz BJ, Kamoun S (2007) Adaptive evolution has targeted the C-terminal domain of the RXLR effectors of plant pathogenic oomycetes. *The Plant Cell* **19:** 2349-2369

Wu H, Brennwald P (2010) The function of two Rho family GTPases is determined by distinct patterns of cell surface localization. *Molecular and Cellular Biology* **30:** 5207-5217

Wu H, Rossi G, Brennwald P (2008) The ghost in the machine: small GTPases as spatial regulators of exocytosis. *Trends in Cell Biology* **18:** 397-404

Xu J-R, Urban M, Sweigard JA, Hamer JE (1997) The CPKA gene of *Magnaporthe grisea* is essential for appressorial penetration. *Molecular Plant-Microbe Interactions* **10:** 187-194

Xu JR (2000) Map kinases in fungal pathogens. *Fungal Genetics and Biology* **31:** 137-152

Xu JR, Hamer JE (1996) MAP kinase and cAMP signaling regulate infection structure formation and pathogenic growth in the rice blast fungus *Magnaporthe grisea*. *Genes & Development* **10:** 2696-2706

Xu JR, Staiger CJ, Hamer JE (1998) Inactivation of the mitogen-activated protein kinase Mps1 from the rice blast fungus prevents penetration of host cells but allows activation of plant defense responses. *Proceedings of the National Academy of Sciences of the United States of America* **95:** 12713-12718

Yaeno T, Li H, Chaparro-Garcia A, Schornack S, Koshiba S, Watanabe S, Kigawa T, Kamoun S, Shirasu K (2011) Phosphatidylinositol monophosphate-binding interface in the oomycete RXLR effector AVR3a is required for its stability in host cells to modulate plant immunity. *Proceedings of the National Academy of Sciences of the United States of America* **108:** 14682-14687

Yaeno T, Shirasu K (2013) The RXLR motif of oomycete effectors is not a sufficient element for binding to phosphatidylinositol monophosphates. *Plant Signaling & Behavior* **8:** e23865

Yan X, Li Y, Yue X, Wang C, Que Y, Kong D, Ma Z, Talbot NJ, Wang Z (2011) Two novel transcriptional regulators are essential for infection-related morphogenesis and pathogenicity of the rice blast fungus *Magnaporthe oryzae*. *PLoS Pathogens* **7:** e1002385

Ye W, Chen X, Zhong Z, Chen M, Shi L, Zheng H, Lin Y, Zhang D, Lu G, Li G, Chen J, Wang Z (2014) Putative RhoGAP proteins orchestrate vegetative growth, conidiogenesis and pathogenicity of the rice blast fungus *Magnaporthe oryzae*. *Fungal Genetics and Biology* **67:** 37-50

Yi M, Chi MH, Khang CH, Park SY, Kang S, Valent B, Lee YH (2009) The ER chaperone LHS1 is involved in asexual development and rice infection by the blast fungus *Magnaporthe oryzae*. *The Plant Cell* **21:** 681-695

Yi M, Valent B (2013) Communication between filamentous pathogens and plants at the biotrophic interface. *Annual Review of Phytopathology* **51:** 587-611

Yoshida K, Saitoh H, Fujisawa S, Kanzaki H, Matsumura H, Yoshida K, Tosa Y, Chuma I, Takano Y, Win J, Kamoun S, Terauchi R (2009a) Association genetics reveals three novel avirulence genes from the rice blast fungal pathogen *Magnaporthe oryzae*. *The Plant Cell* **21:** 1573-1591

Zajac A, Sun X, Zhang J, Guo W (2005) Cyclical regulation of the exocyst and cell polarity determinants for polarized cell growth. *Molecular Biology of Cell* **16:** 1500-1512

Zarsky V, Kulich I, Fendrych M, Pecenkova T (2013) Exocyst complexes multiple functions in plant cells secretory pathways. *Current Opinion in Plant Biology* **16:** 726-733

Zeigler RS (1998) Recombination in *Magnaporthe grisea*. *Annual Review of Phytopathology* **36:** 249-275

Zhang H, Tang W, Liu K, Huang Q, Zhang X, Yan X, Chen Y, Wang J, Qi Z, Wang Z, Zheng X, Wang P, Zhang Z (2011) Eight RGS and RGS-like proteins orchestrate growth, differentiation, and pathogenicity of *Magnaporthe oryzae*. *PLoS Pathogens* **7:** e1002450

Zhang H, Wu Z, Wang C, Li Y, Xu J-R (2014a) Germination and infectivity of microconidia in the rice blast fungus *Magnaporthe oryzae*. *Nature Communications* **5:** 4518

Zhang X, Bi E, Novick P, Du L, Kozminski KG, Lipschutz JH, Guo W (2001) Cdc42 interacts with the exocyst and regulates polarized secretion. *The Journal of Biological Chemistry* **276:** 46745-46750

Zhang X, Orlando K, He B, Xi F, Zhang J, Zajac A, Guo W (2008) Membrane association and functional regulation of Sec3 by phospholipids and Cdc42. *Journal of Cell Biology* **180:** 145-158

Zhang Z, Qin G, Li B, Tian S (2014b) Knocking out Bcsas1 in *Botrytis cinerea* impacts growth, development, and secretion of extracellular proteins, which decreases virulence. *Molecular Plant-Microbe Interactions* **27:** 590-600

Zhao X, Kim Y, Park G, Xu JR (2005) A mitogen-activated protein kinase cascade regulating infection-related morphogenesis in *Magnaporthe grisea*. *The Plant Cell* **17:** 1317-1329

Zhao X, Xu JR (2007) A highly conserved MAPK-docking site in Mst7 is essential for Pmk1 activation in *Magnaporthe grisea*. *Molecular Microbiology* **63:** 881-894

Zheng W, Chen J, Liu W, Zheng S, Zhou J, Lu G, Wang Z (2007) A Rho3 Homolog Is Essential for Appressorium Development and Pathogenicity of *Magnaporthe grisea*. *Eukaryotic Cell* **6:** 2240-2250

Zheng W, Zhao Z, Chen J, Liu W, Ke H, Zhou J, Lu G, Darvill AG, Albersheim P, Wu S, Wang Z (2009) A Cdc42 ortholog is required for penetration and virulence of *Magnaporthe grisea*. *Fungal genetics and biology* **46:** 450-460

Zhou X, Liu W, Wang C, Xu Q, Wang Y, Ding S, Xu JR (2011) A MADS-box transcription factor MoMcm1 is required for male fertility, microconidium production and virulence in *Magnaporthe oryzae*. *Molecular Microbiology* **80:** 33-53

Zhou X, Zhang H, Li G, Shaw B, Xu JR (2012) The Cyclase-associated protein Cap1 is important for proper regulation of infection-related morphogenesis in *Magnaporthe oryzae*. *PLoS Pathogens* **8:** e1002911

Appendix 1

Giraldo, M.C., Dagdas, Y.F., Gupta, Y.K., Mentlak, T.A., Yi, M., Martinez-Rocha, A.L., Saitoh, H., Terauchi, R., Talbot, N.J. and Valent, B. (2013) Two distinct secretion systems facilitate tissue invasion by the rice blast fungus *Magnaporthe oryzae*. *Nature Communications* **4**: 1996. doi: 10.1038/ncomms2996.

nature COMMUNICATIONS

ARTICLE

Received 15 Nov 2012 | Accepted 9 May 2013 | Published 18 Jun 2013

DOI: 10.1038/ncomms2996 OPEN

Two distinct secretion systems facilitate tissue invasion by the rice blast fungus *Magnaporthe oryzae*

Martha C. Giraldo[1,*], Yasin F. Dagdas[2,*], Yogesh K. Gupta[2], Thomas A. Mentlak[2,†], Mihwa Yi[1], Ana Lilia Martinez-Rocha[2,†], Hiromasa Saitoh[3], Ryohei Terauchi[3], Nicholas J. Talbot[2] & Barbara Valent[1]

To cause plant diseases, pathogenic micro-organisms secrete effector proteins into host tissue to suppress immunity and support pathogen growth. Bacterial pathogens have evolved several distinct secretion systems to target effector proteins, but whether fungi, which cause the major diseases of most crop species, also require different secretory mechanisms is not known. Here we report that the rice blast fungus *Magnaporthe oryzae* possesses two distinct secretion systems to target effectors during plant infection. Cytoplasmic effectors, which are delivered into host cells, preferentially accumulate in the biotrophic interfacial complex, a novel plant membrane-rich structure associated with invasive hyphae. We show that the biotrophic interfacial complex is associated with a novel form of secretion involving exocyst components and the Sso1 *t*-SNARE. By contrast, effectors that are secreted from invasive hyphae into the extracellular compartment follow the conventional secretory pathway. We conclude that the blast fungus has evolved distinct secretion systems to facilitate tissue invasion.

[1] Department of Plant Pathology, Kansas State University, Manhattan, Kansas 66506, USA. [2] School of Biosciences, University of Exeter, Exeter, EX4 4QD, UK. [3] Iwate Biotechnology Research Center, Kitakami, Iwate 024-0003, Japan. * These authors contributed equally to this work. † Present addresses: Cambridge Consultants Ltd, Cambridge, CB4 0DW, UK (T.A.M.); Department of Molecular Phytopathology and Genetics, University of Hamburg, Biozentrum Klein Flottbek, D-22609 Hamburg, Germany (A.L.M.-R). Correspondence and requests for materials should be addressed to B.V. (email: bvalent@ksu.edu).

Biotrophic pathogens grow in intimate contact with living host cells and deliver effector proteins into and around these host cells[1–4]. In pathogenic bacteria, effectors serve a variety of functions, including induction of host cell entry by intracellular pathogens, modulation of host cell signalling and suppression of immune responses. These distinct functions are associated with specific forms of secretion that operate during pathogenesis[5,6]. Eukaryotic microbial pathogens, such as fungi and oomycetes, possess even larger numbers of effector proteins that are secreted during host infection[3,4,7,8]. They serve to suppress immunity[9–11], modulate metabolism[12] and prevent recognition of the invading microbe[13,14]. Although the functions of most of these effectors are still unknown, it is increasingly clear that fungal effectors are delivered both to the inside of host cells, as well as to the host–pathogen interface during infection.

The ascomycete fungus *Magnaporthe oryzae* causes rice blast, the most serious disease of cultivated rice and a major threat to global food security[15–17]. Additionally, a wheat-adapted population of *M. oryzae* has recently emerged to cause wheat blast disease in South America, and this fungus now also poses a threat to global wheat production[18,19]. To cause disease, the fungus uses a special infection cell called an appressorium, which ruptures the rice cuticle and allows the fungus entry into the epidermal cells[16,20,21]. *M. oryzae* then invades rice tissue using specialized filamentous invasive hyphae (IH), which successively occupy living rice cells[22] and colonize tissue extensively before the appearance of disease symptoms. Host cells are initially invaded by narrow tubular primary hyphae that subsequently develop into enlarged, bulbous IH (Fig. 1a)[22]. Morphologically, bulbous IH are constricted at septal junctions, resembling pseudohyphae produced by the human fungal pathogen *Candida albicans*[23,24]. Differentiation to a specialized invasive hypha recurs for each new filamentous hypha that enters a living host cell (Fig. 1a), and this differentiation process appears critical for disease development.

During biotrophic invasion, *M. oryzae* expresses many low-molecular-weight biotrophy-associated secreted (Bas) proteins, including known effector proteins, and these proteins possess classical signal peptides, which facilitate delivery into the endoplasmic reticulum (ER)[8,25,26]. The ER chaperone Lhs1 is furthermore required for secretion of effectors[27]. Previous *in planta* analyses have involved live-cell imaging of *M. oryzae* strains secreting chimeric effector proteins labelled with carboxy-terminal green fluorescent protein (GFP), monomeric red fluorescent protein (mRFP) or monomeric Cherry (mCherry). Secreted effectors show distinct patterns of accumulation within the extra-invasive hyphal membrane (EIHM) compartment enclosing IH growing in rice cells[14,25,28]. Apoplastic effectors, which do not enter host cells, are generally dispersed and retained within the EIHM compartment, where they outline the entire IH. By contrast, cytoplasmic effectors preferentially accumulate in the biotrophic interfacial complex (BIC)[28], a membrane-rich structure that initially appears adjacent to primary hyphal tips, but is later positioned subapically as IH develop within rice cells (Fig. 1a). Fluorescent effector proteins that accumulate in BICs appear to be translocated across the EIHM into the cytoplasm of living rice cells[28]. Translocation of effectors into rice cells has been most clearly visualized by expression of fluorescent effector fusion proteins with an artificially added C-terminal nuclear localization signal (NLS). The NLS serves to enhance the sensitivity of effector detection in host cells by concentrating them in the rice nucleus. Using this sensitive assay, it has been shown that some translocated cytoplasmic effectors move ahead of the invading pathogen, into three to four layers of surrounding rice cells, presumably to prepare these cells for fungal colonization[28].

The distinct localization patterns of cytoplasmic and apoplastic effectors within the EIHM compartment raise questions regarding the mechanism by which effectors are secreted by IH within living plant cells. Protein secretion associated with apical tip growth in filamentous fungi involves the Spitzenkörper, the vesicle supply centre feeding vesicles to growing hyphal tips[29–32]. The three-component polarisome complex nucleates actin cables for transporting vesicles to the growth point. Near the polarized secretion site, vesicles dock with the exocyst, a complex of eight proteins that has been implicated in tethering vesicles to the target membrane before fusion. However, it is becoming clear that the exocyst has a role at many sites in a cell as a spatiotemporal regulator of membrane trafficking in response to diverse signals[33]. Fusion of secretory vesicles to the plasma membrane is then directed by SNAREs (soluble *N*-ethylmaleimide-sensitive factor attachment protein receptors), involving a v-SNARE on the vesicle and a t-SNARE on the membrane. Hyphal growth and secretion in filamentous fungi was thought to occur exclusively at the hyphal tips, but this no longer appears to be the case[29]. In *Trichoderma reesei* and *Aspergillus oryzae*, exocytosis mediated by SNARE proteins can also occur in subapical hyphal compartments[34,35].

In this study, we focus on investigating how the fungus secretes effectors during host cell invasion. We were specifically interested in determining whether effectors destined for translocation to host cells follow the same secretory route as those that accumulate in the apoplast. We present evidence for two distinct secretory pathways in *M. oryzae*. We show that BICs are plant-derived, membrane-rich interfacial structures associated with accumulation of effectors that ultimately enter host cells, and that subapical BIC-associated IH cells are enriched in secretion machinery components. Using a combination of pharmacological and gene functional analyses, we show that the conventional fungal ER-Golgi secretion pathway is involved in secretion of apoplastic effectors, but not cytoplasmic effectors, and conversely, that cytoplasmic effectors require exocyst components Exo70 and Sec5 for efficient secretion. Taken together, our results are consistent with operation of two distinct secretory pathways for effector delivery during plant infection by the rice blast fungus.

Results

The biotrophic interfacial complex is a plant-derived structure. To define the location and structure of the BIC, we first generated fungal transformants expressing fluorescently labelled plasma membrane (Fig. 1b) and cytoplasmic (Supplementary Fig. S1) markers, together with BIC-localized cytoplasmic effectors such as Pwl2, which prevents pathogenicity towards weeping lovegrass (*Eragrostis curvula*)[36]. The fungal plasma membrane was visualized by expression of the *M. oryzae* membrane ATPase Pma1 as a translational fusion to GFP (Fig. 1b). During growth inside rice cells, fungal transformants expressing Pma1:GFP and Pwl2:mRFP consistently showed red fluorescence of BIC-localized Pwl2:mRFP outside the green fluorescence in the labelled fungal plasma membrane, confirming that the BIC lies outside the fungal plasma membrane. We then generated transgenic rice lines expressing the fluorescently labelled plasma membrane marker Lti6B-GFP and the ER marker HDEL-GFP. Imaging of fungus expressing Pwl2:mRFP invading these fluorescently labelled rice lines provided evidence that BICs are associated with concentrated regions of plant plasma membrane and ER (Fig. 1c,d). When considered together, these results demonstrate that the BIC is a plant-derived interfacial structure and that effectors must be secreted by the invading fungus in order to be observed so specifically at the BIC.

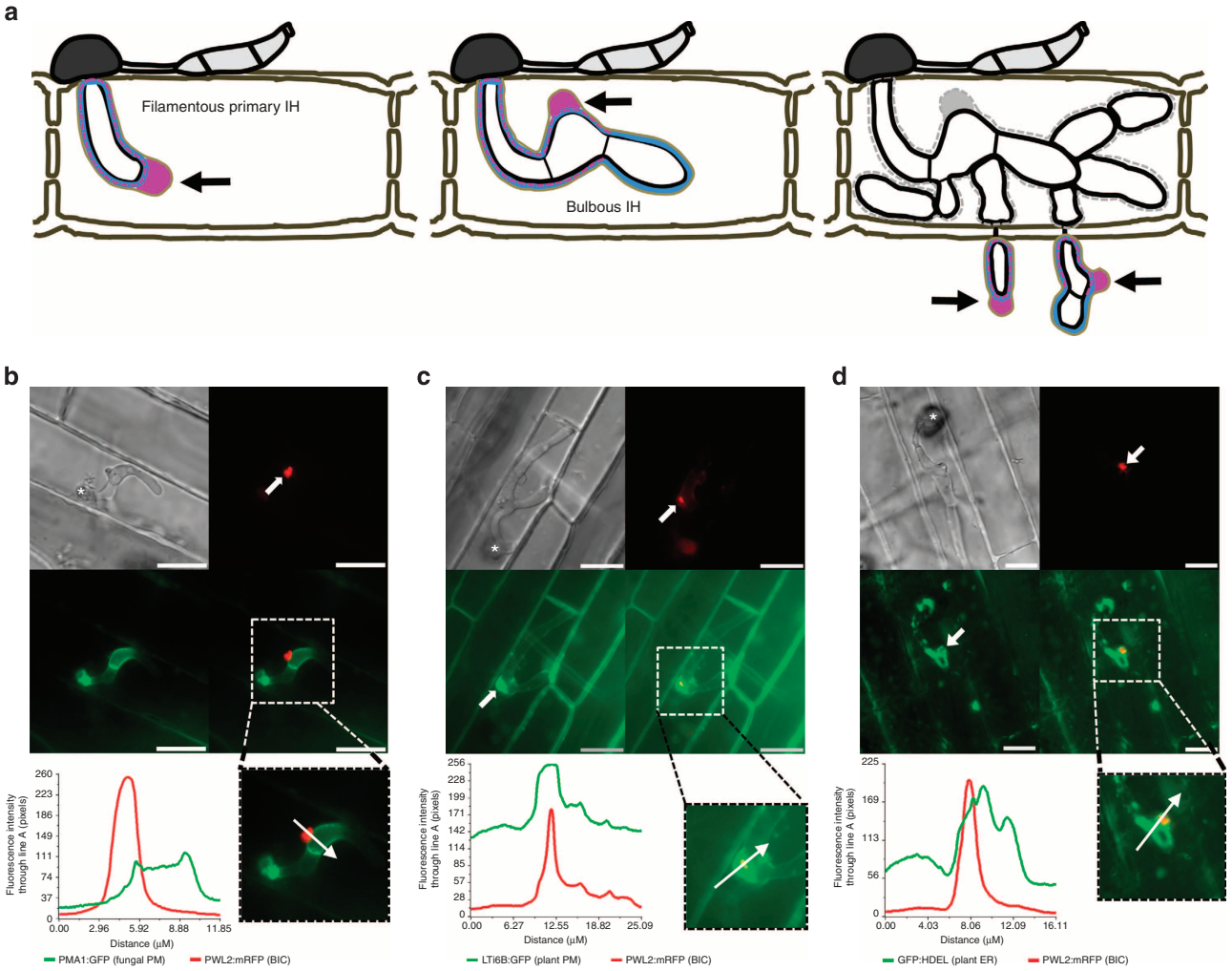

Figure 1 | The biotrophic interfacial complex is a plant-derived membrane-rich structure. (**a**) Schematic representation of the differentiation of a filamentous primary invasive hypha (left, ~22–25 h post inoculation, h.p.i.) into a pseudohyphal-like bulbous invasive hypha (middle, ~26–30 h.p.i.) in a first-invaded rice cell. This differentiation occurs for each new hypha invading a living neighbour cell (right, ~36–40 h.p.i.). Cytoplasmic effectors show preferential accumulation in the BIC (black arrows), which is first located in front of the growing primary hyphal tips, and then remains behind beside the first-differentiated bulbous IH cell. Typical accumulation patterns for cytoplasmic (magenta) and apoplastic (blue) effectors are shown within the EIHM (tan) compartment enclosing the IH. The EIHM appears to lose integrity when the fungus has moved into neighbour cells (dotted line). (**b**–**d**) Live cell imaging of *M. oryzae* infection of rice sheath epidermal cells with the BIC (red) visualized by accumulation of IH-secreted Pwl2:mRFP. Clockwise, images are DIC; mRFP (white arrow indicates BIC); merged GFP (green) and mRFP (red); and GFP alone. Below, white arrow in the inset shows the path for fluorescence intensity distribution linescans on the left. (**b**) The BIC (red) is located outside the fungal plasma membrane (green), which was visualized by expression of *M. oryzae* ATPase Pma1:GFP, here imaged at 23 h.p.i. Lack of co-localization between Pwl2:mRFP and Pma1:GFP, indicated by separate subcellular distribution maxima, confirms that the BIC does not contain fungal plasma membrane. (**c**) The BIC (red) co-localized with intense fluorescence from a rice plasma membrane marker LTi6B:GFP (green), visualized after infection of transgenic rice (at 24 h.p.i.). Note that the plant plasma membrane marker also outlined the entire IH, consistent with invagination around the fungus during cell invasion. Co-localization of fluorescence intensity maxima indicates that the BIC contains material derived from plant plasma membrane. (**d**) The BIC (red) co-localized with fluorescence from rice ER marker GFP:HDEL (green) expressed in transgenic plants and imaged at 24 h.p.i. Fluorescence intensity maxima demonstrate plant ER localized with and closely surrounding the BIC. White asterisks indicate appressoria. Scale bars, 10 μm.

Organization of secretory complexes within invasive hyphae of *M. oryzae*. To investigate the mechanisms of effector secretion by IH inside rice cells, we identified *M. oryzae* orthologues of genes implicated in polarized growth and secretion (Supplementary Fig. S2 and Supplementary Table S1)[23,30,32,33]. These genes encoded the myosin motor regulatory component Mlc1 (MGG_09470.6) (associated with the Spitzenkörper in *C. albicans*[23]), polarisome component Spa2 (MGG_03703.6) and exocyst component Exo70 (MGG_01760.6). We also identified genes encoding v-SNARE Snc1 (MGG_12614.6) and t-SNARE Sso1 (MGG_04090.6), which together mediate docking and fusion of vesicles with the plasma membrane target site[35]. All genes were expressed in *M. oryzae* under control of their native promoters and with C-terminal translational fusions of GFP, except for Snc1, which was expressed with an amino-terminal fusion of GFP. Each putative secretion component localized with fluorescence concentrated at the tips of vegetative hyphae growing on agar medium, as expected (Fig. 2). Spitzenkörper localization of Mlc1:GFP was confirmed by co-localization with the Styryl dye FM4-64, the endocytotic tracer dye that is a generally accepted Spitzenkörper marker (Fig. 2a)[23,37–39]. These secretory components also concentrated in the growing tips of

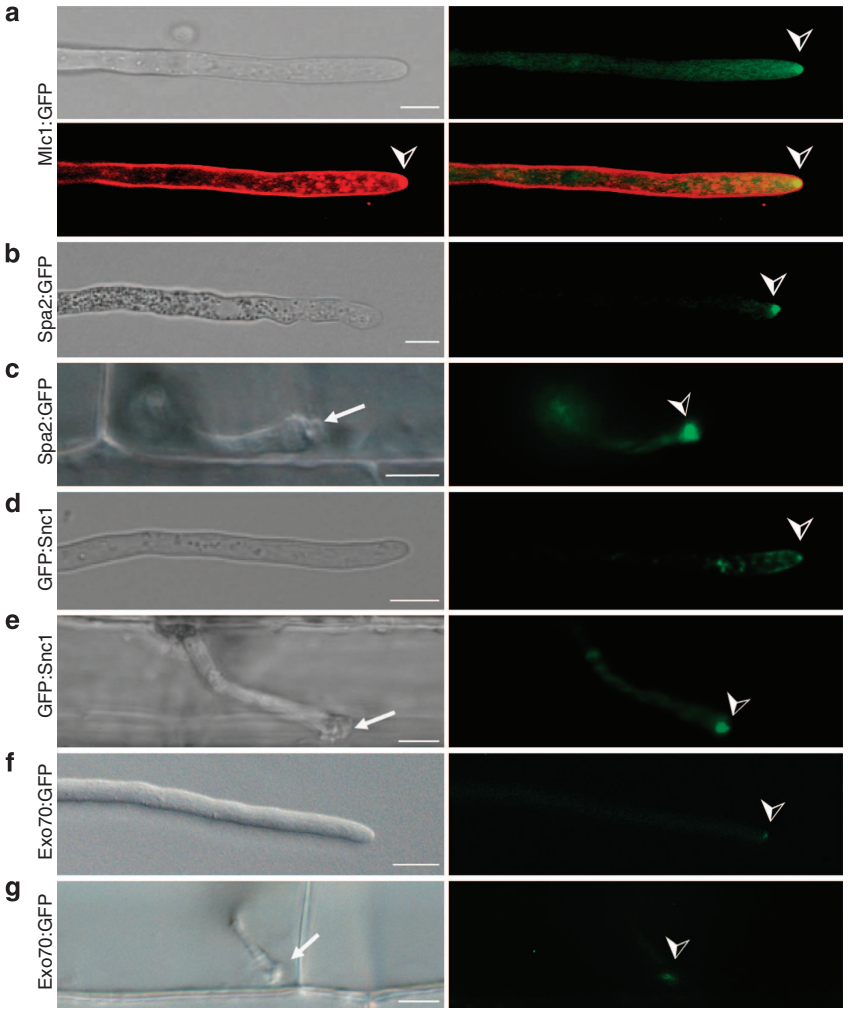

Figure 2 | Secretion components localize similarly in vegetative and primary hyphae. Fluorescent secretory components (➢) were imaged in *M. oryzae* filamentous vegetative hyphae *in vitro* (**a**,**b**,**d**,**f**) and in tubular primary hyphae growing in rice cells (**c**,**e**,**g**). BICs (white arrows) were observed adjacent to the primary hyphal tips even without fluorescent labelling. (**a**) Spitzenkörper marker Mlc1:GFP (green) co-localizes (yellow) with the endocytic tracker dye FM4-64 (red) at tips of vegetative hyphae. This confocal image was acquired 10 min after FM4-64 addition. Images clockwise from upper left are bright-field; GFP; merged GFP and FM4-64; and FM4-64 alone. Similarly, Mlc1:GFP identifies Spitzenkörper in primary hyphae inside rice cells (Fig. 3a). (**b**–**g**) Images from left to right are bright-field; and GFP alone. (**b**) Polarisome component Spa2:GFP localizes to the tip of a vegetative hypha. (**c**) Polarisome component Spa2:GFP concentrates at the primary hyphal tip behind the BIC at 22 h.p.i. (**d**) v-SNARE GFP:Snc1 localizes at the vegetative hyphal tip. (**e**) v-SNARE GFP:Snc1 localizes in a bright fluorescent punctum near the primary hyphal tip at 24 h.p.i. (**f**) Exocyst component Exo70:GFP localizes at the vegetative hyphal tip. (**g**) Exocyst component Exo70:GFP localizes at the primary hyphal tip at 24 h.p.i. Scale bars, 5 μm.

primary hyphae adjacent to BICs (Figs 2c,e,g and 3a). Therefore, secretory machineries of vegetative and primary IH appear to be similarly organized.

Although Mlc1:GFP identified Spitzenkörper at primary hyphal tips *in planta* (Fig. 3a), Spitzenkörper were not observed at the hyphal growth points after differentiation of bulbous IH (Fig. 3b). This result is consistent with loss of the ball-like Spitzenkörper after differentiation of *C. albicans* hyphae into pseudohyphae[23]. In bulbous IH, Mlc1:GFP identified a fluorescent spot near each septum as well as a single larger fluorescent spot in the subapical BIC-associated cell, which was no longer growing (Fig. 3b). In contrast, polarisome marker Spa2:GFP remained localized at hyphal growth points (Fig. 3c), and was not observed in BIC-associated IH cells. Similarly to Mlc1:GFP, the SNARE proteins GFP:Snc1 and Sso1:GFP and exocyst protein Exo70:GFP each showed significant focal fluorescence in subapical BIC-associated cells in addition to fluorescence elsewhere in the hyphae (Fig. 3d–f). For example, GFP:Snc1 also localized as smaller vesicles, especially at hyphal growth points (Fig. 3d). In subsequently invaded cells, all markers first showed significant fluorescence at tips of the initially tubular hyphae that entered each rice cell. After differentiation to bulbous IH, all markers except Spa2:GFP showed significant localization in subapical BIC-associated IH cells. This is shown for Sso1:GFP fluorescence in the seven visible hyphae growing in a second-invaded cell (Fig. 3g). We conclude that filamentous primary hyphae and pseudohyphal-like bulbous IH are distinct morphological cell types and that switching between tubular and bulbous IH *in planta* may involve a spatiotemporal reorientation of secretory machinery. Additionally, after differentiation and further growth, we conclude that subapical bulbous IH cells associated with BICs are capable of active secretion.

Brefeldin A treatment identifies distinct effector secretion pathways. To test the nature of fungal secretion, we first exposed *M. oryzae* IH to Brefeldin A (BFA), which inhibits conventional

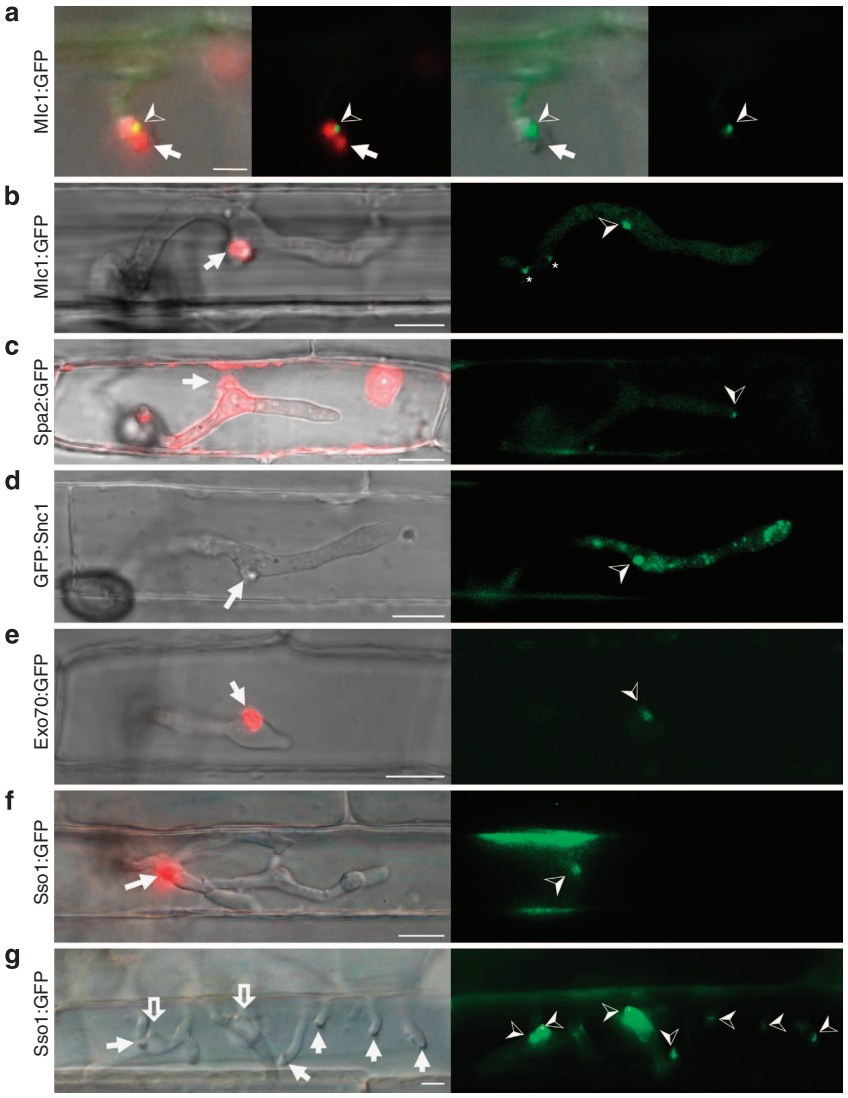

Figure 3 | BIC-associated IH cells contain components of the secretory machinery. All images are representative of at least five biological replicates with >50 images each. BICs are labelled by arrows in all panels and by red fluorescence from Pwl2:mRFP in all panels except **d** and **g**. Unless mentioned otherwise, images left to right are: merged bright-field and mRFP (red); and GFP alone (green). (**a**) The myosin regulatory light chain Mlc1:GFP (➢) labels the Spitzenkörper at the primary hyphal tip before hyphal differentiation at 24 h.p.i. Images left to right: merged bright-field, GFP and mRFP; merged GFP and mRFP; merged bright-field and GFP; and GFP alone. Scale bar, 5 μm. (**b**) After differentiation of bulbous IH at 27 h.p.i., Mlc1:GFP accumulates in a large fluorescent punctum in the BIC-associated bulbous IH cell (➢) and near septa (⋆). Spitzenkörper-like fluorescence is not observed in growing bulbous IH tips. (**c**) Polarisome component Spa2:GFP localizes as a distinct punctum at the tip of growing IH (➢) at 27 h.p.i. Spa2 fluorescence is not observed in the subapical BIC-associated IH cell. In this image, saturated fluorescence from Pwl2:mRFP labels the rice cytoplasm and nucleus (⋆). This saturated Pwl2:mRFP fluorescence is seen in the EIHM compartment surrounding the BIC-associated cells, as previously reported[28]. (**d**) v-SNARE GFP:Snc1 localizes to a large fluorescent punctum (➢) in the BIC-associated IH cell and to smaller vesicles in growing IH at 27 h.p.i. Images left to right: bright-field; and GFP alone. (**e**) Faint fluorescence from exocyst component Exo70:GFP can be observed in the subapical BIC-associated cell at 28 h.p.i. (**f**) t-SNARE Sso1:GFP (➢) localizes in the BIC-associated IH cell near the BIC in a first-invaded rice cell at 27 h.p.i. (**g**) t-SNARE Sso1:GFP (➢) in a second-invaded cell accumulated near BICs, as crescents at the tips of five primary IH (white arrows), and as puncta in two BIC-associated IH cells after differentiation (outline arrows). Shown at 40 h.p.i. (as described in Fig. 1a, right panel). Images left to right: bright-field; and GFP alone. Scale bars, 10 μm unless stated otherwise.

ER-to-Golgi secretion in fungi[40]. For these experiments, we used a *M. oryzae* strain expressing both apoplastic effector Bas4:GFP[25] and cytoplasmic effector Pwl2:mCherry:NLS (Fig. 4a). We found that the apoplastic effector Bas4:GFP was retained in the hyphal ER within 3 h of exposure of infected rice tissue to BFA, but cytoplasmic effector Pwl2:mCherry:NLS still exhibited BIC accumulation with no observable fluorescence inside the hyphal ER, even with longer periods of exposure (Fig. 4b). The distinct BFA localization patterns for Pwl2 and Bas4 were independent of the fluorescent proteins used and the added NLS, indicating that effector sequences controlled the distinct secretion properties (Supplementary Fig. S3a). To determine whether these effects were general, we tested additional cytoplasmic effectors AVR-Pita (ref. 8) (Fig. 4c), Bas1 (ref. 25) (Fig. 4c) and Bas107 (Supplementary Fig. S3b). Secretion and BIC localization of all three continued in the presence of BFA with no visible

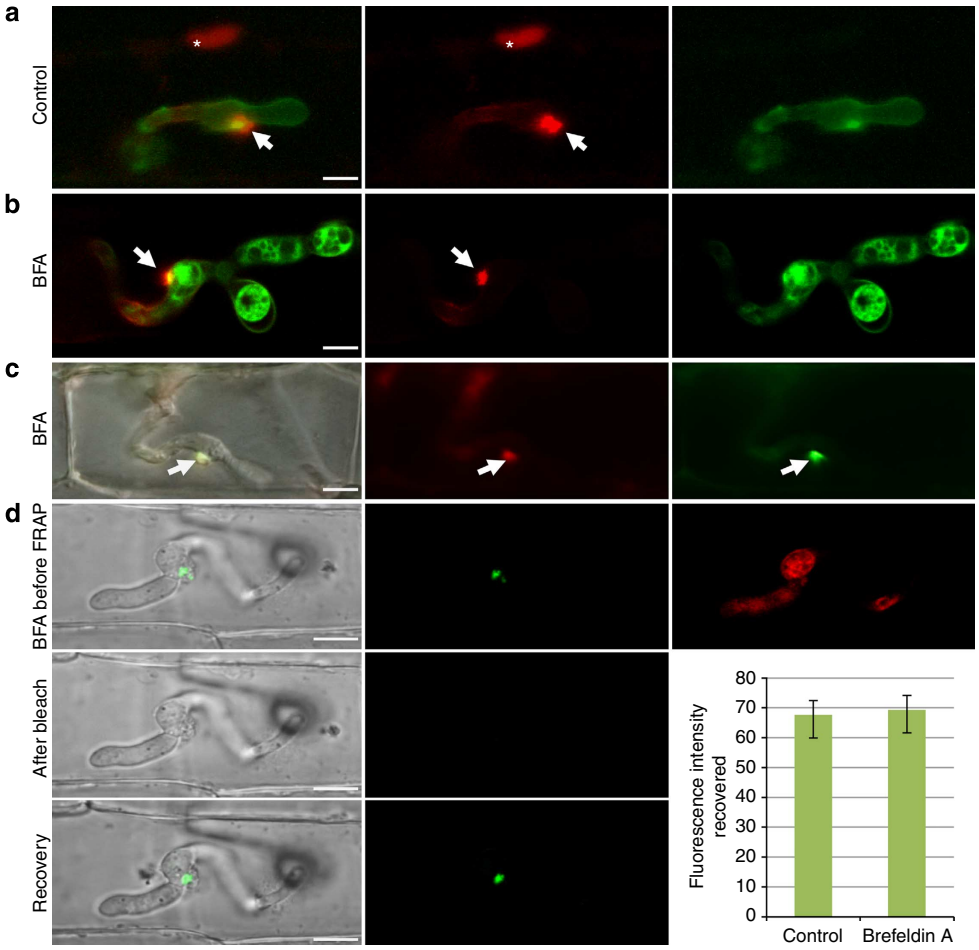

Figure 4 | Brefeldin A blocks secretion of apoplastic but not of cytoplasmic effectors. (**a**–**c**) Images left to right: either merged bright-field, mCherry and GFP or merged mCherry and GFP; mCherry alone; and GFP alone. (**a**) After secretion, cytoplasmic effector Pwl2:mCherry:NLS (red) shows preferential BIC localization (arrow) and translocation into the rice cell, where it accumulates in the rice nucleus (⋆). Bas4:GFP shows apoplastic localization outlining the IH. (**b**) In the presence of BFA, Pwl2:mCherry:NLS remains BIC-localized (arrow), but Bas4:GFP (green) is retained in the fungal ER, imaged with the same transformant in (**a**) 10 h after exposure to BFA. (**c**) Cytoplasmic effectors Bas1:mRFP (red, middle) and AVR-Pita:GFP (green, right) still co-localized in the BIC (arrow) after 5 h exposure to BFA. (**d**) Fluorescence recovery after photobleaching (FRAP) demonstrates continuous secretion of Pwl2:GFP into the BIC in the presence of BFA. Rice tissue infected by a fungal strain expressing Pwl2:GFP and Bas4:mRFP was incubated in BFA for 3 h before photobleaching of Pwl2:GFP in the BIC. Secretion of Bas4:mRFP had been blocked at this point. FRAP results were identical in the presence or absence of BFA ($P = 0.019$). Bars show mean fluorescence intensity recovery after bleaching (mean ± s.d., four FRAP experiments). Images left to right before photobleaching: merged bright-field and GFP; GFP alone; and mRFP alone. Images left to right after photobleaching and recovery: merged bright-field and GFP; and GFP alone. Scale bars, 10 μm.

accumulation of fluorescence inside IH. By contrast, secretion of additional apoplastic effectors Slp1:GFP[14] and Bas113:mRFP was blocked by BFA treatment (Supplementary Fig. S3c).

To confirm that secretion of Pwl2:GFP into BICs continued in the presence of BFA, we performed fluorescence recovery after photobleaching (FRAP) analysis. Using transformants expressing both Pwl2:GFP and Bas4:mRFP, we photobleached Pwl2:GFP in subapical BICs and then monitored fluorescence recovery over time in the presence or absence of BFA. For BFA-treated tissues, retention of Bas4:mRFP in the hyphal ER confirmed that the treatment was effective before fluorescence in the BICs was photobleached. As expected from previous results[28], full recovery of fluorescence in BICs occurred within 3 h. Identical recovery rates were observed in the presence or absence of BFA (Fig. 4d), indicating that the fungus continues to secrete cytoplasmic effector protein into BICs in the presence of BFA. During fungal invasion of rice cells, BFA therefore reproducibly blocked secretion of apoplastic effectors, but not BIC accumulation of cytoplasmic effectors.

We tested whether the fungal cytoskeleton is important for effector secretion using the microtubule inhibitor methyl 1-(butylcarbamoyl)-2-benzimidazolecarbamate (MBC) and the actin inhibitor latrunculin A (LatA). Secretion of Bas4:mRFP was impaired when infected rice tissues were treated with MBC or LatA, but secretion of Pwl2:GFP was not visibly impaired (Supplementary Fig. S4). FRAP experiments again confirmed that Pwl2:GFP continued to accumulate in BICs in the presence of MBC or LatA, further supporting the operation of distinct effector secretion mechanisms.

Efficient secretion of cytoplasmic effectors requires the exocyst complex. We next investigated the protein secretion components necessary for effector secretion. In yeast, Exo70 and Sec5 are subunits of the octameric exocyst complex implicated in spatio-temporal regulation of membrane trafficking[33]. We produced a series of targeted gene replacement mutants for the *M. oryzae EXO70* and *SEC5* genes in strains expressing fluorescent effectors

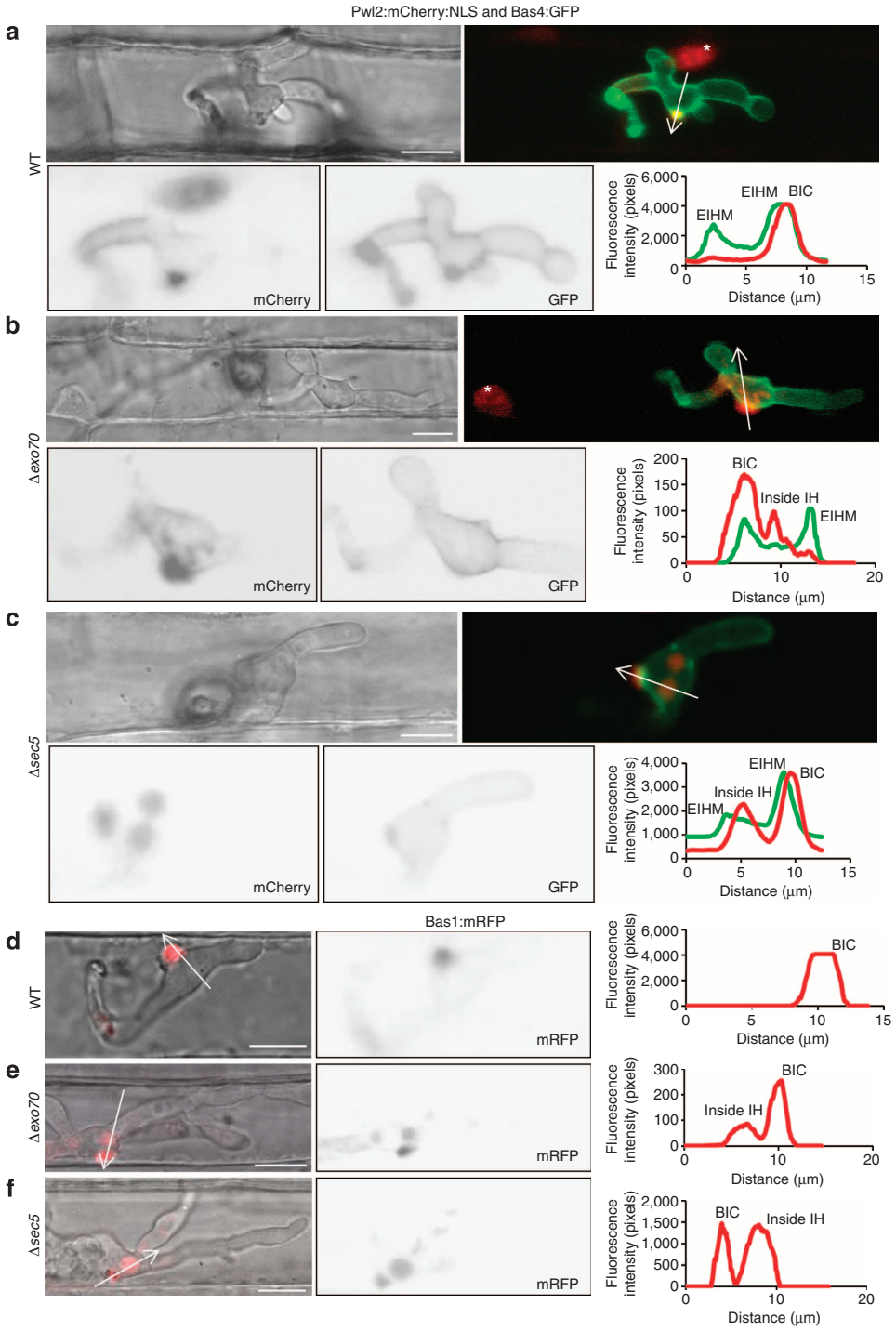

Figure 5 | Secretion of cytoplasmic effectors involves exocyst components Exo70 and Sec5. (**a**–**c**) Wild-type strain Guy11 and corresponding mutants expressed Pwl2:mCherry:NLS and Bas4:GFP. Images clockwise from the upper left: bright-field; merged mCherry (red) and GFP (green); fluorescence intensity linescans for mCherry (red) and GFP (green) along the path of the white arrow; single channel GFP or mCherry fluorescence shown as black and white inverse images, respectively. (**a**) Pwl2:mCherry:NLS in wild type shows preferential BIC localization, translocation and accumulation in the rice nucleus (white asterisk) with no fluorescence observed in the BIC-associated IH cell. Bas4:GFP localizes to the EIHM compartment. (**b**) Δ*exo70* mutant shows partial retention of Pwl2:mCherry:NLS, predominantly in the BIC-associated IH cell. Bas4:GFP secretion appears normal. Internal red fluorescence in the BIC-associated IH cell is further visualized by a black and white inverse image (lower left) and by fluorescence intensity scans, which show red fluorescence between the peaks of green fluorescence marking the boundary of the EIHM. Faint red fluorescence in the rice nucleus (white asterisk) is consistent with effector secretion being only partially blocked in the mutants. (**c**) Δ*sec5* mutant showing partial retention of Pwl2:mCherry:NLS inside the BIC-associated IH cell, but no retention of Bas4:GFP, as further visualized by black and white inverse images and fluorescence intensity scans. (**d**–**f**) Images left to right: merged bright-field and mRFP; single channel mRFP fluorescence as a black and white inverse image; and corresponding fluorescence intensity linescan. (**d**) Wild type Guy11 expressing cytoplasmic effector Bas1:mRFP. Bas1:mRFP fluorescence is not observed inside wild type IH cells. (**e**) Bas1:mRFP expressed by an Δ*exo70* mutant shows significant retention inside the IH, predominantly in the BIC-associated cells. (**f**) Bas1:mRFP expressed by an Δ*sec5* mutant strain shows significant retention of Bas1:mRFP inside the IH, predominantly in the BIC-associated cells. Linescans shown are representative of wild type ($n = 20$) and knockout mutants ($n = 20$ for each). Scale bars, 10 μm.

(Supplementary Fig. S5). These mutants formed normal-appearing IH in first-invaded rice cells. Compared to isogenic wild-type strains imaged in the same experiment (Fig. 5a,d), Δ*exo70* and Δ*sec5* mutant IH showed significant accumulation of two different cytoplasmic effectors inside BIC-associated cells, indicating that cytoplasmic effector secretion was not efficient in these mutants (Fig. 5b,c,e,f). Consistent with impaired effector secretion, we generally observed decreased fluorescence intensity in the BIC and in host nuclei. Secretion of Pwl2:mCherry:NLS was impaired in 60 of 65 randomly imaged infection sites for Δ*exo70* mutants (Fig. 5b) and in 37 of 40 randomly imaged infection sites for Δ*sec5* mutants (Fig. 5c). Effector fluorescence inside the IH occurred in the form of small vesicles or vacuole-like puncta. Fluorescence intensity distribution scans confirmed significant retention of cytoplasmic effector fluorescence inside IH cells. Importantly, in ~80% of infection sites with mutant IH, the internal cytoplasmic effector fluorescence was observed in the BIC-associated IH cells and not observed in subsequently formed IH cells. In the remaining infection sites, relatively low levels of Pwl2 fluorescence were observed in some non-BIC-associated IH cells, consistent with low basal levels of expression in these cells at later stages of cell invasion[28]. Similar impaired secretion was observed for independent transformants expressing a different cytoplasmic effector, Bas1:mRFP (Fig. 5d–f). That is, fluorescence from Bas1:mRFP was retained inside BIC-associated IH cells in Δ*exo70* mutants (in 22 of 28 imaged infection sites) and in Δ*sec5* mutants (in 23 of 27 imaged infection sites). Conversely, secretion of the apoplastic effector Bas4 was not impaired in these mutants (Fig. 5b,c).

Partial retention of these cytoplasmic effectors inside mutant BIC-associated IH cells contrasts with results of extensive imaging of BIC-accumulated effectors in wild-type strains[14,25,28], in which fluorescence from cytoplasmic effectors was not observed to be retained inside IH cells. Additionally, Δ*exo70* and Δ*sec5* mutants showed significant pathogenicity defects on two different rice varieties, when assayed at our independent locations (Fig. 6a,b). This significant loss of pathogenicity would be consistent with these mutants showing inefficient secretion of numerous cytoplasmic effectors with a role in rice blast disease. We conclude that the exocyst is critical both for efficient secretion into BICs and for fungal pathogenicity.

A t-SNARE Sso1 is required for normal BIC development. Targeted gene replacement of the *M. oryzae* t-SNARE *SSO1* (Supplementary Fig. S5) produced mutants with both reduced pathogenicity (Fig. 6a,b) and a BIC developmental defect (Fig. 7a–c). In contrast to wild-type strains, independent Δ*sso1* mutants showed two points of focal accumulation of cytoplasmic effectors. One appeared to be a normal BIC adjacent to the first-differentiated IH cell and the second was a focal fluorescent region adjacent to the primary hypha before the point of differentiation. This 'double BIC' phenotype was observed in 32 of 40 random IH expressing Pwl2:mCherry:NLS and in 25 of 30 random IH expressing Bas1:mRFP. This abnormal secretion pattern for cytoplasmic effectors was not observed previously with wild-type strains or mutants defective in other secretion pathway genes. When considered together with the localization pattern of Sso1:GFP (Fig. 3f,g), these results implicate the t-SNARE Sso1 in accumulation of effectors at the BIC.

Discussion

In this report, we have provided evidence that *M. oryzae* possesses two distinct routes by which it secretes effector proteins during biotrophic invasion of rice (Fig. 8). Apoplastic effectors accumulate extracellularly at the host–pathogen interface and are actively secreted via the conventional secretory process previously defined in filamentous fungi. As expected, this process is inhibited by BFA, implicating Golgi-dependent secretion. By contrast, cytoplasmic effectors destined for delivery inside rice cells are secreted by a different pathway involving the exocyst complex and insensitive to BFA treatment.

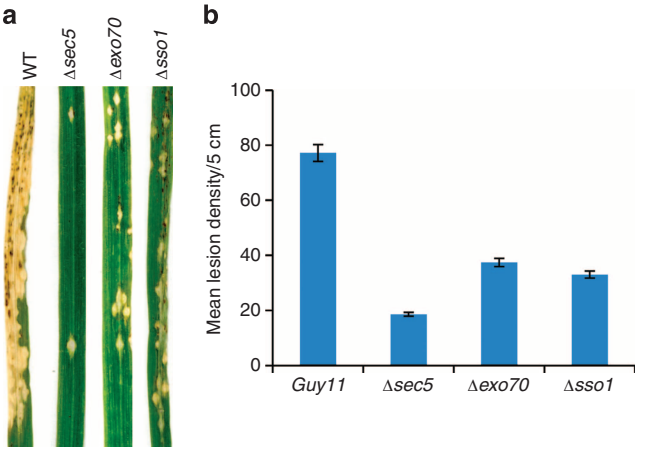

Figure 6 | Exocyst component and t-SNARE mutants suggest roles in pathogenicity. (**a**) Targeted deletions of the *SEC5*, *EXO70* and *SSO1* genes in the aggressive Chinese field isolate O-137 (WT) resulted in a significant reduction in pathogenicity on a fully susceptible rice cultivar YT-16 in whole plant spray inoculation assays at Kansas State University. Numbers of lesions formed and lesion sizes were both reduced. (**b**) Similar pathogenicity defects were observed after inoculation of mutants in the Guy11 (WT) background on rice cultivar CO-39 at the University of Exeter. These data are presented as a bar chart showing the frequency of lesions formed per 5 cm of CO-39 leaf surface ($P<0.05$ for all mutants; $n=30$ for each mutant; mean ± s.d., three experiments).

Previous studies have highlighted the presence of a membrane-rich complex, the BIC, at the host–pathogen interface during rice blast infection[28]. We have now clearly shown that the BIC is a plant-derived interfacial structure that lies outside of the plasma membrane and cell wall of the fungus in a region rich in plant plasma membrane and ER. We have also shown that the fungal exocyst components Exo70 and Sec5 have roles in an unconventional secretory mechanism for blast effectors, which lead to their accumulation at the BIC. Both Δ*exo70* and Δ*sec5* mutants show inefficient cytoplasmic effector secretion but are still viable inside rice cells, suggesting that there is functional redundancy in the system. Indeed, yeast Exo70 and Sec3 are both exocyst subunits identified as having a role in docking secretory vesicles to active sites of exocytosis[33]. It appears that Exo70 function can be at least partially fulfilled by Sec3 or some unknown component. The exocyst component Sec5 appears to function by interacting with Exo70 and Sec3 to mediate polarized targeting of secretory vesicles to the plasma membrane. Individually, Exo70 and Sec5 are required for efficient secretion of both cytoplasmic effectors we tested. The large pathogenicity defect associated with these mutants could be explained if many cytoplasmic effectors utilize the same unconventional secretion pathway and are inefficiently secreted. The individual IH that we observe in first-invaded cells would fail to thrive during subsequent colonization, and either produce smaller lesions than wild-type IH, or fail to produce macroscopic lesions at all (Fig. 6).

Both mutant analysis and localization results indicate that the t-SNARE Sso1 has a role in IH development and effector secretion. The Δ*sso1* mutant consistently produces second BIC-

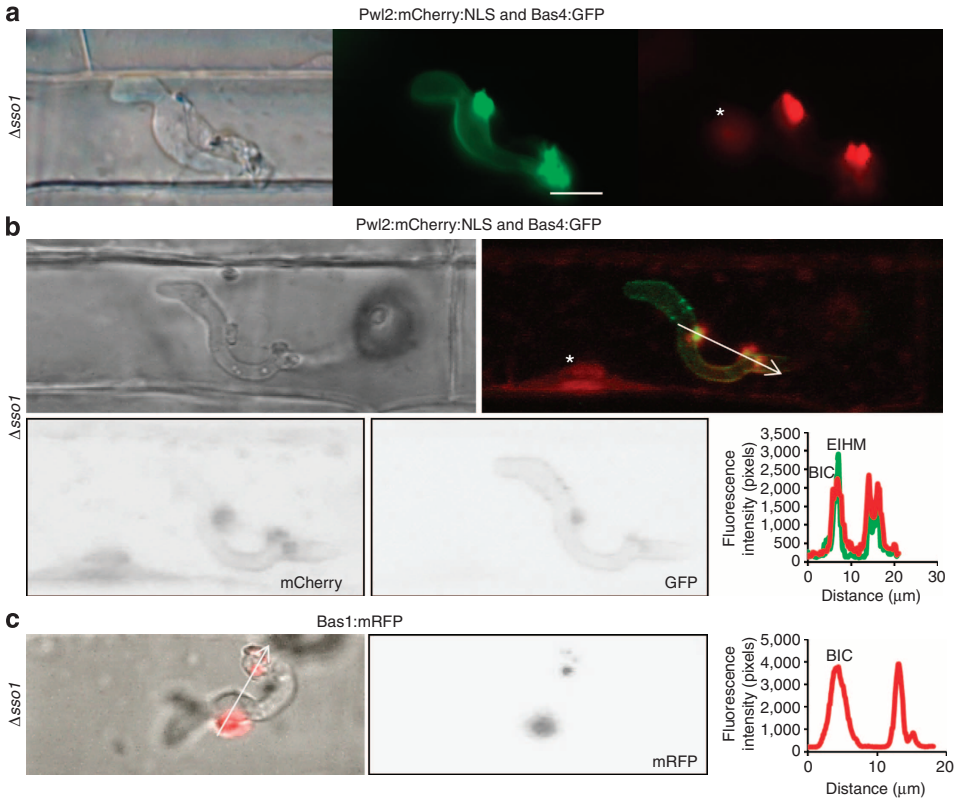

Figure 7 | t-SNARE mutants suggest a role in BIC development. (**a**) Δ*sso1* mutant showing inappropriate secretion of Pwl2:mCherry:NLS during plant infection. In addition to BICs in the expected location, second fluorescent foci occurred midway along the primary hyphae. Images left to right: bright-field; GFP (green); and mCherry (red). (**b**) Another infection site in which Pwl2:mCherry:NLS expressed by an Δ*sso1* mutant strain shows inappropriate secretion. Images clockwise from the upper left: bright-field; merged mCherry (red) and GFP (green); fluorescence intensity linescans for mCherry (red) and GFP (green) along the white arrow; single channel GFP or mCherry fluorescence shown as black and white inverse images. (**c**) Bas1:mRFP expressed by an Δ*sso1* mutant shows inappropriate secretion. Images left to right: merged bright-field and mRFP; mRFP fluorescence shown as black and white inverse image; and fluorescence intensity linescan along the white arrow. Rice nuclei are indicated by a white asterisk. Linescans shown are representative of wild type ($n = 20$) and knockout mutants ($n = 20$ for each). Scale bars, 10 μm.

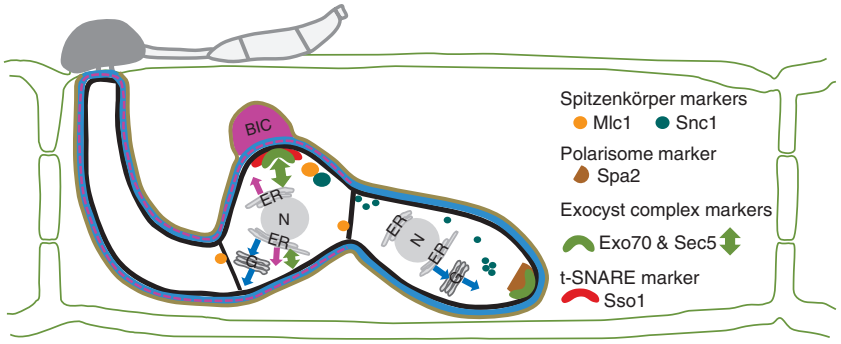

Figure 8 | Model for effector secretion by *M. oryzae*. This cartoon shows a bulbous IH at 26–30 h.p.i. inside a rice cell. The EIHM (tan) continues around the BIC. Apoplastic effectors (blue), including Bas4, Bas113 and Slp1, accumulate in the EIHM compartment surrounding the IH, resulting in uniform outlining of the IH. These apoplastic effectors follow the conventional, BFA-sensitive, Golgi-dependent secretion pathway. In contrast, cytoplasmic effectors (magenta), including Pwl2, AVR-Pita, Bas1 and Bas107, accumulate in the BIC beside the first-differentiated bulbous IH cell. To a lesser extent, as observed at saturated fluorescence exposure levels (Fig. 3c), cytoplasmic effectors (magenta dotted line) also accumulate inside the EIHM surrounding the BIC-associated cells (the primary hypha and first-differentiated bulbous IH cell), but they do not outline the subsequently formed bulbous IH cells. These cytoplasmic effectors follow a nonconventional, BFA-insensitive secretion pathway involving exocyst and SNARE proteins.

like regions of focal effector accumulation midway along the primary hyphae (Fig. 7). This Sso1:GFP localization pattern is consistent with specialized exocytic pathways employing different surface SNAREs at different hyphal sites for cytoplasmic effector secretion and for hyphal growth. There is precedent for the involvement of SNARE proteins in secretion from subapical regions of hyphae. The industrially important cellulolytic filamentous fungus *T. reesei* has two pathways for exocytosis, which employ different t-SNARE proteins at distinct sites in the hyphae[35].

Secretion of cytoplasmic effectors by a distinct pathway that is predominantly localized to BIC-associated cells is consistent with

the BIC being important in effector delivery or sequestration by the host. BICs have been hypothesized as the site of translocation of cytoplasmic effectors into the rice cytoplasm based on a strong correlation between preferential BIC localization of known effectors (such as Pwl2, Avr-Pita and AvrPiz-t) and evidence supporting their translocation to the rice cytoplasm[8,11,28]. Several aspects of this study are consistent with the idea that BIC-associated bulbous IH cells actively secrete cytoplasmic effectors. First, BIC-associated bulbous IH cells contain concentrated fluorescent foci of GFP-labelled secretory pathway components, the myosin regulatory light chain Mlc1, exocyst component Exo70, v-SNARE Snc1 and t-SNARE Sso1. The only exception to this was the polarisome component Spa2, which we observed only in growing hyphal cells. Retention of Spa2 at bulbous IH growth points after differentiation resembles retention of Spa2 at pseudohyphal growth points after differentiation in *C. albicans*[23]. Second, fluorescent cytoplasmic effectors accumulate at BICs following photobleaching, and this process is BFA insensitive. Third, cytoplasmic effector proteins accumulate predominantly inside the BIC-associated cells of Δ*exo70* and Δ*sec5* mutants rather than at hyphal tips, suggesting that they may be secreted predominantly from BIC-associated cells. These results are consistent with new evidence that expression of cytoplasmic effectors is highly upregulated in BIC-associated cells compared to lower basal levels of expression throughout the IH at later infection stages of host cell invasion[28]. We also found that the t-SNARE Sso1 not only localized adjacent to the BIC, but that mutants lacking this gene showed defects in normal BIC development. When considered together, these observations support a central role for the BIC as a destination for secretion of effectors that are ultimately taken up by rice cells.

In summary, our results provide evidence that targeting fungal effectors to distinct host compartments may require separate, specialized secretory processes in the rice blast fungus, *M. oryzae*. Identifying how these processes function will prove pivotal in controlling rice blast disease and also determining the nature and evolution of exocyst processes in fungal pathogens.

Methods

Live-cell imaging of *M. oryzae* hyphae. Fungal transformants were stored in dried filter papers at −20 °C, and cultured on oatmeal agar plates at 24 °C under continuous light[41]. From fresh fungal cultures, a small plug cut from the hyphal growth zone was placed on the edge of a sterile water agar-coated microscope slide and incubated in a humid chamber for 16–18 h. *M. oryzae* vegetative hyphae were imaged while growing at a rate of 5–10 μm min^{-1} on these slides. New fungal transformants were evaluated at 16–18 h post inoculation (h.p.i.) using vegetative hyphae to confirm fluorescence expression. Active growth was documented by time-lapse imaging using AxioVisionLE software, version 4.8. Independent transformants were selected for use based on the highest intensity of the fluorescent marker. These transformants were evaluated during infection *in planta* by rice sheath inoculations. Rice sheath inoculations were performed as described[22] using the susceptible rice line YT-16. Briefly, 5-cm-long sheath pieces from 3-week-old plants were placed in a glass container under high humidity conditions. Sheaths were placed on acrylic stands to avoid contact with wet paper and to hold epidermal cells directly above the mid-vein horizontally flat for uniform inoculum distribution in the trimmed sheath pieces. A spore suspension (~200 μl of a suspension of 2×10^4 spores ml^{-1} in 0.25% gelatin, Cat. #G-6650, Sigma-Aldrich) was injected into one end of the sheath using a 200-μl pipette. Each segment was trimmed at 22–36 h.p.i. and imaged immediately. Conventional epifluorescence and differential interference contrast microscopy was performed with a Zeiss Axioplan 2 IE MOT microscope, using a ×63 1.2 NA (numerical aperture) C-Apochromat water immersion objective lens. Images were acquired using a Zeiss AxioCam HRc camera and analysed with Zeiss Axiovision digital image-processing software, version 4.8. Fluorescence was observed with an X-Cite® 120 (EXFO Life Sciences) mercury lamp source. The filter sets used were: GFP (excitation 480 ± 10 nm, emission 510 ± 10 nm, filter set 41020, Chroma Tech. Corp., Rockingham, VT) and mRFP, mCherry or FM4-64 (excitation 535 ± 25 nm, emission 610 ± 32 1/2 nm, Zeiss). Confocal imaging was performed with a Zeiss Axiovert 200 M microscope equipped with a Zeiss LSM 510 META system using two water immersion objectives, ×40/1.2 NA and ×63/1.2 NA C-Apochromat. Excitation/emission wavelengths were 488 nm/505–550 nm for EGFP, and 543 nm/560–615 nm for mRFP, mCherry and FM4-64. Images were acquired and processed using LSM 510 AIM version 4.2 SP1 software.

Identification of *M. oryzae* secretory pathway genes. Sequence data were accessed from the *Saccharomyces* Genome Database (SGD) (http://www.yeastgenome.org/sitemap.html) under the following accession numbers MLC1/YGL106W, SNC1/YAL030W, SPA2/YLL021W, SEC5/YDR166C, SSO1/YPL232W and EXO70/YJL085W. Analysis of the predicted protein sequences was performed using BLASTP[42] from NCBI GeneBank (http://www.ncbi.nlm.nih.gov/genbank/), Broad Institute's *Magnaporthe grisea* Genome Database (http://www.broadinstitute.org/annotation/genome/magnaporthe_grisea/MultiHome.html), MGOS (http://www.mgosdb.org/), SGD (http://www.yeastgenome.org/sitemap.html) and the Biological General Repository for Interaction Datasets (BioGRID) database (http://www.thebiogrid.org). Multiple protein sequence alignments were used to find diagnostic patterns to characterize protein families and to detect homology between *M. oryzae* orthologue sequences and existing families of sequences. These protein sequence alignments were performed using CLUSTALW2 from EMBL-EBI (http://www.ebi.ac.uk/Tools/clustalw2/index.html). In ClustalW2 (ref. 43), the guide trees, used to guide the multiple alignment, were calculated by a distance matrix method using the Neighbour Joining tree_BLOSUM62 (ref. 44). *M. oryzae* genes selected were *MLC1* (MGG_09470), *SNC1* (MGG_12614), *SPA2* (MGG_03703), *EXO70* (MGG_01760), *SEC5* (MGG_07150), and *SSO1* (MGG_04090). Further details are listed in Supplementary Table S1.

FM4-64 staining and treatment with pharmacological inhibitors. Fungal transformants expressing secretion machinery components were treated with FM4-64 (4 μg ml^{-1} in water). An aqueous 17 mM stock solution of FM4-64 (Cat # 13320, Invitrogen, Carlsbad, CA) was made and stored at −20 °C as described[45]. Vegetative hyphae at ~16–18 h.p.i. on a water agar slide were incubated for 5–30 min in a 10-μM aqueous solution of FM4-64 for uniform staining. *In planta*, inoculated trimmed leaf sheaths, ~24 h.p.i., were incubated in a 10-μM aqueous working solution for 1–5 h. To examine the effects of brefeldin A (BFA) (Sigma) on IH secretion of effectors *in planta*, we prepared stock solutions of BFA, 10 mg ml^{-1}, in dimethyl sulphoxide (DMSO, Sigma) according to Bourett and Howard[46]. We incubated the leaf sheath tissue at 27–28 h.p.i. (2×10^4 spores ml^{-1} in 0.25% gelatin solution) in 50 μg ml^{-1} BFA (0.1% DMSO). Treatments with the microtubule inhibitor methyl 1-(butylcarbamoyl)-2-benzimidazolecarbamate (MBC, the active ingredient in the fungicide benomyl) and the actin inhibitor LatA were performed on infected sheath tissue to examine the effects of hyphal cytoskeletal organization. Stock solutions of 10 mg ml^{-1} MBC (Sigma) and 100 μg ml^{-1} latrunculin A (Sigma) were prepared according to Czymmek *et al.*[47]. For *in planta* experiments with both drugs, we prepared working solutions of 50 μg ml^{-1} in 0.1% DMSO and treated the inoculated tissue as described for BFA.

Fluorescence recovery after photobleaching. Experiments were performed using a Zeiss LSM 510 confocal microscope with a 488-nm argon laser and a C-Apochromat ×40/1.2 NA water immersion objective at ×2 optical zoom. For FRAP analyses, the specific region of interest (ROI) covering the entire fluorescence in the BIC was selected for bleaching. We used 20 bleaching iterations at 100% laser power for a BIC containing cytoplasmic effector Pwl2:GFP fusion protein. Image scans were taken with the acousto-optic tunable filter attenuated to 5% laser power immediately before and after bleaching. Images were recorded up to 3 h after bleaching of the BIC region. During these time periods, the ROI showed from 70% to complete recovery. For quantitative analyses, the GFP fluorescence recovery curves were measured as the mean intensity of ROI pixels using the LSM software (version 4.2 SP1), normalized and graphed using Microsoft Excel.

Vector construction and Agrobacterium-mediated transformation of *M. oryzae*. Unless noted otherwise, transformation cassettes to observe *M. oryzae* fluorescently labelled cellular components and effector proteins were constructed containing the entire protein coding sequence with its native promoter (~1 kb) in a translational fusion with GFP, mRFP or mCherry. The GFP gene used was the EGFP gene from Clontech. The mRFP gene was obtained from Campbell *et al.*[48]. The mCherry gene from Shaner *et al.*[49] was isolated from pAN583. The plasmid containing the PWL2 promoter and coding sequence fused to a nuclear targeting mCherry:NLS sequence was obtained from Khang *et al.*[28] Each cassette was cloned into the pBHt2 binary vector for fungal transformation by *A. tumefaciens*[50] and for selection of positive transformants using resistance to hygromycin or geneticin (G418). Details of plasmid construction and corresponding fungal transformants used in this study are listed in Supplementary Tables S2 and S3, respectively. *M. oryzae* field isolates O-137 (ref. 51) and Guy11 (ref. 52), and laboratory strain CP987 (ref. 51) were used as recipients. Fungal transformants were purified by isolation of single spores and 7–10 independent transformants were analysed per gene. In GenBank, the sequence data for the effector genes used in this study are under U26313 for PWL2, FJ807764 for Bas1, AF207841 for AVR-Pita1, MGG_10020.6 for Bas107, FJ807767 for Bas4, MGG_05785.6 for Bas113 and MGG_10097.6 for Slp1.

Targeted gene replacements in *M. oryzae* and whole plant infection assays. Targeted gene replacements for *EXO70*, *SEC5* and *SSO1* were carried out using the split marker method[53]. A 1.4-kb hygromycin resistance cassette or a 2.8-kb sulphonylurea resistance cassette replaced the coding sequence of each gene. Sequence data for these genes can be found in the GenBank/EMBL databases under MGG_ numbers listed in Supplementary Table S1. Sequences for flanking regions were retrieved from the *M. oryzae* genome database at the Broad Institute (http://www.broadinstitute.org/annotation/fungi/magnaporthe/). Approximately 1.0 kb of flanking sequences were used for homologous recombination, and positive transformants were confirmed by DNA gel blot analysis (Supplementary Fig. S5). At least two positive transformants were used for further analysis of every gene in each background. Whole plant infection assays for assessing mutant phenotypes were performed by spray inoculation of 2–3-week-old rice plants as described[41]. All results reported are based on at least three independent assays at each location.

Generation of transgenic rice plants. Gene fusions for expressing the plant plasma membrane marker low-temperature inducible protein 6B, LTi6B:GFP[54] and the ER marker GFP:HDEL[55] were transformed into rice cultivar *Oryza sativa* cv Sasanishiki[56] using standard rice transformation. Putative transformants of rice were selected on 100 μg ml^{-1} hygromycin, confirmed by DNA gel blot, and expression checked by qRT–PCR, immunoblotting and epifluorescence microscopy.

References

1. Goldberg, D. E. & Cowman, A. F. Moving in and renovating: exporting proteins from Plasmodium into host erythrocytes. *Nat. Rev. Microbiol.* **8,** 617–621 (2010).
2. Koeck, M., Hardham, A. R. & Dodds, P. N. The role of effectors of biotrophic and hemibiotrophic fungi in infection. *Cell Microbiol.* **13,** 1849–1857 (2011).
3. Bozkurt, T. O., Schornack, S., Banfield, M. J. & Kamoun, S. Oomycetes, effectors, and all that jazz. *Curr. Opin. Plant Biol.* **15,** 483–492 (2012).
4. Rafiqi, M., Ellis, J. G., Ludowici, V. A., Hardham, A. R. & Dodds, P. N. Challenges and progress towards understanding the role of effectors in plant-fungal interactions. *Curr. Opin. Plant Biol.* **15,** 477–482 (2012).
5. Alfano, J. R. & Collmer, A. Type III secretion system effector proteins: double agents in bacterial disease and plant defense. *Annu. Rev. Phytopathol.* **42,** 385–414 (2004).
6. Galan, J. E. & Collmer, A. Type III secretion machines: bacterial devices for protein delivery into host cells. *Science* **284,** 1322–1328 (1999).
7. Schirawski, J. *et al.* Pathogenicity determinants in smut fungi revealed by genome comparison. *Science* **330,** 1546–1548 (2010).
8. Valent, B. & Khang, C. H. Recent advances in rice blast effector research. *Curr. Opin. Plant Biol.* **13,** 434–441 (2010).
9. Birch, P. R. *et al.* Towards understanding the virulence functions of RXLR effectors of the oomycete plant pathogen *Phytophthora infestans*. *J. Exp. Bot.* **60,** 1133–1140 (2009).
10. Hogenhout, S. A., Van der Hoorn, R. A., Terauchi, R. & Kamoun, S. Emerging concepts in effector biology of plant-associated organisms. *Mol. Plant Microbe Interact.* **22,** 115–122 (2009).
11. Park, C. H. *et al.* The *Magnaporthe oryzae* effector AvrPiz-t targets the RING E3 ubiquitin ligase APIP6 to suppress pathogen-associated molecular pattern-triggered immunity in rice. *Plant Cell* **24,** 4748–4762 (2012).
12. Djamei, A. *et al.* Metabolic priming by a secreted fungal effector. *Nature* **478,** 395–398 (2011).
13. de Jonge, R. *et al.* Conserved fungal LysM effector Ecp6 prevents chitin-triggered immunity in plants. *Science* **329,** 953–955 (2010).
14. Mentlak, T. A. *et al.* Effector-mediated suppression of chitin-triggered immunity by *Magnaporthe oryzae* is necessary for rice blast disease. *Plant Cell* **24,** 322–335 (2012).
15. Fisher, M. C. *et al.* Emerging fungal threats to animal, plant and ecosystem health. *Nature* **484,** 186–194 (2012).
16. Wilson, R. A. & Talbot, N. J. Under pressure: investigating the biology of plant infection by *Magnaporthe oryzae*. *Nat. Rev. Microbiol.* **7,** 185–195 (2009).
17. Guo-Liang Wang & Valent, Barbara (eds.) *Advances in Genetics, Genomics and Control of Rice Blast Disease* (Springer Science and Business Media, New York, 2009).
18. Cruz, C. D. *et al.* Preliminary assessment of resistance among U.S. wheat cultivars to the *Triticum* pathotype of *Magnaporthe oryzae*. *Plant Dis.* **96,** 1501–1505 (2012).
19. Urashima, A. S., Lavorent, N. A., Goulart, A. C. P. & Mehta, Y. R. Resistance spectra of wheat cultivars and virulence diversity of *Magnaporthe grisea* isolates in Brazil. *Fitopatol. Bras.* **29,** 511–518 (2004).
20. Dagdas, Y. F. *et al.* Septin-mediated plant cell invasion by the rice blast fungus, *Magnaporthe oryzae*. *Science* **336,** 1590–1595 (2012).
21. Fernandez, J. & Wilson, R. A. Why no feeding frenzy? Mechanisms of nutrient acquisition and utilization during infection by the rice blast fungus *Magnaporthe oryzae*. *Mol. Plant Microbe Interact.* **25,** 1286–1293 (2012).
22. Kankanala, P., Czymmek, K. & Valent, B. Roles for rice membrane dynamics and plasmodesmata during biotrophic invasion by the blast fungus. *Plant Cell* **19,** 706–724 (2007).
23. Crampin, H. *et al.* *Candida albicans* hyphae have a Spitzenkörper that is distinct from the polarisome found in yeast and pseudohyphae. *J. Cell Sci.* **118,** 2935–2947 (2005).
24. Sudbery, P., Gow, N. & Berman, J. The distinct morphogenic states of *Candida albicans*. *Trends Microbiol.* **12,** 317–324 (2004).
25. Mosquera, G., Giraldo, M. C., Khang, C. H., Coughlan, S. & Valent, B. Interaction transcriptome analysis identifies *Magnaporthe oryzae* BAS1-4 as biotrophy-associated secreted proteins in rice blast disease. *Plant Cell* **21,** 1273–1290 (2009).
26. Saitoh, H. *et al.* Large-scale gene disruption in *Magnaporthe oryzae* identifies MC69, a secreted protein required for infection by monocot and dicot fungal pathogens. *PLoS Pathog.* **8,** e1002711 (2012).
27. Yi, M. *et al.* The ER chaperone LHS1 is involved in asexual development and rice infection by the blast fungus *Magnaporthe oryzae*. *Plant Cell* **21,** 681–695 (2009).
28. Khang, C. H. *et al.* Translocation of *Magnaporthe oryzae* effectors into rice cells and their subsequent cell-to-cell movement. *Plant Cell* **22,** 1388–1403 (2010).
29. Read, N. D. Exocytosis and growth do not occur only at hyphal tips. *Mol. Microbiol.* **81,** 4–7 (2011).
30. Steinberg, G. Hyphal growth: a tale of motors, lipids, and the spitzenkörper. *Eukaryot. Cell* **6,** 351–360 (2007).
31. Sudbery, P. Fluorescent proteins illuminate the structure and function of the hyphal tip apparatus. *Fungal Genet. Biol.* **48,** 849–857 (2011).
32. Riquelme, M. *et al.* Architecture and development of the *Neurospora crassa* hypha—a model cell for polarized growth. *Fungal Biol.* **115,** 446–474 (2011).
33. Heider, M. R. & Munson, M. Exorcising the exocyst complex. *Traffic* **13,** 898–907 (2012).
34. Hayakawa, Y., Ishikawa, E., Shoji, J. -y., Nakano, H. & Kitamoto, K. Septum-directed secretion in the filamentous fungus *Aspergillus oryzae*. *Mol. Microbiol.* **81,** 40–55 (2011).
35. Valkonen, M. *et al.* Spatially segregated SNARE protein interactions in living fungal cells. *J. Biol. Chem.* **282,** 22775–22785 (2007).
36. Sweigard, J. A. *et al.* Identification, cloning, and characterization of *PWL2*, a gene for host species specificity in the rice blast fungus. *Plant Cell* **7,** 1221–1233 (1995).
37. Atkinson, H. A., Daniels, A. & Read, N. D. Live-cell imaging of endocytosis during conidial germination in the rice blast fungus, *Magnaporthe grisea*. *Fungal Genet. Biol.* **37,** 233–244 (2002).
38. Fischer, R., Zekert, N. & Takeshita, N. Polarized growth in fungi; interplay between the cytoskeleton, positional markers and membrane domains. *Mol. Microbiol.* **68,** 813–826 (2008).
39. Fischer-Parton, S. *et al.* Confocal microscopy of FM4-64 as a tool for analysing endocytosis and vesicle trafficking in living fungal hyphae. *J. Microsc.* **198,** 246–259 (2000).
40. Chardin, P. & McCormick, F. Brefeldin A: the advantage of being uncompetitive. *Cell* **97,** 153–155 (1999).
41. Valent, B., Farrall, L. & Chumley, F. G. *Magnaporthe grisea* genes for pathogenicity and virulence identified through a series of backcrosses. *Genetics* **127,** 87–101 (1991).
42. Altschul, S. F. *et al.* Gapped BLAST and PSI-BLAST: a new generation of protein database search programs. *Nucleic Acids. Res.* **25,** 3389–3402 (1997).
43. Thompson, J. D., Higgins, D. G. & Gibson, T. J. CLUSTAL W: improving the sensitivity of progressive multiple sequence alignment through sequence weighting, position-specific gap penalties and weight matrix choice. *Nucleic Acids. Res.* **22,** 4673–4680 (1994).
44. Saitou, N. & Nei, M. The neighbor-joining method: a new method for reconstructing phylogenetic trees. *Mol. Biol. Evol.* **4,** 406–425 (1987).
45. Bolte, S. *et al.* FM-dyes as experimental probes for dissecting vesicle trafficking in living plant cells. *J. Microsc.* **214,** 159–173 (2004).
46. Bourett, T. M. & Howard, R. J. Brefeldin A-induced structural changes in the endomembrane system of a filamentous fungus, *Magnaporthe grisea*. *Protoplasma* **190,** 151–163 (1996).
47. Czymmek, K. J. *et al.* Live-cell imaging of tubulin in the filamentous fungus *Magnaporthe grisea* treated with anti-microtubule and anti-microfilament agents. *Protoplasma* **225,** 23–32 (2005).
48. Campbell, R. E. *et al.* A monomeric red fluorescent protein. *Proc. Natl Acad. Sci. USA* **99,** 7877–7882 (2002).
49. Shaner, N. C. *et al.* Improving the photostability of bright monomeric orange and red fluorescent proteins. *Nat. Methods.* **5,** 545–547 (2008).
50. Khang, C. H., Park, S. -Y., Lee, Y. -H. & Kang, S. A dual selection based, targeted gene replacement tool for *Magnaporthe grisea* and *Fusarium oxysporum*. *Fungal Genet. Biol.* **42,** 483–492 (2005).

51. Orbach, M. J., Farrall, L., Sweigard, J. A., Chumley, F. G. & Valent, B. A telomeric avirulence gene *AVR-Pita* determines efficacy for the rice blast resistance gene *Pi-ta*. *Plant Cell* **12,** 2019–2032 (2000).
52. Leung, H., Borromeo, E. S., Bernardo, M. A. & Notteghem, J. L. Genetic analysis of virulence in the rice blast fungus *Magnaporthe grisea*. *Phytopathology* **78,** 1227–1233 (1988).
53. Kershaw, M. J. & Talbot, N. J. Genome-wide functional analysis reveals that infection-associated fungal autophagy is necessary for rice blast disease. *Proc. Natl Acad. Sci. USA* **106,** 15967–15972 (2009).
54. Kurup, S. *et al.* Marking cell lineages in living tissues. *Plant J.* **42,** 444–453 (2005).
55. Zheng, H. *et al.* A Rab-E GTPase mutant acts downstream of the Rab-D subclass in biosynthetic membrane traffic to the plasma membrane in tobacco leaf epidermis. *Plant Cell* **17,** 2020–2036 (2005).
56. Yoshida, K. *et al.* Association genetics reveals three novel avirulence genes from the rice blast fungal pathogen *Magnaporthe oryzae*. *Plant Cell* **21,** 1573–1591 (2009).

Acknowledgements

We thank Melinda Dalby for technical support and Timothy Todd for support and discussions at KSU. This work was supported by a grant from the Biotechnology and Biological Sciences Research Council to N.J.T., a Halpin Scholarship to Y.F.D. and Y.K.G., a Sainsbury studentship from Gatsby Charitable Foundation to T.A.M., and a European Research Council Advanced Investigator award to N.J.T.; by grants from the National Research Initiative Competitive Grants Program (Grants 2008-35600-18809 and 2010-65108-20538) from the USDA National Institute of Food and Agriculture to B.V.; and a Grant-in-Aid by MAFF (Genomics for Agricultural Innovation PMI-0010), PROBRAIN and MEXT, Japan (Grant-in-Aid for Scientific Research on Innovative Areas 23113009) to R.T. and H.S. We acknowledge support from the COBRE Confocal Microfluorometry and Microscopy Core at KSU, funded by CVM-KSU and NIH Grant P20 RR-017686. This is contribution # 13-140-J from the Agricultural Experiment Station at KSU.

Author contributions

B.V. and N.J.T. developed the research plan and experimental strategy. M.C.G. helped to design the research plan and designed experiments, constructed fluorescently-tagged *M. oryzae* strains and carried out live cell imaging experiments using laser confocal microscopy, FRAP and inhibitor analysis. Y.F.D. helped to design experiments, constructed fluorescently-tagged *M. oryzae* strains and a range of targeted deletion mutants. Y.K.G. and T.A.M contributed equally to the study, as joint second authors. Y.K.G. generated *M. oryzae* exocyst mutants, fluorescently-tagged strains to define exocyst components and carried out pathogenicity assays. T.A.M. designed and constructed transgenic rice and *M. oryzae* lines expressing fluorescent membrane markers to define the BIC using laser enhanced epifluorescence microscopy. M.Y. and A.L.M.-R generated vectors and characterized *M. oryzae* strains. H.S. and R.T. generated transgenic rice lines. All authors analysed data and contributed to writing the paper, led by B.V. and N.J.T.

Additional information

Supplementary Information accompanies this paper on www.nature.com/naturecommunications.

Competing financial interests: The authors declare no competing financial interests.

Reprints and permission information is available online at http://www.nature.com/reprintsandpermissions/

How to cite this article: Giraldo, M. C. *et al.* Two distinct secretion systems facilitate tissue invasion by the rice blast fungus *Magnaporthe oryzae*. *Nat. Commun.* 4:1996 doi: 10.1038/ncomms2996 (2013).

List of Supplementary Movies